



Thèse

2007

Open Access

This version of the publication is provided by the author(s) and made available in accordance with the copyright holder(s).

---

## Differential proteomic analysis of STAT6 knock-out mice reveals new regulatory function in glucose and lipid homeostasis

---

Iff, Joël

### How to cite

IFF, Joël. Differential proteomic analysis of STAT6 knock-out mice reveals new regulatory function in glucose and lipid homeostasis. Doctoral Thesis, 2007. doi: 10.13097/archive-ouverte/unige:698

This publication URL: <https://archive-ouverte.unige.ch/unige:698>

Publication DOI: [10.13097/archive-ouverte/unige:698](https://doi.org/10.13097/archive-ouverte/unige:698)

**UNIVERSITÉ DE GENÈVE**

Section des Sciences Pharmaceutiques

Département de Physiologie Cellulaire  
et Métabolisme

**FACULTÉ DES SCIENCES**  
Professeur Gérard Hopfgartner

**FACULTÉ DE MÉDECINE**  
Professeur Jean-Louis Carpentier  
Docteur Ildiko Denes Carpentier

---

**Differential Proteomic Analysis of STAT6 Knock-out Mice  
Reveals New Regulatory Function in Glucose and Lipid  
Homeostasis**

**THÈSE**

présentée à la Faculté des sciences de l'Université de Genève  
pour obtenir le grade de Docteur ès sciences, mention sciences pharmaceutiques

par

**Joël IFF**

de

Genève (GE)

Thèse N° 3908

GENÈVE

Atelier de reproduction de la Section de physique

2007



**UNIVERSITÉ  
DE GENÈVE**

**FACULTÉ DES SCIENCES**

**Doctorat ès sciences  
mention sciences pharmaceutiques**

Thèse de *Monsieur Joël IFF*

intitulée :

**"Differential Proteomic Analysis of STAT6 Knock-out Mice  
Reveals New Regulatory Function in Glucose  
and Lipid Homeostasis"**

La Faculté des sciences, sur le préavis de Messieurs J.-L. CARPENTIER, professeur ordinaire et directeur de thèse (Faculté de médecine – Département de physiologie cellulaire et métabolisme), G. HOPFGARTNER, professeur ordinaire et co-directeur de thèse (Section des Sciences Pharmaceutiques), I. DENES CARPENTIER, docteur et co-directeur de thèse (Faculté de médecine – Département de physiologie cellulaire et métabolisme), C. WOLLHEIM, professeur ordinaire (Faculté de médecine – Département de physiologie cellulaire et métabolisme), B. DOMON, docteur (Eidgenössische Technische Hochschule Zürich – Institute of Molecular systems biology – Zürich, Switzerland), autorise l'impression de la présente thèse, sans exprimer d'opinion sur les propositions qui y sont énoncées.

Genève, le 26 octobre 2007

**Thèse - 3908 -**

  
**Le Doyen, Jean-Marc TRISCONE**

N.B.- La thèse doit porter la déclaration précédente et remplir les conditions énumérées dans les "Informations relatives aux thèses de doctorat à l'Université de Genève".

**Nombre d'exemplaires à livrer par colis séparé à la Faculté : - 7 -**

## Remerciements

En tout premier lieu j'aimerais remercier mon directeur de thèse, le Professeur Jean-Louis **Carpentier** pour m'avoir accueilli dans son laboratoire dans le département de physiologie cellulaire et métabolisme de la Faculté de Médecine. Ces années m'ont permis d'élargir mes connaissances et de nouer des contacts qui ont été très enrichissants.

Toute ma gratitude s'adresse au Professeur Gérard **Hopfgartner** qui a accepté d'être mon co-directeur et répondant de la Faculté des Sciences. Sa présence a permis de tisser des liens étroits entre la Faculté de Médecine et la Section des sciences pharmaceutiques et a abouti à une collaboration fructueuse. Ses nombreux et précieux conseils ont toujours été les bienvenus tant sur le plan scientifique que sportif.

Mes remerciements les plus sincères s'adressent au Docteur Ildiko **Szanto**, mon superviseur de thèse, qui a été, à la fois très exigeante, mais qui m'a également laissé beaucoup de liberté.

Je remercie également chaleureusement le Professeur Claes **Wollheim** et le Docteur Bruno **Domon** pour avoir accepté d'évaluer ce travail et d'y participer en tant que membres du jury.

Je tiens également à souligner toute ma reconnaissance au Docteur Emmanuel **Varesio** pour ses nombreuses relectures, corrections, précieux conseils, ainsi que pour ses discussions riches et variées. Je tiens également à le remercier pour les nombreuses heures qu'il a passé à analyser les données protéomiques.

Un grand merci également à Nathalie **Oudry** qui a été également très impliquée dans la partie protéomique de ce travail.

J'aimerais également remercier tous mes collègues du Laboratoire, Michelangelo **Foti**, Margot **Fournier**, Gilles **Erba**, Christine **Maeder**, Céline **Manzin**, Sarah **Mouche**, Moulay **Moukil**, Geneviève **Porcheron**, Manlio **Vinciguerra** et Wei **Wang**, qui ont su m'aider, m'inspirer et partager leur savoir-faire scientifique.

Je remercie également toutes les personnes qui ont eu une influence positive par leur présence et leur soutien durant ces années : Michael **Allimann**, Olivier **Chastonay**, Raphaël **Guanella**, Nicolas **Holzer**, Thierry **Schaub**, Patrick **Surber** et Albert **Villa** qui ont su m'inspirer par leurs accompagnements sportifs, œnologiques ou gastronomiques.

Un immense merci à mes parents, Roland et Rose-Marie **Iff** ainsi qu'à mon frère Sylvain **Iff** qui m'ont aidés et rendus un nombre incalculable de précieux services.

Finalement qu'aurais-je fait sans Elodie **Privat** qui m'a encouragé, soutenu, aidé, conseillé et qui a eu plusieurs impacts décisifs sur mes choix durant ces années ?

Un grand merci à tous

Joël Iff



## Résumé de la thèse

Ces dernières années, la majorité des cas d'hospitalisation liés au système cardio-vasculaire, rénal ou oculaire ont été en relation avec des complications liées au diabète. La prise en charge de cette maladie est donc devenue une préoccupation majeure de santé publique. Dans tous les cas de figure, le facteur déclencheur de cette pathologie est le résultat d'une perturbation du métabolisme du glucose et des lipides qui a pour conséquence une élévation de la glycémie. Il existe deux dysfonctionnements principaux liés à cette élévation de glycémie. Le premier (diabète de type I) est dû à une incapacité des cellules  $\beta$  pancréatiques de sécréter de l'insuline. La raison de cette destruction est principalement due à une réaction auto-immune contre les îlots de Langerhans qui sécrètent l'insuline. Le deuxième (diabète de type II) est la conséquence d'excès alimentaires à répétition, conduisant à une accumulation lipidique et un état inflammatoire au niveau des tissus adipeux. Cette inflammation provoque la libération de cytokines pro-inflammatoires (TNF $\alpha$ , IL-6), responsables de la diminution de l'effet de l'insuline, et qui agissent principalement au niveau des tissus adipeux, du muscle et de la production de glucose par le foie. Les taux de glucose circulants ne sont donc plus en mesure d'être abaissés par ces organes, ce qui entraîne une augmentation des sécrétions d'insuline par le pancréas, qui finit par s'épuiser et perdre ainsi sa capacité à produire de l'insuline. L'organisme se trouve ainsi dans l'incapacité de s'opposer à une élévation de la glycémie. Les effets néfastes d'une glycémie élevée finissent pas entraîner des complications micro- et macrovasculaires qui sont les conséquences de l'inflammation et de l'accumulation de lipides dans les vaisseaux sous forme d'athéromes.

Pour mieux comprendre l'implication des signaux pro-inflammatoires sur la sensibilité à l'insuline de tissus périphériques tels que muscle, foie et tissus adipeux, la démarche utilisée lors de ce travail a consisté à considérer le scénario inverse, à savoir étudier l'impact d'une suppression de signaux anti-inflammatoires sur le métabolisme. Les conséquences d'une telle suppression devraient, en théorie, provoquer le même effet qu'une sécrétion d'effets pro-inflammatoires. Nous avons donc choisi un modèle de souris dépourvues de STAT6, une protéine nécessaire à la transmission des signaux anti-inflammatoires d'IL-4 et IL-13. Ces deux cytokines ont par ailleurs un rôle protecteur au niveau du foie. Pour évaluer les conséquences de la suppression de ce facteur de transmission nous avons comparé le protéome du foie de souris STAT6 KO avec celui de souris contrôle. Les différences d'expression des protéines ont été étudiées par le biais de deux approches

protéomiques complémentaires. La première (gel 2D) a permis de visualiser l'ensemble du protéome et d'identifier puis d'analyser les protéines qui présentaient des modifications ou dont l'expression était différente. La deuxième approche (réactif iTRAQ couplé avec LC-MS/MS) a permis d'analyser tous les peptides du foie et de mettre en évidence les protéines différemment exprimées. Grâce à leur complémentarité ces techniques nous ont permis d'obtenir des résultats bien supérieurs à ce que permet l'une ou l'autre de ces techniques prises individuellement. Afin de valider la confiance des résultats obtenus par protéomique, nous avons confirmé chaque protéine d'intérêt de manière quantitative, soit au niveau de l'ARN messager (Taqman), soit au niveau des protéines (Western Blot).

Cette approche protéomique nous a finalement permis d'identifier un certain nombre de protéines liées au stress cellulaire qui étaient en nette augmentation dans les foies STAT6 KO (GRP78, GLO1). De plus, l'augmentation d'une protéine liée au transport lipidique (FABP1) nous a suggéré un dérèglement du métabolisme des acides gras, dérèglement que nous avons pu mettre en évidence en soumettant nos souris à une alimentation riche en graisse. A la suite de ce régime, le foie des souris STAT6 KO contenait beaucoup plus de dépôts lipidiques (cholestérol, triglycérides) que celui des souris contrôle. Les souris STAT6 KO présentaient également des taux plasmatiques lipidiques très nettement supérieurs. Contrairement à nos suppositions qui stipulaient qu'une suppression de facteurs anti-inflammatoires provoquerait une diminution de la sensibilité à l'insuline, les souris STAT6 KO n'ont pas présenté de résistance à l'insuline mais plutôt une intolérance au glucose. De plus, conscients que cette observation pouvait avoir une implication clinique, nous avons mesuré l'expression de STAT6 dans le foie de patients souffrant d'une stéatose hépatique, similaire à celle observée sur notre modèle de souris KO ainsi que sur un modèle de souris obèses (Ob/Ob). Les niveaux de cette protéine étaient nettement inférieurs à ceux observés chez les patients sains. Cette observation ouvre donc la porte à une nouvelle possibilité de dépister cette maladie de manière précoce et de lier l'incidence de la stéatose hépatique à une prédisposition génétique. Une approche thérapeutique peut finalement être envisagée à l'aide d'un agoniste STAT6 afin de réduire l'incidence des troubles liés à la stéatose hépatique.

## Table of content

Remerciements	i
Résumé de la thèse	iii
Abbreviations	vii
1. Introduction	1
Part A – STAT6 and its potential role in metabolism	1
1.1 Metabolic diseases, related complications and inflammation	3
1.1.1 Diabetes mellitus	3
1.1.1.1 Type 1 diabetes	3
1.1.1.2 Type 2 diabetes	4
1.1.1.3 Diabetes related complications	7
1.2 Inflammation and insulin resistance	10
1.2.1 The inflammatory response	12
1.2.1.1 Innate immune response	12
1.2.1.2 Adaptive immune response	14
1.2.2 Crosstalk between metabolism and inflammation in the adipose tissue and the liver	15
1.2.3 Cytokine signaling, the JAK/STAT pathway	18
1.2.3.1 Cytokines	18
1.2.3.2 Cytokine receptors	19
1.2.3.3 Signal initiation and termination through cytokine receptors	21
1.2.4 Insulin signaling	28
1.2.5 Crosstalk points	29
1.2.6 Oxidative stress	30
1.2.7 IL-4 and IL-13 signaling	32
1.3 Diabetes-related liver damage: the role of IL-4 and IL-13	34
1.4 Bibliography	36
Part B – Proteomic tools	47
1.6 What is proteomics?	49
1.6.1 Gene quantification	49
1.6.2 Protein synthesis and its regulation	51
1.6.3 Correlation between genome and proteome	52
1.6.4 Proteome complexity	53
1.6.5 Ultimate protein tool: mass spectrometry	57
1.6.6 Identification of biomarkers and “therapeutic targets”	63
1.7 Quantitative methods for proteomic studies	66
1.7.1 Densitometric comparison in 2D gel electrophoresis	68
1.7.2 Sample preparation	68
1.7.3 First dimension: Isoelectric focusing (IEF)	68
1.7.4 Second dimension: SDS-PAGE	69
1.7.5 Protein detection	71
1.7.6 Fluorescent dye	72
1.7.7 Radiolabelling of proteins	75
1.7.8 2-DE analysis	75
1.7.9 Post-Translational Modifications	76
1.8 Liquid-based techniques	78
1.8.1 Quantitation based on precursor ions	79

---

1.8.2	Quantitation based on reporter ions	84
1.8.3	Label free quantitation approach	86
1.9	Bibliography	87
2.	Differential proteomic analysis of STAT6 knock-out mice reveals new regulatory function in liver lipid homeostasis	93
2.1	Abbreviations	94
2.2	Abstract	99
2.3	Introduction	96
2.4	Experimental Procedures	97
2.5	Results	103
2.5.1	Comparison of Differentially Expressed Proteins Detected by 2-DE Gel and iTRAQ 2D nLC-MS/MS Analysis	103
2.5.2	Increased Expression of Major Urinary Proteins	108
2.5.3	Expression of Stress-related Proteins in STAT6 Knock-out Mice	110
2.5.4	Increased Lipid Deposition in the Livers of STAT6 Knock-out Mice	113
2.5.5	Changes in the Expression of Glucose Homeostasis Enzymes	117
2.5.6	In silico Promoter Analysis	119
2.6	Discussion	123
2.7	Acknowledgements	133
2.8	References	133
2.9	Supplementary Material	147
3.	STAT6 deficient mice display age-dependent hepatosteatosis and glucose intolerance	159
3.1	Introduction	160
3.2	Experimental Procedures	163
3.3	Results	165
3.3.1	Starving hyperglycemia and hypoinsulinemia in STAT6 KO mice	165
3.3.2	STAT6 KO mice are glucose intolerant	167
3.3.3	Liver lipid storage and mobilization in STAT6 KO mice	169
3.3.4	Histological changes in the liver and the white adipose tissue of STAT6 KO mice	172
3.3.5	Differential protein and gene expression in the liver and white adipose tissue of STAT6 KO mice	174
3.3.6	Insulin signaling in the livers of STAT6 KO mice	179
3.3.7	Expression of STAT6 in liver steatosis	179
3.4	Discussion	181
3.5	Acknowledgements	183
3.6	References	183
4.	Conclusion and perspectives	189

## Abbreviations

1D	one dimension
2-DE	two dimensional electrophoresis
11 $\beta$ -HSD1	11 $\beta$ -Hydroxysteroid Dehydrogenase type 1
Acrp30	adiponectin
AKT	serine threonine kinase
APC	antigen presenting cell
AQUA	absolute quantification
CAP	<i>Cbl</i> -associated protein
CBP	CREB binding protein
cICAT	cleavable isotope-coded affinity tag
CID	collision induced dissociation
CREB	cAMP response element binding protein
CRP	C-reactive protein
Cy	cyanine dye
DTT	dithiothreitol
DIGE	differential gel electrophoresis
EDRN	early detection research network
EGF	epidermal growth factor
emPAL	exponentially modified protein abundance index
ER	endoplasmic reticulum
ESI	electrospray ionization
FAT-1	fatty-acid transporter 1
FFA	free fatty acid
HDL	high density lipoprotein
HPLC	high performance liquid chromatography
ICAT	isotope-coded affinity tag
ICPL	Isotope-Coded Protein Label
IDDM	insulin diabetes mellitus
IEF	isoelectric focusing
IFN	interferon
Ig	immunoglobulin
IGF1	insulin like growth factor 1
IKK $\alpha$	I $\kappa$ B Kinase $\alpha$
IL	interleukin
IL-1 RA	interleukin 1 receptor antagonist
IPG	immobilized pH gradient
IMAC	immobilized metal affinity chromatography
IR	insulin receptor
I/R	ischemia reperfusion
IRS	insulin receptor substrate
ISRE	interferon stimulated response element
iTRAQ	isotope-tagged amine-reactive reagents for relative and absolute quantitation
JAK	janus kinase
JNK	c-Jun N-terminal kinases
KO	knock out
LC-MS/MS	liquid chromatography tandem mass spectrometry
LXR	liver X receptor
MALDI	matrix assisted laser desorption/ionization
MARS	multiple affinity removal system
MCAT	mass-coded abundance tagging
MHC	major histocompatibility complex
MS	mass spectrometry
MudPIT	multidimensional identification technology
MW	molecular weight
NAFLD	non fatty liver disease
NASH	non alcoholic hepatosteatosis

---

NCOA	nuclear coactivator
NEFA	non esterified fatty acid
NFκB	nuclear Factor κB
NIDDM	non insulin diabetes mellitus
NK	natural killer lymphocyte
NKT	natural killer T cell
PAGE	polyacrylamide gel electrophoresis
PAI	protein abundance index
PAMP	pathogen associated molecular pattern
p/CIP	co-integrin protein
pI	isoelectric point
PDK4	pyruvate dehydrogenase kinase 4
PGC	PPARγ coactivator
PI3K	phosphatidylinositol 3
PIAS	protein inhibitor of activated stat
PMF	peptide mass fingerprint
PPAR	peroxisome proliferating-activated receptor
PRR	pathogen recognition receptor
PTM	post-tranlational modification
RBP4	retinol binding protein 4
ROS	reactive oxygen species
SAGE	serial analysis of gene expression
SCID	severe combined immunodeficiency
SDS	sodium dodecyl sulfate
SH2	src homology 2
SHP	SH2 containing protein
SILAC	stable isotope labelling by amino acids in cell culture
SOCS	suppressor of cytokine signalling
SRC	sterol receptor coactivator
STAT	signal transducer and activator of transcription
Tc	cytotoxic T cell
TCR	T cell receptor
T <sub>H</sub> 1	t helper 1 cell
T <sub>H</sub> 2	t helper 2 cell
TLR	toll like receptor
TNF	Tumor Necrosis Factor
TOF	time of flight
Treg	regulatory T cell
TMT	tandem mass tag
TZD	thiazolidinedione
WHO	world health organisation
WT	wild type

# **1. Introduction**

## **Part A**

### **STAT6 and its Potential Role in Metabolism**



---

## 1.1 Metabolic diseases, related complications and inflammation

### 1.1.1 *Diabetes mellitus*

Diabetes mellitus and its complications are one of the leading causes of morbidity and death across the globe, thus being responsible for a substantial proportion of worldwide health care expenditures (1). Recent estimations indicate that 171 million people (2.8% of the population) in the world live with diabetes and the number of affected patients will double by 2030 to reach 366 million (4.4%) (2). One of the most critical factors involved in the regulation of glucose homeostasis and the development of diabetes is insulin. Depending on the implication of this hormone, two major types of diabetes are indexed. Nomenclatures have evolved from juvenile- and adult- onset diabetes to insulin-dependent (IDDM) and non-insulin-dependent diabetes (NIDDM) and finally, according to the current state of knowledge, to type 1 and type 2 diabetes mellitus (DM) (3). Type 1 DM (IDDM), is characterized by a serious impairment of insulin production, while type 2 DM (NIDDM), is characterized by a decrease in peripheral insulin efficiency, along with decreased pancreatic insulin production (4).

#### 1.1.1.1 *Type 1 diabetes*

Type 1 diabetes accounts for approximately 5-10% of all cases of diabetes (5). It is characterized by an incapacity of pancreatic islet  $\beta$ -cells to produce insulin leading to a state of insulin deficiency (5). Originally, its prevalence was considered to be mainly age dependent, most of the patients being children or young adults, hence its historical name of “juvenile diabetes”. However, recent data suggest that only 50-60% of all the patients are younger than 16-18 years (5). Type 1 diabetes has a strong genetic component and the main etiology seems to be an autoimmune response against insulin producing cells, triggered by different, currently not yet fully uncovered environmental factors (3, 5). Exposure to one or more of these triggers, *e.g.* viruses (enteroviruses, congenital rubella), toxins (nitrosamines) or food (milk protein, gluten) is a major accelerating factor in the evolution of the disease leading to the destruction of the insulin producing  $\beta$ -cell (5).

Therefore, type 1 diabetes requires exogenous insulin intake to adjust blood glucose to a physiological level. Without this external supply, type 1 diabetes is fatal. Opposite to type 2 diabetes, patients affected by this disease are not obese, but rather suffer of weight loss (5).

#### *1.1.1.2 Type 2 diabetes*

According to the WHO, type 2 diabetes accounts for around 90% of all diabetes cases worldwide (6). Type 2 diabetes is a heterogeneous, polygenic disease. It is characterized by the combination of a resistance to insulin's action in peripheral tissues and a defect in pancreatic islet  $\beta$ -cell insulin secretion. Patients suffering from type 2 diabetes develop insulin resistance years before the clinical appearance of insulin deficiency (7). This delay is due to the capacity of the  $\beta$ -cells to increase insulin release sufficiently to overcome the gradually developing insulin resistance (8). This compensatory mechanism can delay the onset of overt hyperglycemia leading to belated diagnosis when complications have already arisen. Therefore, early diagnosis and the identification of predisposing risk factors are of primary importance.

To date, several risk factors have been identified to be linked to the development of type 2 diabetes, classified as non-modifiable and modifiable (9). The non-modifiable risk factors include genetic factors, age and gender, or previous gestational diabetes. Although genetic factors contributing to the onset of type 2 diabetes are still elusive, difference between ethnic groups implies a significant genetic contribution (10). Contrary to the non modifiable risk factors, the modifiable risk factors can be reduced by the patient's goodwill to lose weight, increase physical activity and improve nutrition. Type 2 diabetes leads to a variety of associated complications resulting from the onset of simultaneous dysfunctions in several organs. The organs most frequently affected are the cardiovascular system, the kidney and the eye. These complications are due to the presence of a long term increase in blood glucose level, accompanied by disturbances in other serum metabolites, most notably the metabolites of lipid homeostasis. The cause of this homeostatic imbalance is a malfunction of the complex regulatory network relating the pancreas, liver, muscle, fat and brain. This accurately regulated network is

responsible for keeping serum glucose levels within physiological boundaries at all time in order to maintain proper organ functioning. Serum glucose levels are determined by the net balance between the inflow from intestinal glucose absorption and hepatic glucose production, and the outflow due to peripheral glucose uptake. The precise coordination of these processes secures the maintenance of physiological glucose levels after food consumption or during periods of fasting. A simplified overview of the regulatory mechanisms is provided in *Figure 1*.

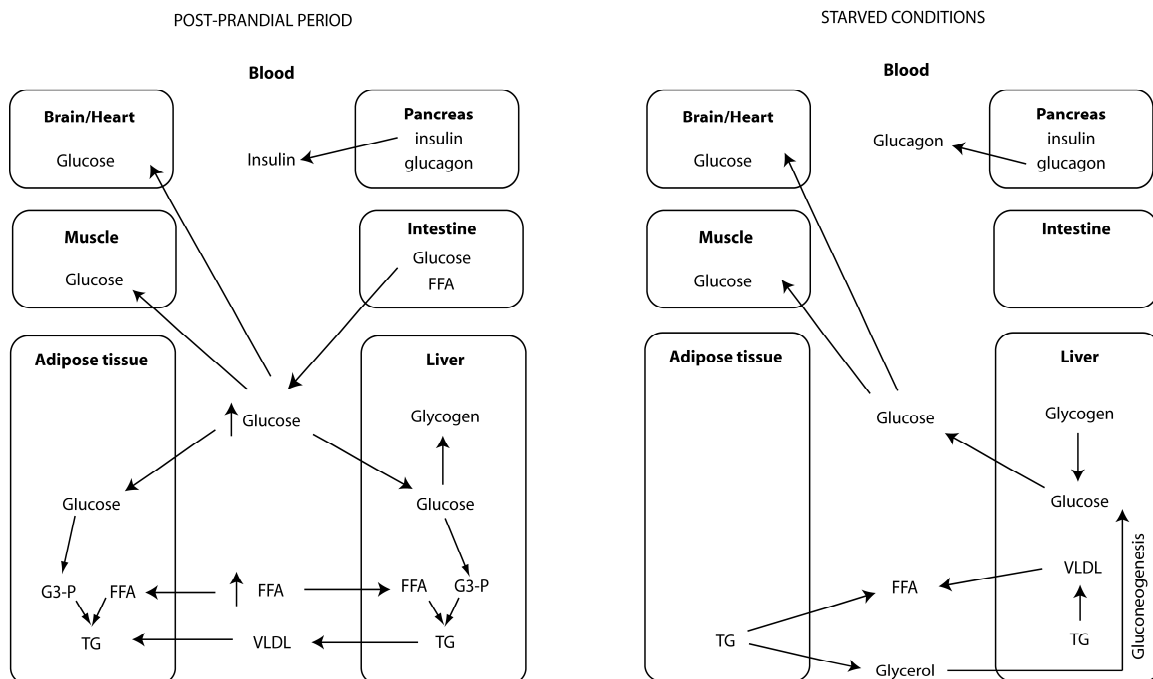


**Figure 1:** Glucose and free fatty acid (FFA) metabolism under fed (left) and starved (right) conditions. The liver stocks energy as glycogen and the adipose tissue as triglycerides (TG). Glucose is metabolized into glycerol 3 phosphate (G3-P) which can produce triglyceride when associated with free fatty acid.

After food intake, during the post-prandial period, the rise in blood glucose levels rapidly stimulates insulin and inhibits glucagon secretion in pancreatic  $\beta$ - and  $\alpha$ - cells. The increased insulin/glucagon ratio leads to a concerted action in different organs to facilitate cellular glucose uptake and storage in the form of glycogen in the liver and muscle, or in the form of triglycerides (TG) in adipocytes (*Figure 1*) (11). By contrast, during fasting, the lowering in blood glucose level triggers liver glycogen degradation

---

and glucose production incorporating glycerol derived from degradation of triglycerides in the adipose tissue. These mechanisms ensure the buildup of stocks in nutrition-rich conditions and usage of these stocks to provide the necessary energy-supply for vital organs e.g. the brain and heart for their proper functioning in periods of starving.

The core mechanism of the deregulation of the above described system is a vicious circle resulting from repeated dietary excesses finally exhausting  $\beta$ -cell insulin secretion capacity, thus leading to permanently elevated glucose and non esterified / free fatty acid (NEFA/FFA) levels. The development of this process and the role of peripheral organs are depicted in *Figure 2*. Impaired insulin action in the hypothalamus leads to increased food intake, despite the presence of already developed obesity, provoking the onset of insulin resistance (8, 12). Decreased insulin action in liver leads to uncontrolled glucose production, raising glucose levels in the circulation. This rise in blood glucose level is further aggravated by an impaired glucose uptake in muscle. The increased lipolysis in adipose tissue results in the release of non esterified fatty acids (NEFAs) in the circulation, accelerating the development of peripheral insulin resistance in the muscle and liver. In addition, NEFAs exert a deleterious effect on  $\beta$ -cell function thus initiating a vicious circle.

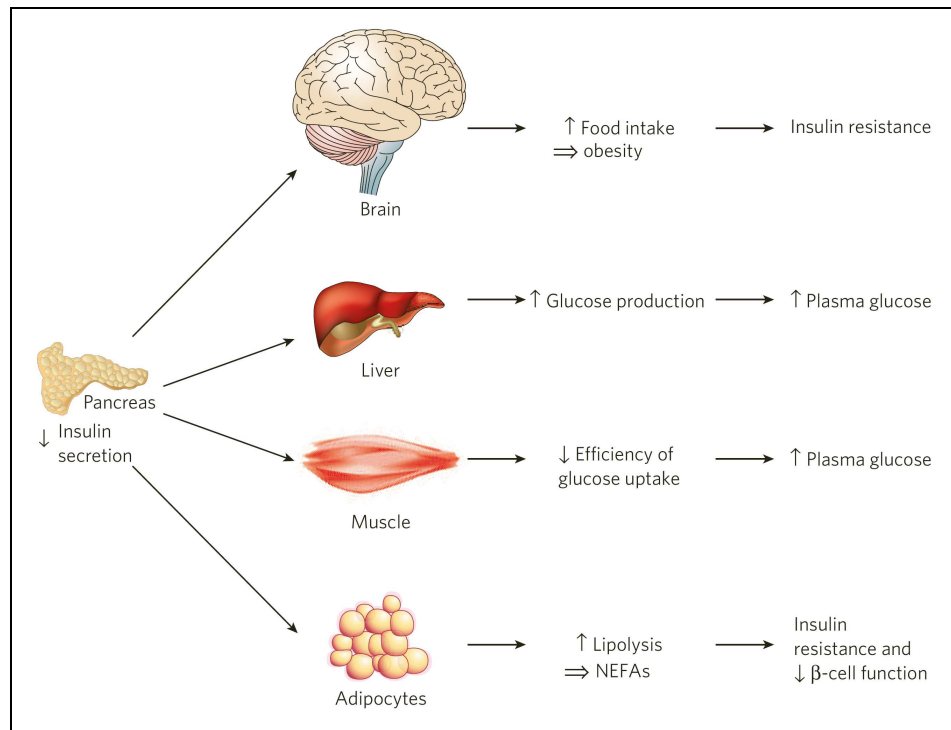


**Figure 2:** Model of development of type 2 diabetes described by Kahn (et al.) (8).

### 1.1.1.3 Diabetes related complications

The persistence of insulin resistance, hyperglycemia and elevated FFA levels leads to multiple complications of serious consequences. Thus, understanding the metabolic and signaling pathways provoking the onset of these complications is an important healthcare objective (12). Notably, these metabolic alterations damage the vasculature resulting in a variety of micro- and macrovascular disorders. The microvascular damages provoke nephropathy, retinopathy, neuropathy and cardiovascular disorders. Diabetic nephropathy is the major cause of renal transplantation and a leading cause of dialysis need, while diabetic retinopathy is the most common cause of acquired blindness (5). Neuropathy can cause either generalized dysfunction (cardiac or erectile) or peripheral dysfunctions inducing skin ulceration and gangrene. These symptoms are usually accompanied by macrovascular complications *e.g.* ischemic heart disease, stroke and peripheral vascular disease. Macrovascular complications are of

extreme importance as cardiovascular diseases are responsible for about 70% of all deaths among the people living with type 2 diabetes. Moreover, diabetes is the major cause for limb amputation (13).

Obesity and type 2 diabetes has also negative effects on liver function. A major liver disease related to type 2 diabetes is the development of non alcoholic fatty liver disease (NAFLD) characterized by liver lipid accumulation. This lipid accumulation can provoke the onset of inflammation leading to nonalcoholic steatohepatitis (NASH) and further in time to cirrhosis in a small percentage of affected individuals. In cirrhosis liver tissue is replaced by fibrotic tissue, leading to a loss of liver function (*Figure 3*) (14). This step might be the starting point for the development of hepatocellular carcinoma (HCC).

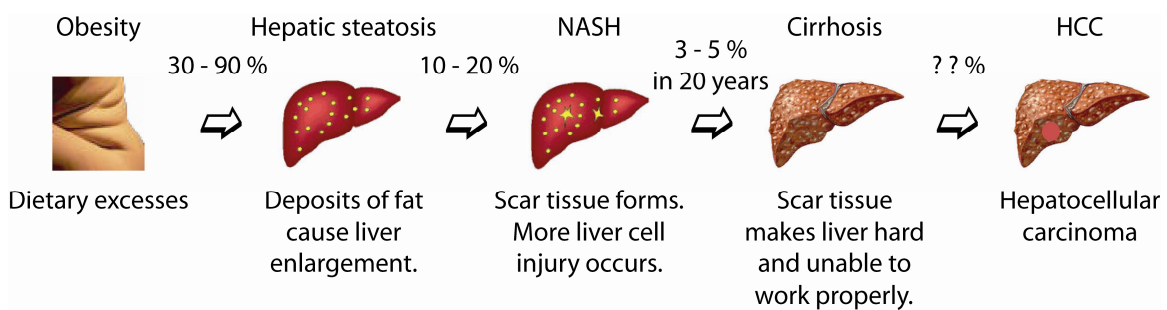


**Figure 3:** Model of the stages of non alcoholic fatty liver disease (NAFLD). Disease evolves from hepatic steatosis characterized by lipid accumulation, to inflammatory nonalcoholic steatohepatitis (NASH), cirrhosis and finally hepatocellular carcinoma (HCC).

Incidence of diabetes-related complication has been demonstrated to be reduced by 25% after tight control of glycemia (15). Control of blood glucose levels can be achieved by using different approaches including exercise, weight loss and pharmacological treatment. There is an ample choice of agents available to treat type 2 diabetes.

Type 2 diabetes often requires insulin supplementation to obtain adequate glycemic control in combination with an oral hypoglycemic agent. Different oral hypoglycemic agents target different organs and metabolic processes. These mechanisms include the reduction of glucose intestinal absorption, the increase of  $\beta$ -cell insulin production, or the improvement of peripheral fat and liver insulin sensitivity. For example,  $\alpha$ -glucosidase inhibitors diminish glucose absorption from the gastro-intestinal tracts by inhibiting a carbohydrate metabolizing enzyme on the intestine mucosa, reducing therefore glucose epithelial transportation. The most frequent prescribed therapeutic agent, the biguanids (*e.g.* metformin), reduces glucose production in the liver by inhibiting gluconeogenesis and promoting peripheral glucose utilization by increasing glucose transporter translocation in muscle and liver (16, 17). The second most frequently prescribed class, the sulfonylureas (*e.g.* tolbutamid) acts on multiple targets. This type of compound stimulates insulin secretion through an activation of insulin exocytosis in the pancreatic  $\beta$ -cell by blocking ATP dependent potassium channels (18). Sulfonylureas also directly lower glucose level by increasing its storage in the form of glycogen in the liver and lower circulating free fatty acid levels by reducing lipolysis in the adipose tissue. A good example for multiple actions is the thiazolidinediones (TZDs) (*e.g.* rosiglitazone). TZDs improve insulin sensitivity through the activation of the peroxisome proliferating-activated receptor  $\gamma$  (PPAR $\gamma$ ). Due to the main localization of this receptor in the adipose tissue this class acts by altering the expressions of certain adipose genes *e.g.* fatty-acid transporter 1 (FAT-1), *Cbl*-associated protein (CAP) or 11  $\beta$ -Hydroxysteroid Dehydrogenase type 1 (11  $\beta$ -HSD1). These alterations will result in a decrease in the level of circulating free fatty acid (FFAs) and thus will improve insulin sensitivity in muscle and liver (*Figure 4*) (19). In addition, PPAR $\gamma$  agonists possess an indirect effect by suppressing the expression of circulating insulin resistance factors (*e.g.* the pro-inflammatory cytokines such as Tumor Necrosis Factor  $\alpha$  (TNF $\alpha$ ), and resistin) and enhancing the expression of insulin sensitizing factors (*e.g.* adiponectin (Acrp30)).

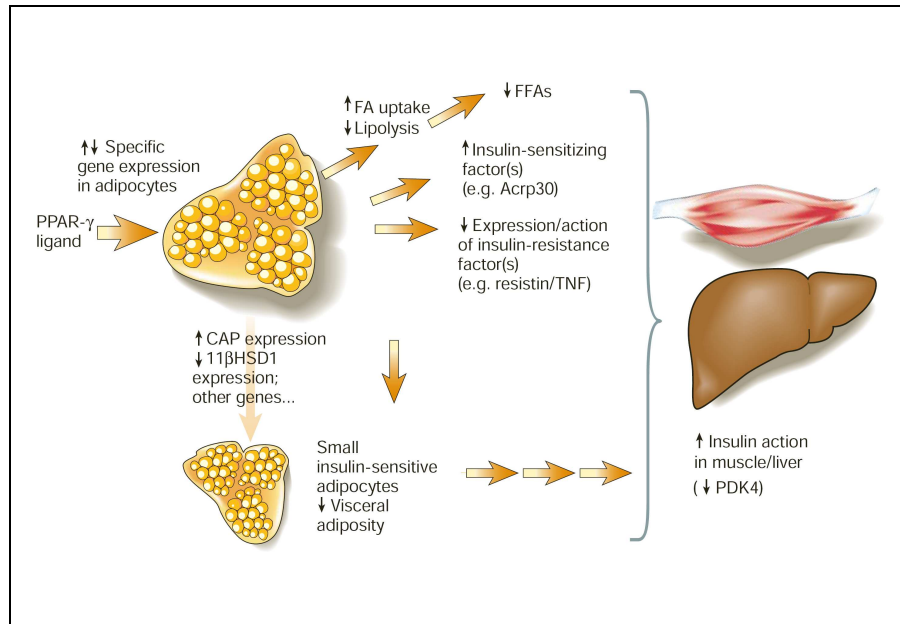


**Figure 4:** Potential mechanisms of insulin sensitization by peroxisome proliferating-activated receptor  $\gamma$  (PPAR $\gamma$ ) ligands from D. Moller (19).

## 1.2 Inflammation and insulin resistance

Metabolic and immune systems are the two major systems ensuring survival. The first one by regulating nutrition and energy availability, and the second one by protecting from infections (20). In fact, many hormones, cytokines, signaling proteins, transcription factors and lipid derivatives can function in both signaling systems providing logical connecting “crosstalk” points between them (20).

Adipose tissue and liver are the main examples where linkage between immune and metabolic systems exists. These tissues possess a particular structural organization where immunological cells are highly represented. For example, in case of liver, two-third of the total cell population is represented by the hepatocytes but the remaining cells are immune population. This heterogeneous population contains multiple cell types residing within the hepatic sinusoid, including Kupffer cells (the macrophages of the liver), B and T lymphocytes, natural killer (NK) lymphocytes and dendritic cells. These

cells are of crucial importance in the recognition of pathogens but also contribute to the inflammatory process that evolves with liver damage as a result of the onset of diabetes (21). *Figure 5* shows configuration of principal metabolic (adipocytes and hepatocytes) and immune cells (macrophages, granulocytes, lymphocytes and dendritic cells) in adipose tissue and in liver. This spatial conformation close allows interaction between metabolic and immune cells and supplies these cells a rapid access to blood vessels for cytokine release which provides a molecular mean of communication between inflammatory cells residing in different organs (22). In order to appreciate the contribution of inflammatory processes to the development of metabolic disorders, it is important to provide a short overview of the immune system and the inflammatory response.

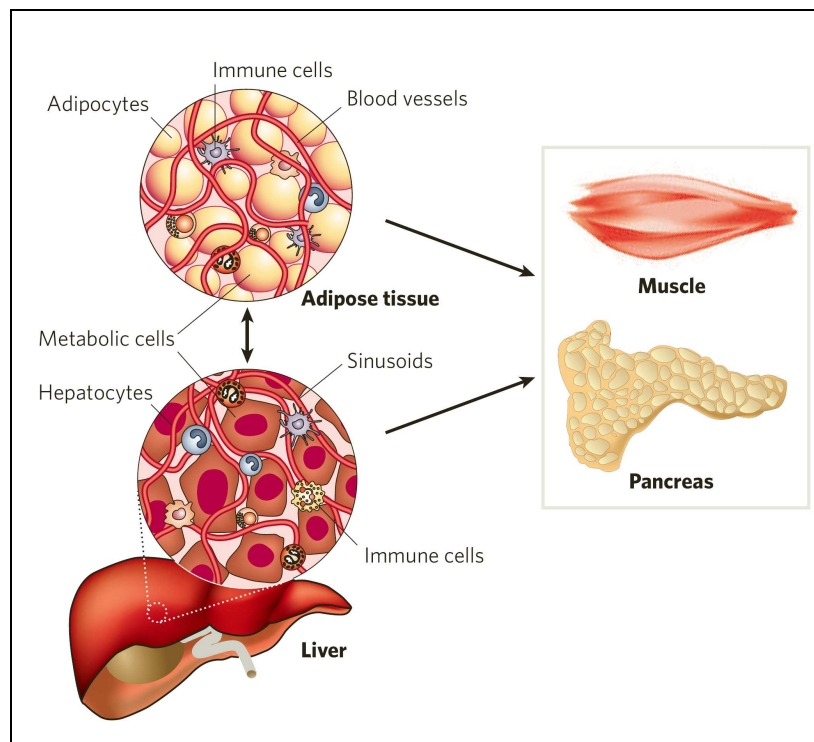


**Figure 5:** Configuration of principal metabolic (adipocytes and hepatocytes) and immune (macrophages, granulocytes, lymphocytes and dendritic cells) cells in liver and adipose tissue from Hotamisligil (22).

---

### ***1.2.1 The inflammatory response***

The immune system provides a non-specific/innate and specific/acquired immune response against foreign invading agents.

#### ***1.2.1.1 Innate immune response***

Innate immunity provides the first immediate, but non specific response against external threat, thus it plays a crucial role in the recognition of “self” from “non self”. It is the starting point of an inflammatory response leading to an activation of a complex network consisting of various immune cell types. These recognition mechanisms involve complement’s proteins for the recognition of bacterias, NK lymphocytes for the recognition of viruses and eosinophil granulocytes for the recognition of parasites. The system is activated when Toll Like Receptors (TLRs), expressed on Antigen Presenting Cells (APCs) (macrophages and dendritic cells) recognize Pathogen-Associated Molecular Patterns (PAMPs), which are present on the surface of the invading micro-organism. This activation leads to the production of different inflammatory mediators, termed chemokines with distinct functions. Interleukin 6 (IL-6) and IL-8 recruit leukocytes, TNF $\alpha$  and IL-1 activate tissue permeabilization, while TNF $\alpha$  also activates APCs. Release of TNF $\alpha$  by phagocytes (macrophages and dendritic cells) is required to increase vascular permeability and vasodilatation promoting leukocytes recruitment. Vascular permeabilization, vasodilatation and recruitment of leukocytes are crucial to attract innate cells at the infectious place leading to the state of acute inflammation. Within a few days, this first immune response is followed by a second adaptive response providing much more specific defense on a long term basis. This second response cannot be activated without the first innate immune response (*Figure 6*).

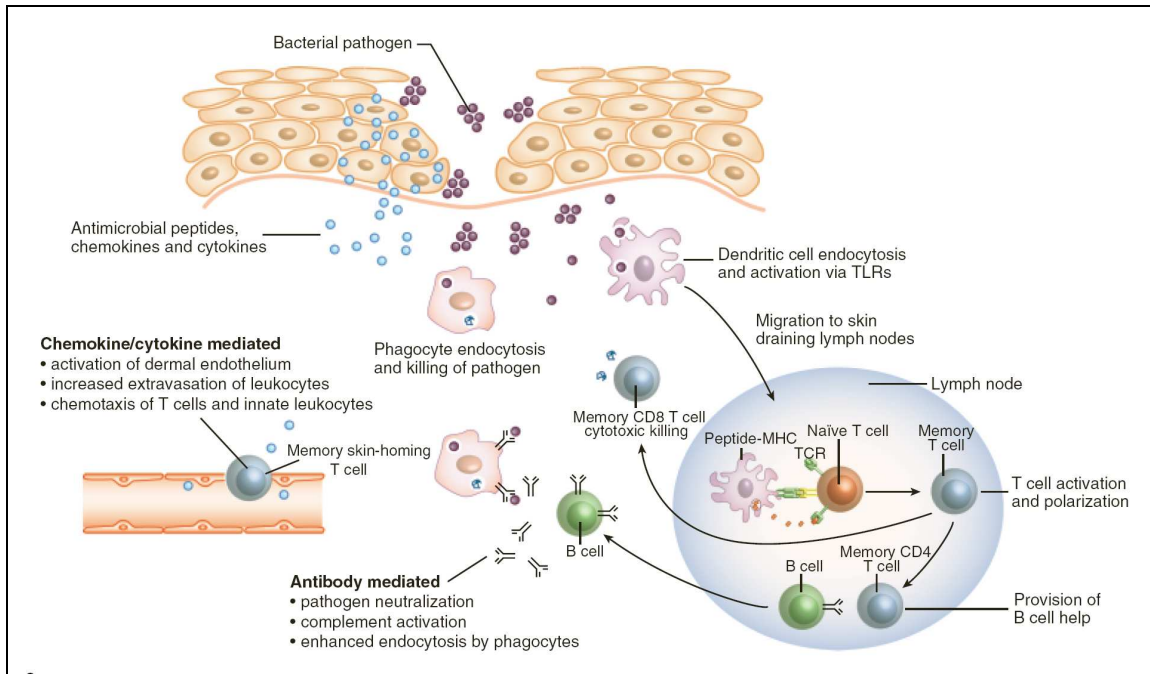


**Figure 6:** Interaction between innate and adaptive immunity in response to bacterial infection of the skin from Clark (*et al.*) (23).

Interconnection between immune and metabolic pathways is reinforced by several examples. As mentioned before, inflammation is accompanied by increased levels of  $\text{TNF}\alpha$  and  $\text{IL-6}$ . Elevated  $\text{TNF}\alpha$  and  $\text{IL-6}$  levels are characteristic of obesity and are linked to tissue lipid accumulation.  $\text{TNF}\alpha$  and  $\text{IL-6}$  may be released by adipocytes, leading to a state of subacute inflammation and insulin resistance in the adipose tissue. Another example is the Toll Like Receptor 4 (TLR4). TLR4 is the receptor for bacterial wall lipopolysaccharide (LPS) thus plays an important role in pathogen recognition by triggering a primary inflammatory reaction. This receptor may also be activated by free fatty acid in adipocytes and macrophages, inducing an inflammatory response in these cells (24). Thus, TLR provides a crucial crosstalk point between the metabolic and inflammatory pathways in circumstances like obesity, when circulating free fatty acids levels are high. The physiopathological relevance of TLR4 was recently demonstrated by Shi (*et al.*) by showing that TLR4 deficient mice are protected against high fat diet induced insulin resistance (24). These two pathways,  $\text{TNF}\alpha$  overexpression or overgrowth in intestinal bacteria causes NAFLD in liver. By blocking  $\text{TNF}\alpha$  effects with

antibodies or decontaminating intestine, NAFLD damages are reduced (25). Finally, it is known that key molecules in the mediation of inflammation are eicosanoids (leukotrienes, prostaglandins). Interestingly, all these molecules derive from the same precursor, a fatty acid called arachidonic acid (26, 27). These examples demonstrate that crosstalk between immune and metabolic responses are of crucial importance.

### ***1.2.1.2 Adaptive immune response***

The second type of inflammatory reaction is the adaptive/humoral immunity. As mentioned before, it takes place a few days after the first encounter with the antigen and provides a long term, specific response to a given agent. The activation of this reaction is initiated by the dendritic cells, which are important players of the first/innate response as well. Dendritic cells are capable of stimulating a special population of T lymphocytes: the naïve T helper cells. These cells are termed “naïve” as they have not yet encountered antigen. After stimulation by dendritic cells, naïve T helper cells differentiate into  $T_{H1}$ ,  $T_{H2}$  or T regulatory (Treg) cells. The decision for naïve T cell to become either T helper 1 ( $T_{H1}$ ) or T helper 2 ( $T_{H2}$ ) is made during the direct contact to a dendritic cell through the T Cell Receptor (TCR) and a co-signal: CD28. A viral exposition to dendritic cell elicits  $T_{H1}$ , whereas a parasitic exposition elicits  $T_{H2}$  response (23).  $T_{H1}$  cell maturation is initiated by IL-12 while IL-4, produced by mast cells, basophils, granulocytes and other differentiated  $T_{H2}$  lymphocytes, initiates maturation of  $T_{H2}$  cells.  $T_{H1}$  cell typically produce interferon  $\gamma$  ( $IFN\gamma$ ), activate macrophages and stimulate cytotoxic T cells ( $T_C$ ).  $T_{H1}$  response is also called cellular mediated immunity. By contrast, mature  $T_{H2}$  cells produce IL-4, IL-5 and IL-13 and elicit B lymphocyte antibody production (humoral immunity).  $T_{H2}$  maturation process seems to occur mostly via STAT6, a specific transcription factor termed Signal Transducer and Activator of Transcription (28-32). The function of the third type of cells, the regulatory T cells (Treg), is modulating the activation of other T cells (*Figure 7*).

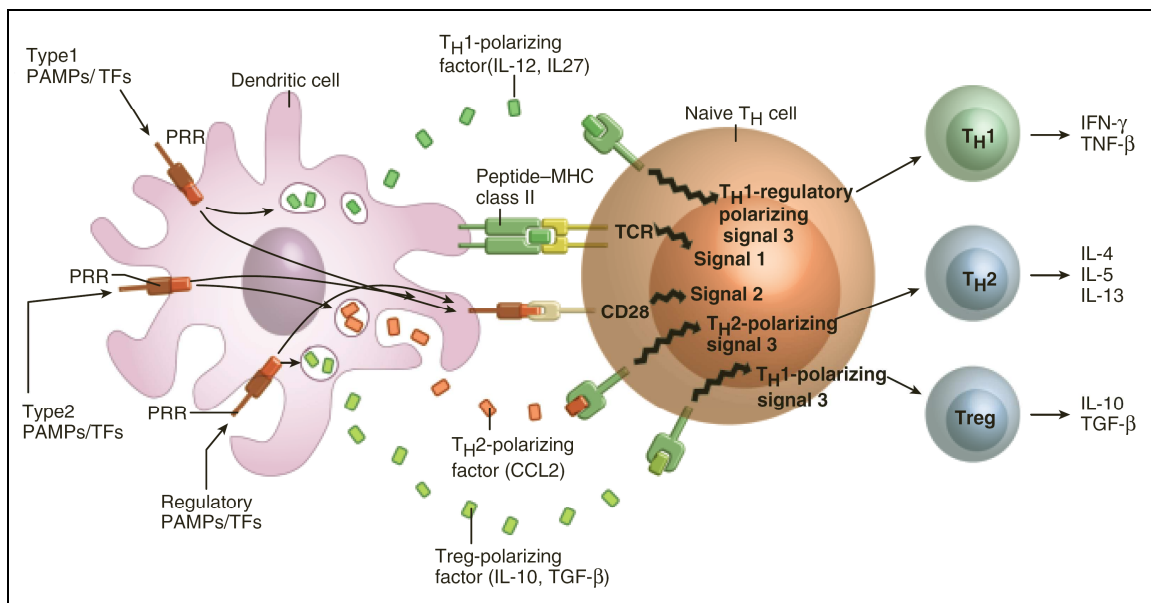


**Figure 7:** *T* helper cell differentiation after dendritic cell stimulation, adapted from Clark (et al.) (23).

### 1.2.2 Crosstalk between metabolism and inflammation in the adipose tissue and the liver

As shown before immune and metabolic cells form an intertwining network in the adipose tissue and the liver. Adipose tissue contain adipocytes, the most abundant cell, but also pre-adipocytes (not yet loaded with lipids), endothelial cells (barrier between circulation and metabolic cells), fibroblasts (required to maintain structure), leukocytes and macrophages (33). Adipocytes, beside their role of lipid storage cells, possess the ability to produce certain pro- and anti-inflammatory cytokines termed adipokines providing again a link between adipose tissue and inflammation (33). The pro-inflammatory cytokines such as  $\text{TNF}\alpha$ , IL-6, IL-1 mediate inflammatory reactions but they also play a direct role in metabolic processes by modulating different signaling steps of the insulin receptor, and exerting a hyperglycemic effect (33). By contrast inhibiting pro-inflammatory effects of IL-1 with IL-1 receptor antagonist (IL-1RA), has a counteractive effect in insulin resistance and diabetes (34). Similarly, adiponectin plays an anti-inflammatory role by inhibiting the production of  $\text{TNF}\alpha$  and  $\text{IFN}\gamma$  and promoting production of IL-10 and the IL-1 Ra in monocytes and macrophages, and has an anti-

hyperglycemic effect by increasing insulin sensitivity (33, 35). Taken together, these examples suggest a pro-hyperglycemic effect for inflammatory signals and an anti-hyperglycemic effect for anti-inflammatory signals.

The pathway leading from adipose tissue expansion to the development of systemic insulin resistance is depicted in (*Figure 8*). The connection between the elevated levels of inflammatory cytokines and the development of insulin resistance allows to use TNF $\alpha$ , IL-6 and C-reactive protein (CRP) serum levels as markers to predict the development of type 2 diabetes mellitus and cardiovascular diseases (33, 36).

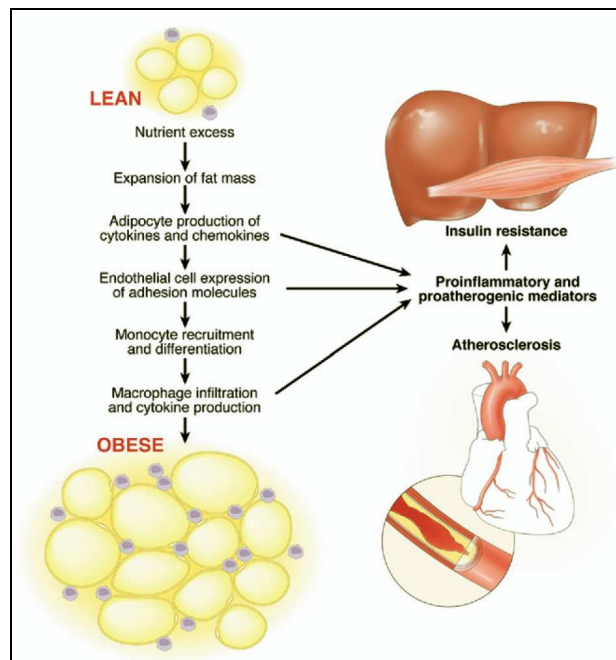


**Figure 8:** Potential mechanism for obesity induced inflammation from Shoelson (*et al.*) (21).

Another diabetic complication related to inflammation is the non alcoholic fatty liver disease (NAFLD). NAFLD is usually accompanied by the elevation of inflammatory mediators and activation of inflammatory signaling pathways in liver. This state of subacute inflammatory response in the liver is similar to the one seen with the accumulation of lipid in the adipocytes (37). Moreover, proinflammatory cytokines produced by the adipocytes (TNF $\alpha$ , IL-6) are carried to the liver through the portal

circulation and contribute actively to the hepatic inflammation. These proinflammatory signal as well as the free fatty acids (FFAs) derived from the adipose tissue or released by hepatocytes upon the activation of transcription factor termed Nuclear Factor  $\kappa$  B (NF $\kappa$ B) will lead to the activation of a specific type of hepatic macrophages, termed Kupffer cells (*Figure 9*) (37). This specific hepatic type of cells accounts for over 5% of total cells mass (37). This inflammation will be amplified by the participation of the other resident immune cells: the T and B lymphocytes, NK cells and dendritic cells. These damages lead generally to nonalcoholic hepatostatitis (NASH) with presence activated hepatic stellate cells provoking fibrosis which can proceed to cirrhosis and hepatocellular carcinoma (38).

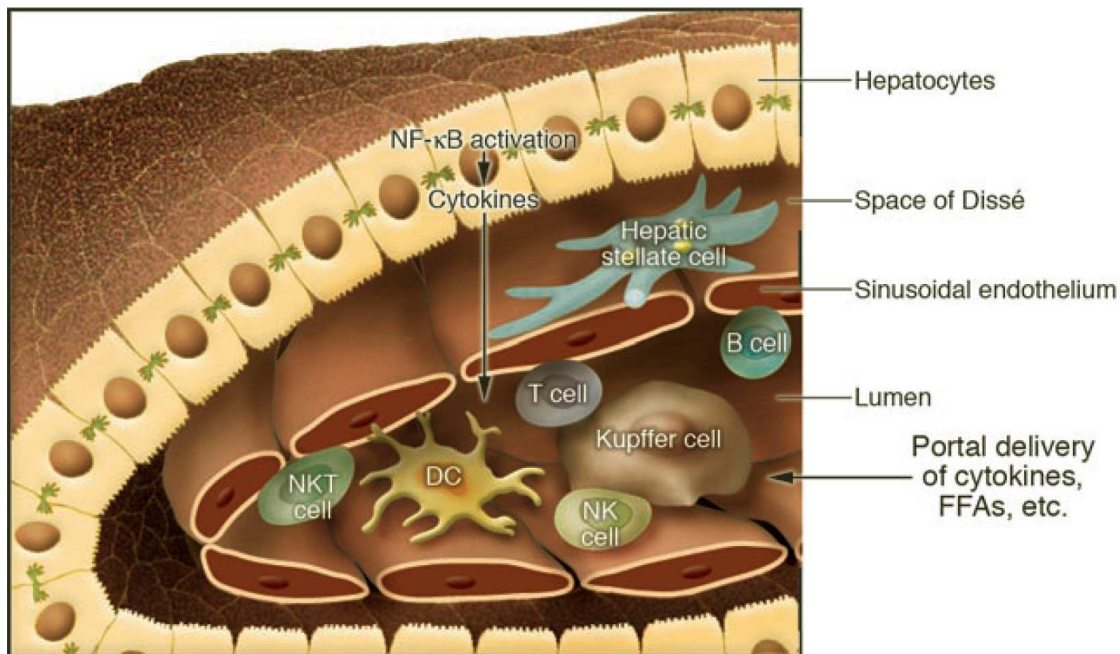


**Figure 9:** Potential mechanisms for adiposity-induced inflammation in the liver from Shoelson *et al.* (37).

### ***1.2.3 Cytokine signaling, the JAK/STAT pathway***

As discussed before, elevated glucose and FFA levels trigger gluco- and lipotoxicity, resulting in cellular oxidative stress and the upregulation of inflammatory cytokines, most importantly in liver and in the adipose tissue (37). The major signaling pathways activated by cytokines is the Janus kinase/ Signal Transducer and Activator of Transcription (Jak/STAT) signal transduction system (39). This system consists of a complex cascade of protein phosphorylation which is able to transmit signal inside the cell and initiate transcription from a broad range of genes. Almost forty different cytokines and several hormones act through Jak/STAT pathway activating a large variety of receptors. The cytokines include IL-1 to IL-12, interferon (IFN) and leptin, while the hormones using this network are growth hormone and prolactin. Taken together, due to the contribution of cytokines in the immune system, Jak/STAT pathway is of crucial importance in the innate and adaptive immune response.

#### ***1.2.3.1 Cytokines***

Cytokine have first been classified into type 1 (T<sub>H</sub>1-like) and type 2 (T<sub>H</sub>2-like) according to the type of T cell that has produced them. This nomenclature has been, later, extended to all cell types producing cytokines (40, 41). In general, type 1 cytokines promote the development of a strong cellular immune response (IL-2, IL-12, IFN  $\gamma$ , TNF  $\beta$ ), whereas type 2 cytokines promote a strong humoral immune response (IL-4, IL-5, IL-6, IL-10, IL-13) (*Table 1*) (41). This complex response is achieved by the same cytokine eliciting a cell type specific response due to a particular combination of the Jak/STAT pathway.

**Table 1:** The nomenclature and functions of well-defined T-cell cytokines, adapted from C. Janeway (*et. Al.*) (42).

Cytokine	T-cell source	Effect on			
		B cells	T cells	Macrophages	Hematopoietic cells
Interleukin 2 (IL-2)	naïve T cell, T <sub>H</sub> 1, T <sub>C</sub>	Growth	Growth	-	Stimulates NK growth
Interferon $\gamma$ (IFN $\gamma$ )	T <sub>H</sub> 1, T <sub>C</sub>	Differentiation	Inhibits TH2 cell growth	Activation, production of MHC	Activates NK cells
Interleukin 4 (IL-4)	T <sub>H</sub> 2	Activation, growth	Growth	Activation	Increase growth of mast cells
Interleukin 5 (IL-5)	T <sub>H</sub> 2	Differentiation	-	Inhibits macrophage activation	Increase eosinophil growth and differentiation
Interleukin 10 (IL-10)	T <sub>H</sub> 2	Production of MHC	Inhibits cytokine release	Inhibits cytokine release	Increase growth of mast cells
Interleukin 3 (IL-3)	T <sub>H</sub> 1, T <sub>H</sub> 2, T <sub>C</sub>	-	-	-	Growth factor
Tumor Necrosis Factor $\alpha$ (TNF $\alpha$ )	T <sub>H</sub> 1, T <sub>H</sub> 2, T <sub>C</sub>	-	-	Activation	-

### 1.2.3.2 Cytokine receptors

Once released in the media, cytokines can act on neighboring or more distant cells and bind a family of receptors called cytokine receptors (43). The interaction between the cytokine and this specific receptor is required to transmit the message inside the cell and to initiate a response. Cytokine receptors are present on many different immune and non immune cell types including T and B cells and macrophages, as well as hematopoietic, endothelial, epithelial, and muscle cells, fibroblast and hepatocytes. Cytokine receptors are composed of two subunits, which, upon activation, associate and form dimers. These receptors are divided into two types: type 1 and type 2 (*Table 2*) (44). Type I receptors are composed of either heterodimers, which are formed after association of the cytokine receptor chain with a choice of three different common chains ( $\gamma$  chain,  $\beta$  chain or gp130) or homodimers, which are formed after association of two cytokine receptor chains. Depending on the subunit association of homo- or hetero-dimers, these receptors bind different cytokines. The  $\gamma$  chain is associated with IL-2, IL-4, IL-7, IL-9, and IL-15 receptor chains, the  $\beta$  chain is associated with IL-3 and IL-5 receptor chain, while gp130

forms hetero-dimer with IL-6 and IL-11 receptor chains. IL-12 and leptin receptors are also related to gp130. Finally, homodimeric receptors bind growths hormone, prolactin, erythropoietin and thrombopoietin (*Table 2*) (45). The group of type II receptors contains the interferon (IFN) and IL-10 receptors.

In general,  $\gamma$  chain receptors mediate growth and maturation of lymphocytes (46, 47).  $\beta$  chain receptors mediate the production of myelomonocytic cells, including myeloid, erythroid and megakaryocytic lineages (48), while gp130 receptors mediate immune, hematopoietic, and thrombopoietic responses (49). Class II cytokine receptors including IFN $\alpha/\beta$  and IFN $\gamma$  receptors are primarily involved in antiviral and inflammatory modulation (50).

**Table 2:** Cytokines and the Jak-STAT signaling pathway, adapted from Leonard (*et al.*) (50).

Type I Cytokines	Jaks	STATs
<i>Cytokines whose receptors share <math>\gamma_c</math></i>		
IL-2, IL-7, IL-9, IL-15	Jak1, Jak3	Stat5a, Stat5b, Stat3
IL-4	Jak1, Jak3	Stat6
IL-13*	Jak1, Jak2, Tyk2	Stat6
<i>Cytokines whose receptors share <math>\beta_c</math></i>		
IL-3, IL-5	Jak2	Stat5a, Stat5b
<i>Cytokines whose receptors share gp130</i>		
IL-6, IL-11	Jak1, Jak2, Tyk2	Stat3
IL-12 <sup>+</sup>	Jak2, Tyk2	Stat4
Leptin <sup>+</sup>		Stat3
<i>Cytokines with homodimeric receptors</i>		
Growth hormone	Jak2	Stat5a, Stat5b, Stat3
Prolactin	Jak2	Stat5a, Stat5b
Erythropoietin	Jak2	Stat5a, Stat5b
Thrombopoietin	Jak2	Stat5a, Stat5b
<u>Type II Cytokines</u>		
<i>Interferons</i>		
IFN $\alpha$ , IFN $\beta$	Jak1, Tyk2	Stat1, Stat2
IFN $\gamma$	Jak1, Jak2	Stat1
IL-10 <sup>‡</sup>	Jak1, Tyk2	Stat3

\*IL-13 does not share  $\gamma_c$  but uses IL-4R $\alpha$ .

<sup>+</sup>IL-12 and leptin do not share gp130, but their receptors are related to gp130.

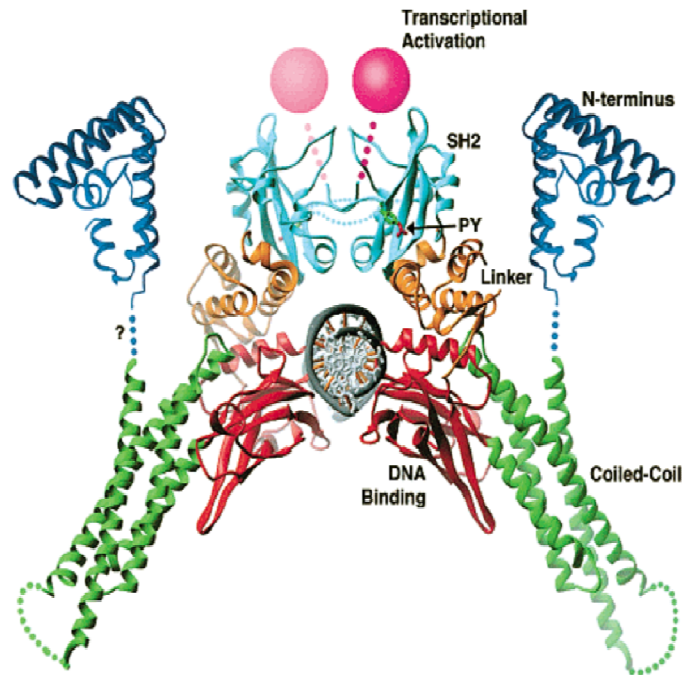
<sup>‡</sup>IL-10 is not an interferon, but its receptor is a type II cytokine receptor.

### ***1.2.3.3 Signal initiation and termination through cytokine receptors***

As mentioned before, cytokines bind to their receptor subunit, allowing dimerization with other subunits, depending on the type of cytokine and this association will activate a signal transduction cascade of protein phosphorylation. However, as the cytokine receptor family lacks intrinsic tyrosine kinase activity, cytokine receptors cannot activate their own tyrosine phosphorylation required for the phosphorylation cascade (51). To bypass this issue, Jak protein tyrosine kinases, are constitutively associated with the cytosolic part of the receptor chain, promoting tyrosine phosphorylation upon receptor ligand binding (52). Jaks are therefore essential to propagate the cytokine signaling cascade (53). Moreover, this Jaks-STAT system can transduce signal with a combinations of four Jak (Jak1, Jak2, Jak3 and Tyk2) and seven STAT (STAT1, STAT2, STAT3, STAT4, STAT5a, STAT5b and STAT6) proteins. This rich number of combination suggests commonality across the Jak-STAT signaling system thus signal and cell-specificity will depend on the Jak/STAT combination (39, 45, 50, 54). To be able to integrate signal from different physiological responses, a single cell expresses multiple cytokine receptors at its surface. Receptors required for hemopoietic cell development and proliferation use Jak2, while common  $\gamma$ -chain receptors, essential for the development and maintenance of lymphocytes, use Jak1 and Jak3, whereas other receptors use only Jak1 (39, 55). Receptors using Jak3, Tyk2, or a combination of Jak2/Tyk2 and Jak3 have not been described. In human, Tyk2 seem to be activated by a broad range of cytokines involved in innate and acquired immunity (56). As seen previously, STATs are mainly activated by Jaks due to a lack of intrinsic catalytic domain in the cytokine receptors. However, STATs may also be directly phosphorylated through receptor tyrosine kinases by growth factors like epidermal growth factor (EGF), platelet-derived growth factor (PDGF) and insulin (57).

STAT proteins possess the same general structure which is conserved through the seven family members. They are approximately 750 to 800 amino acids in lengths with the exception of STAT2 and STAT6, which contain approximately 850 amino acids (50). In order to function properly, every STAT protein is composed of four distinct domains (*Figure 10*).

A.



B.



**Figure 10:** Dimerized structure (A.) and domains (B.) of STAT proteins from Horvath (58).

These domains include from N-terminal to C-terminal, a DNA binding domain (DNA) which is required for the recognition of the DNA binding site. The SH2 domain (SH2) is required for receptor recruitment and for homodimerization. The carboxy terminus domain, called transactivation domain (TAD) is required to initiate and increase rate of gene transcription through recruiting other transcriptional factors. Finally, a tyrosine residue (Y) is required for STAT phosphorylation leading to the activation of the protein. The coiled-coil (C-C) and linker (Link) domains are important for the structural organization of the protein but have no direct effect on activation or physiological function.

The classical Jak/STAT signaling pathway is demonstrated in *Figure 11* using the IL-4/IL-13 receptor as models. IL-4 and IL-13 are two major anti-inflammatory cytokines, mediating signal Jak/STAT pathway through STAT6. Moreover, IL-13 possesses many of the same effects than IL-4. IL-4 is produced by T<sub>H</sub>2 cells, basophils, mast cells and eosinophils. Once secreted, this cytokine can activate IL-4 receptor chain located on various cell types, including T and B cells, hematopoietic, endothelial, epithelial, muscle, fibroblast, hepatocyte and brain tissues (59, 60). IL-4 plays a critical role in the differentiation of naïve T cells and class switching in B cell antibody production. IL-13 is mainly secreted by T<sub>H</sub>2 cells and its receptor is present on B cells, basophils, eosinophils, mast cells, endothelial cells, fibroblasts, monocytes, macrophages, respiratory epithelial cells and smooth muscle cells (61). IL-13 can inhibit pro-inflammatory cytokine production in monocytes and macrophages (62, 63).

Once activated IL-4 receptor (IL-4R) needs to be heterodimerized with the gamma common chain, also involved in IL-2 signaling in order to activate the Jak-STAT cascade. IL-13 can bind IL-4 R $\alpha$  and recruit  $\gamma$  chain as well, but can also activate a complex between IL-4 R $\alpha$  receptor and IL-13 receptor chain (IL-13 R $\alpha$ ). Finally IL-13 binds IL-13 R $\alpha$  with low affinity but when paired with IL-4R it binds IL-13 with high affinity (61). The specificity resides in the presence or absence of IL-13 receptor on the targeted cell.

Receptor activation initiates its dimerization, which brings into proximity two Jak proteins, constitutively associated with the cytosolic part of the receptor (39, 50, 64). This proximity allows Jak activation, which results in a trans-phosphorylation of the receptor cytosolic chain (65). The resulting phosphorylation will conduct to the recruitment of latent cytosolic STAT by creating docking site for the Src homology 2 (SH2) domain of the STATs. SH2 domain, first described in the activity of retroviral oncoprotein v-FPS is now attributed to a large family of molecular-interaction domains that organize the localization, communication and activities of proteins (66-68). SH2 domain of different STATs differ sufficiently to recognize different receptor phosphorylated motifs, which increases STAT specificity (50). Once recruited to the receptor, STAT monomer, associated with the tyrosine phosphorylated receptor, will be

in turn phosphorylated by Jak. This STAT phosphorylation will allow homo- or hetero-dimerization through reciprocal phosphotyrosine SH2 domain interaction. Once activated by tyrosine phosphorylation, STAT protein can dimerize and migrate to the nucleus, where they activate transcription of targeted genes.

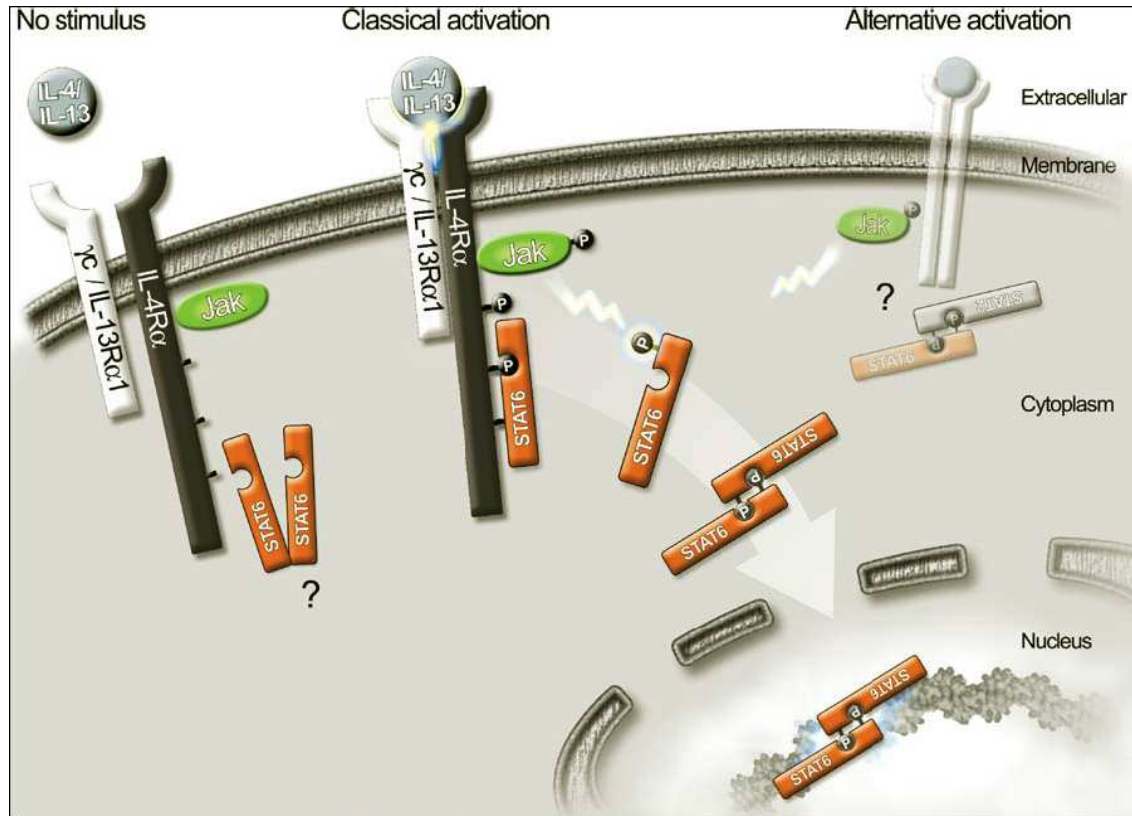


**Figure 11:** The IL-4/IL-13 Jak-STAT signaling pathway from Hebenstreit (et al.) (69).

Once induced STAT DNA binding activity can be detected in the nucleus within minutes of cytokine binding (50). The preferred binding sites for STAT transcription factors consist of the palindromic TTC(N3)GAA or TTC TTC(N4)GAA motifs, although some variation exists even in the TTC/GAA sequence (50, 69). STAT proteins bind to the DNA too far from RNA polymerase II to initiate transcription. This distance requires contact with other proteins to facilitate the activation of the transcription. For this reason, STAT6 interacts with a wide variety of other transcription factors and serves as a recruitment platform for different members of the transcriptional machinery (70-74).

The coactivators mainly interact through the C-terminal transactivation domain and contribute to the specificity of the transcriptional activation despite of high similar DNA binding sequences (69). Two important factors involved in the initiation of transcription by STAT6 are p300/CBP, the binding protein for cAMP response element Binding protein (CREB) and p100. CBP is required to relax chromatin near transcription sites and serves a bridging factor to the previously described transcription machinery. Two other factors are important for the initiation of the transcription: the co-integrating protein (p/CIP) or nuclear receptor co-activator-3 (NCoA-3) and Steroid Receptor Co-activator 1 (SRC-1) or NCoA-1 (72, 75). *Figure 12* depicts the interaction between these co-activators in the initiation of transcription by STAT6. Recently, Goenka (*et al.*) have identified a new co-factor called CoaSt6 (collaborator of STAT6), a poly(ADP-ribose)polymerase, which associates with STAT6 and enhances its transcriptional activity by chromatin decondensation (76).

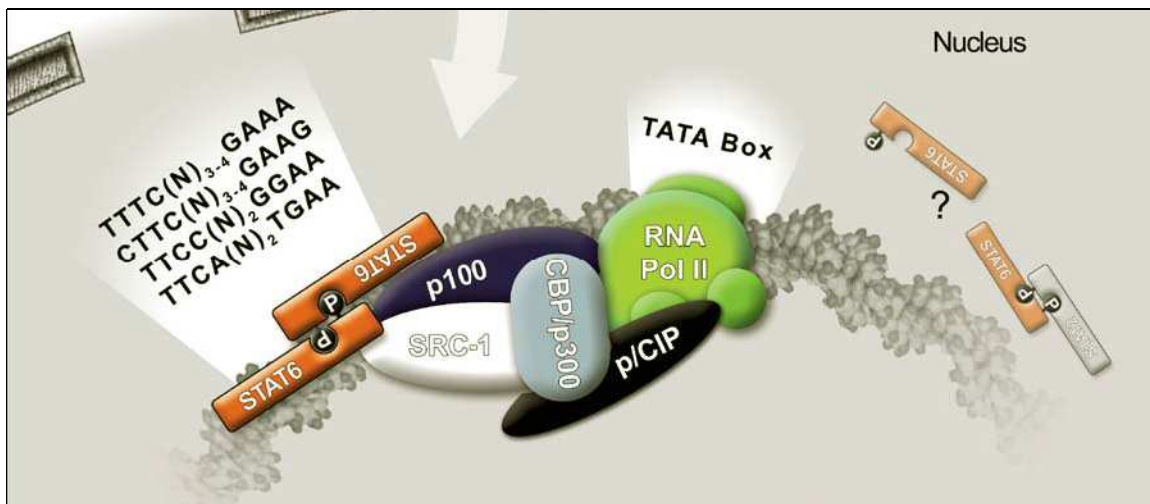


**Figure 12:** Coactivators involved in STAT6 activation of transcription process from Hebenstreit (69).

Finally, different STAT6 isoforms have been identified. STAT6a is identical to STAT6 with shorter mRNA untranslated region, whereas STAT6b displays the same biological functions with a shorter amino-terminal region and finally, STAT6c acts as a dominant-negative isoform due to deletion of SH2 domain (69).

Signal termination is achieved by activating a negative regulatory system. STATs become inactive by dephosphorylation and monomerization. The negative regulatory proteins activated by STATs are Suppressor of Cytokine Signaling (SOCS), SH2 containing Protein tyrosine phosphatase (SHP) and Protein Inhibitors of Activated Stats (PIAS). SOCS acts in a negative feedback to suppress further signaling. Under this inactive configuration it migrates back to the cytosol (77). SOCS can also target Jak to help proteasomes degradation and block STATs recruitment to the receptor. Moreover, SHP dephosphorylates STAT in the nucleus while PIAS target STATs in the nucleus to be degraded in the proteasomes.

This complex system shows crosstalk between other signaling pathways. For example, the receptor IL-4, once phosphorylated by Jak can recruit and activate STAT6, but also the Insulin Receptor Substrate 1 and 2 (IRS-1/2). This activation is due to the fact, that a part of this receptor is highly homologous to the insulin and insulin growth factor 1 (IGF-1) receptors which activate the IRS-1/2 signaling pathway (78). Indeed, STAT6 and IRS-2 have been shown to interact and promoting both IL-4 induced proliferative and differentiating responses and IRS-2 was downregulated STAT6 knock out T<sub>H</sub>1 cells suggesting a complex interaction between these two IL-4 induced mediators (79). This common pathway between STAT6 and IRS-1/2 suggest a likely crosstalk point between IL-4/IL-13 and insulin mediated signaling.

Other examples for the crosstalk between the JAK/STAT mediated and the metabolic pathway includes studies showing that insulin can stimulate STAT3 phosphorylation (80). Indeed, STAT3 has been recently shown to regulate hepatic gluconeogenic gene expression and ameliorate glucose intolerance in diabetic rodents. In addition, IL-6, an anti-inflammatory cytokine, protects against the development of fatty liver by activating STAT3 and regulate the expression of various glucose and lipid homeostasis genes (81).

In spite of the structural homology and the high similarity of the target DNA binding sequence, analysis of the different STAT knock-out mice revealed a different role for each of these proteins (39). All four Jaks and seven STATs family members have

been deleted in mice, in addition to the creation of conditional knock-out mice, when losses were lethal (*Stat3*, combined deficiency of *Stat5a* and *Stat5b*) (39). The phenotypes of the mice deficient for different Jak and STAT proteins are described in *Table 3*.

**Table 3:** Phenotypes of mice deficient in various Jaks and STATs adapted from Leonard (*et al.*) (50).

<u>Jaks</u>	
Jak1:	Severe Combined Immunodeficiency similar to X-linked SCID
Jak2:	Embryonic lethal owing to a defect of erythropoiesis
Jak3:	Severe Combined Immunodeficiency similar to X-linked SCID
Tyk2:	Susceptible to parasite infections
<u>STATS</u>	
Stat1:	Defective signaling in response to type I and type II IFNs
Stat2:	Susceptible to viral infections
Stat3:	Fetal lethal. Implantation occurs, but fetal growth is blunted
Stat4:	Defective Th1 development, consistent with the role of IL-12 in activating Stat4 and promoting Th1 development
Stat5a:	Defective lobuloalveolar development in the breast
Stat5b:	Required for sexual dimorphism of body growth rates, similar to Laron-type dwarfism, a human disease due to growth hormone resistance. Defective GM-CSF signaling in bone marrow-derived macrophages. Defective IL-2-induced IL-2R $\alpha$ expression in splenic T cells
Stat6:	Defective Th2 development, consistent with the role of IL-4 for Stat6 and Th2 development

Jak1 deficient mice present severe defect in lymphopoiesis and show perinatal lethality (82). Deletion of Jak2 is lethal due to incomplete erythropoiesis. Jak3 deficient mice display Severe Combined Immunodeficiency (SCID), similar to human X-linked SCID (83-87). This human genetic disorder is characterized by a deficiency of common X chain leading to a T and B cell deficiency. Finally, contrary to other Jaks, where inactivation leads to a complete loss of the respective cytokine receptor signal, Tyk2 deficient mice expose reduced responses to IFN $\alpha/\beta$  and IL-12, and are prone to parasite infections (88).

STAT1 deficiency in mice leads to a lack of innate immunity toward viral disease and severe defects in IFN immune response (89, 90). However, these mice keep the

ability to respond to other cytokines, and have no major abnormality in development (64). STAT2 deficient mice display increased vulnerability to viral infection (91). STAT3 deficiency leads to embryonic lethality. However, selective disruption of STAT3 in T cell and macrophages revealed the vital role of STAT3 in response to IL-2, IL-6 and IL-10 (64). Liver specific STAT3 knock out mice have been generated and display impaired cell proliferation (92). STAT4 knock-out mice present impaired activation by IL-12 in T<sub>H</sub>1 cell development (93, 94). STAT5 has two distinctive isoforms: STAT5a and STAT5b. These isoforms share more than 90% amino acid homology (95). Both isoforms have been deleted in mice in addition to a double deletion. Stat5a deficient mice show a loss of prolactin signaling with impaired mammary development during pregnancy (96). In addition, STAT5b deficient mice possess a defect in growth hormone signaling with loss of sexual growth (97). Moreover, STAT5a/b double deficient mice contain no NK lymphocytes. Finally, STAT6 deficient mice show a defect in T<sub>H</sub>2 cell differentiation resulting in defective IgE class switch (31, 98, 99). Taken together these data give evidence that STAT, proteins play a crucial role in modulating pro- and anti-inflammatory responses. Finally, we should note that deletion of STAT proteins is less damaging than Jaks', except in the case of STAT3. This difference is due to the multiplicity of roles of Jaks compared to STATs. Most of the Jaks are activated by many different cytokines, by contrast STAT activation is much more stimulospecific.

#### ***1.2.4 Insulin signaling***

To better understand the relationship between insulin and cytokine receptor signaling, a closer look at the signaling network of insulin is required as well. Insulin receptor (IR), once activated, gets autophosphorylated by its intrinsic tyrosine kinase activity. The phosphorylated tyrosines provide docking sites for several downstream signaling molecules. Two different pathways can be activated by insulin, the metabolic pathway (glucose, lipid and protein metabolism), and the mitogenic pathway (cell growth and protein and DNA synthesis). Depending on the pathway, different molecules are recruited to the cytosolic part of the receptor. Insulin receptor substrate 1-4 (IRS 1-4) proteins are main IR partners in the transmission of both pathways. Once phosphorylated, these proteins are recruited to the receptor. This phosphorylation will activate

phosphatidylinositol 3 (PI3) kinase and the serine/treonine kinase (AKT) in the case of metabolic pathway, while Ras and extracellular regulated kinase (ERK) are activated in case of mitogenic pathway. One of the major points of crosstalk, the signaling between cytokine and insulin implies IRS proteins (*Figure 13*).

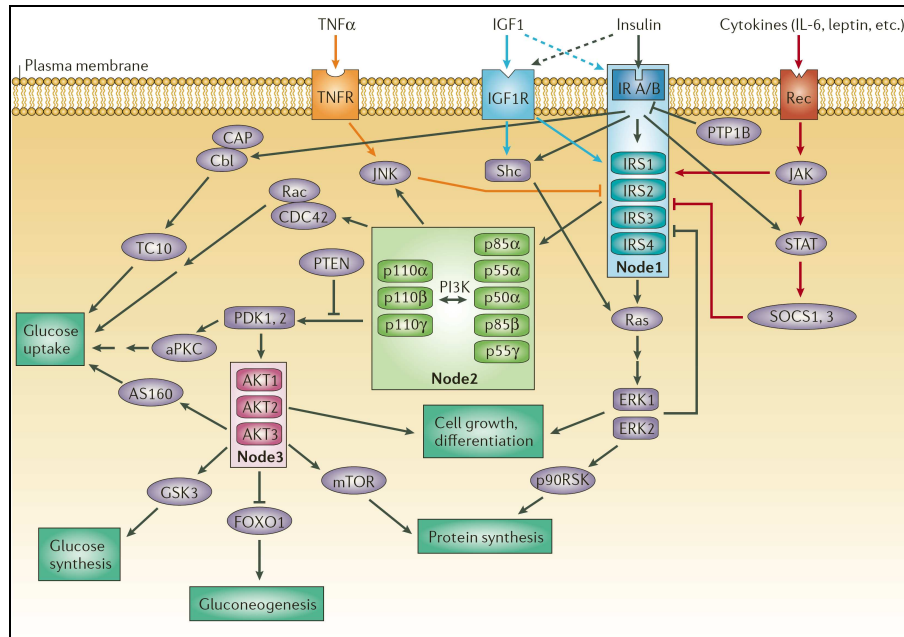


**Figure 13:** Mechanism insulin action and crosstalk between insulin, TNF and cytokine signaling from Taniguchi (*et al.*) (100).

### 1.2.5 Crosstalk points

IRS proteins provide one of the major sites of interaction with inflammatory activators. For example, IRS proteins can be activated by IL-4 and leptin through tyrosine phosphorylation by Janus Kinases (Jaks) (50, 101). By contrast, TNF $\alpha$  can inhibit IRS signal transmission through serine phosphorylation of IRS1 by c-Jun N-terminal kinases (JNK). The JNK pathway provides a crosstalk mechanism also for the endoplasmic reticulum (ER) stress. One of the negative regulators of the cytokine receptor pathway is Suppressor of Cytokine Signaling (SOCS). Activation of this protein due to sustained cytokine effects will lead to the inactivation of IRS proteins (*Figure 14*). A summary of metabolic (FFA) and cytokine induced insulin resistance is provided in *Figure 15*.

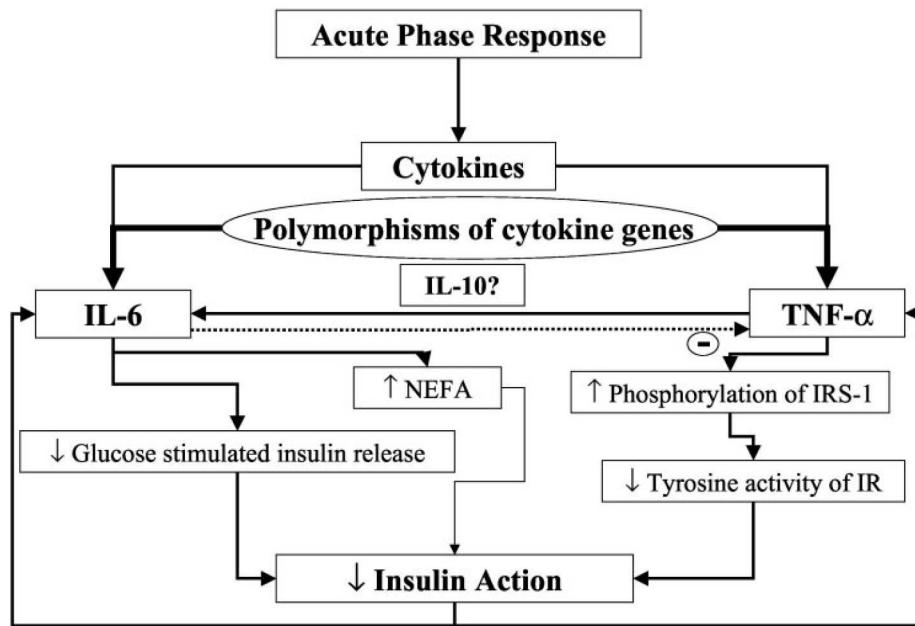


**Figure 14:** Mechanism insulin action and crosstalk between insulin, TNF and cytokine signaling from Fernandez-Real (et al.) (102).

### 1.2.6 Oxidative stress

In addition to crosstalk at the pathway level, interaction between transcription factors mediating inflammation and insulin action exists. Intracellular stress such as ER stress or excess reactive oxygen species (ROS) production by mitochondria can also activate the same pathways (20). For example typical inflammation signaling pathways, like the JNK and Nuclear Factor  $\kappa$ B (NF $\kappa$ B), and I $\kappa$ B Kinase  $\alpha$  (IKK $\alpha$ ) are activated in response to these factors. These mediators can also be activated by fatty acids leading to the inhibition of insulin action (Figure 17).

Lipids can also activate the transcription factors PPAR and liver X receptors (LXR) and promote lipid transport and metabolism. These transcription factors are also involved in inflammatory reactions. A balance between these two processes (inflammation and lipid metabolism) must be found for optimizing cell functions (103).

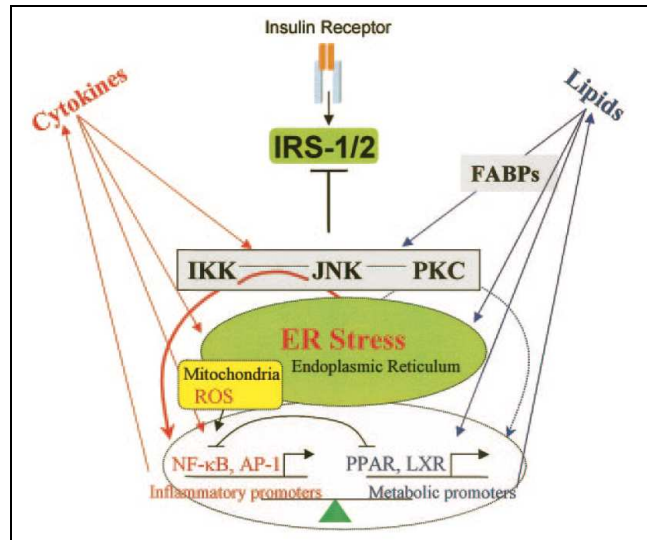


**Figure 15:** Molecular pathways integrating stress and inflammatory responses with insulin action from G. Hotamisligil (103).

The summary of the molecular mechanisms of glucose, free fatty acid, cytokine and ROS mediated liver damage is summarized in *Figure 16*.

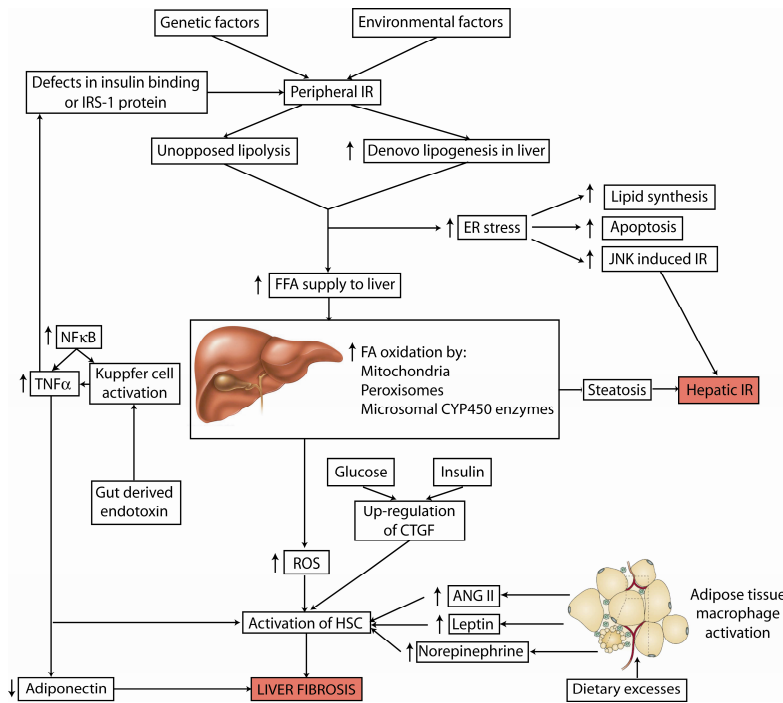


**Figure 16:** Increased inflammation leads to a peripheral insulin resistance.

---

### ***1.2.7 IL-4 and IL-13 signaling***

Both IL-4 and IL-13 can mediate signal transduction by STAT6 activation. For that reason IL-4 and IL-13 share many functional properties and induce many of the same responses as IL-4 among airway hypersensitivity, mucus hypersecretion, inflammatory bowel disease and parasitic nematode expulsion (104-110).

Depending on the cell type, STAT6 activates distinctive types of response. 35 different STAT6 targeted genes have been identified, many of which are associated with  $T_H2$  process (69). Depending on the cell type, every known Jak, including Jak1, Jak2, Jak3 and Tyk2, has been shown to be activated preceding STAT6 phosphorylation (69). Accordingly, IL-13 IL-4 can also increase expression of class II MHC in B cells and upregulate the expression of the IL-4 receptor (111, 112). Finally IL-4 plays an important role in cell adhesion by inducing expression of vascular cell adhesion molecule-1 (VCAM-1) and down-regulating the expression of E-selectin (113, 114). These process are required to favorite the recruitment of T cells and eosinophils, rather than granulocytes, into a peripheral site of inflammation (115). Table 4 gives an exhaustive list of the promoters containing the STAT6 consensus binding sequence. Except E-selectin and CD40, all of the listed proteins are positively regulated by STAT6 (69). Another immune aspect of STAT6 is the infiltration of  $T_H2$  cells and eosinophils into sites of allergic inflammation (69).

**Table 4:** STAT6 binding motif containing protein adapted from Hebenstreit (69).

Locus	Year	Reference	GenBank accession no	Species
Immunoglobulin/class switch				
AID	2004	(116)	NM_020661, NM_009645	Human, mouse
Germline $\gamma$ 1	1993	(117)	D78345, M12389	Human, mouse
Germline $\gamma$ 3	1999	(118)	D78345	Human
Germline $\gamma$ 4	2002	(119)	X56796	Human
Germline $\epsilon$	1993	(117, 120)	K01318, U17387	Human, mouse
Cytokines				
FIZZ1	2003	(121)	NM_020509	Mouse
IL-4	1997	(122, 123)	NM_021283, NM_000589	Mouse, human
sIL-1ra	1996	(124)	NM_031167	Mouse
Lymphotoxin a	1998	(125)	NM_000595	Human
Chemokines				
Eotaxin-1/CCL11	1999	(126)	NM_002986	Human
Eotaxin-3/CCL26	2001	(127)	NM_006072	Human
TARC	2005	(128)	NM_002987	Human
Ym1	2002	(129)	NM_009892	Mouse
Adhesion molecules				
$\beta$ (3) Integrin	2001	(130)	NM_016780	Mouse
E-selectin	1997	(114)	NM_000450	Human
P-selectin	1999	(131)	BC068533	Human
Enzymes				
12/15-Lipoxygenase	2000	(132)	NM_001140	Human
3 $\beta$ -Hydroxysteroid dehydrogenase/isomerase type 1	1999	(133)	AF252254	Human
Arginase I	2004	(134)	NM_007482	Mouse
Receptors				
CD23	1993	(117, 120)	NM_002002, NM_013517	Human, mouse
CD40	2000	(135)	NM_001250	Human
$\delta$ -Opioid receptor	2004	(136)	NM_013622	Mouse
IL-13R $\alpha$ 2	2003	(137)	NM_000640	Human
IL-4R $\alpha$	1996	(138)	NM_001008699	Human
MHC-II	1988	(139)	NM_008206	Mouse
$\mu$ -Opioid receptor	2001	(140)	NM_001008504	Human
Polymeric Ig receptor	2000	(141)	NM_002644	Human
Intracellular signaling				
Bcl-x <sub>L</sub>	2001	(142)	NM_009743	Mouse
SOCS-1	2003	(143)	NM_003745	Human
Miscellaneous				
Angiotensinogen	1998	(144)	NM_134432	Rat
$\alpha$ 1(I) procollagen	2004	(145)	NM_000088	Human
$\alpha$ 2(I) procollagen	2004	(145)	AF004877	Human
$\beta$ -Casein	1997	(146)	NM_017120	Rat
RAD50 locus control region	2004	(147)	NM_009012	Mouse
Trefoil factor-3	2004	(148)	BC017859	Human

### 1.3 Diabetes-related liver damage: the role of IL-4 and IL-13

The implication of the anti-inflammatory signaling through IL-4, IL-13 and STAT6 in metabolic disease has never been reported. Different studies have evaluated the implication of IL-4 or IL-13 in the incidence of liver disease and these cytokines seems to have a deleterious effect on liver T cell mediated hepatotoxicity. For example a study showed that IL-4 and deficient mice was protected from Concanavalin A induced hepatitis and IL-13 knock-out mice were protected from acetaminophen overload (149). Finally overexpression of IL-4 has been recently reported to promote hepatocyte apoptosis. These examples suggest a deleterious effect of IL-4 and IL-13 in certain liver function. Similarly, by suppressing STAT6 anti-inflammatory effect, Lentsch (*et al.*) observed an augmentation of pro-inflammatory cytokines production leading to leukocytes accumulation and significant hepato-cellular injury (150). By contrast, STAT6 is protective against ischemia/reperfusion induced injury which leads to cellular damage by inducing fluctuations in oxygen, nutrition and energy availability (151-153). These disorders are also a characteristic feature of metabolic disturbances, most notably glucose intolerance and insulin resistance. The relationship between hypoxia, metabolism and liver injury is highlighted by studies demonstrating that intermittent hypoxia induces alterations in lipid homeostasis and predisposes to liver injury (151-153). Notably, STAT6 is not only expressed in immune related cells but also in different other cell types, raising the possibility of a broader physiological significance from previously supposed. Indeed, STAT6 has been shown to be involved in adipocyte differentiation, kidney epithelial cell mechanosensation, regulation of apoptosis in human hepatoma cells as well as inflammatory reaction in lung epithelial cells (154-156). Therefore, STAT6-deficient mice, in addition to impaired immune functionality display severe and multiple disorders (157).

In addition to its protective role in ischemia/reperfusion, STAT6 has been shown to be involved in atherosclerosis. Indeed, STAT6 KO mice develop more severe aortic wall lipid accumulation upon high fat diet feeding and, in humans, it was identified as one of the three up-regulated genes in atherosclerotic coronary plaques (158, 159).

Recently, STAT6 was reported to play a role in fatty acid oxidation in macrophages. This protein modulates lipid metabolism and cellular proliferation in alternatively activated macrophages (156, 160). STAT6 is intimately involved in this process, contributing to the switch between glycolytic and lipolytic metabolism. Interestingly, STAT6 provide a counterbalance to the transcription factor Hypoxia Induced Factor  $\alpha$  (HIF $\alpha$ ) allowing resulting in an increase in lipolytic activity and allowing wound healing (*Figure 17*).

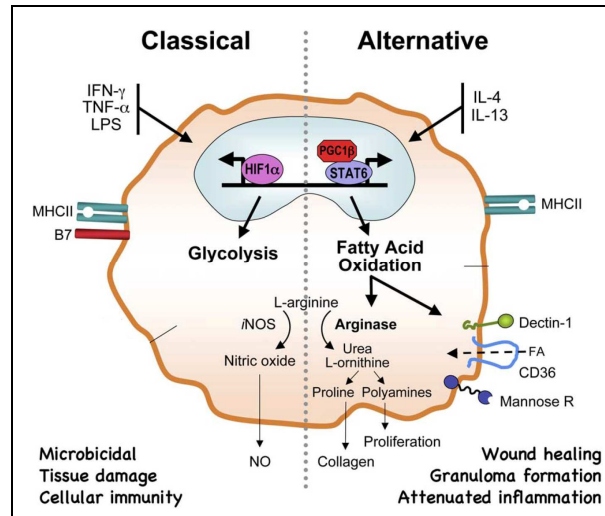


**Figure 17:** STAT6 activation can lead to fatty acid oxidation in the macrophage from Lacy-Hulbert (*et al.*) (161).

Hepatocyte are master regulators of glucose and lipid metabolism and are known to express STAT6 (154). Despite of the growing evidence of the involvement of STAT6 in non-immune cell function the role of STAT6 has never been evaluated in the context of the development of metabolic diseases and their related complications. To explore this potential new function, the liver proteomes of wild type and STAT6 knock-out mice were compared using two different quantitative techniques, namely 2D-PAGE gel electrophoresis and a combination of 2D nanoscale LC-MS/MS with iTRAQ labeling technique. These techniques will be reviewed in the next chapter.

## 1.4 Bibliography

1. King H, Rewers M. (1993) Global estimates for prevalence of diabetes mellitus and impaired glucose tolerance in adults. WHO Ad Hoc Diabetes Reporting Group. *Diabetes Care* **16**: 157-177.
2. Wild S, Roglic G, Green A, Sicree R, King H. (2004) Global prevalence of diabetes: estimates for the year 2000 and projections for 2030. *Diabetes Care* **27**: 1047-1053.
3. Rother KI. (2007) Diabetes treatment--bridging the divide. *N Engl J Med* **356**: 1499-1501.
4. (1999) Definition, Diagnosis and Classification of Diabetes Mellitus and its Complications. World Health Organization.
5. Daneman D. (2006) Type 1 diabetes. *Lancet* **367**: 847-858.
6. Zimmet P, Alberti KG, Shaw J. (2001) Global and societal implications of the diabetes epidemic. *Nature* **414**: 782-787.
7. McMahon GT, Arky RA. (2007) Inhaled insulin for diabetes mellitus. *N Engl J Med* **356**: 497-502.
8. Kahn SE, Hull RL, Utzschneider KM. (2006) Mechanisms linking obesity to insulin resistance and type 2 diabetes. *Nature* **444**: 840-846.
9. Alberti KG, Zimmet P, Shaw J. (2007) International Diabetes Federation: a consensus on Type 2 diabetes prevention. *Diabet Med* **24**: 451-463.
10. Shai I, Jiang R, Manson JE, et al. (2006) Ethnicity, obesity, and risk of type 2 diabetes in women: a 20-year follow-up study. *Diabetes Care* **29**: 1585-1590.
11. Shepherd PR, Kahn BB. (1999) Glucose transporters and insulin action--implications for insulin resistance and diabetes mellitus. *N Engl J Med* **341**: 248-257.
12. Petersen KF, Shulman GI. (2006) Etiology of insulin resistance. *Am J Med* **119**: S10-16.
13. Olefsky JM. (2001) Prospects for research in diabetes mellitus. *Jama* **285**: 628-632.
14. Tilg H, Hotamisligil GS. (2006) Nonalcoholic fatty liver disease: Cytokine-adipokine interplay and regulation of insulin resistance. *Gastroenterology* **131**: 934-945.
15. Bretzel RG, Voigt K, Schatz H. (1998) The United Kingdom Prospective Diabetes Study (UKPDS) implications for the pharmacotherapy of type 2 diabetes mellitus. *Exp Clin Endocrinol Diabetes* **106**: 369-372.
16. Boccuzzi SJ, Wogen J, Fox J, Sung JC, Shah AB, Kim J. (2001) Utilization of oral hypoglycemic agents in a drug-insured U.S. population. *Diabetes Care* **24**: 1411-1415.
17. Bailey CJ, Turner RC. (1996) Metformin. *N Engl J Med* **334**: 574-579.
18. Proks P, Reimann F, Green N, Gribble F, Ashcroft F. (2002) Sulfonylurea stimulation of insulin secretion. *Diabetes* **51 Suppl 3**: S368-376.
19. Moller DE. (2001) New drug targets for type 2 diabetes and the metabolic syndrome. *Nature* **414**: 821-827.
20. Wellen KE, Hotamisligil GS. (2005) Inflammation, stress, and diabetes. *J Clin Invest* **115**: 1111-1119.

21. Shoelson SE, Herrero L, Naaz A. (2007) Obesity, inflammation, and insulin resistance. *Gastroenterology* **132**: 2169-2180.
22. Hotamisligil GS. (2006) Inflammation and metabolic disorders. *Nature* **444**: 860-867.
23. Clark R, Kupper T. (2005) Old meets new: the interaction between innate and adaptive immunity. *J Invest Dermatol* **125**: 629-637.
24. Shi H, Kokoeva MV, Inouye K, Tzamelis I, Yin H, Flier JS. (2006) TLR4 links innate immunity and fatty acid-induced insulin resistance. *J Clin Invest* **116**: 3015-3025.
25. Li Z, Yang S, Lin H, et al. (2003) Probiotics and antibodies to TNF inhibit inflammatory activity and improve nonalcoholic fatty liver disease. *Hepatology* **37**: 343-350.
26. Christie PE, Henderson WR, Jr. (2002) Lipid inflammatory mediators: leukotrienes, prostaglandins, platelet-activating factor. *Clin Allergy Immunol* **16**: 233-254.
27. Heller A, Koch T, Schmeck J, van Ackern K. (1998) Lipid mediators in inflammatory disorders. *Drugs* **55**: 487-496.
28. Seder RA, Paul WE, Davis MM, Fazekas de St Groth B. (1992) The presence of interleukin 4 during in vitro priming determines the lymphokine-producing potential of CD4+ T cells from T cell receptor transgenic mice. *J Exp Med* **176**: 1091-1098.
29. Akimoto T, Numata F, Tamura M, et al. (1998) Abrogation of bronchial eosinophilic inflammation and airway hyperreactivity in signal transducers and activators of transcription (STAT)6-deficient mice. *J Exp Med* **187**: 1537-1542.
30. Malaviya R, Uckun FM. (2002) Role of STAT6 in IgE receptor/FcepsilonRI-mediated late phase allergic responses of mast cells. *J Immunol* **168**: 421-426.
31. Shimoda K, van Deursen J, Sangster MY, et al. (1996) Lack of IL-4-induced Th2 response and IgE class switching in mice with disrupted Stat6 gene. *Nature* **380**: 630-633.
32. Swain SL, Weinberg AD, English M, Huston G. (1990) IL-4 directs the development of Th2-like helper effectors. *J Immunol* **145**: 3796-3806.
33. Tilg H, Moschen AR. (2006) Adipocytokines: mediators linking adipose tissue, inflammation and immunity. *Nat Rev Immunol* **6**: 772-783.
34. Perrier S, Darakhshan F, Hajdouch E. (2006) IL-1 receptor antagonist in metabolic diseases: Dr Jekyll or Mr Hyde? *FEBS Lett* **580**: 6289-6294.
35. Rosen ED, Spiegelman BM. (2006) Adipocytes as regulators of energy balance and glucose homeostasis. *Nature* **444**: 847-853.
36. Despres JP, Lemieux I. (2006) Abdominal obesity and metabolic syndrome. *Nature* **444**: 881-887.
37. Shoelson SE, Lee J, Goldfine AB. (2006) Inflammation and insulin resistance. *J Clin Invest* **116**: 1793-1801.
38. Cave M, Deaciuc I, Mendez C, et al. (2007) Nonalcoholic fatty liver disease: predisposing factors and the role of nutrition. *J Nutr Biochem* **18**: 184-195.
39. Murray PJ. (2007) The JAK-STAT signaling pathway: input and output integration. *J Immunol* **178**: 2623-2629.

40. Bloom BR, Salgame P, Diamond B. (1992) Revisiting and revising suppressor T cells. *Immunol Today* **13**: 131-136.
41. Lucey DR, Clerici M, Shearer GM. (1996) Type 1 and type 2 cytokine dysregulation in human infectious, neoplastic, and inflammatory diseases. *Clin Microbiol Rev* **9**: 532-562.
42. Janeway CAJ. (2001) Immunobiology 5th edition. Library of Congress.
43. Kishimoto T, Taga T, Akira S. (1994) Cytokine signal transduction. *Cell* **76**: 253-262.
44. Bazan JF. (1990) Structural design and molecular evolution of a cytokine receptor superfamily. *Proc Natl Acad Sci U S A* **87**: 6934-6938.
45. O'Sullivan LA, Liongue C, Lewis RS, Stephenson SE, Ward AC. (2007) Cytokine receptor signaling through the Jak-Stat-Socs pathway in disease. *Mol Immunol* **44**: 2497-2506.
46. Gaffen SL. (2001) Signaling domains of the interleukin 2 receptor. *Cytokine* **14**: 63-77.
47. Parrish-Novak J, Dillon SR, Nelson A, et al. (2000) Interleukin 21 and its receptor are involved in NK cell expansion and regulation of lymphocyte function. *Nature* **408**: 57-63.
48. Mangi MH, Newland AC. (1999) Interleukin-3 in hematology and oncology: current state of knowledge and future directions. *Cytokines Cell Mol Ther* **5**: 87-95.
49. Ito H. (2003) IL-6 and Crohn's disease. *Curr Drug Targets Inflamm Allergy* **2**: 125-130.
50. Leonard WJ, O'Shea JJ. (1998) Jaks and STATs: biological implications. *Annu Rev Immunol* **16**: 293-322.
51. Remy I, Wilson IA, Michnick SW. (1999) Erythropoietin receptor activation by a ligand-induced conformation change. *Science* **283**: 990-993.
52. Ihle JN, Kerr IM. (1995) Jaks and Stats in signaling by the cytokine receptor superfamily. *Trends Genet* **11**: 69-74.
53. Darnell JE, Jr., Kerr IM, Stark GR. (1994) Jak-STAT pathways and transcriptional activation in response to IFNs and other extracellular signaling proteins. *Science* **264**: 1415-1421.
54. Copeland NG, Gilbert DJ, Schindler C, et al. (1995) Distribution of the mammalian Stat gene family in mouse chromosomes. *Genomics* **29**: 225-228.
55. Alves NL, Arosa FA, van Lier RA. (2007) Common gamma chain cytokines: dissidence in the details. *Immunol Lett* **108**: 113-120.
56. Minegishi Y, Saito M, Morio T, et al. (2006) Human tyrosine kinase 2 deficiency reveals its requisite roles in multiple cytokine signals involved in innate and acquired immunity. *Immunity* **25**: 745-755.
57. Coffey PJ, van Puijenbroek A, Burgering BM, et al. (1997) Insulin activates Stat3 independently of p21ras-ERK and PI-3K signal transduction. *Oncogene* **15**: 2529-2539.
58. Horvath CM. (2000) STAT proteins and transcriptional responses to extracellular signals. *Trends Biochem Sci* **25**: 496-502.
59. Ohara J, Paul WE. (1987) Receptors for B-cell stimulatory factor-1 expressed on cells of haematopoietic lineage. *Nature* **325**: 537-540.

60. Lowenthal JW, Castle BE, Christiansen J, et al. (1988) Expression of high affinity receptors for murine interleukin 4 (BSF-1) on hemopoietic and nonhemopoietic cells. *J Immunol* **140**: 456-464.
61. Hershey GK. (2003) IL-13 receptors and signaling pathways: an evolving web. *J Allergy Clin Immunol* **111**: 677-690; quiz 691.
62. Coffman RL, Ohara J, Bond MW, Carty J, Zlotnik A, Paul WE. (1986) B cell stimulatory factor-1 enhances the IgE response of lipopolysaccharide-activated B cells. *J Immunol* **136**: 4538-4541.
63. Vitetta ES, Ohara J, Myers CD, Layton JE, Krammer PH, Paul WE. (1985) Serological, biochemical, and functional identity of B cell-stimulatory factor 1 and B cell differentiation factor for IgG1. *J Exp Med* **162**: 1726-1731.
64. Imada K, Leonard WJ. (2000) The Jak-STAT pathway. *Mol Immunol* **37**: 1-11.
65. Chen W, Khurana Hershey GK. (2007) Signal transducer and activator of transcription signals in allergic disease. *J Allergy Clin Immunol* **119**: 529-541; quiz 542-523.
66. Pawson T, Gish GD, Nash P. (2001) SH2 domains, interaction modules and cellular wiring. *Trends Cell Biol* **11**: 504-511.
67. Koch CA, Anderson D, Moran MF, Ellis C, Pawson T. (1991) SH2 and SH3 domains: elements that control interactions of cytoplasmic signaling proteins. *Science* **252**: 668-674.
68. Sadowski I, Stone JC, Pawson T. (1986) A noncatalytic domain conserved among cytoplasmic protein-tyrosine kinases modifies the kinase function and transforming activity of Fujinami sarcoma virus P130gag-fps. *Mol Cell Biol* **6**: 4396-4408.
69. Hebenstreit D, Wirnsberger G, Horejs-Hoeck J, Duschl A. (2006) Signaling mechanisms, interaction partners, and target genes of STAT6. *Cytokine Growth Factor Rev* **17**: 173-188.
70. Abu-Amer Y. (2001) IL-4 abrogates osteoclastogenesis through STAT6-dependent inhibition of NF-kappaB. *J Clin Invest* **107**: 1375-1385.
71. Biola A, Andreau K, David M, et al. (2000) The glucocorticoid receptor and STAT6 physically and functionally interact in T-lymphocytes. *FEBS Lett* **487**: 229-233.
72. Litterst CM, Pfitzner E. (2001) Transcriptional activation by STAT6 requires the direct interaction with NCoA-1. *J Biol Chem* **276**: 45713-45721.
73. Valineva T, Yang J, Palovuori R, Silvennoinen O. (2005) The transcriptional co-activator protein p100 recruits histone acetyltransferase activity to STAT6 and mediates interaction between the CREB-binding protein and STAT6. *J Biol Chem* **280**: 14989-14996.
74. Yang J, Aittomaki S, Pesu M, et al. (2002) Identification of p100 as a coactivator for STAT6 that bridges STAT6 with RNA polymerase II. *Embo J* **21**: 4950-4958.
75. Arimura A, vn Peer M, Schroder AJ, Rothman PB. (2004) The transcriptional co-activator p/CIP (NCoA-3) is up-regulated by STAT6 and serves as a positive regulator of transcriptional activation by STAT6. *J Biol Chem* **279**: 31105-31112.
76. Goenka S, Cho SH, Boothby M. (2007) Collaborator of Stat6 (CoaSt6)-associated poly(ADP-ribose) polymerase activity modulates Stat6-dependent gene transcription. *J Biol Chem* **282**: 18732-18739.

77. O'Shea JJ, Gadina M, Schreiber RD. (2002) Cytokine signaling in 2002: new surprises in the Jak/Stat pathway. *Cell* **109 Suppl**: S121-131.
78. Keegan AD, Nelms K, White M, Wang LM, Pierce JH, Paul WE. (1994) An IL-4 receptor region containing an insulin receptor motif is important for IL-4-mediated IRS-1 phosphorylation and cell growth. *Cell* **76**: 811-820.
79. Huang H, Paul WE. (1998) Impaired interleukin 4 signaling in T helper type 1 cells. *J Exp Med* **187**: 1305-1313.
80. Ceresa BP, Pessin JE. (1996) Insulin stimulates the serine phosphorylation of the signal transducer and activator of transcription (STAT3) isoform. *J Biol Chem* **271**: 12121-12124.
81. Inoue H, Ogawa W, Ozaki M, et al. (2004) Role of STAT-3 in regulation of hepatic gluconeogenic genes and carbohydrate metabolism in vivo. *Nat Med* **10**: 168-174.
82. Rodig SJ, Meraz MA, White JM, et al. (1998) Disruption of the Jak1 gene demonstrates obligatory and nonredundant roles of the Jaks in cytokine-induced biologic responses. *Cell* **93**: 373-383.
83. Neubauer H, Cumano A, Muller M, Wu H, Huffstadt U, Pfeffer K. (1998) Jak2 deficiency defines an essential developmental checkpoint in definitive hematopoiesis. *Cell* **93**: 397-409.
84. Parganas E, Wang D, Stravopodis D, et al. (1998) Jak2 is essential for signaling through a variety of cytokine receptors. *Cell* **93**: 385-395.
85. Nosaka T, van Deursen JM, Tripp RA, et al. (1995) Defective lymphoid development in mice lacking Jak3. *Science* **270**: 800-802.
86. Park SY, Saijo K, Takahashi T, et al. (1995) Developmental defects of lymphoid cells in Jak3 kinase-deficient mice. *Immunity* **3**: 771-782.
87. Thomis DC, Gurniak CB, Tivol E, Sharpe AH, Berg LJ. (1995) Defects in B lymphocyte maturation and T lymphocyte activation in mice lacking Jak3. *Science* **270**: 794-797.
88. Karaghiosoff M, Neubauer H, Lassnig C, et al. (2000) Partial impairment of cytokine responses in Tyk2-deficient mice. *Immunity* **13**: 549-560.
89. Durbin JE, Hackenmiller R, Simon MC, Levy DE. (1996) Targeted disruption of the mouse Stat1 gene results in compromised innate immunity to viral disease. *Cell* **84**: 443-450.
90. Meraz MA, White JM, Sheehan KC, et al. (1996) Targeted disruption of the Stat1 gene in mice reveals unexpected physiologic specificity in the JAK-STAT signaling pathway. *Cell* **84**: 431-442.
91. Park C, Li S, Cha E, Schindler C. (2000) Immune response in Stat2 knockout mice. *Immunity* **13**: 795-804.
92. Haga S, Ogawa W, Inoue H, et al. (2005) Compensatory recovery of liver mass by Akt-mediated hepatocellular hypertrophy in liver-specific STAT3-deficient mice. *J Hepatol* **43**: 799-807.
93. Kaplan MH, Sun YL, Hoey T, Grusby MJ. (1996) Impaired IL-12 responses and enhanced development of Th2 cells in Stat4-deficient mice. *Nature* **382**: 174-177.
94. Thierfelder WE, van Deursen JM, Yamamoto K, et al. (1996) Requirement for Stat4 in interleukin-12-mediated responses of natural killer and T cells. *Nature* **382**: 171-174.

95. Mui AL, Wakao H, O'Farrell AM, Harada N, Miyajima A. (1995) Interleukin-3, granulocyte-macrophage colony stimulating factor and interleukin-5 transduce signals through two STAT5 homologs. *Embo J* **14**: 1166-1175.
96. Liu X, Robinson GW, Wagner KU, Garrett L, Wynshaw-Boris A, Hennighausen L. (1997) Stat5a is mandatory for adult mammary gland development and lactogenesis. *Genes Dev* **11**: 179-186.
97. Udy GB, Towers RP, Snell RG, et al. (1997) Requirement of STAT5b for sexual dimorphism of body growth rates and liver gene expression. *Proc Natl Acad Sci U S A* **94**: 7239-7244.
98. Takeda K, Tanaka T, Shi W, et al. (1996) Essential role of Stat6 in IL-4 signalling. *Nature* **380**: 627-630.
99. Kaplan MH, Schindler U, Smiley ST, Grusby MJ. (1996) Stat6 is required for mediating responses to IL-4 and for development of Th2 cells. *Immunity* **4**: 313-319.
100. Taniguchi CM, Emanuelli B, Kahn CR. (2006) Critical nodes in signalling pathways: insights into insulin action. *Nat Rev Mol Cell Biol* **7**: 85-96.
101. Szanto I, Kahn CR. (2000) Selective interaction between leptin and insulin signaling pathways in a hepatic cell line. *Proc Natl Acad Sci U S A* **97**: 2355-2360.
102. Fernandez-Real JM, Ricart W. (2003) Insulin resistance and chronic cardiovascular inflammatory syndrome. *Endocr Rev* **24**: 278-301.
103. Hotamisligil GS. (2005) Role of endoplasmic reticulum stress and c-Jun NH2-terminal kinase pathways in inflammation and origin of obesity and diabetes. *Diabetes* **54 Suppl 2**: S73-78.
104. Grunig G, Warnock M, Wakil AE, et al. (1998) Requirement for IL-13 independently of IL-4 in experimental asthma. *Science* **282**: 2261-2263.
105. Wills-Karp M, Luyimbazi J, Xu X, et al. (1998) Interleukin-13: central mediator of allergic asthma. *Science* **282**: 2258-2261.
106. Wills-Karp M. (2004) Interleukin-13 in asthma pathogenesis. *Immunol Rev* **202**: 175-190.
107. Zhu Z, Homer RJ, Wang Z, et al. (1999) Pulmonary expression of interleukin-13 causes inflammation, mucus hypersecretion, subepithelial fibrosis, physiologic abnormalities, and eotaxin production. *J Clin Invest* **103**: 779-788.
108. Wynn TA. (2003) IL-13 effector functions. *Annu Rev Immunol* **21**: 425-456.
109. Grecnis RK, Bancroft AJ. (2004) Interleukin-13: a key mediator in resistance to gastrointestinal-dwelling nematode parasites. *Clin Rev Allergy Immunol* **26**: 51-60.
110. Finkelman FD, Shea-Donohue T, Morris SC, et al. (2004) Interleukin-4- and interleukin-13-mediated host protection against intestinal nematode parasites. *Immunol Rev* **201**: 139-155.
111. Noelle R, Krammer PH, Ohara J, Uhr JW, Vitetta ES. (1984) Increased expression of Ia antigens on resting B cells: an additional role for B-cell growth factor. *Proc Natl Acad Sci U S A* **81**: 6149-6153.
112. Ohara J, Paul WE. (1988) Up-regulation of interleukin 4/B-cell stimulatory factor 1 receptor expression. *Proc Natl Acad Sci U S A* **85**: 8221-8225.

113. Thornhill MH, Wellicome SM, Mahiouz DL, Lanchbury JS, Kyan-Aung U, Haskard DO. (1991) Tumor necrosis factor combines with IL-4 or IFN-gamma to selectively enhance endothelial cell adhesiveness for T cells. The contribution of vascular cell adhesion molecule-1-dependent and -independent binding mechanisms. *J Immunol* **146**: 592-598.
114. Bennett BL, Cruz R, Lacson RG, Manning AM. (1997) Interleukin-4 suppression of tumor necrosis factor alpha-stimulated E-selectin gene transcription is mediated by STAT6 antagonism of NF-kappaB. *J Biol Chem* **272**: 10212-10219.
115. Nelms K, Keegan AD, Zamorano J, Ryan JJ, Paul WE. (1999) The IL-4 receptor: signaling mechanisms and biologic functions. *Annu Rev Immunol* **17**: 701-738.
116. Dedeoglu F, Horwitz B, Chaudhuri J, Alt FW, Geha RS. (2004) Induction of activation-induced cytidine deaminase gene expression by IL-4 and CD40 ligation is dependent on STAT6 and NFkappaB. *Int Immunol* **16**: 395-404.
117. Kotanides H, Reich NC. (1993) Requirement of tyrosine phosphorylation for rapid activation of a DNA binding factor by IL-4. *Science* **262**: 1265-1267.
118. Schaffer A, Cerutti A, Shah S, Zan H, Casali P. (1999) The evolutionarily conserved sequence upstream of the human Ig heavy chain S gamma 3 region is an inducible promoter: synergistic activation by CD40 ligand and IL-4 via cooperative NF-kappa B and STAT-6 binding sites. *J Immunol* **162**: 5327-5336.
119. Agresti A, Vercelli D. (2002) c-Rel is a selective activator of a novel IL-4/CD40 responsive element in the human Ig gamma4 germline promoter. *Mol Immunol* **38**: 849-859.
120. Kohler I, Rieber EP. (1993) Allergy-associated I epsilon and Ec epsilon receptor II (CD23b) genes activated via binding of an interleukin-4-induced transcription factor to a novel responsive element. *Eur J Immunol* **23**: 3066-3071.
121. Stutz AM, Pickart LA, Trifilieff A, Baumruker T, Prieschl-Strassmayr E, Woisetschlager M. (2003) The Th2 cell cytokines IL-4 and IL-13 regulate found in inflammatory zone 1/resistin-like molecule alpha gene expression by a STAT6 and CCAAT/enhancer-binding protein-dependent mechanism. *J Immunol* **170**: 1789-1796.
122. Curiel RE, Lahesmaa R, Subleski J, et al. (1997) Identification of a Stat-6-responsive element in the promoter of the human interleukin-4 gene. *Eur J Immunol* **27**: 1982-1987.
123. Kubo M, Ransom J, Webb D, Hashimoto Y, Tada T, Nakayama T. (1997) T-cell subset-specific expression of the IL-4 gene is regulated by a silencer element and STAT6. *Embo J* **16**: 4007-4020.
124. Ohmori Y, Smith MF, Jr., Hamilton TA. (1996) IL-4-induced expression of the IL-1 receptor antagonist gene is mediated by STAT6. *J Immunol* **157**: 2058-2065.
125. Worm MM, Tsytsykova A, Geha RS. (1998) CD40 ligation and IL-4 use different mechanisms of transcriptional activation of the human lymphotoxin alpha promoter in B cells. *Eur J Immunol* **28**: 901-906.
126. Matsukura S, Stellato C, Plitt JR, et al. (1999) Activation of eotaxin gene transcription by NF-kappa B and STAT6 in human airway epithelial cells. *J Immunol* **163**: 6876-6883.

127. Hoeck J, Woisetschlager M. (2001) Activation of eotaxin-3/CCL126 gene expression in human dermal fibroblasts is mediated by STAT6. *J Immunol* **167**: 3216-3222.
128. Wirnsberger G, Hebenstreit D, Posselt G, Horejs-Hoeck J, Duschl A. (2006) IL-4 induces expression of TARC/CCL17 via two STAT6 binding sites. *Eur J Immunol* **36**: 1882-1891.
129. Welch JS, Escoubet-Lozach L, Sykes DB, Liddiard K, Greaves DR, Glass CK. (2002) TH2 cytokines and allergic challenge induce Ym1 expression in macrophages by a STAT6-dependent mechanism. *J Biol Chem* **277**: 42821-42829.
130. McHugh KP, Kitazawa S, Teitelbaum SL, Ross FP. (2001) Cloning and characterization of the murine beta(3) integrin gene promoter: identification of an interleukin-4 responsive element and regulation by STAT-6. *J Cell Biochem* **81**: 320-332.
131. Khew-Goodall Y, Wadham C, Stein BN, Gamble JR, Vadas MA. (1999) Stat6 activation is essential for interleukin-4 induction of P-selectin transcription in human umbilical vein endothelial cells. *Arterioscler Thromb Vasc Biol* **19**: 1421-1429.
132. Conrad DJ, Lu M. (2000) Regulation of human 12/15-lipoxygenase by Stat6-dependent transcription. *Am J Respir Cell Mol Biol* **22**: 226-234.
133. Gingras S, Simard J. (1999) Induction of 3beta-hydroxysteroid dehydrogenase/isomerase type 1 expression by interleukin-4 in human normal prostate epithelial cells, immortalized keratinocytes, colon, and cervix cancer cell lines. *Endocrinology* **140**: 4573-4584.
134. Pauleau AL, Rutschman R, Lang R, Pernis A, Watowich SS, Murray PJ. (2004) Enhancer-mediated control of macrophage-specific arginase I expression. *J Immunol* **172**: 7565-7573.
135. Nguyen VT, Benveniste EN. (2000) IL-4-activated STAT-6 inhibits IFN-gamma-induced CD40 gene expression in macrophages/microglia. *J Immunol* **165**: 6235-6243.
136. Borner C, Woltje M, Holtt V, Kraus J. (2004) STAT6 transcription factor binding sites with mismatches within the canonical 5'-TTC.GAA-3' motif involved in regulation of delta- and mu-opioid receptors. *J Neurochem* **91**: 1493-1500.
137. David MD, Bertoglio J, Pierre J. (2003) Functional characterization of IL-13 receptor alpha2 gene promoter: a critical role of the transcription factor STAT6 for regulated expression. *Oncogene* **22**: 3386-3394.
138. Kotanides H, Reich NC. (1996) Interleukin-4-induced STAT6 recognizes and activates a target site in the promoter of the interleukin-4 receptor gene. *J Biol Chem* **271**: 25555-25561.
139. Boothby M, Gravallesse E, Liou HC, Glimcher LH. (1988) A DNA binding protein regulated by IL-4 and by differentiation in B cells. *Science* **242**: 1559-1562.
140. Kraus J, Borner C, Giannini E, et al. (2001) Regulation of mu-opioid receptor gene transcription by interleukin-4 and influence of an allelic variation within a STAT6 transcription factor binding site. *J Biol Chem* **276**: 43901-43908.

141. Schjerven H, Brandtzaeg P, Johansen FE. (2000) Mechanism of IL-4-mediated up-regulation of the polymeric Ig receptor: role of STAT6 in cell type-specific delayed transcriptional response. *J Immunol* **165**: 3898-3906.
142. Masuda A, Matsuguchi T, Yamaki K, Hayakawa T, Yoshikai Y. (2001) Interleukin-15 prevents mouse mast cell apoptosis through STAT6-mediated Bcl-xL expression. *J Biol Chem* **276**: 26107-26113.
143. Hebenstreit D, Luft P, Schmiedlechner A, et al. (2003) IL-4 and IL-13 induce SOCS-1 gene expression in A549 cells by three functional STAT6-binding motifs located upstream of the transcription initiation site. *J Immunol* **171**: 5901-5907.
144. Mascareno E, Dhar M, Siddiqui MA. (1998) Signal transduction and activator of transcription (STAT) protein-dependent activation of angiotensinogen promoter: a cellular signal for hypertrophy in cardiac muscle. *Proc Natl Acad Sci U S A* **95**: 5590-5594.
145. Buttner C, Skupin A, Rieber EP. (2004) Transcriptional activation of the type I collagen genes COL1A1 and COL1A2 in fibroblasts by interleukin-4: analysis of the functional collagen promoter sequences. *J Cell Physiol* **198**: 248-258.
146. Moriggl R, Berchtold S, Friedrich K, et al. (1997) Comparison of the transactivation domains of Stat5 and Stat6 in lymphoid cells and mammary epithelial cells. *Mol Cell Biol* **17**: 3663-3678.
147. Lee DU, Rao A. (2004) Molecular analysis of a locus control region in the T helper 2 cytokine gene cluster: a target for STAT6 but not GATA3. *Proc Natl Acad Sci U S A* **101**: 16010-16015.
148. Blanchard C, Durual S, Estienne M, et al. (2004) IL-4 and IL-13 up-regulate intestinal trefoil factor expression: requirement for STAT6 and de novo protein synthesis. *J Immunol* **172**: 3775-3783.
149. Jaruga B, Hong F, Sun R, Radaeva S, Gao B. (2003) Crucial role of IL-4/STAT6 in T cell-mediated hepatitis: up-regulating eotaxins and IL-5 and recruiting leukocytes. *J Immunol* **171**: 3233-3244.
150. Lentsch AB, Kato A, Davis B, Wang W, Chao C, Edwards MJ. (2001) STAT4 and STAT6 regulate systemic inflammation and protect against lethal endotoxemia. *J Clin Invest* **108**: 1475-1482.
151. Li J, Grigoryev DN, Ye SQ, et al. (2005) Chronic intermittent hypoxia upregulates genes of lipid biosynthesis in obese mice. *J Appl Physiol* **99**: 1643-1648.
152. Li J, Thorne LN, Punjabi NM, et al. (2005) Intermittent hypoxia induces hyperlipidemia in lean mice. *Circ Res* **97**: 698-706.
153. Savransky V, Nanayakkara A, Vivero A, et al. (2007) Chronic intermittent hypoxia predisposes to liver injury. *Hepatology* **45**: 1007-1013.
154. Aoudjehane L, Podevin P, Scatton O, et al. (2007) Interleukin-4 induces human hepatocyte apoptosis through a Fas-independent pathway. *Faseb J* **21**: 1433-1444.
155. Low SH, Vasanth S, Larson CH, et al. (2006) Polycystin-1, STAT6, and P100 function in a pathway that transduces ciliary mechanosensation and is activated in polycystic kidney disease. *Dev Cell* **10**: 57-69.
156. Shum BO, Mackay CR, Gorgun CZ, et al. (2006) The adipocyte fatty acid-binding protein aP2 is required in allergic airway inflammation. *J Clin Invest* **116**: 2183-2192.

- 
157. Zimmermann N, Mishra A, King NE, et al. (2004) Transcript signatures in experimental asthma: identification of STAT6-dependent and -independent pathways. *J Immunol* **172**: 1815-1824.
  158. Huber SA, Sakkinen P, David C, Newell MK, Tracy RP. (2001) T helper-cell phenotype regulates atherosclerosis in mice under conditions of mild hypercholesterolemia. *Circulation* **103**: 2610-2616.
  159. Satterthwaite G, Francis SE, Suvarna K, et al. (2005) Differential gene expression in coronary arteries from patients presenting with ischemic heart disease: further evidence for the inflammatory basis of atherosclerosis. *Am Heart J* **150**: 488-499.
  160. Vats D, Mukundan L, Odegaard JI, et al. (2006) Oxidative metabolism and PGC-1beta attenuate macrophage-mediated inflammation. *Cell Metab* **4**: 13-24.
  161. Lacy-Hulbert A, Moore KJ. (2006) Designer macrophages: oxidative metabolism fuels inflammation repair. *Cell Metab* **4**: 7-8.



# **1. Introduction**

## **Part B**

### **Proteomic Tools**



---

## 1.6 What is proteomics?

Proteomics is a widely used method to identify protein structure and functions. Proteins play various crucial roles in organisms such as catalyzing chemical reactions with high speed and high specificity (enzymes), transmitting a signal to distant cells (hormones) or recognizing immune identity (antibodies). Proteins are also very important in different other tasks such as transducing signals inside cells, transporting ligand or maintaining cell structure. Because of this large panel of function and distribution in the organism, proteomics is the method of choice to study and identify these large varieties of proteins. Moreover, proteomics can help discovering therapeutic targets or biomarkers candidates by comparing two different types of samples for example control and treated.

The word proteome describes an entire organism's protein content. The study and identification of this complex mixture of proteins received the name "proteomics". This nomenclature comes from the analogy of the word "genomics", which describes an organism's gene content, applied to an organism's protein content. The former goal of studying proteins was to determine all the protein produced by the DNA and, therefore, give a complete overview of the protein complement of the genome (1). But scientists noticed the limits of this approach due to the particular and multiple functions of proteins. Most of the proteins possess specific conformation or modification called post-translational modification (PTM) in order to be functional. For that reason, the basic study of protein expression became limited. Therefore, proteomics expanded from primary protein identification to post-translational modifications and protein-protein interactions studies.

### *1.6.1 Gene quantification*

The completion of the Human Genome Project in 2003 has offered new opportunities of understanding cell biology (2). The availability of this sequence database has become a starting point to open large possibilities for biomedical research, and to discover mechanisms involved in the functional regulation of a cell or a tissue (2, 3). The crucial goal of identifying and sequencing the 20'000 to 25'000 genes of the human genome was to use the genetic sequences to predict the translated proteins and to investigate their roles and interactions (3). Moreover, high throughput technologies allowing determining thousand of genes expression pattern were decisive in the understanding of biological processes.

The global pattern of gene expression is used to identify candidate that might be involved in disease processes (4). Therefore, measuring mRNA levels is one of the appropriate techniques to elucidate gene functions. The two most frequent used techniques include DNA microarray technology (gene chip) and serial analysis of gene expression (SAGE). DNA microarray technology is based on immobilizing probe sequences at predetermined positions that will hybridise complementary fluorescent labelled mRNA extracted from experimental material (5). By quantifying the labels, the relative abundance of mRNA is determined (*Figure 1*).

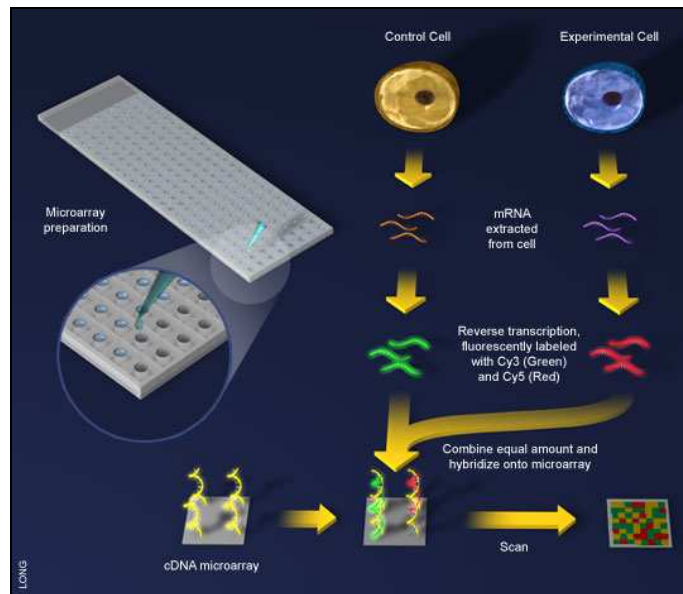


**Figure 1:** DNA microarray technology from Columbia University, New York. A fluorescent dye is labelled with mRNA extracted from control (green) or treated (red) cells. This mRNA is hybridized with cDNA present on microarray and the intensity of fluorescence describes the amount of mRNA present in the sample.

This technique allows identifying 2-3 fold changes in expression, but smaller changes are more difficult to detect due to cross-hybridisation that diminish specificity (6). On the opposite, SAGE is based on the generation of unique, short sequence tags from each mRNA molecule in the cell (7). The frequency of presence of each tag provides absolute quantification of mRNA expression. However, errors can occur if the tag is not unique or if low copy-number genes are present (6).

### 1.6.2 Protein synthesis and its regulation

These mRNA used to quantify genes are functional products of the four base pair containing DNA. Once translated, these newly synthesized short sequences migrate to the cytosol where they are translated into a combination of the twenty corresponding amino acids. Finally, the assembly of amino acids, called a polypeptide, is folded into functional protein with the help of chaperones. These folded proteins will act as functional product of the gene (*Figure 2*).

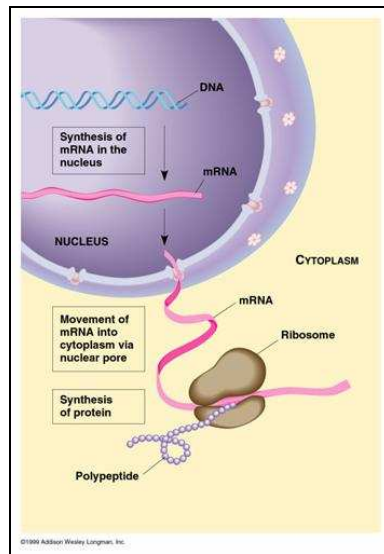


**Figure 2:** Protein synthesis from Addison Wesley, Longman. DNA is transcribed into corresponding mRNA, which will then be translated into corresponding polypeptides. Proteins are a three dimensional folding of these polypeptides.

Many different steps are involved in the regulation of protein synthesis from their corresponding genes. These include DNA transcription, mRNA translation and additional transformation steps. Different factors can regulate this flow of information. Every step of the synthesis can be influenced by a specific type of modification which can control the amount of final functional product. These different modifications include transcriptional and post-transcriptional control (alternative splicing), translational and degradation control, activation control (PTM) and catalytic control (stability) (*Figure 3*). Due to these multiple control steps, the correlation between mRNA level and protein amount is low.

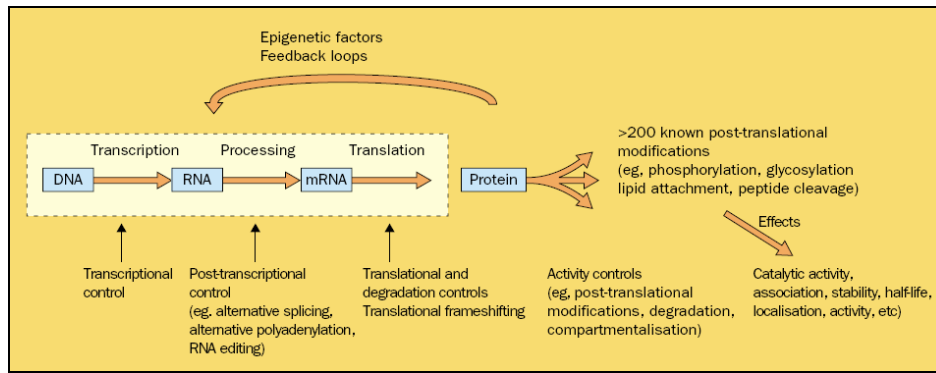


**Figure 3:** Regulation and modification of gene products from DNA to proteins from R. Banks (et al.) (8). Protein synthesis can be regulated at many different steps including transcription, processing and translational. These modifications reduce correlation between mRNA and protein level. Finally additional modifications (PTM) and diverse external factors can affect protein structure and stability.

In addition to these modifications, protein polymorphism can influence activity of protein. Moreover, the majority of proteins may be targeted by many additional PTM in order to be activated and fulfil their physiological role. For example, phosphorylation is a reversible modification adjusting folding and function of proteins including enzyme activity (9). Another modification, glycosylation is involved in various biological events, including cell recognition, adhesion and cell-cell interaction (11-13). These protein modification studies have been developed to supplement proteomics and are therefore called phosphoproteomics and glycoproteomics. Moreover, the specific study of glycomes and their genomic or pathologic relationship with organisms is called glycomics. These different approaches opened a new opportunity to overcome the non linear relationship between genome and physiological effect (14, 15).

### 1.6.3 Correlation between genome and proteome

One of the aims of sequencing the human genome was to measure genes and their correlation with corresponding functional proteins. As shown previously, correlation between mRNA and proteins is not perfect due to the large amount of post-translational modifications. As expression or function of proteins is modulated at many points, gene quantification cannot provide accurate results. Moreover, proteins are the functional product of the cell and are therefore expected to provide more relevant information than gene quantification. The first

studies that revealed poor mRNA protein correlation were conducted using two dimensional gel electrophoresis (2-DE) (16, 17). These studies allowed measuring the Pearson correlation coefficient between mRNA translational product and protein. This coefficient measures the tendency of the variable to increase or decrease together and ranges from -1 to 1. A value close to 1 shows a linear relationship between the two variables and a value close to -1 show an increase when the other variable decreases. A value of 0 means no correlation between the two variables. The Pearson coefficient between protein and mRNA varies from 0.46 to 0.76 (6). These studies give the proof about mRNA not being a reliable indicator of protein levels.

Most of the protein-based therapeutic compounds imply PTM which can affect protein properties relevant to their therapeutic application. Therefore, a correct understanding of human complexity implied knowing the total number of genes in addition to the proteome that is created through differential splicing of mRNA, protein post-translational modifications and the release of active products after physiological activation (10). For example, the 20'000 to 25'000 genes are translated to a total of 67'764 non redundant human proteins (human IPI database, v. 3.33 - release 13.09.2007) (11). However this result may vary depending on the protein database. Unfortunately, one of the limitations of proteomics is the incapacity of identifying factors that determine ultimately protein effects, like pH, hypoxia or drug administration. However this limitation can be overcome by studying metabolites of cell products. Metabolomics became widely used to give a metabolic profile of the physiological relevance of the end-products of gene expression.

#### ***1.6.4 Proteome complexity***

The large amount of proteins present in organisms makes proteomic a very challenging science. Moreover, these products vary from conditions to conditions, from cell to cell and represent a large dynamic range. Biological fluids, cells or tissues are therefore extremely complex to be analyzed. For that reason, different techniques exist to simplify the proteome and their choice depends on the type of matrix used. For example, most proteins of interest in the identification of a biomarker or therapeutic candidates are pooled in only 4% of an entire plasma sample. The 96% left are represented by the 12 most abundant proteins and are therefore not of interest in most of the studies (*Figure 4*). On the opposite, when using cell or tissue, separating organelles can be useful if a subset of the proteome needs to be studied.

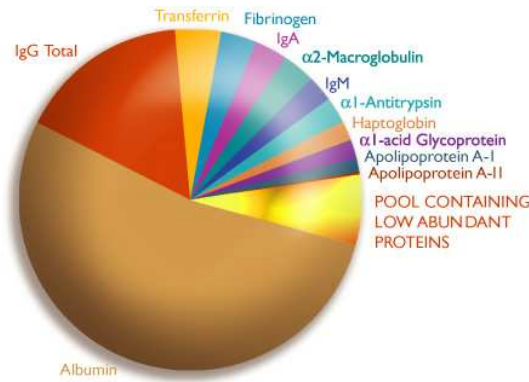


**Figure 4:** 12 proteins comprise up to 96% of the protein mass in plasma from the Plasma Protein Institute (12); drawing by Beckman Coulter. These proteins include albumin, immunoglobulin G (IgG), transferrin, fibrinogen, immunoglobulin A (IgA), α2-macroglobulin, immunoglobulin M (IgM), α1-antitrypsin, haptoglobin, α1-acid glycoprotein and apolipoprotein A1 and A2.

This huge variation in the proteome abundance has been studied by Anderson (*et al.*) who suggested a range in copy numbers of probably 7-8 orders of magnitude in human cells (13). This range can even be larger when comparing the most abundant plasma protein (albumin) with a single protein copy present in the plasma and released by a single necrosed cell (kininogen) (14). Moreover, this variation can reach up to 12 orders of magnitude. This huge variation can be represented, at the earth level by comparing order 10 (10'000 km) to order 1 (1 cm) (Figure 5).

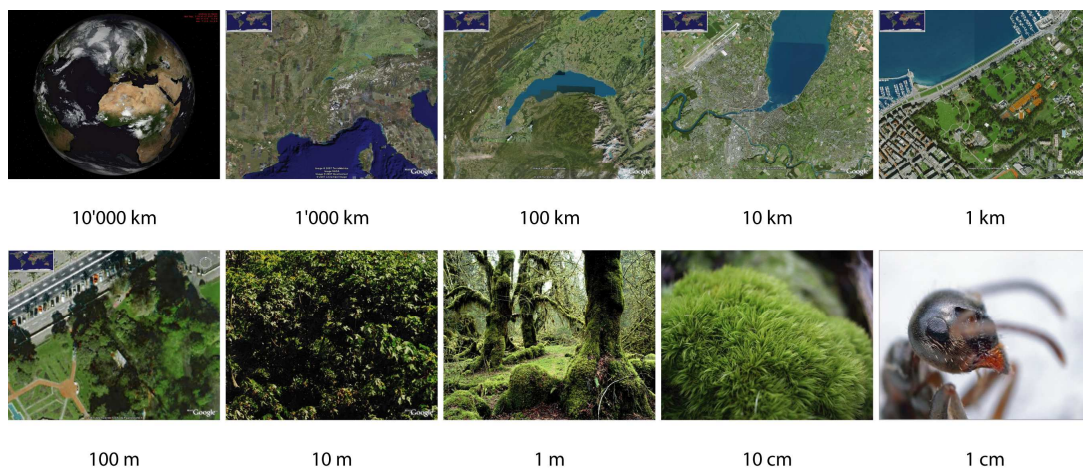


**Figure 5:** Ten orders of magnitude represented at the earth level, adapted from B. Domon. Earth represents order 10 (10'000 km) and ant represents order 1 (1 cm).

When analyzing plasma, depletion of most abundant proteins is often used and can be crucial to perform high quality analysis. This strategy consists of removing the most abundant proteins by immunodepletion and keeping the small fraction of interest. This process is necessary to avoid important biological information being lost (15). Several columns are now commercially available and *Figure 6* shows the Multiple Affinity Removal System (MARS) LC column as an example.

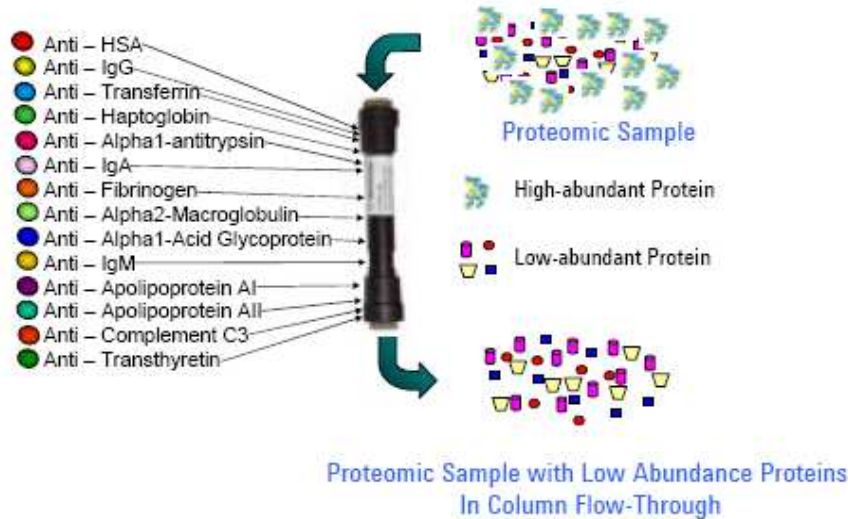


**Figure 6:** The MARS Human-14 LC column from Agilent Technologies removes fourteen abundant plasma proteins.

On the opposite, when working with cell culture or tissues several fractionation strategies exist to lower sample complexity and to analyze subsets of the total proteome called subproteomes. Zhang (*et al.*) have classified subproteome profiling strategies into three categories (*Figure 7*) (16).

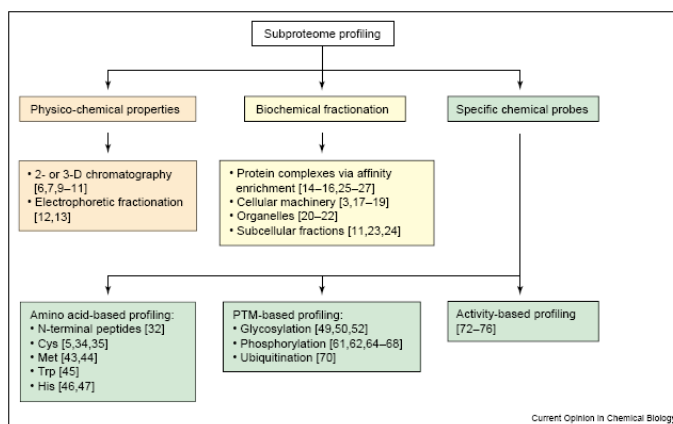


**Figure 7:** Strategies for subproteome profiling from Zhang (et al.). Numbers in brackets are related to references in the original paper (16).

Finally, separative techniques can be applied to all types of samples to analyze proteins. These techniques are based on physico-chemical properties of proteins or peptides, and include two-dimensional gel electrophoresis (2-DE) and multidimensional protein identification technology (MudPIT). Another technique such as differential centrifugation is an appropriate solution to concentrate the different organelles in the cell (Figure 8). Typically, a sucrose gradient is used to enrich or separate the different cytosolic, nuclear, mitochondrial and/or microsomal (endoplasmic reticulum) fractions (17).

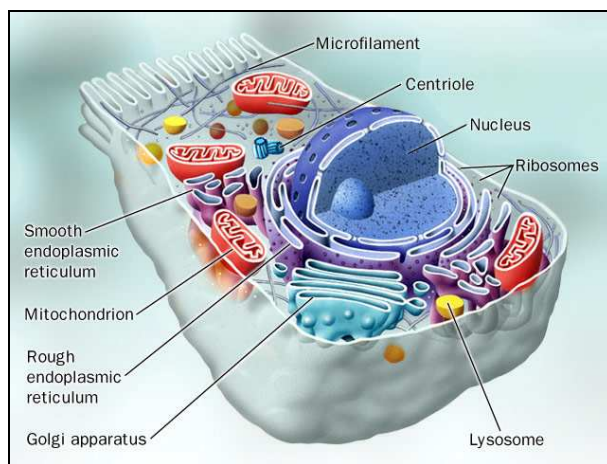


**Figure 8:** Structure of the eukaryote cell from Chemistry pictures. This structure includes nucleus, ribosome, rough endoplasmic reticulum, golgi apparatus, centrioles, lysosomes, mitochondrion, smooth endoplasmic reticulum and microfilaments. In order to simplify proteome, these organelles can be separated.

Specific antibodies are used to immunoprecipitate and isolate a particular subset of protein including receptor complexes. Moreover, specific phospho- or glycan-antibodies can capture phospho- or glycoproteins and can be useful when PTM identification is required. Finally, chemical probes are used to pull-down proteins containing the adequate targets (e.g. specific amino acids, phosphate group or sugar moiety, etc.).

### ***1.6.5 Ultimate proteomic tool: mass spectrometry***

One of the reasons of the rapid proteomic expansion is the improvement of technique efficiency and development of new technologies including nanoscale liquid chromatography coupled with tandem mass spectrometry (LC-MS/MS) or matrix-assisted laser desorption/ionisation (MALDI) (18). These techniques are based on mass spectrometry (MS) (immune-MS, MS profiling), on protein arrays (antibody arrays, reversed phase arrays), on RNA assays (oligonucleotide microarrays, gene chips) or on DNA assays (chromatin immunoprecipitation, high-density DNA microarrays) (27, 28). Proteomics is now the most widely used approach to evaluate differential expression on tissues, biofluids, and enzymatic pathways as well as disease and toxicological screening (19).

*Figure 9* explains a typical workflow in a proteomic study. A protein population is usually extracted from a biological sample. This protein population is then separated by single or multiple dimension gel electrophoresis and then digested (trypsin, endoproteinase) prior to the mass spectrometry identification analysis. An alternative approach consists of digesting protein first and separating peptides by high performance liquid chromatography (HPLC) before the identification analysis. Peptides are then ionized using an electrospray ionization (ESI) or matrix-assisted laser desorption/ionization (MALDI) and analysed by various different mass spectrometers including quadrupole or Time of Flight (TOF). Finally, the obtained peptide-sequencing are searched against protein databases using database-searching softwares (Sequest, Mascot, etc.). Examples of the reagents or techniques used at each step of this workflow are given beneath each arrow.

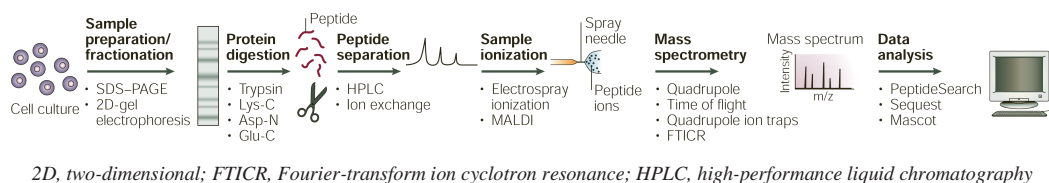


**Figure 9:** Typical workflow in proteomic studies from Steen (*et al.*) (20).

The use of tandem mass spectrometry (MS/MS) for protein analysis has been elaborated during those last twenty years. Before the existence of this tool, applied to protein analysis, the method of choice for the analysis of amino acids sequences was the Edman degradation. The principle is based on the sequential removal of an amino acid from the N-terminus of protein and on the identification of this cleaved amino acid. Shimonishi (*et al.*) proposed in 1980 to combine mass spectrometry and Edman degradation by measuring the mass of the peptides after amino acid removal (21). However, the extension of this approach to biological samples was confronted to a fundamental problem. This problem consisted to transfer highly polar, completely non-volatile molecules with a mass of several kDa into a gas phase without damages (20). After several improvements the identification of peptides with mass spectrometry took a radical change in the 1990s with the development of two ionization methods for large molecules: electrospray ionisation (ESI) by Fenn (*et al.*) and matrix-assisted laser desorption/ionisation (MALDI) by Karas (*et al.*) (32, 33). Moreover as well as the rapid increase of the number of available protein sequences databases contributed to this expansion. The discovering of these two methods became the starting point of the proteomic approach called peptide mass fingerprinting (PMF), based on the measure of the peptide mass composition and on its correlation with theoretical masses computed from protein sequences databases (34, 35). Different software has been proposed to identify proteins from PMF data, such as Mascot, ProFound or Aldente (22). Finally, another identifying approach used with ESI was based on the correlation of MS/MS spectra with theoretical peptides fragment mass found in databases (23).

The mass spectrometer is the key element in the identification of peptide mass. This powerful tool is composed of three elements: an ionization source, a mass analyzer and a detector. The ESI and MALDI are the most commonly used ionization sources (20). When using MALDI the sample must be co-crystallized within an ultraviolet absorbing matrix which is a low-molecular weight aromatic acid. During irradiation, a focused laser of suitable wavelength target the matrix and makes the molecules sublime and transfer into the gas phase

(20). The formed ions are then accelerated by electric potentials into a mass analyser. Contrary to the MALDI, ESI source can spray peptides solution under high-voltage (several kV) to create highly positive charged micro droplets and generate ionized peptides (*Figure 10*). The liquid, eluting from the chromatography column contains the peptides which are electrostatically dispersed. Once the droplets are nebulized, the solvent evaporates which decreases the size and increases the charge density of the particle.

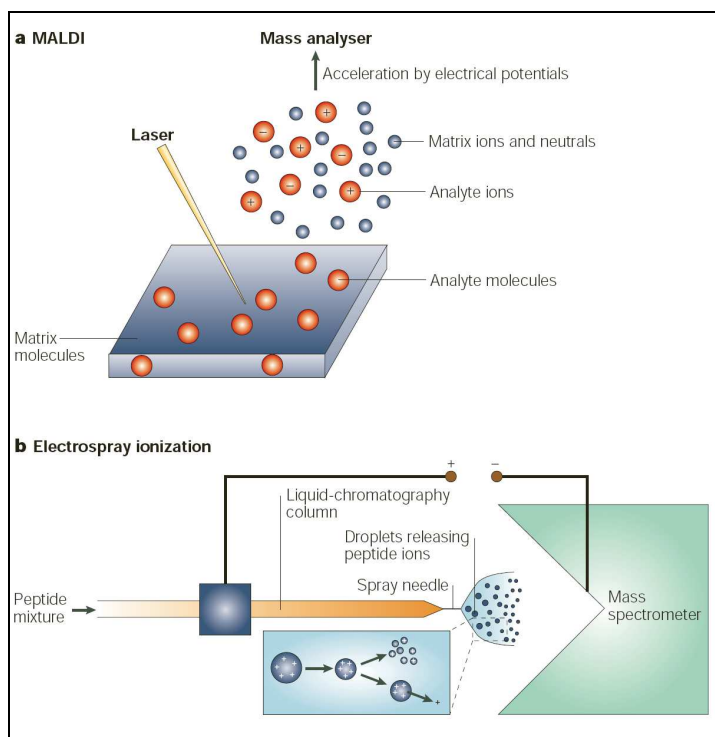


**Figure 10:** Two ionization techniques: matrix-assisted laser desorption/ionization (MALDI) (a) and electrospray ionization (ESI) (b) from Steen (et al.) (20). MALDI consists of targeting peptides with a laser which will ionize these peptides. ESI consists of applying a current between the end needle of a HPLC and the mass spectrometer. This current will ionize peptides.

Finally, the ionized molecules are injected into the mass spectrometer and peptide fragmentation is induced by collision with environmental gas. This collision causes an amide bond cleavage, creating b-ions when the charge is retained by the amino-terminal fragment or y-ions when it is retained by the carboxy-terminal fragment (*Figure 11*) (20). Some other types of fragments (e.g. a-ions) can also be produced depending on the type of ionisation (e.g. MALDI) and mass spectrometer.

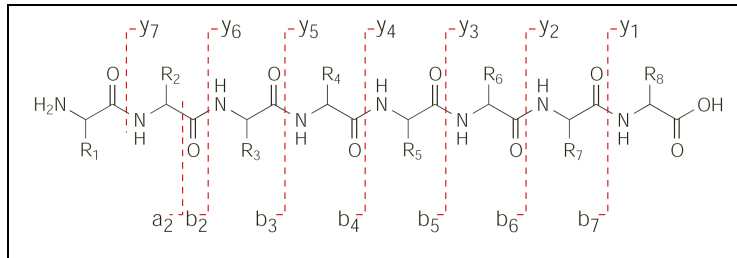


**Figure 11:** Fragmentation process during mass spectrometer collision from Steen (et al.) (20). *b*-ions represent fragments retaining charge at the amino-terminal and *y*-ions represent fragment retaining charge at the carboxy-terminal fragment.

The mass analyzer separates the peptide ions according to their mass over charge ratio ( $m/z$ ). This ratio is then recorded by the detector. Redundancy can be reduced by the use of an exclusion list containing the previously fragmented precursor ions (24). Each selected peptide can then be fragmented after collision induced dissociation (CID) into different fragment ions and be recorded as the MS/MS spectrum. This spectrum is composed of the  $m/z$  ratio of the precursor ion corresponding to its mass and charge state, as well as some *b*- and *y*-ions representing part of the amino acid sequence of the peptide (Figure 12). Each peak of the HPLC run represents a group of the most abundant peptides (a). The amount of peptides is therefore given by the height of each peak. The spectrometer can then select the most abundant peptides present in each peak and measure their total mass (MS) (b). Finally, these selected peptides are fragmented and the MS/MS sequence of each peptide gives their exact sequence (c).

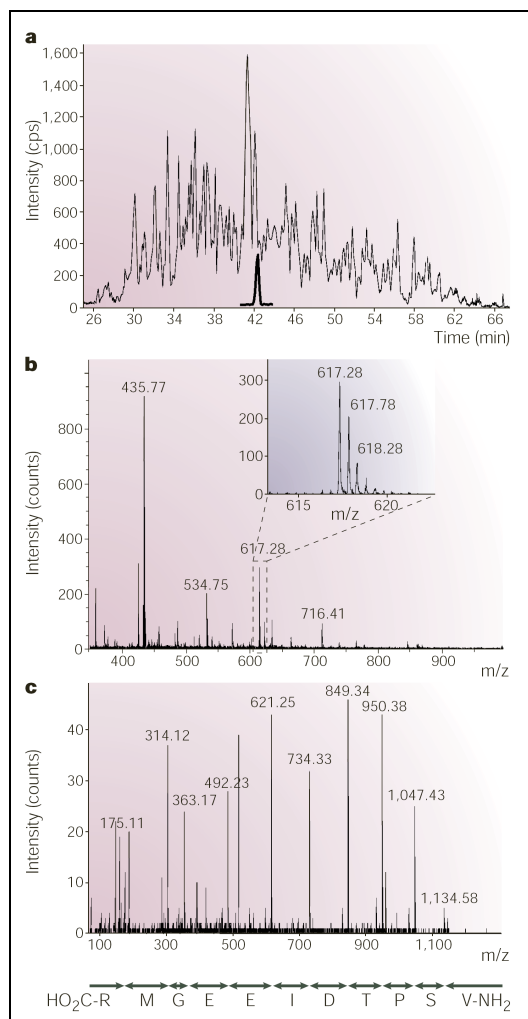


**Figure 12:** Chromatogram (a), MS (b) and MS/MS (c) spectra of a mixture of peptides separated on a HPLC column from Steen (et al.) (20). Mass spectrometer select the most intense peptides in each chromatogram peaks. Then mass of these peptides is determined during MS. Finally each peptide is fragmented and their sequence is given during MS/MS.

Three different approaches are commonly used to determine the correct identity of analyzed peptides (Figure 13). The first one, called Peptide Sequence Tags, (PeptideSearch) is based on interpretative models where it is assumed that each MS/MS spectrum contains at least a continuous serie of fragment ions giving a short amino acids sequence called amino acid tag (panel a). Together with the amino terminal mass ( $m_1$ ) and the carboxy terminal mass ( $m_3$ ), the peptidic sequence tag is searched in the database to match the complete peptide sequence (20). The second approach (panel b) is based on descriptive models like the Sequest algorithm, which mathematically correlates the experimental MS/MS spectrum with the

theoretical predicted MS/MS spectrum. The quality of the match is then quantified to give a cross correlation score reflecting the similarity between the spectra (20). The third approach (panel c) implies statistical and probability models. The Mascot search engine, which is based on the MOWSE scoring algorithm (25), evaluates all the matches between the input MS/MS spectrum and peptide sequences from the database. A probability (P) that the match is a random event is calculated for each peptide and a score is returned as  $-10 \times \log_{10}(P)$  for better convenience. Further information on database searching software can be found in recent reviews (26, 27).

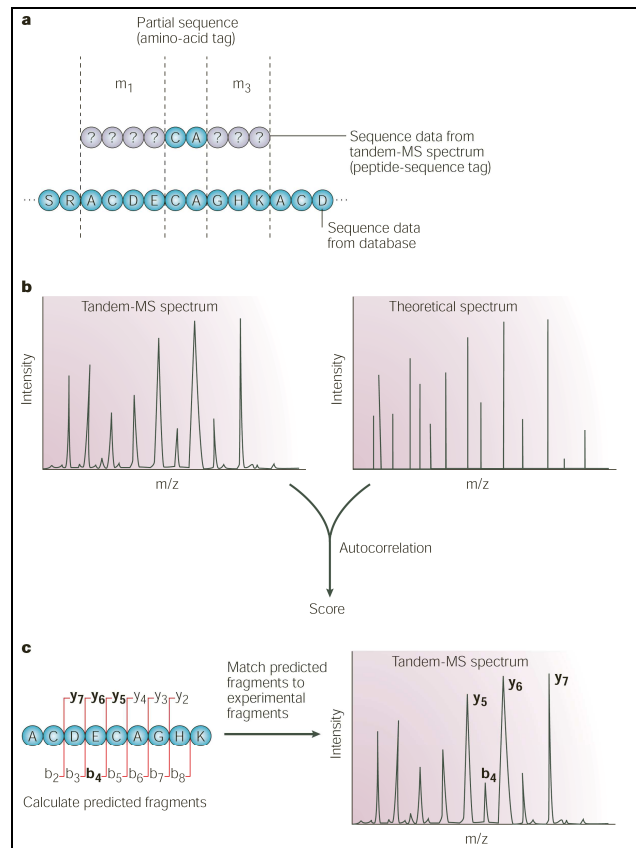


**Figure 13:** Different approaches in the identification of peptides from Steen (et al.) (20). These approaches consist of (a) matching sequence against a database with most intense fragments, (b) determining similarities with theoretical spectrum and (c) calculation of all predicted fragments contained in the database.

### 1.6.6 Identification of biomarkers and “therapeutic targets”

One of the main applications to proteomics is the identification of biomarkers. Biomarkers can be defined as a characteristic measured as an indicator of normal, pathological or pharmacological responses to a therapeutic treatment (28). These indicators are required to monitor diseases or therapeutic efficiency because of their intensity increasing after the disease becomes pathological.

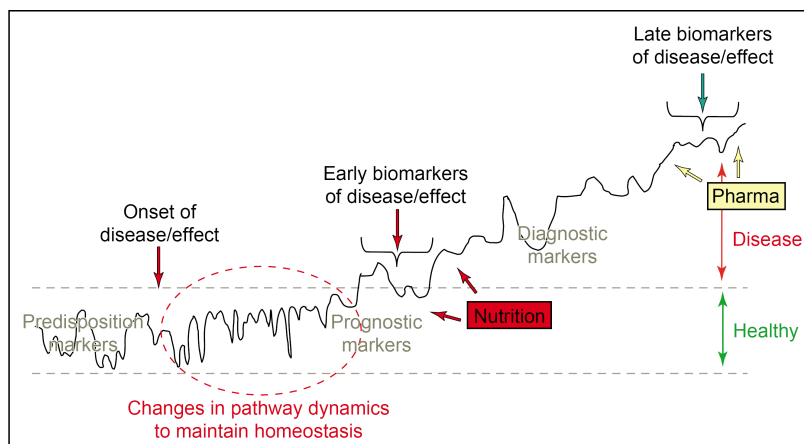


**Figure 14:** Development of diseases from healthy to disease state by monitoring biomarkers evolution from Van der Greef (et al.) (29).

For many human diseases, currently existing biomarkers are inadequate for early detection. The problem comes from the specific release of these biomarkers when disease has already occurred, making monitoring difficult (Figure 14) (19). Another drawback comes from the long validation process that occurred in the biomarkers discovery and identification before proteomics has emerged. This process was based on gene expression analysis, followed by validation of a candidate at the protein level using antibody assays (Figure 15) (30). Obtaining suitable antibodies against biomarker candidates followed by validation in plasma samples are the most time-consuming steps (30). Proteomics gave therefore new opportunities in this identification process.

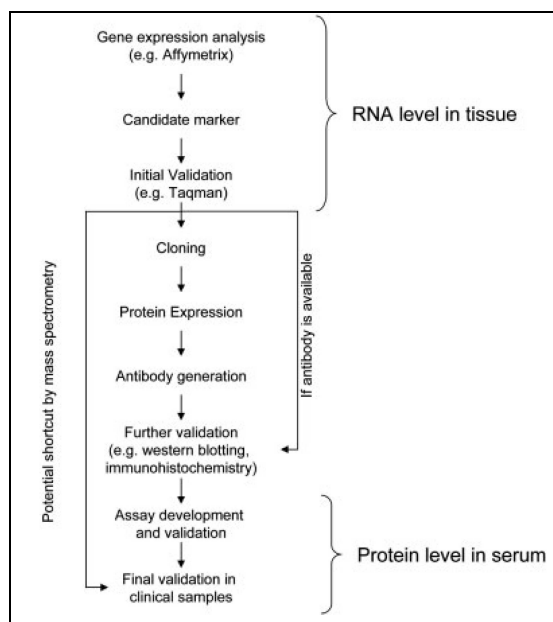


**Figure 15:** Biomarkers discovery and validation workflow from Immler (et al.) (30). The discovery starts with gene expression studies followed by antibody validation. This validation step can be avoided with the use of mass spectrometry.

The aim of applying proteomic to biomarkers is to help identifying new proteins in the early detection of disease. Moreover, proteomics allows simplifying the workflow by avoiding antibody validation using multi-dimensional separation followed by MS quantification. The quantification can be achieved using isotopically labelled synthetic peptide as internal standard (30). Finally, the clinical validation is performed using an Enzyme-Linked ImmunoSorbent Assay (ELISA). Proteomics, PTM evaluation and protein interconnection are complementary approaches in the identification of new biomarkers. By comparing control and treated models, or healthy and pathological patients, these approaches are very useful in the identification and the characterisation of new biomarkers candidates. *Table 1* represents biomarkers commonly used to identify diseases. Most of them are released after damages and new candidates of early detection would be useful.

**Table 1:** Protein biomarkers in diseases from the Plasma Proteome Institute. Biomarkers can identify different type of disease, including cardiac damages, cancer, inflammation, liver damage, coagulation disorders, allergy and infectious diseases.

Cardiac damage	Tnl, CK-MB, Mb, MPO, BNP
Cancer	PSA, CA-125, Her-2
Inflammation	CRP, SAA, cytokines, RF
Liver Damage	ALT, ALP, AST, GGT (enzyme assays)
Coagulation	AT-III, proteins C&S, fibrinogen, VWF
Allergy	IgE against various antigens
Infectious disease	HIV-I, Hepatitis BsAg

Finally, they can contribute to the designing of clinical trials by evaluating the safety and efficacy of the investigated compound or by providing information for guidance in dosing and thus minimizing inter-individual variation in response (28).

Applying proteomics in the identification of biomarkers can be used by three different approaches. The first one, called protein profiling tries to identify molecular signatures, or unique features within mass spectral profile, characterizing biological samples, specifically human serum samples (31). This approach is however restricted to the most abundant proteins. This unique profile is represented by the plot of the mass over charge ( $m/z$ ) ratio versus intensity of each detected peptide across many samples using a MALDI mass spectrometer. This approach however underestimates the complexity of the proteome and the difficulty of identifying the peak of interests. The two other methods: two-dimensional gel electrophoresis and liquid-based approaches. These different methods are used in all the different phases involved in the discovery and development of a biomarker and represented in *Table 2*.

**Table 2:** The five phases involved in the development and testing of disease biomarkers as proposed by the Early Detection Research Network (EDRN) from Duncan (*et al.*) (31). Phase I is the discovery phase, phase II is the validation phase, phase III is the pre-clinical phase, phase IV is the prospective clinical phase and phase V is the large scale clinical phase.

Phase I	Exploratory studies to identify potentially useful biomarkers (i.e., the “discovery” phase).
Phase II	Biomarkers are studied to determine their capacity for distinguishing between people with cancer and those without (i.e., the “validation” phase).
Phase III	Studies to assess the capacity of a biomarker to detect preclinical disease by testing the marker against tissues collected longitudinally from research cohorts.
Phase IV	Prospective screening studies.
Phase V	Definitive large-scale population studies to determine the overall impact of screening on health outcomes in the target population.

## 1.7 Quantitative methods for proteomic studies

Mass Spectrometry (MS)-based techniques allow analyzing large amount of protein. This method has the advantage of allowing quantitative approach. Quantitative studies involves a differential level of expression between two experimental conditions and are therefore the most common approach in proteomics. This approach can give an absolute or relative amount of proteins in the sample and may be used specifically in certain type of experiment, such as toxicology. To perform an acute quantitative measurement, complex protein samples must be simplified before protein identification. Researchers have access to a variety of different separative techniques including 2-D gel electrophoresis, combined with different staining and visualization methods, as well as liquid-based approaches, including proteins or peptides labelling, to process and analyze their samples. The workflow for protein identification using different separative techniques is illustrated in *Figure 16*. This workflow contains the following steps: reduction of complexity, protein targeting (in case of 2-DE gel), protein digestion, peptides ms/ms analysis, peptide identification and protein identification by grouping peptides.

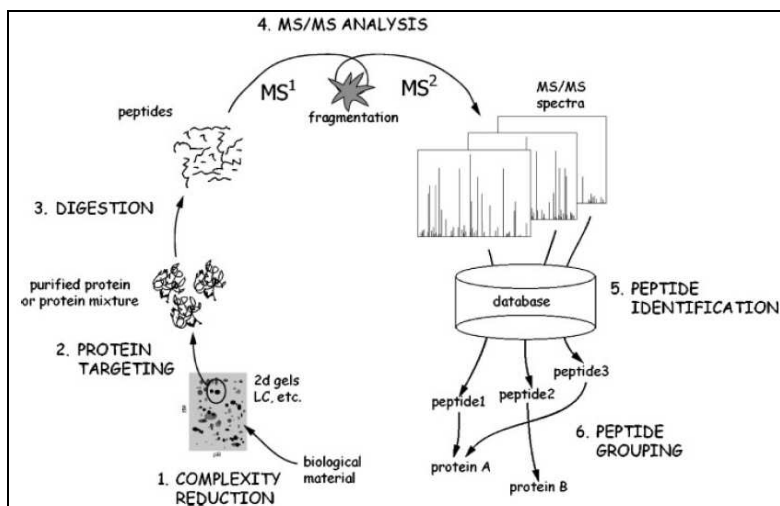


**Figure 16:** Workflow for protein identification based on tandem mass spectrometry from P. Hernandez (24). The different phases implied in peptide identification include protein separation, isolation, digestion and peptide fragmentation. Finally a database is used to group peptides and identify protein.

The quantitative techniques can be divided into two groups, called the gel-based approaches, including 2D polyacrylamid gel electrophoresis (2D-PAGE), Differential Gel Electrophoresis (DIGE) technology and the liquid-based approaches where multidimensional LC-MS/MS is used in conjunction with different protein/peptide labelling techniques such as ( $O$ -18, cICAT, SILAC, iTRAQ, etc.). The Table below gives an extensive overview of the techniques used today to achieve high throughput analysis (Table 3).

**Table 3:** Quantitative techniques based either on 2-DE or on liquid-based approach.

Densitometric comparison in 2 DE	Liquid-based quantification
<b>Visible stain</b> Coomassie, Silver	<b>Precursor ion</b> $^{18}O$ , AQUA, cICAT, ICPL, Metabolic labelling, SILAC
<b>Fluorescent dye</b> DIGE, SYPRO	<b>Reporter ion</b> iTRAQ, tandem mass tag
<b>Radiolabelled detection</b> Different isotope	<b>Label free</b> Replicate, emPAI, average

---

### ***1.7.1 Densitometric comparison in 2D gel electrophoresis***

Two dimensional gel electrophoresis (2-DE) is one of the most frequently used method for separating proteins (6). The immobilized pH gradient (IPG) and 2-DE technique has first been described by Patrick O'Farrell in 1975 and extensively reviewed by Angelika Görg in 2004 (44, 45). Several improvements have been made to this method in the past few years in 1993, 2000 and 2004 (46-48). Principle of 2-DE is to separate proteins on the basis of their charge (*i.e.* pI) in the first dimension and their molecular weight in the second. This process is used to isolate each protein that will be compared, once labelled, between two experimental conditions.

### ***1.7.2 Sample preparation***

Appropriate sample preparation is critical for obtaining optimized 2-DE results. The process should allow the complete solubilisation, disaggregation, denaturation and reduction of the proteins contained in the sample. These steps are very important to obtain a well-focussed first dimensional separation. Among the reagents used, urea solubilises and unfolds most proteins to their linear conformation, detergent solubilises hydrophobic proteins and minimizes protein aggregation and reducing agent cleaves disulfide bonds to allow proteins to unfold completely. Proteins are therefore denatured into their linear structure (polypeptides), losing their three dimensional conformations, avoiding intermolecular interactions. Finally, polypeptides must be protected from protease liberated from cell disruption by using protease inhibitors such as leupeptin or aprotinin. If a subset of the tissue or cell is of interest, protein fractionation technique or reduction of the pI range may be used.

### ***1.7.3 First dimension: Isoelectric focusing (IEF)***

Proteins are then separated by isoelectric focusing (IEF) after a current is running through the solution. The sample is often loaded in the first dimension by rehydration of a commercial IPG strip. This technique allows larger quantities of protein to be loaded, reduces the formation of precipitate and avoids problems of leakage compared with cup loading. IEF is an electrophoretic method that separates proteins according to their isoelectric point (pI). The current makes the charged polypeptides migrate through an immobilized pH gradient gel strip until they reach their isoelectric point. The pI is the specific pH at which the sum of

negatively charged amino acids is equal to the sum of positively charged amino acids. In other words, the protein pI corresponds to a net charge of zero (*Figure 17*).

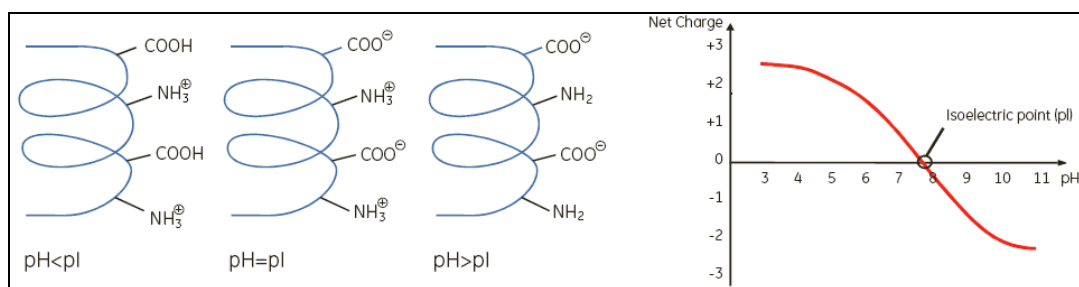


**Figure 17:** Net charge of a protein versus the pH of its environment from 2-D electrophoresis, principles and methods, GE Healthcare Life Sciences. The pH of the environment influences the overall charge of a protein. Once pH equals pI, the net charge of this protein equals zero.

Once the pI is reached, the protein stops migrating. An appropriate first dimensional separation requires selecting a first-dimension pH range corresponding to the complexity of the sample. For example, a pH of 3-10 is often used for an overview of total protein distribution. To obtain a more detailed overview of the sample it is possible to combine pH 4-7 and 6-9 or even narrower pH window of one unit. Now such strips are manufactured which improve resolution and reproducibility.

#### 1.7.4 Second dimension: SDS-PAGE

After IEF, SDS-PAGE (sodium dodecyl sulphate -polyacrylamid gel electrophoresis) is performed. This approach is an electrophoresis method for separating proteins according to their molecular weight (MW). The gel strip containing proteins is placed on the top of a precast polyacrylamid gel containing sodium dodecyl sulphate. The first dimensional focused proteins migrate on the second dimension after applying an electric current. The intrinsic electrical charge of the sample proteins is not influencing the separation due to the presence of SDS in the sample and the gel. By forming micelles around the proteins, SDS masks the overall protein charge, allowing the migration occur according to the molecular weight. Beside SDS, a reducing agent such as dithiothreitol (DTT) is also added to break disulfide bound. Reduction and prevention of re-oxidation is crucial for cleavage of intra- and intermolecular disulfide bonds (32). This step is necessary to achieve complete protein

---

unfolding necessary for a proper migration. By adding SDS and DTT in the sample solution, proteins follow a linear relationship between the logarithm of the molecular weight and the relative distance of migration of the SDS-protein complex. In addition, an alkylating agent is added, iodoacetamide to alkylate sulfhydryl groups and preventing their reoxydation by binding covalently to cystein groups. This step is crucial for acute spot identification by MS (32). The difficult issues with 2-DE are to solubilise correctly proteins, to elute without streaking alkaline or hydrophobic membrane proteins, to migrate properly low or high molecular weight proteins and to accurately and reproducibly quantify stained proteins.

Once separated, proteins have to be fixed and visualized. Most common detection methods of proteins on 2-DE gels include staining with anionic dyes (*e.g.* Coomassie Blue), silver-staining, fluorescence labelling, and radioactive isotopes labelling, using autoradiography or phosphor-imaging (32). Proteins are most often detected with visible staining (silver stain, Coomassie blue) or with fluorescent tags (33). Protein visualization methods should be highly sensitive, possess a high linear dynamic range, reproducible, and compatible with identification processes, such as MS (32). Finally, in order to compare the density of two spots, gels must be scanned with a densitometer. These images are then aligned digitally, and pairs of gels are compared spot by spot to reveal changes in abundances. 2-DE is the major method of separating proteins, although it is considered a labour-intensive and low throughput technique with poor reproducibility (6). Identification of protein has been improved with commercial nonlinear IPG strips allowing reducing the pI range, therefore reducing the overlapping spots. This approach allows the loading of a more important amount of sample, increasing the sensitivity of the method. The drawback is the increased amount of gels that has to be run to cover the whole pI range. Protein separation with 2-DE gel require considerable manual manipulation, however they provide the separation of several thousand soluble proteins with resolution as yet unequalled by other methods of protein preparation (*Figure 18*) (33). Several improvements have been made to reduce the manual manipulation, like automated spot picker but this method will never be fully automated.

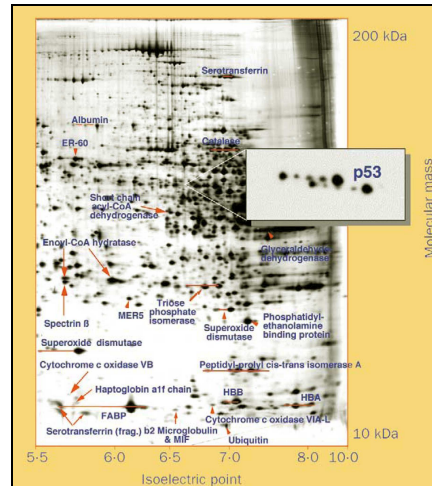


**Figure 18:** Example of silver stained 2-dimensional gel electrophoresis and some identified proteins from *R. Banks* (8). X axis represents the isoelectric point (pI) of the protein and the Y axis represents the molecular weight (Mw) of the protein.

### 1.7.5 Protein detection

The major challenge while detecting protein with visible staining is the range of concentration of individual proteins which differ between six or seven orders of magnitude and from several millions of copies per cell for highly abundant proteins (*i.e.* glycolytic enzymes) to a few copies per cell for low abundant proteins (32). The two most common used techniques for the visualization of protein is Coomassie Blue and silver staining. Those two staining reagents possess the required properties enumerated below, although Coomassie has a lower sensitivity which is one of its limitations. Coomassie blue is an anionic dye and the sensitivity of protein detection can be as low as 5 ng, although the actual limit of detection depends on the individual protein and is closer to 200-500 ng per spot (32). Even if colloidal dispersion of Coomassie blue has been reported to be more sensitive, this staining is still much less sensitive than the other staining methods (34). Because of its low price, ease of use and compatibility with MS, this method is the most commonly used. Typically a hundred spots can be visualized on a gel with milligrams of tissue loaded.

Silver staining is much more sensitive so that 1000–3000 proteins per gel can be visualized and this high sensitivity staining can detect as little as 0.1 ng of protein (47, 51). There is a wide spot variability and even staining artefact in presence of DNA or lipopolysaccharide which can result in background staining of the gel. This staining method

is not stoichiometric and much less reproducible than Coomassie, due to the individual development of the staining procedure which makes it less suitable for quantitative analysis (32). Finally this staining technique is time consuming because protein must get rid of formaldehyde and glutaraldehyde contained in the fixing solution to avoid protein modification during the mass spectrometer analysis (35).

### 1.7.6 Fluorescent dye

Fluorescent dyes often provide greater sensitivity and broader linear dynamic responses when compared to colorimetric staining as shown on *Figure 19* (36). An advantage of this approach is that the detection of the signal covers a much wider range than for the non-fluorescent alternatives. This approach allows avoiding the superimposition of two gel images resulting in warping the gels to overlay and compare them. This technical manipulation makes image comparison and spot detection complex, particularly when protein variations are subtle. The traditional visible approach often implies to run several replicates to be confident. This requires the creation of a “control master gel” which can be compared with a “treated master gel” and is thus time consuming.

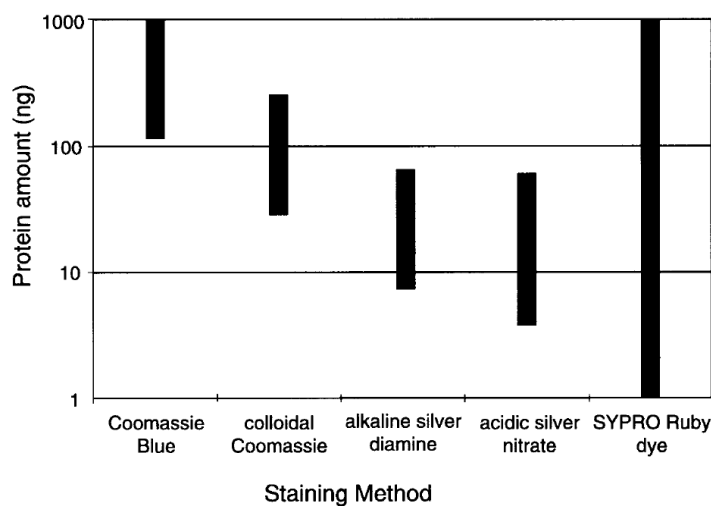


**Figure 19:** The linear dynamic range of commonly employed protein gel stains adapted from F. Patton (36). The staining method influences the total amount of protein being visible. Coomassie blue is less sensitive than silver staining and SYPRO covers a wider dynamic range but requires a laser detector.

There are two types of fluorescent dyes: covalent, prior to IEF and non covalent labelling, post-electrophoretic protein staining. Covalent dyes include DIGE (Differential Gel Electrophoresis) and are incorporated to proteins before running the gel. Two protein samples are pre-labelled with amine reactive fluorescent dye, consisting of two cyanine dyes (Propyl-Cy3 and Methyl-Cy5), enabling to run two samples on the same gel (37). These two fluorophores are similar but spectrally distinct (*Figure 20*). Their N-hydroxysuccinimidyl esters reacts by nucleophilic substitution with lysine amine groups on proteins to form an amide (38). The dyes have very close molecular masses and are positively charged to be able to react with the charge on the lysine group. To avoid multiple dyes labelling on the same protein, the ration protein/dye must be kept low.

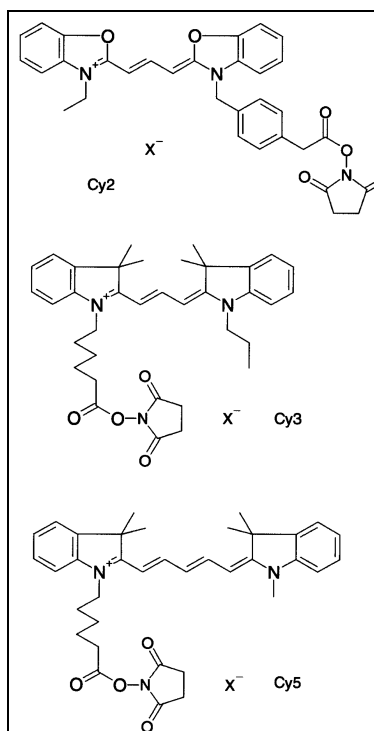


**Figure 20:** Structure of cyanine dyes: Cy2, Cy3 and Cy5 from Tonge (*et al.*) (38).

This technique has the advantage to avoid technical variations and eliminates the need to detect spots on two separate gels. Using the traditional 2-DE approach implies to repeat the procedure three to six times in order to reduce technical variability. The comparison can be made without warping the gels. This approach has the advantage of reducing the number of gel required to make a statistical comparison and raise the confidence of the detection and quantification of changing spots (38). The dyes are now commercially available with Cy2,

Cy3 and Cy5. The third dye is used as internal standard for minimizing experimental variations. The major challenge with this pre-electrophoretic protein binding is the protein mass modification due to the addition of the label migration. Since only 1-2% of the proteins are labelled in the samples, there is a shift in migrating over the samples on the second dimension between the labelled and unlabelled protein which might cause problem of protein identification. More than 95 percent of the protein can be significantly shifted away from the labelled protein in the MW dimension particularly at lower protein masses which can cause problem during automated spot picking excision from the gel for MS identification (54, 55). *Figure 21* show migrating differences between green and red dye (circled spots). The exact positions where the maximum amounts of the considered protein are located are thus missed, leading to a loss of sensitivity of the MS analyses and resulting in a reduced reliability and sequence coverage (39).

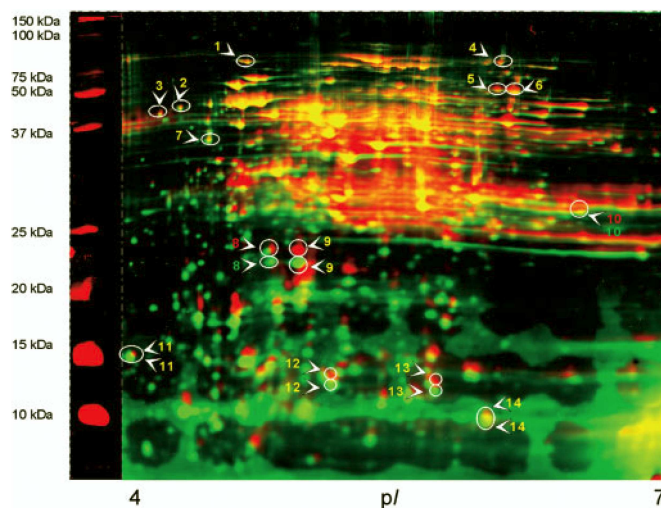


**Figure 21:** *Overlay fluorescence image of 2-DE gel after Cy5 (red) and Ruby or Deep Purple (DP) (green) staining illustrating the labelling-induced shifts in spot position particularly in low molecular masses from Hrebicek (39).*

The other type of dyes is the non-covalent binding including ruthenium-based SYPRO dyes and is incorporated by intercalation of fluorophores into the micelles coating the proteins. These fluorophores are non fluorescent in aqueous solutions and become fluorescent upon association with SDS-protein complexes. This procedure is accomplished in a single step which can be easily automated. Since SYPRO dyes are not present during electrophoresis, this approach avoids protein aberrant migration.

### ***1.7.7 Radiolabelling of proteins***

This approach, combined with electronic detection methods offer a highly sensitive detection method. Radiolabelling can be achieved by incorporating different radioactive isotopes ( $^3\text{H}$ ,  $^{14}\text{C}$ ,  $^{32}\text{P}$ ,  $^{33}\text{P}$ ,  $^{35}\text{S}$ ,  $^{131}\text{I}$  or  $^{125}\text{I}$ ) into proteins. These isotope-labelled proteins can be detected either with autoradiography or fluorography using X-ray films exposure. This technique may need several days or weeks to reach desired sensitivity. The alternative of this time consuming approach is the exposure of the radiolabelled gel to a storage-phosphor screen which can be scanned with a He-Ne laser on a phosphor-imager. This laser densitometer can help reaching very low levels of radioactivity with a very high linear dynamic range. This approach can also be used when incorporating isotope during protein synthesis (Stable Isotope Labelling by Amino acids in Cell culture) (SILAC).

The major limitation of most visible or fluorescent staining approach is their lower sensitivity compared to electronic detection methods of radiolabelled proteins or liquid-based labelled peptides. Typically, only proteins expressed at higher level than 10<sup>3</sup> copies/cell can be detected on standard 2-DE gels by using fluorescent dye technologies, whereas less than a dozen copies of a protein/cell can be visualized with the most sensitive electronic detection methods for radiolabelled proteins (32).

### ***1.7.8 2-DE Analysis***

In theory, the analysis of up to 15'000 proteins should be possible in one gel, but, according to the principles and methods of 2-D Electrophoresis from Amersham Biosciences, 5'000 detected protein spots means a very good separation (32). Protein identification based on MS/MS spectra is a challenging issue mainly due to identification algorithms. Among the difficulties we can mention expected or unexpected modifications of the peptide sequences, polymorphisms, errors in databases, missed or non-specific cleavages, unusual fragmentation patterns, and single MS/MS spectra of multiple peptides of the same  $m/z$  (24).

---

### ***1.7.9 Post-Translational Modifications***

Phosphoproteomics is the field of increasing importance. The described tools will help characterizing all phosphorylation states or elucidation of the entire cell phosphoproteome. 2-DE gel and phosphoprotein enrichment are complementary techniques to study and analyse this issue. Anyway these approaches lack more molecularly relevant parameters, such as: molecular half-life, synthesis rate, functional competence (presence or absence of mutations), reaction kinetics, the influence of individual gene-products on biochemical flux, the influence of the environment, cell-cycle, stress and disease on gene-products, and the collective roles of multigenic and epigenetic phenomena governing cellular processes (40).

One of the strength of 2-DE is its capability to readily locate post-translationally modified proteins, as they frequently appear as distinctive rows of spots in the horizontal and/or vertical axis of the 2-DE gel. Up to now, several hundred PTMs, including phosphorylation, glycosylation, acetylation, lipidation, sulfation, ubiquitination or limited proteolysis have been reported. Specific staining methods for detection of PTM are employed either directly in the 2-DE gel or, more frequently, after transfer (blotting) onto an immobilizing membrane (32). The two major PTM analysed with the 2-DE approach are phosphorylation and glycosylation. In addition to the traditional protein analysis, new techniques has recently emerged to study PTM and protein-protein interactions (41). Phosphorylation is one of the most abundant PTM and techniques have been optimized these last years to better understand this new approach. These new tools include immunoprecipitation with specific phospho-antibodies, affinity chromatography with Immobilized Metal Affinity Chromatography (IMAC) or titane dioxide (TiO<sub>2</sub>) and chemical modification with phosphoamidate or phosphate  $\beta$ -elimination (9).

Protein phosphorylation is a crucial PTM required for the control of regulatory pathways like receptor signalling, enzyme activities, cell division or degradation of proteins. More than 50% of all proteome are phosphorylated reaching a total of 100'000 estimated phosphorylation sites in the human proteome (42). The major amino acids known to be phosphorylated are serine, threonine, and tyrosine residues. Most of the residues are quantitatively phosphorylated but some may only be transiently phosphorylated. Many techniques are now available to study phosphoproteomics. The major challenge is that

---

phosphorylation happens in the first minutes after the initiation of the signal. The addition of phosphatase inhibitors is thus required. Phosphorylation analysis can be achieved either in 2-DE gel approach or by enrichment of phosphoproteins and peptides. 2-DE gel approach implies using phosphospecific stains like Pro-Q Diamond (Invitrogen), immunoblotting a transferred membrane with specific phospho-antibody or radioactive labelling the phosphate group using  $^{32}\text{P}$ . The most sensitive method is radioactive labelling but this approach might lead to some unspecific phosphorylation. Commercially available phospho-stains are less sensitive and immunoblotting can detect very low amounts (few femtomoles) of phosphoproteins but specificity and sensitivity is strongly dependant on the respective antibodies (9). All these methods can only give an approximation of the result due to co-migrating proteins within the gel.

The enrichment of phosphoproteins and peptides is getting more popular in the phosphoproteomics analysis (42). It consists of immunoprecipitating the sample with specific phospho-antibody, elution of the protein sample through an affinity column which retains phosphoproteins by electrostatic interactions: Immobilized metal-ion affinity chromatography (IMAC) or  $\text{TiO}_2$  or even chemical modification of the phosphate group with phosphoamidate (9).

Glycosylation is the second most frequent PTM and is associated with pathogenesis or biochemical alterations. This protein modification can be detected with Pro-Q Emerald 488 (Invitrogen) which reacts with carbohydrate groups by emitting a green-fluorescent signal. This type of stain allows detection of approximately 5-20 ng of glycoprotein per spot (32). Another approach when detecting glycosylation consists of binding glycoprotein with sugar binding lectins. These lectins might be labelled with different fluorescent molecules or enzymes. When analysing in details glycoprotein composition, a LC-MS based approach is required (32).

## 1.8 Liquid-based techniques

As described previously, proteomics has been used for the quantitative analysis of protein amounts in complex extracts with 2-DE gel. However, the limitations of this approach in terms of throughput and analyzable protein range have elicited the development of other proteomics approaches, based on peptide separations instead of protein separations. The term proteomics is now associated with a great variety of analysis technique from protein identification to characterization and quantification. The techniques described below are thus more often used with a liquid-based approach (LC-MS/MS) but some might be used with 2-DE gel. Yates (*et al.*) described a largely unbiased method for rapid and large-scale proteome analysis by multidimensional liquid chromatography, tandem mass spectrometry, named multidimensional protein identification technology (MudPIT) (43). MudPIT is a technique for the separation and identification of complex protein and peptide mixtures. Rather than use traditional 2D gel electrophoresis, MudPIT separates peptides in 2D liquid chromatography. Typically, peptides are first separated according to their charge state by a cation exchange chromatography (SCX) and then according to their hydrophobicity in the second dimension by reversed-phase chromatography (C18). The separation is normally interfaced directly with the ion source of a mass spectrometer as shown on *Figure 22*.

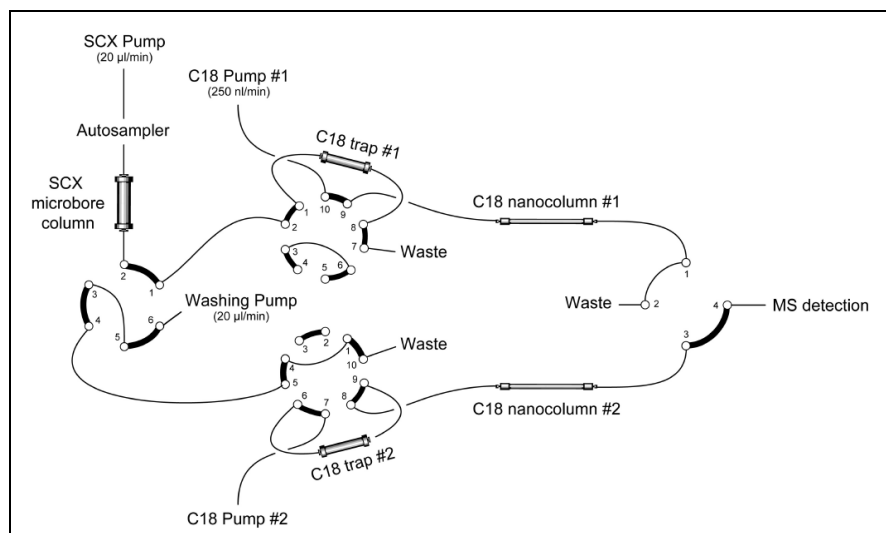


**Figure 22:** 2D dual nanoscale LC-MS/MS from Varesio (*et al.*)(44). Peptide solution is eluted through a cation exchange column (SCX). This column separates peptides according to their charge. Then a C18 nanocolumn separates peptides according to their hydrophobicity. Switching trap column are required to remove gradient salts from solution.

This method is the most suitable using differential labeling when comparing two experimental conditions. The use of stable isotope labelling to code proteome is one of the most recent approaches. These isotopes can be incorporated metabolically (SILAC), chemically either at the protein level (cICAT) or at the peptide level (iTRAQ) or even during the enzymatic cleavage ( $^{18}\text{O}$ ).

### 1.8.1 Quantitation based on precursor ions

Quantification of peptides can be based on precursor ions generated from isotope incorporation in the peptides. Isotope can be enzymatically incorporated into peptides. The most common way is to introduce two atoms of  $^{18}\text{O}$  into the carboxylic acid group of every proteolytic peptide in a protein pool using  $\text{H}_2^{18}\text{O}$ . The incorporation of this isotope can be achieved either with trypsin, Glu-C protease, Lys-C protease and chymotrypsin (*Figure 23*) (61-63). This labelled pool of peptide can be compared with the same pooled control samples labelled with  $^{16}\text{O}$  contained in regular water. This technique has the advantage to label all peptides except the original C-terminus of the protein (33). Stewart (*et al.*) has described a method allowing the conservation of the labelled peptides in natural abundance water without fear of chemical back-exchange with  $\text{H}_2^{16}\text{O}$  by adjusting the pH carefully.

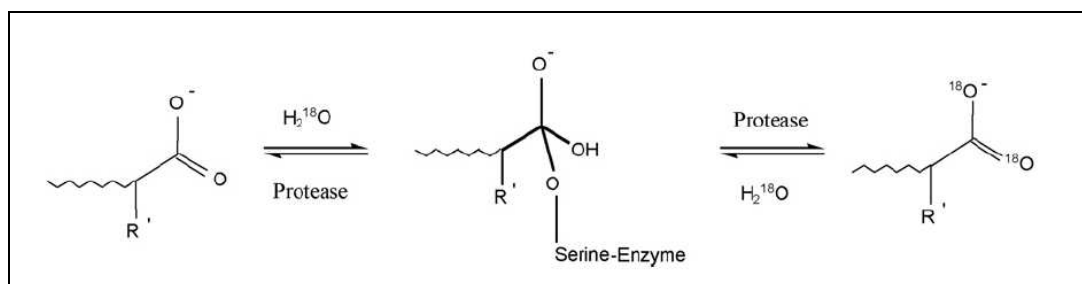


**Figure 23:** Incorporation of two atoms of  $^{18}\text{O}$  by reversible binding of peptides by members of serine protease family from Fenselau (*et al.*) (33).

Another way to analyze peptides based on precursor ions is to incorporate stable synthetic isotope as internal standards to provide absolute quantification. The first example of this technique has been made by Barr (*et al.*) who incorporated deuterium labelled peptides corresponding to the proteolysis counterpart of the apolipoprotein A1 present in the sample (45). This internal standard allows peptides to be quantified because they change their mass but not their chemical behaviour. This technique called AQUA (Absolute Quantification) by

Gygi (*et al.*) allows multiple peptides to be quantified in a single sample and these internal standards peptides are used to precisely and quantitatively measure the absolute level of protein and post-translationally modified proteins (46). Different approaches involve chemical derivation isotope incorporation. The first one has been made in 1999 by Aebersold (*et al.*) who introduced the Isotope-Coded Affinity Tag (ICAT) (47). The method is based on stable isotope dilution techniques coupled with tandem mass spectrometry and allows comparing two biological samples in a single analysis. An affinity reagent is covalently bound to a particular amino acid (cysteine) in all proteins present in the sample (*Figure 24*) and the relative abundance of protein is determined using the ratio between two similar peptides offset by 8 Daltons.

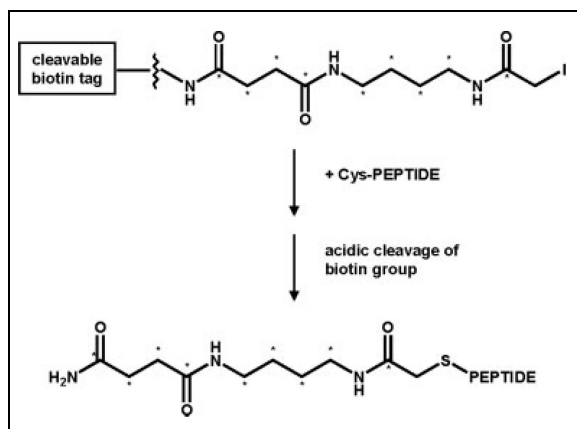


**Figure 24:** Structure of the cleavable Isotope-Coded Affinity Tag (cICAT) tag and labeling of cysteine containing peptides from Leitner (*et al.*) (48). Cystein containing peptides are tagged with cICAT reagent which is coupled with a biotin tag. Then these tagged peptides are extracted from solution with affinity column and analyzed after cleavage of biotin group.

The proteins are then digested into peptides and the labeled peptides are purified with an affinity tag leading to a simplification of the sample mixture. The affinity tag consists of a biotin which will be retained on a streptavidin affinity matrix leading to the extraction and purification of the labeled peptides. The drawbacks of this technique include non specific binding to the matrix and incapacity to extract non cysteine containing proteins. Aebersold simplified his technique by coupling cysteines with solid beads giving a simpler, more efficient and more sensitive aspect to this approach (49). However the limitation to cysteine containing protein may compromise low level analysis. The quantification is based on the difference in mass of the tag between the control and treated experiment at the first stage MS.

Several other similar techniques have been proposed later, based on the chemical modification of proteins or peptides. Münchbach (*et al.*) has elaborated a similar technique to ICAT but based on tagging the peptides on their N-terminal amino acid either with H4 or with D4 reagent. The quantification is then based on the 4 Da difference in the MS spectra instead of the 8 Da or 9 Da difference for ICAT or cleavable isotope coded affinity tag (cICAT) reagents, respectively (*Figure 25*) (50).

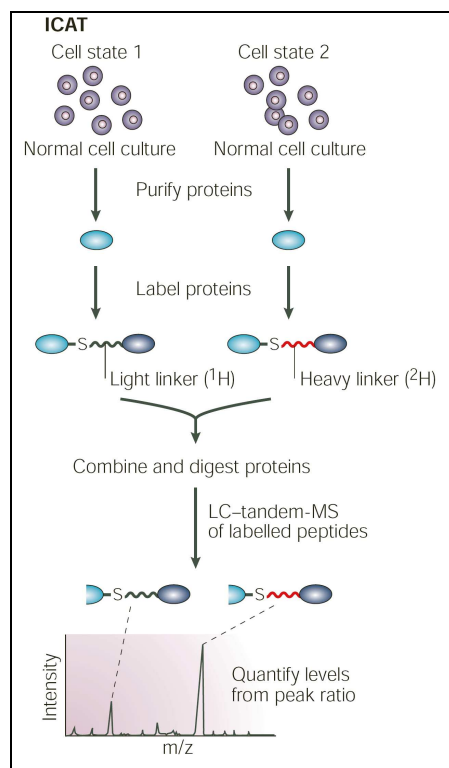


**Figure 25:** Schematic representation of the ICAT method from Steen (*et al.*) (20). Samples are tagged either with light ( $^1\text{H}$ ) or heavy ( $^2\text{H}$ ). Then proteins are extracted and quantification is performed at the MS level where a difference of 8 Da exists between light and heavy.

Cagney modified this method by proposing his Mass-Coded Abundance Tagging (MCAT) based on differential guanidination of C-terminal lysine residue of peptides (51). The principle is based on the modification of a lysine residue using O-methylisourea which transforms the lysine into homoarginine which is 42 Dalton heavier than lysine. Moreover, this modification does not affect the biophysical properties using LC-MS. The quantification is then performed by monitoring the ratio between modified and non-modified proteins. The

next improvement based on differential protein analysis has been made by Goodlett (*et al.*) who proposed a per-methyl esterification of peptides (52). The quantification was based on the difference of the D0- or D3-methanol once separated from the corresponding peptide in the second dimension of the tandem mass spectrometer (MS/MS). Another method based on the relative intensities of extracted ion chromatograms is called Isotope-Coded Protein Label (ICPL). This method is capable of high throughput quantitative proteome profiling and is based on stable isotope tagging at the frequent free amino groups of isolated intact proteins (53). Two different experimental groups are individually alkylated and differentially labeled at the free amino groups with isotope encoded (heavy) or isotope free (light) ICPL tags (53). *Figure 26* describes the workflow of this amine-based tagging.

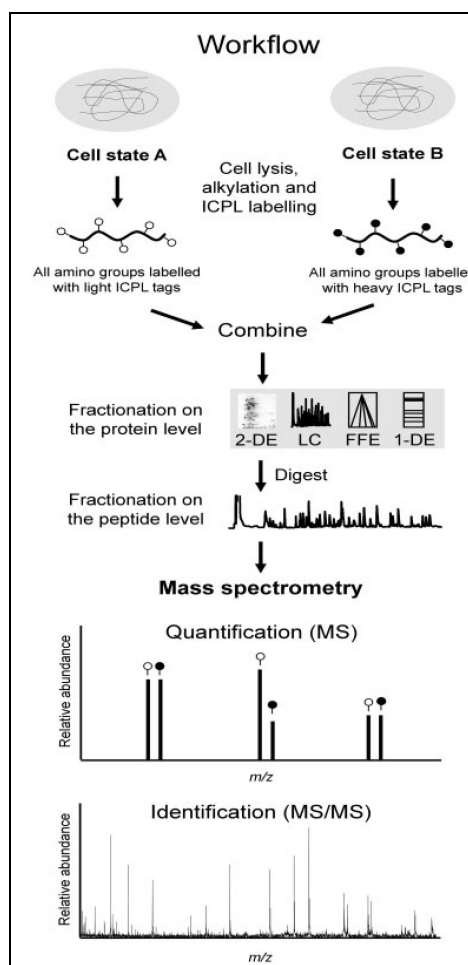


**Figure 26:** Overview of the ICPL workflow from Schmidt (*et al.*) (53).

These stable isotope labeling techniques for proteomics are often based on complex and expensive reagents. A different approach emerged and was based on metabolic

incorporation of labeling protein into protein (54). This approach is particularly adapted to single cells grown in culture and different isotopically enriched amino acids can be used such as arginine, lysine, tyrosine and leucine. An enhanced metabolic labelling technique emerged then from specific incorporation of amino acids in cell into all mammalian proteins. This technique has been described by Ong (*et al.*) and is called SILAC (Stable Isotope Labelling by Amino acids in Cell culture) (55). It allows comparing two different populations of cells which will be labelled either with a normal amino acid or an isotope labelled amino acid. Cell culture media lack an essential amino acid which is replaced, with the same labelled amino acid. This labelled amino acid is then incorporated into all proteins during protein synthesis (Figure 27).

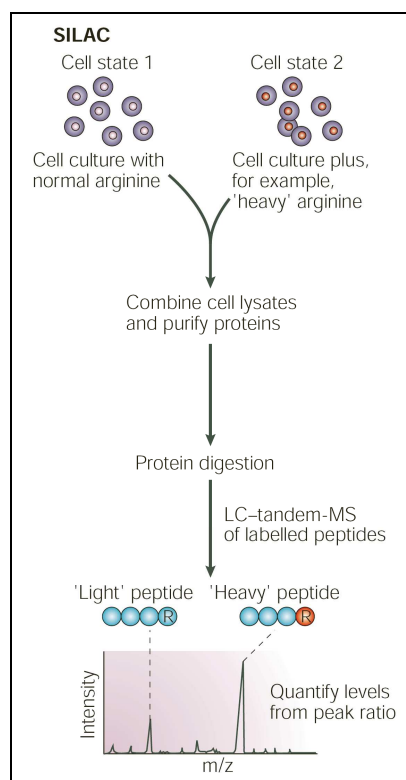


**Figure 27:** Schematic representation of the SILAC method from Steen (*et al.*) (20). Isotopically enriched amino acid is incorporated during cell culture growth, which can be seen as a shift in mass in the MS analysis.

No chemical labelling or affinity purification steps are necessary using this technique which is compatible with all cell culture conditions, including primary cells. Ong (*et al.*) show that incorporation of the labelled amino acid is complete in the proteome and that cells

remain normal in the presence of the labelled media. These incorporations can be used with arginine, lysine, tyrosine and leucine (74-77).

### 1.8.2 Quantitation based on reporter ions

These improvements introduced the iTRAQ reagents (Isotope-Tagged amine-reactive reagents for Relative and Absolute Quantitation) based on a multiplexed set of isobaric reagents that yield amine-derivatized peptides (78). This technique allows quantitative comparison of four different protein pools simultaneously. The quantitative measurements can be done either using LC-MS/MS with electrospray or MALDI with TOF. Each reagent contains a reporter ion whose mass differs of one Dalton from each others (*i.e.*  $m/z$  114, 115, 116, and 117) and a balance moiety that give the same global mass and physico-chemical properties for each tagging reagent. When tagged peptides experience fragmentation, the charge remains on the reporter group and the balance group is removed as a neutral loss (Figure 28).

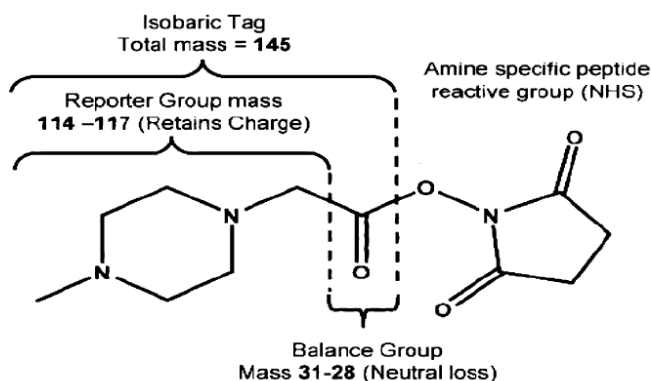


**Figure 28:** Isotope-Tagged amine-reactive reagents for Relative and Absolute Quantitation (iTRAQ) tagging strategy from Fenselau (*et al.*) (33). An isobaric tag of 145, containing a reporter group ranging from 114 to 117 and a balance group containing masses from 31-28 is covalently bound to amino-terminal group of all peptides.

Peptides from four different samples are tagged separately with single channel iTRAQ reagent and then mixed together prior to the analysis (Figure 29). The derivatized peptides are indistinguishable in MS, but exhibit intense low-mass MS/MS signature ions that support quantitation.

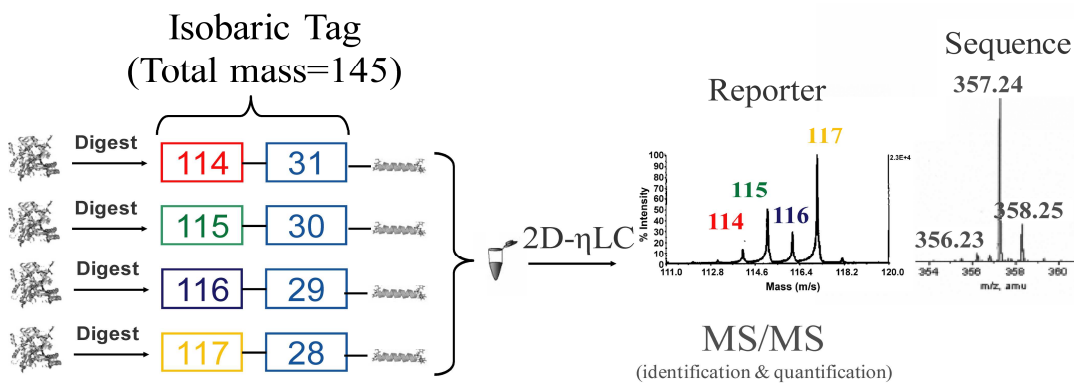


**Figure 29:** *iTRAQ* reporter ion quantitation and peptide identification in four different experimental conditions. Pooled peptide arrives at the same time in the mass spectrometer. The reporter group gives the quantification of each experimental condition.

Each channel is represented by an experimental procedure and the ratios of the same protein coming from four different samples are measured in the MS/MS spectra by comparing reporter ions peak areas (*Figure 30*).

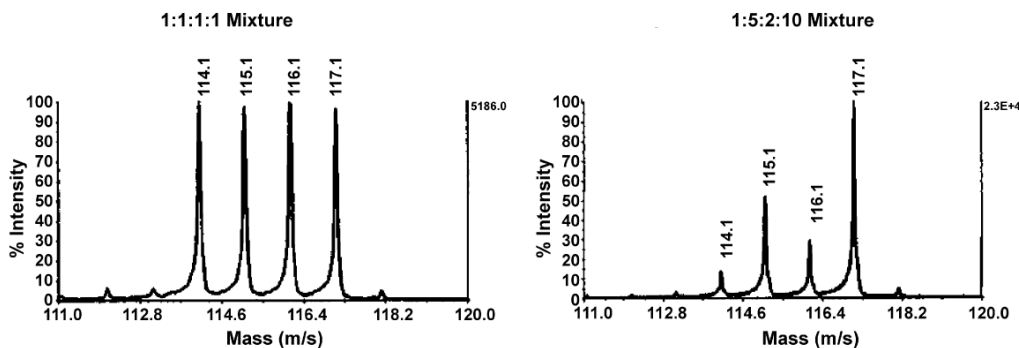


**Figure 30:** *MS/MS* spectra of peptides from an equimolar mixture of four protein samples (left) and a 1:5:2:10 mixture of four protein samples (right) from Fenseleau (33).

Reagents used for this technique are commercially available by Applied Biosystems and a new version with eight reporter ions has been recently developed. The last quantitative approach based on the relative intensities of fragment peaks is called Tandem Mass Tag. This quantitative technique based on reporter ion uses a tagged amino acid, referred to as “tandem mass tags” (TMTs), for the accurate quantification of peptides and proteins (56). These tags are designed to ensure that identical peptides labeled with different TMTs exactly co-migrate

---

in all separations and the term tandem refers to the use of MS/MS for the analysis of these tags. This approach is similar to other peptide isotope labeling techniques like iTRAQ.

### ***1.8.3 Label free quantitation approach***

The quantification of protein between two physiological states can be performed, as seen previously, using protein gel staining or mass-spectrometry-based methods. These methods include differential stable isotope labeling introduced metabolically, enzymatically or even by spiked synthetic peptide standards. All these different methods rely on the addition of a chemical compound on the protein or peptide. On the opposite, label free quantification allows correlating the mass spectrometric signal of intact peptides with protein quantification directly, without any use of external chemical modification (57).

Different label free quantitation approaches have been reported so far. These approaches include replicate protocol, exponentially modified Protein Abundance Index (emPAI) and average method. The replicate protocol is based on an integrated algorithm that automatically detects and quantifies large numbers of peptide peaks aligned according to their  $m/z$  ratio and their elution time (58). These peaks are matched across many different datasets. This approach allows quantifying a large variety of peptides and the method relies on linearity of signal compared to molecular concentration and on reproducibility of sample processing (59).

The emPAI approach is based on the estimation of absolute protein content in a complex mixture using the protein abundance index (PAI) (number of observed peptides divided by the number of observable peptide per protein) (60). This PAI value shows a linear relationship with the logarithm of protein concentration and can be used as a quantitative tool in proteomic studies. Another label-free quantitation method has been reported by Silva (*et al.*) and is based on the rule that the average peak height for the three most intense tryptic peptides per mole of protein is constant within a variation of  $\pm 10\%$ . By adding an internal standard this relationship can give an absolute quantitation of the protein tested by calculating a universal signal response factor (counts/mol) applicable to all the proteins tested in their study (61).

## 1.9 Bibliography

1. Swinbanks D. (1995) Government backs proteome proposal. *Nature* **378**: 653.
2. Moseley FL, Bicknell KA, Marber MS, Brooks G. (2007) The use of proteomics to identify novel therapeutic targets for the treatment of disease. *J Pharm Pharmacol* **59**: 609-628.
3. Levy S, Sutton G, Ng PC, et al. (2007) The Diploid Genome Sequence of an Individual Human. *PLoS Biol* **5**: e254.
4. Ye SQ, Lavoie T, Usher DC, Zhang LQ. (2002) Microarray, SAGE and their applications to cardiovascular diseases. *Cell Res* **12**: 105-115.
5. Schena M, Shalon D, Davis RW, Brown PO. (1995) Quantitative monitoring of gene expression patterns with a complementary DNA microarray. *Science* **270**: 467-470.
6. Hack CJ. (2004) Integrated transcriptome and proteome data: the challenges ahead. *Brief Funct Genomic Proteomic* **3**: 212-219.
7. Velculescu VE, Zhang L, Vogelstein B, Kinzler KW. (1995) Serial analysis of gene expression. *Science* **270**: 484-487.
8. Banks RE, Dunn MJ, Hochstrasser DF, et al. (2000) Proteomics: new perspectives, new biomedical opportunities. *Lancet* **356**: 1749-1756.
9. Reinders J, Sickmann A. (2005) State-of-the-art in phosphoproteomics. *Proteomics* **5**: 4052-4061.
10. Walsh G, Jefferis R. (2006) Post-translational modifications in the context of therapeutic proteins. *Nat Biotechnol* **24**: 1241-1252.
11. <http://www.ebi.ac.uk/IPI/IPIhuman.html>.
12. Anderson NL, Anderson NG. (2002) The human plasma proteome: history, character, and diagnostic prospects. *Mol Cell Proteomics* **1**: 845-867.
13. Anderson NL, Anderson NG. (1998) Proteome and proteomics: new technologies, new concepts, and new words. *Electrophoresis* **19**: 1853-1861.
14. Corthals GL, Wasinger VC, Hochstrasser DF, Sanchez JC. (2000) The dynamic range of protein expression: a challenge for proteomic research. *Electrophoresis* **21**: 1104-1115.
15. Bodovitz S, Joos T. (2004) The proteomics bottleneck: strategies for preliminary validation of potential biomarkers and drug targets. *Trends Biotechnol* **22**: 4-7.
16. Zhang H, Yan W, Aebersold R. (2004) Chemical probes and tandem mass spectrometry: a strategy for the quantitative analysis of proteomes and subproteomes. *Curr Opin Chem Biol* **8**: 66-75.
17. Arnold RJ, Hrnčirova P, Annaiah K, Novotny MV. (2004) Fast proteolytic digestion coupled with organelle enrichment for proteomic analysis of rat liver. *J Proteome Res* **3**: 653-657.
18. Aebersold R, Mann M. (2003) Mass spectrometry-based proteomics. *Nature* **422**: 198-207.
19. Elrick MM, Walgren JL, Mitchell MD, Thompson DC. (2006) Proteomics: recent applications and new technologies. *Basic Clin Pharmacol Toxicol* **98**: 432-441.
20. Steen H, Mann M. (2004) The ABC's (and XYZ's) of peptide sequencing. *Nat Rev Mol Cell Biol* **5**: 699-711.
21. Shimonishi Y, Hong YM, Kitagishi T, Matsuo T, Matsuda H, Katakuse I. (1980) Sequencing of peptide mixtures by Edman degradation and field-desorption mass spectrometry. *Eur J Biochem* **112**: 251-264.
22. Perkins DN, Pappin DJ, Creasy DM, Cottrell JS. (1999) Probability-based protein identification by searching sequence databases using mass spectrometry data. *Electrophoresis* **20**: 3551-3567.

23. Mann M, Wilm M. (1994) Error-tolerant identification of peptides in sequence databases by peptide sequence tags. *Anal Chem* **66**: 4390-4399.
24. Hernandez P, Muller M, Appel RD. (2006) Automated protein identification by tandem mass spectrometry: issues and strategies. *Mass Spectrom Rev* **25**: 235-254.
25. Pappin DJ, Hojrup P, Bleasby AJ. (1993) Rapid identification of proteins by peptide-mass fingerprinting. *Curr Biol* **3**: 327-332.
26. Xu C, Ma B. (2006) Software for computational peptide identification from MS-MS data. *Drug Discov. Today* **11**: 595-600.
27. Sadygov RG, Cociorva D, Yates JR, 3rd. (2004) Large-scale database searching using tandem mass spectra: looking up the answer in the back of the book. *Nat. Methods* **1**: 195-202.
28. (2001) Biomarkers and surrogate endpoints: preferred definitions and conceptual framework. *Clin Pharmacol Ther* **69**: 89-95.
29. van der Greef J, Stroobant P, van der Heijden R. (2004) The role of analytical sciences in medical systems biology. *Curr Opin Chem Biol* **8**: 559-565.
30. Immler D, Greven S, Reinemer P. (2006) Targeted proteomics in biomarker validation: detection and quantification of proteins using a multi-dimensional peptide separation strategy. *Proteomics* **6**: 2947-2958.
31. Duncan MW, Hunsucker SW. (2005) Proteomics as a tool for clinically relevant biomarker discovery and validation. *Exp Biol Med (Maywood)* **230**: 808-817.
32. Gorg A, Weiss W, Dunn MJ. (2004) Current two-dimensional electrophoresis technology for proteomics. *Proteomics* **4**: 3665-3685.
33. Fenselau C. (2006) A review of quantitative methods for proteomic studies. *J Chromatogr B Analyt Technol Biomed Life Sci.*
34. Neuhoff V, Arold N, Taube D, Ehrhardt W. (1988) Improved staining of proteins in polyacrylamide gels including isoelectric focusing gels with clear background at nanogram sensitivity using Coomassie Brilliant Blue G-250 and R-250. *Electrophoresis* **9**: 255-262.
35. Nishihara JC, Champion KM. (2002) Quantitative evaluation of proteins in one- and two-dimensional polyacrylamide gels using a fluorescent stain. *Electrophoresis* **23**: 2203-2215.
36. Patton WF. (2000) A thousand points of light: the application of fluorescence detection technologies to two-dimensional gel electrophoresis and proteomics. *Electrophoresis* **21**: 1123-1144.
37. Unlu M, Morgan ME, Minden JS. (1997) Difference gel electrophoresis: a single gel method for detecting changes in protein extracts. *Electrophoresis* **18**: 2071-2077.
38. Tonge R, Shaw J, Middleton B, et al. (2001) Validation and development of fluorescence two-dimensional differential gel electrophoresis proteomics technology. *Proteomics* **1**: 377-396.
39. Hrebicek T, Dürschmid K, Auer N, Bayer K, Rizzi A. (2007) Effect of CyDye minimum labeling in differential gel electrophoresis on the reliability of protein identification. *Electrophoresis* **28**: 1161-1169.
40. Humphery-Smith I, Cordwell SJ, Blackstock WP. (1997) Proteome research: complementarity and limitations with respect to the RNA and DNA worlds. *Electrophoresis* **18**: 1217-1242.
41. Uetz P, Giot L, Cagney G, et al. (2000) A comprehensive analysis of protein-protein interactions in *Saccharomyces cerevisiae*. *Nature* **403**: 623-627.
42. Kalume DE, Molina H, Pandey A. (2003) Tackling the phosphoproteome: tools and strategies. *Curr Opin Chem Biol* **7**: 64-69.

43. Washburn MP, Wolters D, Yates JR, 3rd. (2001) Large-scale analysis of the yeast proteome by multidimensional protein identification technology. *Nat Biotechnol* **19**: 242-247.
44. Tschappat V, Varesio E, Signor L, Hopfgartner G. (2005) The application of 2-D dual nanoscale liquid chromatography and triple quadrupole-linear ion trap system for the identification of proteins. *J Sep Sci* **28**: 1704-1711.
45. Barr JR, Maggio VL, Patterson DG, Jr., et al. (1996) Isotope dilution--mass spectrometric quantification of specific proteins: model application with apolipoprotein A-I. *Clin Chem* **42**: 1676-1682.
46. Gerber SA, Rush J, Stemman O, Kirschner MW, Gygi SP. (2003) Absolute quantification of proteins and phosphoproteins from cell lysates by tandem MS. *Proc Natl Acad Sci U S A* **100**: 6940-6945.
47. Gygi SP, Rist B, Gerber SA, Turecek F, Gelb MH, Aebersold R. (1999) Quantitative analysis of complex protein mixtures using isotope-coded affinity tags. *Nat Biotechnol* **17**: 994-999.
48. Leitner A, Lindner W. (2006) Chemistry meets proteomics: the use of chemical tagging reactions for MS-based proteomics. *Proteomics* **6**: 5418-5434.
49. Zhou H, Ranish JA, Watts JD, Aebersold R. (2002) Quantitative proteome analysis by solid-phase isotope tagging and mass spectrometry. *Nat Biotechnol* **20**: 512-515.
50. Munchbach M, Quadroni M, Miotto G, James P. (2000) Quantitation and facilitated de novo sequencing of proteins by isotopic N-terminal labeling of peptides with a fragmentation-directing moiety. *Anal Chem* **72**: 4047-4057.
51. Cagney G, Emili A. (2002) De novo peptide sequencing and quantitative profiling of complex protein mixtures using mass-coded abundance tagging. *Nat Biotechnol* **20**: 163-170.
52. Goodlett DR, Keller A, Watts JD, et al. (2001) Differential stable isotope labeling of peptides for quantitation and de novo sequence derivation. *Rapid Commun Mass Spectrom* **15**: 1214-1221.
53. Schmidt A, Kellermann J, Lottspeich F. (2005) A novel strategy for quantitative proteomics using isotope-coded protein labels. *Proteomics* **5**: 4-15.
54. Beynon RJ, Pratt JM. (2005) Metabolic labeling of proteins for proteomics. *Mol Cell Proteomics* **4**: 857-872.
55. Ong SE, Blagoev B, Kratchmarova I, et al. (2002) Stable isotope labeling by amino acids in cell culture, SILAC, as a simple and accurate approach to expression proteomics. *Mol Cell Proteomics* **1**: 376-386.
56. Thompson A, Schafer J, Kuhn K, et al. (2003) Tandem mass tags: a novel quantification strategy for comparative analysis of complex protein mixtures by MS/MS. *Anal Chem* **75**: 1895-1904.
57. Bantscheff M, Schirle M, Sweetman G, Rick J, Kuster B. (2007) Quantitative mass spectrometry in proteomics: a critical review. *Anal Bioanal Chem* **389**: 1017-1031.
58. Radulovic D, Jelveh S, Ryu S, et al. (2004) Informatics platform for global proteomic profiling and biomarker discovery using liquid chromatography-tandem mass spectrometry. *Mol Cell Proteomics* **3**: 984-997.
59. Wang W, Zhou H, Lin H, et al. (2003) Quantification of proteins and metabolites by mass spectrometry without isotopic labeling or spiked standards. *Anal Chem* **75**: 4818-4826.
60. Ishihama Y, Oda Y, Tabata T, et al. (2005) Exponentially modified protein abundance index (emPAI) for estimation of absolute protein amount in proteomics by the number of sequenced peptides per protein. *Mol Cell Proteomics* **4**: 1265-1272.

- 
61. Silva JC, Gorenstein MV, Li GZ, Vissers JP, Geromanos SJ. (2006) Absolute quantification of proteins by LCMSE: a virtue of parallel MS acquisition. *Mol Cell Proteomics* **5**: 144-156.

## **2. Proteomic study**

**Differential Proteomic Analysis of  
STAT6 Knock-out Mice Reveals New  
Regulatory Function in Liver Lipid  
Homeostasis**



---

## Differential Proteomic Analysis of STAT6 Knock-out Mice Reveals New Regulatory Function in Liver Lipid Homeostasis

Joël Iff<sup>‡\*</sup>, Estelle Gueneau<sup>§</sup>, Wei Wang<sup>‡</sup>, Nathalie Oudry<sup>§</sup>, Gérard Hopfgartner<sup>§,§</sup>, Emmanuel Varesio<sup>§,§\*</sup> and Ildiko Szanto<sup>‡¶</sup>

From the <sup>‡</sup> Department of Cellular Physiology and Metabolism, the <sup>§</sup> SVS-MS Mass Spectrometry Core Facility and the <sup>¶</sup> Department of Rehabilitation and Geriatrics, University of Geneva, 1211 Geneva 4, Switzerland; and the <sup>§</sup> Life Sciences Mass Spectrometry Laboratory, School of Pharmaceutical Sciences, University of Geneva, University of Lausanne, 1211 Geneva 4, Switzerland

*\* These authors contributed equally to this work.*

Running title: STAT6 Controls Liver Lipid Homeostasis

Corresponding author:

Emmanuel Varesio, Life Sciences Mass Spectrometry, School of Pharmaceutical Sciences, University of Geneva, 20, bd d'Yvoy, CH-1211 Geneva 4, Switzerland.

Phone: +41 (0)22 37 96757

Fax: +41 (0)22 37 96808

E-mail: [emmanuel.varesio@pharm.unige.ch](mailto:emmanuel.varesio@pharm.unige.ch)

## 2.1 Abbreviations

2-DE: two-dimensional gel electrophoresis ; 2D-nLC-MS/MS: two-dimensional nanoscale LC tandem mass spectrometry ; %T: total monomer concentration; %C : weight percentage of crosslinker; ACAA2: 3-ketoacyl-CoA thiolase ; ACAT2: acetyl CoA acetyltransferase ; ACC: acetyl-CoA carboxylase ; acetyl-CoA: acetyl coenzyme A ; ACLY: ATP-citrate synthase ; ACSM1: medium-chain acyl-CoA synthetase ; AGEs: advanced glycation endproducts ; AHR: aryl hydrocarbon receptor ; AHRE: aryl hydrocarbon receptor element ; APBP/AP56: 56 kDa acetaminophen-binding protein ; ARE: antioxidant responsive element ; ARG1: arginase 1; ARNT: aryl hydrocarbon receptor nuclear translocator ; ATP5B: ATP synthase isoform 5B ; BCA: bicinchoninic acid ; BHB: beta-hydroxybutyrate ; BPB: bromo phenol blue ; CAT: catalase ; CCl<sub>4</sub>: carbon tetrachloride ; CPT1: carnitin-palmytoil CoA transferase 1 ; CSAD: cysteine sulfinic acid decarboxylase ; CYCS: Cytochrome C protein, somatic ; CYP7A1: cytochrome family 7 subunit A isoform 1 ; FABP1 : fatty acid-binding protein ; FADH<sub>2</sub>: flavin adenine dinucleotide ; FAS: fatty acid synthase ; FBP1: fructose bisphosphatase 1 ; FPP Synthase: Farnesyl pyrophosphate synthase ; G-6-Pase : glucose 6 phosphatase ; GK : glucokinase ; GLO1: glyoxalase 1 ; GPI1: glucose phosphate isomerase 1 ; GPX1: glutathione peroxidase 1 ; GSMT1: glutathione S-transferase 1 ; GSMT2: glutathione S-transferase 2 ; GST: glutathione S-transferase ; GSTP1: glutathione S-transferase P1 ; HO-1: heme oxygenase 1 ; HRP: horseradish peroxidase; HSPA5 / GRP78 : heat shock 70kD protein 5 / glucose related protein 78 ; HSPD1: 60 kDa heat shock protein ; iTRAQ: isotope-tagged amine-reactive reagents for relative and absolute quantitation ; KO: knock-out ; MAT1A: methionine adenosyltransferase 1 ; MMTS: methyl methane-thiosulfate ; mRNA: messenger ribonucleic acid ; MudPIT: multidimensional protein identification technology ; MUP: major urinary protein ; NADH :nicotinamide adenine dinucleotide ; NaF: sodium fluoride ; NAFLD : non-alcoholic fatty liver disease ; nLC: nanoscale liquid chromatography ; NO: nitric oxide ; NOS: nitric oxide synthase ; PCK1: phosphoenolpyruvate carboxykinase ; PGYL: glycogen phosphorylase ; PMA: phorbol 12-myristate 13-acetate ; RGN: regucalcin ; ROS: reactive oxygen species; SAM: senescence accelerated mice ; SBP1: selenium binding protein 1 , SBP2: selenium binding protein 2 ; SCP2: nonspecific lipid-transfer protein ; S.E.M. : Standard Error of the Mean ; SISCAPA : stable isotope standards and capture by anti-peptide antibodies ; SMP30: 30kDa senescence marker protein ; SOCS: suppressor of cytokine signaling ; SOD1: superoxide dismutase 1 ; SRBP4 : serum retinol binding protein 4 ; STAT3, STAT6: signal transducer and activator of

---

transcription 3 and 6; TCDD: tetrachlorodibenzo-*p*-dioxin ; TCEP: Tris(2-carboxyethyl)phosphine ; TEAB: triethylammonium bicarbonate ; TPCK: L-1-tosylamido-2-phenylethyl chloromethyl ketone ; TRACE: time resolved amplified cryptated emission ; UGDH: UDP-glucose 6-dehydrogenase ; WT: wild type.

## 2.2 Abstract

The members of the signal transducer and activator of transcription (STAT) family mediate different cytokine-induced gene transcription. STAT6 is a ubiquitously expressed member of this family transmitting interleukin 4 and 13 (IL-4 and IL-13) signaling. IL-4 and IL-13 exert a protective effect against liver ischemia/reperfusion (I/R) injury. I/R leads to cellular damage in a great part by inducing fluctuations in oxygen, nutrition and energy availability; also a characteristic feature of metabolic disturbances, most notably glucose intolerance and insulin resistance. STAT3, another member of the STAT family, has been recently demonstrated to regulate hepatic gluconeogenic gene expression and ameliorate glucose intolerance in diabetic rodents. Therefore, the aim of our study was to evaluate if STAT6, a homologue molecule highly expressed in the liver, exerts a similar metabolic gene regulatory effect contributing to its protective effect during I/R. To achieve this goal we compared the liver proteomes of wild type and STAT6 knock-out mice using two different quantitative techniques, namely 2D-PAGE gel electrophoresis and a combination of 2D nanoscale LC-MS/MS with iTRAQ labeling technique. Applying these two techniques we identified 20 down-regulated and 28 up-regulated proteins in the knock-out mice. The proteins identified by this comparative proteome analysis indicated a state of hepatocellular stress and a disposition towards liver lipid accumulation in the knock-out mice. The physiological relevance of these results was demonstrated by using independent histological and biochemical methods which confirmed the presence of latent liver steatosis in STAT6-deficient mice. In conclusion, our study revealed a so far unidentified role for STAT6 in the *in vivo* regulation of liver lipid homeostasis and suggests a protective function for STAT6 against metabolic stress in this organ.

---

## 2.3 Introduction

Signal transducer and activator of transcription (STAT) proteins mediate different cytokine-induced gene transcription. STAT6 is a ubiquitously expressed member of the this family involved in interleukin 4 and 13 (IL-4 and IL-13) signaling (reviewed in (1)). Upon stimulation, STAT6 gets tyrosine phosphorylated and translocates into the nucleus as a homodimer. Once in the nucleus, STAT6 modulates gene transcription by binding to a specific palindromic DNA sequence (2, 3). Most STAT6-dependent genes display this sequence in their promoter regions (reviewed in (1)). In addition to its direct gene-regulatory function, STAT6 interacts with a wide variety of other transcription factors and serves as a recruitment platform for the different members of the transcriptional machinery (4-8). Therefore, STAT6-deficient mice display complex STAT6-dependent and -independent transcriptional alterations (9).

Most of the research effort to elucidate the molecular basis for the different effects of STAT6 has been attributed to its essential function in the immune system to pre-dispose T cells towards Th2 type differentiation (10). Recently, however, several studies indicated a function for STAT6 in different other cell types. Notably, STAT6 has been shown to be involved in adipocyte differentiation, kidney epithelial cell mechanosensation, regulation of apoptosis in human hepatoma cells and inflammatory reaction in lung epithelial cells (11-13). In the liver, STAT6 has a protective role against I/R injury (reviewed in (14)). Liver I/R leads to abrupt changes in oxygen supply and alterations of substrates availability required for cellular metabolism. Cytokines play a crucial role in modulating hepatocyte metabolic adaptive responses to the hypoxic insult inflicted by the I/R (15). The relationship between hypoxia, metabolism and liver injury is highlighted by studies demonstrating that intermittent hypoxia induces alterations in lipid homeostasis and predisposes to liver injury (16-18). IL-6, an anti-inflammatory cytokine, protects against the development of fatty liver by activating STAT3 and regulating the expression of various glucose and lipid homeostasis genes (19). IL-4 and IL-13 display a similar protective effect against I/R injury, however the gene expression pattern regulated by their common effector molecule, STAT6, has not yet been investigated.

Therefore, the present study was aimed at exploring the effect of ablation of IL-4 and IL-13 signaling on liver function by analyzing the proteomes of wild type and STAT6 knock-out mice using two current differential proteomic methods and validating the physiological relevance of the identified proteins.

## 2.4 Experimental Procedures

*Animals* - Balb/cJ wild type and STAT6 knock-out male mice were obtained from Charles River Laboratories (L'Arbresle, France) and were kept under regular animal housing conditions. Ob/ob mice, fa/fa rats and their control littermates were purchased from Elevage Janvier (CERJ, Le Genest St Isle, France). The experimental protocol had been accepted by the Ethical Committee of the University of Geneva and the Veterinary Office of the Canton of Geneva. All experiments were carried out in accordance with the regulatory guidelines of the Veterinary Office of the Canton of Geneva on the care and welfare of laboratory animals. Mice had *ad libitum* access to water and standard chow (SDS Dietex, Saint Gratien, France) and were sacrificed at the age of 20 weeks.

*Preparation of Liver Samples and Two-dimensional Gel Electrophoresis* - Mice were anesthetized by isoflurane administration and were sacrificed by decapitation. The liver was immediately removed and crushed in a mortar in presence of liquid nitrogen followed by lyophilization for 48 hours. The resulting dried powder was stored at -80°C until analysis. 2 mg of pooled (n=3) liver samples were dissolved in 400 µL solution containing urea (8 M), CHAPS (4% w/v), dithioerythritol (DTE; 65 mM), Ampholine (2% w/v) and a trace of bromophenol blue (BPB). The total volume of the sample was used for rehydration of a commercial 7 cm nonlinear pH 4–7 IPG strip (GE Healthcare, Otelfingen, Switzerland). Isoelectric focusing (IEF) was carried out using a Multiphor II system at 3500 V for 17 hours as described in (20). The IPG gel was then equilibrated in the first equilibration buffer (50 mM Tris-HCl, 8 M urea, 30% glycerol, 10% SDS, 100 mM DTE) for 5 minutes at room temperature followed by a 5-minute incubation in the second equilibration buffer (50 mM Tris-HCl, 8 M urea, 30% glycerol, 10% SDS, 250 mM iodoacetamide, a trace of BPB). Second dimensional separation was performed on in-house manufactured SDS-PAGE gels (9x8x0.15 cm, 12 %T, 2.6 %C). Proteins were detected using Coomassie brilliant blue stain (Fluka, Buchs, Switzerland). Destaining was performed in a solution containing 40%

methanol and 10% acetic acid followed by extensive wash in water to remove excess destaining reagent.

*Image acquisition and spot picking* - Gels were scanned using a laser densitometer (4000 x 5000 pixels; 12 bits/pixel) (Labscan, GE Healthcare). Liver 2-DE maps (n=3) from pooled STAT6 KO mice were compared to 2-DE maps (n=3) from pooled wild types littermates. Visual and computer-assisted image analysis was performed using the ImageMaster 2D Platinum software v. 6.0 (GE Healthcare). All the significant spots were manually confirmed by visual inspection of the images. Candidate spots were manually excised with a Gel Pal spot picker (Genetix Ltd, Hampshire, UK).

*In-gel Digestion and Nanoscale Liquid Chromatography Mass Spectrometry* – Selected spots were washed twice by dehydration / rehydration cycles with 50 µl of 25 mM NH<sub>4</sub>HCO<sub>3</sub>:acetonitrile (1:2, v/v) and 25 mM NH<sub>4</sub>HCO<sub>3</sub> solutions. After supernatant removal and spots drying by centrifuge-evaporation (RC10.22 - Jouan, France), in-gel tryptic digestion was performed by adding 10-15 µl of a 12.5 ng/µl TPCK-treated porcine trypsin (Promega, Madison, WI, USA) followed by the addition of 30 µl of 25 mM NH<sub>4</sub>CO<sub>3</sub> to rehydrate the spots for 1 hour on ice. Incubation was performed at 37°C for 4.5 hours. Peptides were extracted by adding 30 µl of 25 mM NH<sub>4</sub>HCO<sub>3</sub>:acetonitrile (1:2, v/v) to gel pieces (incubation at room temperature for 20 minutes) and the supernatant was pooled to the first one. Gel spots were finally dehydrated by adding 30 µl of acetonitrile and, after 20 minutes, supernatant was removed and pooled. Combined supernatants were dried down by vacuum-centrifugation and re-solubilized in 4µl of 1% aqueous formic acid. Sample was diluted twice in 0.1% aqueous TFA and 2 µl were analyzed on a nanoscale LC-MS/MS system. This setup consisted of a FAMOS micro-autosampler (LC Packings – Dionex, Amsterdam, The Netherlands), a split-free nanoLC pump (Eksigent, Dublin, CA, USA) delivering a flowrate of 300 nl/min on a PepMap C18 75µm ID column (LC Packings - Dionex). MS/MS spectra were acquired on a QSTAR XL (AB / MDS Sciex, Concord, ON, Canada) mass spectrometer operating in information-dependent acquisition mode with two product ions scans per MS survey scan. Peak list generation was performed by the Mascot Daemon software (v.2.1.0 - Matrix Science, London, UK) using the “AB / MDS Sciex Analyst wiff file” import filter with its default parameters. Protein identification was carried out by searching the Uniref100 database (release 7.4 – 3’334’551 sequences) installed on a Mascot server (v.2.1.0 - Matrix Science) with the following parameters: no taxonomy

restriction, trypsin digestion agent, one missed cleavage allowed, MS and MS/MS  $m/z$  tolerances of 0.2 Da, cysteine carbamidomethylation set as fixed modification and methionine oxidation set as variable modification. The significance threshold for individual MS/MS spectra was set at  $p < 0.05$  and the ion score cut-off to 10 in order to remove low scoring peptides. Protein hits required at least one bold red peptide match in order to remove duplicate homologous protein hits. Only proteins related to rodent species were reported and proteins sharing the same set of peptides were all reported equally.

*Preparation of Liver Samples for iTRAQ Analysis* - Liver samples were lysed by freeze-cracking in presence of liquid nitrogen. Homogenization with a mechanical douncer was performed on ice by adding a Tris buffer (pH 7.4) containing 250 mM sucrose and a tablet of Complete protease inhibitor cocktail per 50 ml of buffer (Roche Diagnostics, Mannheim, Germany). The buffer volume was adjusted in order to obtain liver amounts of 50 mg per 100  $\mu$ l. Organelle enrichment fractionation was performed by differential centrifugation according to Arnold *et al.* (21) and the different fractions were stored at  $-80^{\circ}\text{C}$  for subsequent differential analyses.

*iTRAQ Labeling and Two-dimensional Nanoscale LC Tandem Mass Spectrometry* - Protein concentration of pooled ( $n=3$ ) wild type or STAT6 knock-out cytosolic enriched fractions was determined by the Coomassie Plus Bradford assay (Pierce, Rockford, IL, USA). Differential labeling was performed using iTRAQ reagents (Applied Biosystems) according to the method described by Ross *et al.* (22). In brief, ca. 20  $\mu$ l of 500 mM triethylammonium bicarbonate (TEAB) buffer (pH 8.5) and 1  $\mu$ l of 2% SDS were added to each sample in order to obtain a protein concentration of 5  $\mu\text{g}/\mu\text{l}$ . Proteins were then reduced by the addition of 2  $\mu$ l of 50 mM Tris(2-carboxyethyl)-phosphine (TCEP) followed by an incubation at  $60^{\circ}\text{C}$  for one hour. At room temperature, proteins were alkylated with 1  $\mu$ l of 200 mM methyl methane-thiosulfate (MMTS) reagent. Overnight digestion ( $37^{\circ}\text{C}$ ) was performed by adding 10  $\mu$ l of a 1 mg/ml trypsin aqueous solution. Finally iTRAQ differential labeling was carried out by adding separately 70  $\mu$ l of reagent to the respective tubes containing the pooled wild type or pooled STAT6-KO mice liver cytosolic fractions. After an incubation of one hour at room temperature, labeled samples were combined and evaporated to a final volume of ca. 200  $\mu$ l. Sample pH was adjusted to 3.0 with a 10% (v:v) aqueous formic acid solution before injection in the two dimensional nanoscale LC-MS/MS (2D-nLC-MS/MS) system. Analyses were performed according to the method described by Varesio *et al.* (23) and adapted as

follows: 5  $\mu$ l of sample was injected and cation exchange chromatography was carried out on a 300  $\mu$ m ID x 15 cm Poros 10S SCX column (packed by LC Packings – Dionex) at a flow rate of 6  $\mu$ l/min. A step gradient of twenty KCl fractions ranging from 0 to 300 mM in 10 mM sodium phosphate buffer (pH 3.0):acetonitrile (95:5, v:v) was performed over 24 hours. Each salt fraction containing peptides eluted from the SCX column was trapped onto a PepMap C18 300  $\mu$ m ID x 5 mm cartridge and washed at 20  $\mu$ l/min for 10 min. with a 0.1% aqueous TFA solution to remove salts from the SCX mobile phase. Then, the cartridge was backflushed in line with a C18 nanocolumn (PepMap – 75  $\mu$ m ID x 15 cm, LC Packings - Dionex) at a flowrate of 300 nl/min and peptides were separated over a 30 minutes generic reverse-phase LC gradient (*i.e.* from 0% to 75% of 0.1% formic acid in acetonitrile – 70 min. total runtime). In the meantime the following SCX step was performed and peptides were retained on the second C18 cartridge mounted in parallel on the 10-ports switching valve (Switchos II – LC Packings - Dionex). Mass spectrometry was performed on a QSTAR XL (AB / MDS Sciex) operating in information-dependent acquisition mode with two product ions scans per MS survey scan. The sample was run in triplicate with an exclusion list built from the peptides identified from the previous runs (24). Peak list generation and protein identification were carried out by searching the Uniref100 database (release 7.4 – 3'334'551 sequences) using the ProteinPilot software (v.1.0 – Applied Biosystems). The following parameters were applied: no species restriction, trypsin digestion agent, cysteine residues alkylated by MMTS as fixed modification, search effort was set as thorough ID for the Paragon search algorithm (25). Results were grouped by the ProGroup algorithm (Applied Biosystems) within the ProteinPilot software (26, 27) in order to group proteins sharing the same set of identified peptides. Protein reporting was based on at least two peptides identified with a confidence level higher than 95% and a detected protein threshold (*i.e.* Unused ProtScore) greater than 1.3 corresponding to a confidence level of 95% for the protein identification. As for the 2D-PAGE study, only proteins related to rodent species were reported. Proteins isoforms or members of a protein family sharing the same set of peptides were all reported as being equal hits. The estimation of false-positive identification rate was performed by searching the same dataset against a decoy database made of random sequences generated by the “decoy.pl” script available on the Matrix Science website (28). A false positive rate of 0.55 % was calculated for rodent proteins. Quantitation was performed by taking the peak areas ratio with a correction for the overlapping isotopic contributions from the different reporter ions according to manufacturer's certificate. Experimental labeling bias was also corrected by the software. Peptides used for quantitation were automatically selected

by the software with the default criteria (*i.e.* the sum of reporter ion areas should be greater than 40 counts, peptides with a ratio of 0 or 9999 or peptides shared by several proteins and overlapping precursors were excluded from quantitation) and only peptides with an identification confidence higher than 95% were selected for quantitation. No outlier data points were removed. Results for proteins reported as up- or down-regulated were manually validated.

For both the 2-DE and the iTRAQ differential analyses, liver samples from wild type (n=3) or STAT6-KO (n=3) mice were pooled to obtain two average samples (29). These samples were then analyzed in triplicate by each technique to assess protein expression differences in wild type and STAT6-KO mice liver samples. While technical variability was taken into account at the proteomic level, biological variation was assessed at the mRNA and physiological levels by analyzing several animals separately.

*RNA Preparation and Real-time PCR* – Total RNA was prepared by homogenizing approximately 100-200 mg liver tissue in TRIZOL Reagent (Invitrogen, Basel Switzerland) and was purified by using RNase free DNase in combination with the RNeasy Mini Kit (Qiagen, Homrechtikon, Switzerland). cDNA was synthesized from 2 µg of DNA-free RNA by Superscript II Reverse Transcriptase (Invitrogen). Primers and probes were designed by Primer Express software (Applied Biosystems) and are listed online as Supplementary Material in Table S1. The results were quantified by the  $\Delta\Delta C_t$  method using cyclophilin A as the standard internal non-variable gene to compensate for differences in RNA input and efficiency of cDNA synthesis. Results were expressed as arbitrary units compared to the average expression levels in wild type mice.

*Western Blot Analysis* – Liver tissues were snap frozen in liquid nitrogen immediately upon removal and were stored at -80°C till processing. Tissues were homogenized in lysis buffer (25 mM HEPES, 0.5% Triton X100, 65 mM NaCl, 2.5 mM EDTA, 25 mM sodium pyrophosphate, 50 mM NaF, 2 mM PMSF, 9 mM sodium orthovanadate, one tablet of Complete Inhibitor Cocktail in 20 ml (Roche Diagnostics, Rotkreuz, Switzerland), pH 7.5. Protein concentration was measured by bicinchoninic acid (BCA) method (Pierce, Rockford, IL). Lysates were dissolved in Laemmli buffer (10 mM sodium phosphate - pH 7.0, 0.1% glycerol, 2% SDS, 100 mM DTT and a trace of BPB) and were resolved on a 5-20% gradient polyacrylamide gel. Gels were transferred onto nitrocellulose membranes (GE Healthcare).

Non-specific binding of the antibody was prevented by blocking the membranes with 0.05% polyvinyl alcohol (PVA) followed by incubation with the respective primary antibodies at 4°C overnight. Antibodies were as follows: Ezrin: SC-6407, SOCS3: SC-9023, STAT3: SC-7179 and STAT6: SC-981 (Santa Cruz Biotechnology, Santa Cruz, CA, USA). Blots were then washed 3 times for 5 minutes at room temperature with TBS supplied with 0.1% Tween20, and subsequently incubated with the applicable secondary horseradish peroxidase (HRP)-conjugated antibody: goat anti-rabbit IgG (Biorad, Reinach, Switzerland) or rabbit anti-goat IgG (Sigma-Aldrich, Buch Sitzerland). Signals were revealed by enhanced chemiluminescence (ECL Advanced Western Blot Detection Kit, GE Healthcare) and were recorded in Chemidoc XRS system (Biorad). Quantification of the detected bands was performed by using the Quantity One program (Biorad). Protein expression was related to the amount of ezrin as a non-variable reference protein and was expressed as arbitrary units compared to the average expression in wild type mice.

*Serum Testosterone Measurement* - Blood was collected from the tail vein in heparinized tubes (BD Diagnostics, Basel, Switzerland). Testosterone measurements were performed by TRACE (Time Resolved Amplified Cryptated Emission) method using a commercial kit (Testosterone KRYPTOR kit, BRAHMS GmbH, Hennigsdorf, Germany).

*Determination of Liver Lipid Content* - Liver lipids were extracted according to a modified Bligh and Dyer method (30). Briefly, liver pieces were pulverized in a mortar using liquid nitrogen then left overnight in a chloroform:methanol (2:1, v:v) extraction solution. After filtration, lipids were washed once with water, then three times using 2 mM calcium chloride in water:methanol:chloroform (48:49:3, v:v:v) with the supernatant discarded each time. Finally, lipids were air dried and weighted in order to quantify total lipid amount.

*Statistical Analysis for mRNA expression, serum and lipid content measurements* - Results were analyzed by Student's unpaired *t* test using the SigmaStat software (version 2.0 – SPSS, Chicago, IL, USA). Results with a *p* value less or equal than 0.05 were considered significant.

*In silico Promoter Analysis* - *In silico* promoter analysis was performed using consensus DNA binding sequences as described by Pastorelli *et al.* (31). Briefly, genomic sequences were downloaded from the University of California Santa Cruz (UCSC) genome browser database for the most recent (mm8) assembly. The -5000 and +1000 regions relative

to the RefSeq transcriptional start sites were extracted and searched for the presence of different transcription factor binding motifs (Table VI) using custom Bioperl based scripts generously provided by P.C. Boutros (University of Toronto, Toronto, Canada).

## 2.5 Results

### 2.5.1 Comparison of Differentially Expressed Proteins Detected by 2-DE Gel and iTRAQ 2D nLC-MS/MS Analysis

Pooled mouse liver samples were arrayed on the 2-DE gel system, and proteins were identified by peptide MS/MS sequencing with a nanoscale LC coupled to an orthogonal QqTOF. From the *ca.* 700 spots detected by the visualization software, 10 spots were found to be down-regulated and 25 spots up-regulated in STAT6 knock-out mice after differential analysis by the software and manual validation, corresponding to 7 and 22 proteins, respectively (Fig. 1 shows the acidic pI range 2D gels).

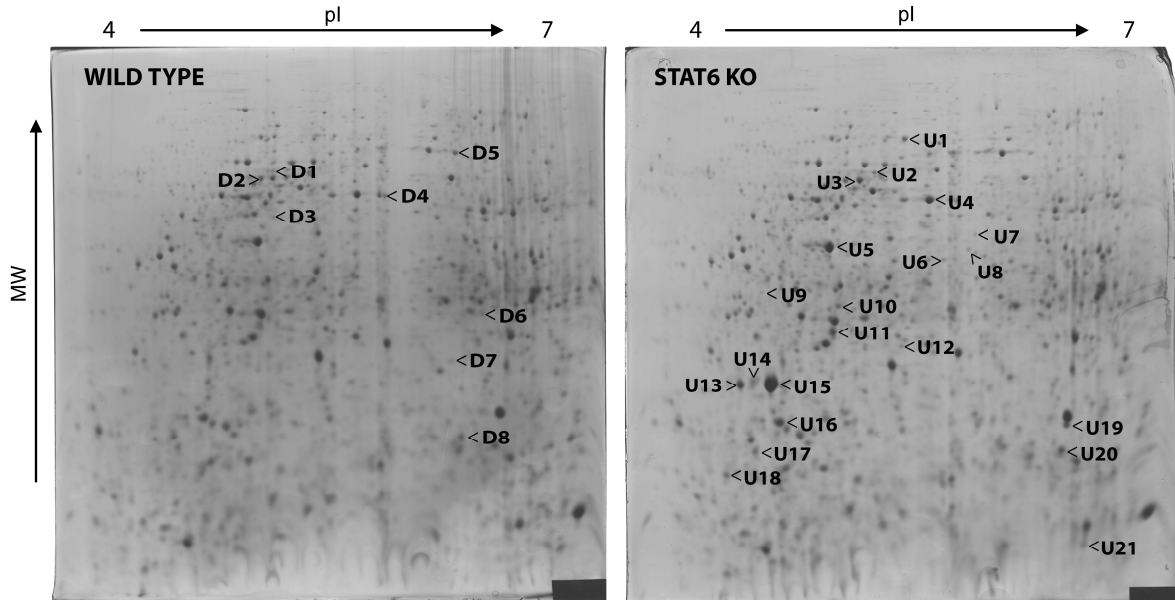


FIG. 1. **Representative 2D PAGE images of the acidic (pI:4-7) range analysis of livers of wild type and STAT6 KO mice.** The labels “D” and “U” mark spots respectively down- or up-regulated in STAT6 knock-out mice. The corresponding protein identities are listed in Tables I and II.

---

In parallel, pooled mouse liver cytosolic fractions were differentially analyzed by 2D-nLC-MS/MS after iTRAQ labeling. From the 155 validated proteins (Table S2 in the Supplementary Material), 16 down-regulated and 17 up-regulated proteins were found in STAT6 knock-out mice. The down- and up-regulated proteins identified by the two methods are listed in Tables I and II, respectively. Altogether there were 20 proteins down-regulated and 28 proteins up-regulated in STAT6-deficient mice, from which 6 and 15 were detected by both methods (marked bold in Table I and II).

Interestingly, selenium binding proteins 1 and 2 (SBP1, SBP2) were regulated in an opposite manner (Table I, #3 and Table II, #7). SBP1 possesses two different isoforms with a difference of six amino acids between their sequences (32, 33). Accordingly, we identified two different spots on the 2D gels corresponding to SBP1a and SBP1b. Spot D5 was identified as SBP1a (Q91X87), while spot D4 could be either of the two isoforms: SBP1a (Q91X87) or SBP1b (P17563) (Fig. 1). Both spots identified as SBP1 were down-regulated in the knock-out mouse. Similar to SBP1, SBP2 (Q63836 or Q9R1Z6) has been identified as three different spots in the gel. SBP2 has two known isoforms (SBP2a and SBP2b) with a difference of only one amino acid between them (33-35). As the peptide containing this particular amino acid has not been identified in our measurement, the spots marked as SBP2 (Fig. 1, U4, U10 and U17) can in fact contain both isoforms. Contrary to SBP1, the expression of SBP2 was up-regulated in STAT6-deficient mice.

**TABLE I Down-regulated proteins in the livers of STAT6 knock-out mice.**

Bold font represents proteins identified both by 2-DE gel and iTRAQ 2D nLC-MS/MS techniques. Spot ID refers to the spot marked in Fig. 1.

Protein number	Gene symbol	Protein Name (Accession number)	2D PAGE			iTRAQ		
			Spot ID §	Sequence coverage	Unique peptides	Sequence coverage	Unique peptides	KO / WT ratio † <i>Mean [95% E.I.] (n)</i>
1	<b>GSTM2</b>	<b>Glutathione S-transferase Mu 2</b> (P15626)	D6	37 %	10	73 %	5	0.64 [0.42 – 0.97] (7)
2	<b>GOT1</b>	<b>Glutamate oxaloacetate transaminase 1</b> (P05201 / Q3UJH8)	D7	9 %	4	10 %	2	0.59 [0.34 – 0.99] (4)
3	<b>SELENBP1</b>	<b>Selenium-binding protein 1</b> (Q91X87 / P17563) Selenium-binding protein 1 (Q91X87)	D4	22 %	10	75%	18	0.73 [0.65 – 0.82] (2)
4	<b>GSTM1</b>	<b>Glutathione S-transferase, Mu 1</b> (Q58ET5)	D8	30 %	14	88 %	19	0.96 [0.75 – 1.24] (32)
			<i>n.s.</i>	39 %	13			
5	<b>DBI</b>	<b>Acyl-CoA-binding protein</b> (P31786 / Q3ULV8 / Q4VWZ5)	<i>n.s.</i>	25 %	3	68 %	2	0.94 [0.58 – 1.53] (16)
6	<b>MAT1A</b>	<b>Methionine adenosyltransferase 1</b> (Q91X83)	D3	5 %	2	29 %	6	0.78 [0.54 – 1.12] (14)
7	KRT18	Keratin complex 1, acidic (Q3TIX1 / Q3TJH6 / Q3TJW7)	D1	13 %	6			
			D2	31 %	15			
8	ASS1	Argininosuccinate synthase (P16460 / Q3UEJ7)				68 %	15	0.87 [0.78 – 0.97] (98)
9	ADH1	Alcohol dehydrogenase 1 (Q3UKA4)				37 %	9	0.73 [0.67 – 0.80] (55)
10	FBP1	Fructose biphosphatase 1 (Q3UEH1)				48 %	15	0.81 [0.67 – 0.97] (48)
11	ETFA	Electron transferring flavoprotein, alpha polypeptide (Q8BMU7 / Q5M7W0 / Q4V9X5 / Q3THD7)				33 %	6	0.87 [0.78 – 0.97] (32)
12	PYGL	Liver glycogen phosphorylase (Q91WP9 / Q3UKJ0)				18 %	10	0.60 [0.49 – 0.74] (15)
13	UGDI1	UDP-glucose 6-dehydrogenase (O70475 / Q3TJ71 / Q3TJE8 / O70199)				26 %	6	0.52 [0.41 – 0.66] (13)
14	FDPS	Farnesyl pyrophosphate synthetase (Q920E5 / Q3TMB3)				16 %	3	0.76 [0.58 – 0.99] (12)
15	TUBA6	Tubulin alpha-6 chain (P68373 / Q3TIZ0 / Q9JUZ2)				24 %	3	0.67 [0.60 – 0.74] (8)
16	GPI1	Glucose phosphate isomerase 1 (Q5RJ13 / Q3UZJ1 / Q3LUX1 / Q3TW50 / Q3TEE7)				13 %	3	0.63 [0.44 – 0.90] (7)
17	ACAT3	Acetyl CoA transferase-like protein (Q8R4V3 / Q80X81)				15 %	2	0.67 [0.55 – 0.81] (7)
	ACAT2	Acetyl CoA acetyltransferase, cytosolic (Q8CAY6)						
18	ACLY	ATP-citrate synthase (Q91V92 / Q3V117 / Q3TED3)				5 %	3	0.51 [0.41 – 0.63] (6)
19	CYCS	Cytochrome C protein, somatic (Q56A15)				37 %	2	0.60 [0.44 – 0.81] (3)
20	CSAD	Cysteine sulfinic acid decarboxylase (Q9DBE0 / Q8K566)				17 %	2	0.67 [0.63 – 0.70] (2)

§ Spot ID corresponds to spot labels shown in Figure 1.

*n.s.* = “not shown” in Figure 1 since these proteins were observed in the alkaline pI range 2D gels.

†) iTRAQ ratios written in italic were statistically not different from 1.0 ( $p > 0.05$ ).

95% E.I. = 95% confidence Error Interval = [(Mean / Error Factor) – (Mean \* Error Factor)], which means that the true protein ratio is found in this interval with a 95% confidence level (135).

(n) = number of peptides used for quantitation.

**TABLE II Up-regulated proteins in the livers of STAT6 knock-out mice.**

Bold font represents proteins identified both by 2-DE gel and iTRAQ 2D nLC-MS/MS techniques. Spot ID refers to the spot marked in Fig. 1.

Protein number	Gene symbol	Protein Name (Accession number)	2D PAGE			iTRAQ		
			Spot ID <sup>§</sup>	Sequence coverage	Unique peptides	Sequence coverage	Unique peptides	KO / WT ratio <sup>†</sup> <i>Mean [95% E.I.] (n)</i>
1	CA3	<b>Carbonic anhydrase 3</b> (P16015)	U21	15 %	3	74 %	16	1.16 [1.02 – 1.31] (130)
2	FABP1	<b>Fatty acid-binding protein   L-FABP</b> (P12710)	<i>n.s.</i>	58 %	9	84 %	9	1.45 [1.26 – 1.66] (101)
3	HBA-A1	<b>Hemoglobin alpha chain</b> (P01942 / Q91VB8 / Q8BPF4 / Q9CY10)	<i>n.s.</i>	31 %	6	89 %	6	1.34 [1.21 – 1.48] (59)
			<i>n.s.</i>	31 %	6			
4	SOD1	<b>Superoxide dismutase [Cu Zn]</b> (P08228)	U19	32 %	4	79 %	6	1.16 [1.04 – 1.29] (44)
5	RGH	<b>Regucalcin   SMP 30</b> (Q64374)	U5	55 %	20	52 %	8	1.37 [1.13 – 1.65] (16)
6	GLO1	<b>Glyoxalase 1   LGUL</b> (Q9CPU0)	U11	36 %	6	47 %	3	2.54 [2.14 – 3.02] (11)
7	SELENBP2	<b>Selenium binding protein 2</b> (Q8R1T6 / Q63836)	U4	50 %	26	79 %	21	1.70 [1.48 – 1.97] (9)
			U10	25 %	12			
			U17	16 %	8			
8	MUP1a	<b>Major urinary protein 1   MUP</b> (Q4FZE8 / Q9CX16)	U13	59 %	16	38 %	3	25.54 [n/a] (1)
			U18	38 %	11			
9	MUP1b	<b>Major urinary protein 1   MUP</b> (Q58EV3 / P11588)	U14	57 %	15			15.73 [5.29 – 46.77] (7) <sup>‡</sup>
10	MUP2	Major urinary protein 2   MUP (P11589)	U15	66 %	25			
11	MUP6	<b>Major urinary protein 6   MUP</b> (P02762)	U13	60 %	16	38 %	3	15.73 [5.29 – 46.77] (7) <sup>‡</sup>
			U18	38 %	11			
12	MUP8, MUP11	<b>Major urinary protein 8 &amp; 11   MUP</b> (P04938)	U13	71 %	16	45 %	3	15.73 [5.29 – 46.77] (7) <sup>‡</sup>
			U18	45 %	11			
13	GPX1	<b>Glutathione peroxidase 1</b> (P11352 / Q5RJH8)	U12	33 %	7	45 %	3	1.33 [1.07 – 1.65] (4)
14 <sup>§</sup>	ALB	<b>Serum albumin</b> (P07724 / Q8C7H3 / Q8C7C7 / Q3TV03)	U8	14 %	8	59 %	24	0.94 [0.88 – 0.99] (127)
15	HSPD1	<b>60 kDa heat shock protein</b> (P63038)	U1	46 %	21	40 %	15	1.03 [0.84 – 1.25] (81)
16	HBB-B1	<b>Hemoglobin beta-1 chain</b> (P02088)	U21	42 %	3	96 %	13	0.97 [0.88 – 1.07] (122)
			<i>n.s.</i>	84 %	11			
17	ACSM1	Medium-chain acyl-CoA synthetase (Q91VA0)	U6	9 %	4			
18	KRT18	Keratin complex 1, acidic (Q3TIX1 / Q3TJH6 / Q3TJW7)	U2	35 %	17			
			U3	49 %	22			
			U9	17 %	8			
19	UOX	Urate oxidase (Q54310 / Q8C7K4)	U70	74 %	11			
20	HSPA5	Heat shock 70kDa protein 5   GRP 78 (Q3TI47 / P20029 / Q3TKF8 / Q3U6V3 / Q3TWF2 / Q3U9G2 / Q3UEM8 / Q9DC41)	U7	11 %	8			
21	CYB5	Cytochrome b-5 (Q544Z9)	U16	41 %	6			
22	ATP5B	ATP synthase, H <sup>+</sup> transp. Mitoch. F1 complex (Q3TFD7 / Q3TWD5 / Q3UB69 / Q3TIP9 / Q3TX28 / Q3U6U4 / Q8C165 / P56480)	U16	10 %	6			
23	GSTP1	Glutathione S-transferase P1 (P19157)				90 %	10	1.66 [1.38 – 2.01] (50)
24	ACAA2	3-ketoacyl-CoA thiolase, mitochondrial (Q8BWT1 / Q3TIT9)				64 %	11	1.13 [1.02 – 1.25] (42)
25	SCP2	Nonspecific lipid-transfer protein (P32020)				29 %	8	1.31 [1.13 – 1.52] (37)
26	NME2	Nucleoside diphosphate kinase B (Q01768)				79 %	5	1.18 [1.07 – 1.31] (9)
27	AKRIC6	Estradiol 17 beta-dehydrogenase 5 (P70694)				65 %	4	1.14 [1.01 – 1.29] (8)
28	TST	Thiosulfate sulfurtransferase (Q545S0)				14 %	2	1.23 [1.09 – 1.39] (7)

- a) Albumin was found to be up-regulated in the 2D PAGE study and down-regulated in the iTRAQ study (see text for details).
- § Spot ID corresponds to spot labels shown in Figure 1.
- n.s.* = “not shown” in Figure 1 since these proteins were observed in the alkaline pI range 2D gels.
- ‡ iTRAQ ratios written in italic were statistically not different from 1.0 ( $p > 0.05$ ).
- 95% E.I. = 95% confidence Error Interval = [(Mean / Error Factor) – (Mean \* Error Factor)], which means that the true protein ratio is found in this interval with a 95% confidence level (135).
- n = number of peptides used for quantitation.
- i) This ratio is the same for the three MUP proteins and was entered as a single entry in Table S2 (MUP 1 / 11&8 / 6 – entry #152)

One protein, *i.e.* albumin, showed conflicting results determined by 2D-PAGE and iTRAQ analysis (Table II, #14). While there was a clear up-regulation in its expression in 2-DE analysis (Fig. 2a), we could not confirm it by iTRAQ analysis (knock-out/wild type ratio of 0.94). To resolve this controversy we measured albumin mRNA expression by real-time PCR analysis. We found no significant differences between the expression levels of the two genotypes, although STAT6-null mice displayed a tendency towards higher expression levels (Fig. 2b). By contrast, serum albumin levels were undistinguishable between wild type and knock-out mice (Fig. 2c). The sensitivity limits of both techniques are clearly illustrated by the lack of identification of STAT6 among the differentially expressed proteins even though STAT6 was readily detected by Western blot analysis (Fig. 2d).

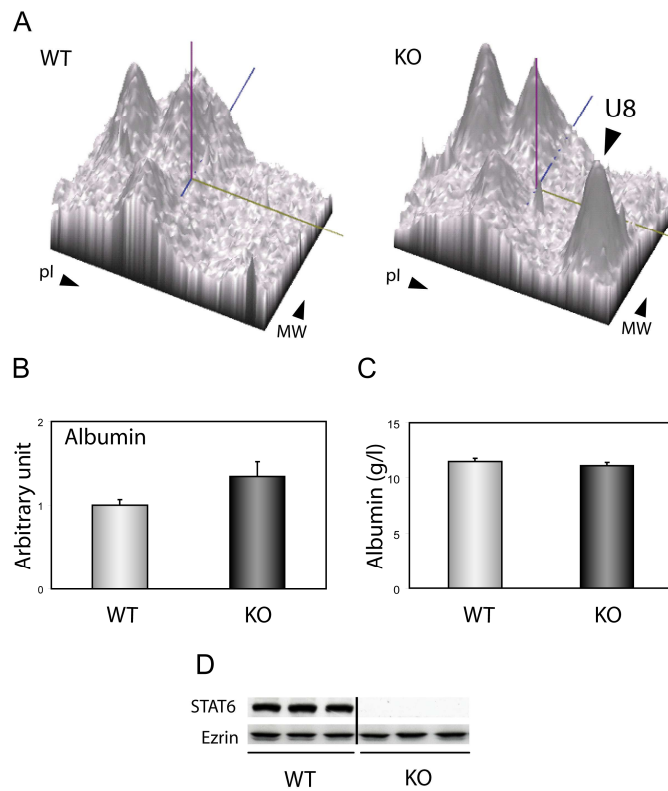


**FIG. 2. Albumin protein and mRNA expression.** A. 3 dimensional representation of the region where albumin (spot U8) migrates on 2D-PAGE gel. B. Expression of albumin mRNA. Each bar represents the average expression level expressed as arbitrary units normalized to the mean of wild type mice  $\pm$  S.E.M. (n=10). C. Plasma levels of albumin (n=6). Data are expressed as mean  $\pm$  S.E.M. D. Detection of STAT6 expression by Western blot analysis. Ezrin is a non-variable protein showing equal protein loading (n=3).

---

### ***2.5.2 Increased Expression of Major Urinary Proteins***

The most prominent change in protein expression was observed in case of the different isoforms of the major urinary proteins (MUP1, MUP6, MUP8 and MUP11) with 15-25-fold increase in the livers of the STAT6-null mice as determined by iTRAQ analysis (Table II, #8, #9, #11 and #12). The enhanced protein expression of MUPs was mirrored in their mRNA levels that showed a more than 500-fold increase in the knock-out mice (Fig. 3a, males). MUPs are synthesized in the liver and secreted in the male urine to serve as territorial marks, therefore MUP expression is generally higher in males than in females (36). In line with its sex-specific expression, female knock-out mice showed a much less robust increase in their MUP expression when compared to males (Fig. 3a, females). Expression of MUP proteins is most commonly induced by testosterone; therefore we compared testosterone levels in wild type and STAT6-deficient male and female mice (Fig. 3b). Contrary to our expectations, we found decreased testosterone levels in the knock-out mice indicating that other factor(s) than testosterone are responsible for the observed increase in MUP expression (Fig. 3b). Testosterone plays an important role in gonadogenesis; therefore we compared histological sections of testis and ovary of wild type and STAT6-null mice (Fig. 3c). Morphological analysis did not reveal aberrant structural organization in any of the organs: the testis showed visibly normal sperm maturation, while the ovary presented all different stages of follicle maturation.

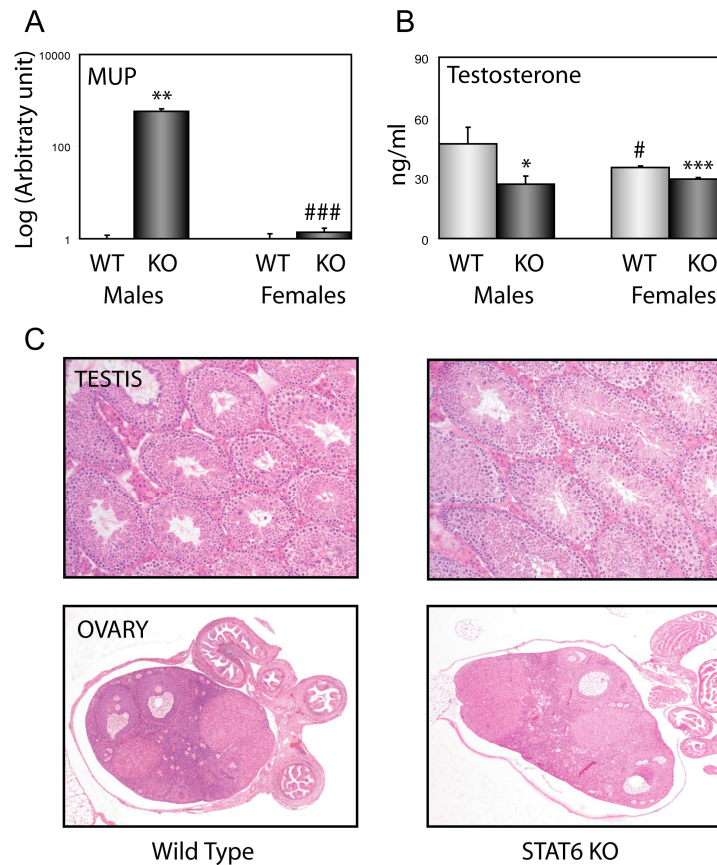


**FIG. 3. MUP mRNA expression and plasma testosterone levels.** A. Quantification of MUP mRNA expression in male and female mice. Each bar represents the average expression level expressed as arbitrary units normalized to the mean of the wild type males  $\pm$  S.E.M. (males: n=5; females: n=11). Y axis is in logarithmic scale. \*\*=  $p \leq 0.01$  wild type vs. knock-out mice; ###=  $p < 0.001$  males vs. females of the same genotype. B. Plasma testosterone levels in male and female mice (n=11). \*= $p \leq 0.05$  and \*\*\*=  $p \leq 0.001$  wild type vs. knock-out mice; #=  $p \leq 0.05$  males vs. females. C. Hematoxylin-eosin staining of testis and ovary (magnification: 5x).

### 2.5.3 Expression of Stress-related Proteins in STAT6 Knock-out Mice

Ten proteins involved in cellular defensive strategies against oxidative, metabolic and heat shock stress showed changes in their expression levels as indicated by the two different proteomic methods: glutathione S-transferase Mu 2 and 1 (GSTM2, GSTM1), methionine adenosyltransferase 1 (MAT1A), superoxide dismutase 1 (SOD1), regucalcin (RGN), lactoylglutathione lyase (GLO1), glutathione peroxidase 1 (GPX1), heat shock protein 60 (HSPD1), heat shock 70 kDa protein 5 (HSPA5) and glutathione S-transferase P1 (GSTP1) (Table I, # 1, 4, 6 and Table II, # 4, 5, 6, 13, 15, 20, 23). Real-time PCR analysis revealed that the increased protein expression was accompanied by an increase in the corresponding mRNA levels of RGN, HSPA5 and GLO1 (Fig. 4a). By contrast, GPX1 and SOD1 mRNA levels were not different between wild type and STAT6-deficient mice suggesting a posttranscriptional mechanism in the regulation of the cellular levels of these proteins (Fig. 4b). Additionally, we evaluated the mRNA expression of catalase, the enzyme responsible for neutralizing H<sub>2</sub>O<sub>2</sub> by converting it into H<sub>2</sub>O. The expression of this enzyme remained unaltered both at the mRNA and the protein levels, suggesting intracellular H<sub>2</sub>O<sub>2</sub> accumulation in the STAT6 knock-out livers (Fig. 4b and Table S2 #17).

To further characterize the hepatocellular stress of the knock-out mice we measured the mRNA expression levels of two important STAT6-related anti-oxidant proteins: heme oxygenase (HO-1) and arginase I (ARG1). Heme oxygenase is intimately involved in interleukin 10 (IL-10)-mediated protection against ischemia/reperfusion induced injury (37). STAT6 is required for IL-10 expression; therefore a previous study suggested that the lack of HO-1 might be an important factor in the development of increased hepatocellular stress in STAT6 knock-out mice (38). In accordance with this concept, a slight decrease in HO-1 expression was observed, though the difference did not reach statistical significance (Fig. 4b). Arginase I (ARG1) is a liver enzyme situated in the endoplasmatic reticulum (ER) and its expression has been shown to be induced by IL-4 in a STAT6-dependent manner (39). Contrary to our expectations, STAT6 knock-out mice displayed not a decrease but an increase in their ARG1 expression suggesting a more complex mechanism in the *in vivo* regulation of basal mRNA transcription of this gene (Fig. 4b). ARG1 competes with the nitric oxide synthase (NOS) for the same substrate (Arginine), therefore an increased ARG1 expression would imply lower hepatocellular nitric oxide (NO) levels (40). Nitric oxide is a protective factor against ischemia-induced hepatocellular injury (41). An increase in ARG1

expression would therefore aggravate the development of cellular stress in the livers of STAT6 knock-out mice through a reduction in nitric oxide availability.

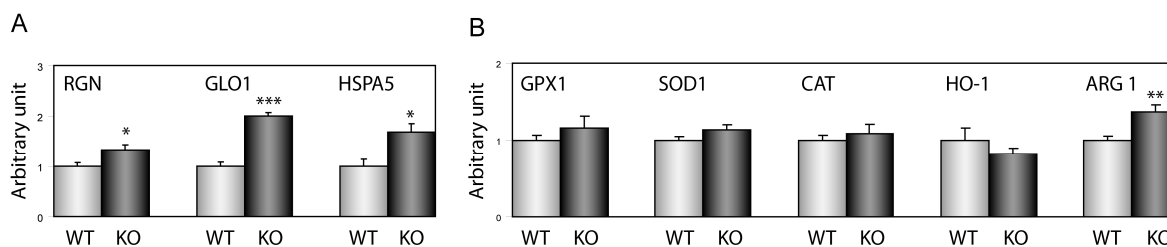


**FIG. 4. Analysis of mRNA expression in the livers of wild type and STAT6 knock-out mice.** A. Verification of up-regulation of proteins identified by both proteomic methods. Each bar represents the average mRNA level expressed as arbitrary units normalized to the mean of wild type controls  $\pm$  S.E.M., (n=5). RGN: regucalcin, GLO1: Lactoylglutathione lyase, HSPA5: Glucose Regulated Protein 78; \*=  $p \leq 0.05$ , \*\*\*=  $p \leq 0.001$ . B. mRNA expression of oxidative stress-related proteins. GPX1-1: Glutathione peroxidase, SOD-1: Superoxide dismutase 1, CAT: Catalase, HO-1: Heme oxidase, ARG1: Arginase I; \*\*=  $p \leq 0.01$ , n=10.

Further proteins involved in the regulation of cellular oxidative state are enzymes involved in the maintenance of reduced glutathione levels within the cell (reviewed in (42)). Glutathione is one of the major cellular protective factors against oxidative stress as it can act as a “buffer” against different reactive oxygen species by a reversible change between a reduced and an oxidized dimer form (GSH, GSSG). It also contributes to the maintenance of proper enzymatic functions by protecting oxidation-sensitive cystein groups situated in the active centers of a large variety of enzymes. The changes in the expression levels of the different members of this complex system identified in the liver proteome of STAT6 knock-out mice indicate a depletion of reduced glutathione pool leading to a decreased cellular capacity against oxidative insult. The summary of the functions of the different proteins of the glutathione system is depicted in Figure 5. Two important detoxifying enzymes using the glutathione system are GPX1 and GLO1. GPX1 catalyzes the reduction of peroxides while GLO1 is involved in the elimination of toxic metabolic by-products (43). Increased amount of GPX1 and GLO1 will result in lower levels of reduced glutathione (GSH), thus impairing the cell’s defensive capacity against oxidative assaults. GSH is the major substrate of glutathione S-transferase Mu 1 (GSTM1). Accordingly, the restrained availability of GSH was reflected in a diminution of GSTM1 expression. The decrease in glutathione availability is aggravated by the down-regulation of a key enzyme involved in its synthesis *e.g.* methione

adenosyltransferase 1 (MAT1A). Thus, decreased glutathione synthesis, coupled to increased GPX1 and GLO1 activity will result in the further exhaustion of GSH pool leading to impaired GST-mediated conjugation and a defective capacity to withstand oxidative stress.

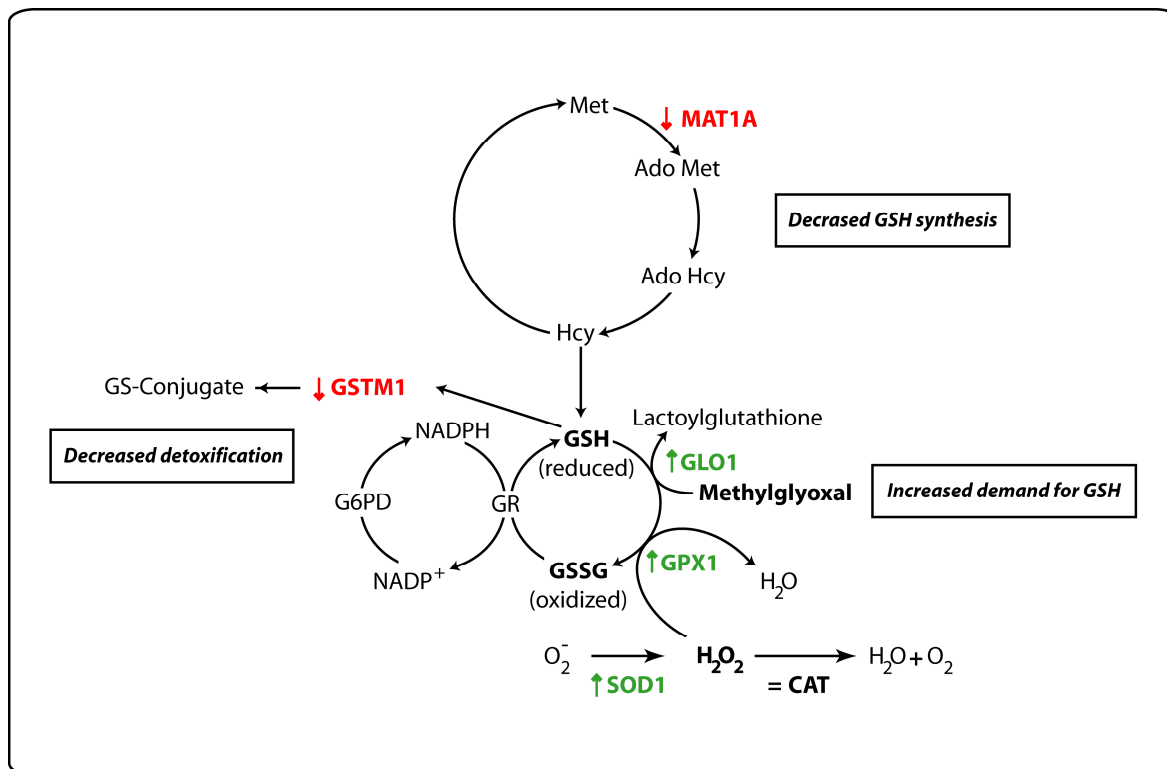


FIG. 5. **Changes in the glutathione biochemical cycle in STAT6 knock-out mice.**

Proteins identified by any of the proteomic approaches as up- or down-regulated in the STAT6 knock-out mice are represented in green and red, respectively. Arrows represent the direction of changes in protein expression (up- or down-regulation), = represents no change. Up-regulated proteins: GLO1: Glyoxalase 1, GPX1: Glutathione peroxidase 1, SOD1: Superoxide dismutase. Down-regulated proteins: GSTM1: Glutathione S-transferase Mu1, MAT1A: Methionine adenosyltransferase 1. Other abbreviations: Ado-Hcy: S-Adenosylhomocystein, Ado Met: S-Adenosyl-N-Methionine, CAT: catalase, G6PD: Glucose-6-Phosphate dehydrogenase, GR: Glutathione reductase, GSH: Glutathione (reduced form), GSSG: Glutathione (oxidized form), Hcy: Homocysteine, Met: Methionine, NADPH: nicotinamide-adenine-dinucleotide phosphate.

#### ***2.5.4 Increased Lipid Deposition in the Livers of STAT6 Knock-out Mice***

Hepatocytes fulfill a complex metabolic role both in lipid and glucose homeostasis. The proteome of the livers of the STAT6 knock-out mice revealed differences in the expression levels of several enzymes involved in both processes. The functions of the different lipid and glucose metabolic enzymes identified by the proteomic comparison and discussed in the following two chapters are summarized in Figure 8.

Liver fatty acid binding protein (FABP1) is involved in the uptake, intracellular transport and esterification of fatty acids (44). FABP1 expression was up-regulated in the livers of STAT6 knock-out mice as demonstrated by both 2-DE gel and iTRAQ analyses (Table II, #2). Cellular FABP1 content is regulated at the transcriptional level (45). Accordingly, we found a corresponding up-regulation of FABP1 mRNA expression in the knock-out mice (Fig. 6a). The physiological relevance of this elevated expression was established by direct quantification of liver lipid content which was significantly increased in the knock-out mice (Fig. 6b). Previous studies conducted in the STAT6-deficient mice failed to describe morphological signs of hepatic lipid accumulation when examined by hematoxylin-eosin staining (46). In accordance with these studies we found no gross structural alterations in similarly stained liver sections (Fig. 6c, upper panels). However, when applying the neutral lipid dye Oil-red-O, the generalized lipid deposition in the livers of the knock-out mice became evident (Fig. 6c, lower panels).

Increased lipid accumulation can reflect increased fatty acid uptake, an increase in the rate of fatty acid synthesis or a decrease in mitochondrial fatty acid  $\beta$ -oxidation. In contrast to the increased lipid storage we actually observed a decrease in the amount of ATP-citrate synthase (ACLY), an enzyme involved in the first step of fatty acid and cholesterol biosynthesis (Table I, #18). To better characterize the changes in fatty acid synthesis we assessed the mRNA expressions of two key regulatory lipogenic enzymes, acetyl-CoA carboxylase (ACC) and fatty acid synthase (FAS), which are regulated at the transcriptional level. None of the two enzymes showed significant alterations in their mRNA levels confirming that the observed lipid accumulation is not due to enhanced fatty acid synthesis (Fig. 6d). Exogenous fatty acids taken up by the liver can be oxidized during starvation or be used for triglyceride synthesis in fed conditions. FABP1 has been demonstrated to regulate fatty acid uptake and esterification but also mitochondrial  $\beta$ -oxidation under starving

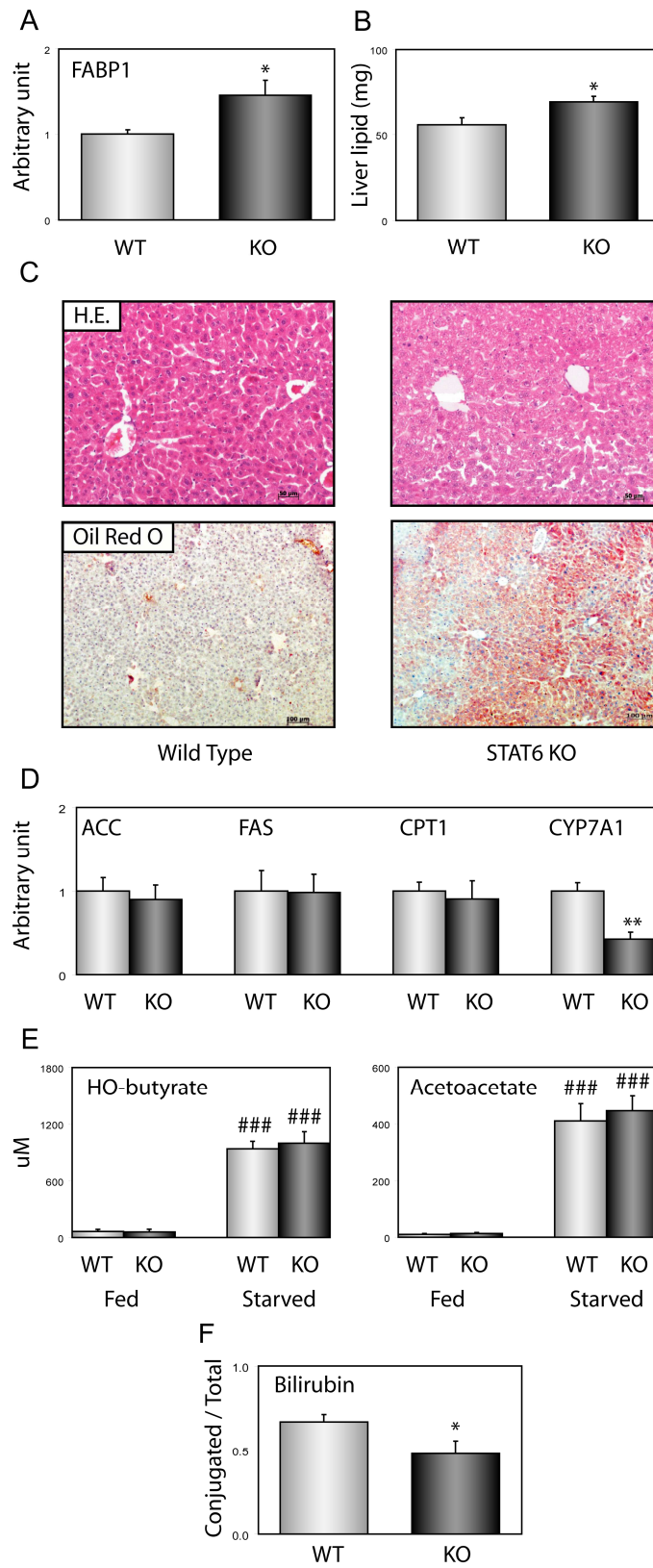
conditions when circulating fatty acid levels are high. Increased FABP1 levels in the STAT6 knock-out mice may therefore indicate increased triglyceride synthesis but also enhanced fatty acid  $\beta$ -oxidation. Indeed, we identified two  $\beta$ -oxidation-related enzymes whose expression was up-regulated: the medium-chain acyl-CoA synthetase (ACSM1) and the 3-ketoacyl-CoA thiolase (ACAA2) (Table II, # 17 and 24). Moreover, an increase in fatty acid  $\beta$ -oxidation is also indirectly suggested by the upregulation of the mitochondrial ATP synthase F1 complex (ATP5B) (Table II, # 22) involved in the oxidation of the NADH and FADH<sub>2</sub> produced during this process and in the Krebs's cycle. The rate limiting step of  $\beta$ -oxidation is the acyl-CoA transport across the mitochondrial membrane by the carnitin-palmytoil CoA transferase 1 (CPT1). CPT1 mRNA levels were not different between wild type and knock-out mice suggesting that the increase in fatty acid oxidation was within the limits of physiological capacity of this transporter (Fig. 6d). Fatty acid uptake in the liver is elevated during starvation. This elevation leads to increased triglyceride synthesis but also to enhanced acetyl-CoA production which might saturate the Krebs's cycle's eliminating capacity. Accumulation of acetyl-CoA results in the formation of beta-hydroxybutyrate (BHB) and acetoacetate, commonly referred to as "ketone bodies". In line with the similar mRNA expression levels of CPT1 we found identical BHB and acetoacetate levels in wild type and knock-out mice regardless if mice were fed or were challenged by overnight starving (Fig. 6e). This finding again suggests that the increased liver lipid content found in the STAT6 knock-out mice is the result of enhanced triglyceride synthesis and that the alterations in mitochondrial  $\beta$ -oxidation enzymes reflect an increase in fatty acid availability most likely due to the up-regulation of FABP1 expression.

iTRAQ analysis also revealed decreased expression of several enzymes involved in the cholesterol / bile acid synthesis pathway *e.g.* acetyl CoA acetyltransferase (ACAT2), farnesyl pyrophosphate synthetase (FPP Synthase) and cysteine sulfinic acid decarboxylase (CSAD) (Table I, #17, 14 and 20). In accordance with the decreased expression of these proteins we found diminished mRNA expression of CYP7A1, the rate-limiting enzyme of bile acid synthesis in rodents (Fig. 6d).

Liver plays a crucial role in the metabolism of bile acids and heme, the major functional component of hemoglobin. Bile acids are conjugated with taurin or glycin, while the degradation product of heme, bilirubin, is conjugated with glucorinic acid. The livers of STAT6 knock-out mice showed decreased expression of two key enzymes of these two

conjugating pathways: the cysteine sulfinic acid decarboxylase (CSAD) and the UDP-glucose 6-dehydrogenase (UGDH) (Table I, #20 and 13). The decreased expression of CSAD is in line with the decreased expression of several enzymes of the cholesterol/bile acid synthesis pathway. The physiological importance of the observed decrease in UGDH expression was reflected by a significant decrease in the ratio of conjugated bilirubin in the STAT6 knock-out mice (Fig. 6f).

**FIG. 6. Changes in liver lipid homeostasis in STAT6 knock-out mice (*see next page*).** A. mRNA expression of the Fatty Acid Binding Protein 1 (FABP1). Each bar represents the average mRNA level expressed as normalized to the mean of the controls  $\pm$ S.E.M.; n=5, \*=p $\leq$ 0.05. B. Total liver chloroform/methanol-extractable lipid content. n=9, \*= p $\leq$ 0.05. C. Hematoxylin-eosin (H.E.) (magnification 20x) and Oil red O (magnification 10x) staining of liver sections. D. mRNA expression of enzymes involved in lipid metabolism. Each bar represents the average mRNA level expressed as arbitrary units normalized to the mean of the wild type controls  $\pm$  S.E.M. ACC: Acetyl CoA Carboxylase, FAS: Fatty Acid Synthase, CPT1: Carnitin Palmoyltransferase 1, CYP7A1: Cytochrome 7A1. n=5, \*=p $\leq$ 0.01. E. Ketone body concentrations. Each bar represents the mean values  $\pm$ S.E.M. n= 9, ###=p $\leq$ 0.001 fed vs. starved state in mice of the same genotype. HO-butyrate: hydroxybutyrate. F. Ratio of conjugated plasma bilirubin. Data are expressed as the mean  $\pm$  S.E.M. n= 9, \*= p $\leq$  0.05.



### 2.5.5 Changes in the Expression of Glucose Homeostasis Enzymes

The two proteomic methods identified several differentially expressed proteins involved in glucose homeostasis regulation. Namely, we found a decrease in the expression levels of fructose biphosphatase 1 (FBP1), glycogen phosphorylase (PYGL) and glucose phosphate isomerase 1 (GPI1) (Table I, #10, 12, 16). Phosphoenolpyruvate carboxykinase (PCK1) is another key regulatory enzyme of gluconeogenesis whose expression is mainly regulated at the transcriptional level. Accordingly, we found a decrease in PCK1 mRNA expression (Fig. 7a), which is in keeping with the decreased FBP1 expression suggesting decreased gluconeogenesis. The altered FBP1 and PCK1 expression was a singular feature as two other rate limiting enzymes involved in glucose synthesis/utilization, glucose 6 phosphatase (G-6-Pase) and glucokinase (GK), did not show any significant variations in their expression levels (Fig. 7a). PCK1 expression has been shown to be regulated by another member of the STAT family, STAT3. The signaling of STAT family members is negatively modulated by the Suppressor of Cytokine Signaling (SOCS) proteins. In particular, SOCS3 expression was shown to be STAT6 dependent in HepG2 human hepatoma cells (47). To verify if modifications of STAT3 or SOCS3 expression are responsible for the observed down-regulation of PCK1 expression we evaluated their mRNA and protein levels by real time PCR and Western blot analysis. As judged by these two methods the expression levels of these two proteins remained unchanged in the STAT6 knock-out mice (Fig. 7b and 7c, respectively).

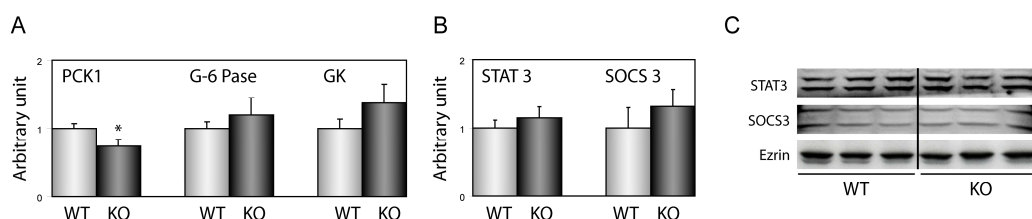


**FIG. 7. Expression of glucose homeostasis enzymes and proteins involved in cytokine signaling.** A. mRNA expression of glucose homeostasis enzymes. PCK1: Phosphoenolpyruvate carboxykinase, G-6 Pase: G-6 Phosphatase, GK: Glucokinase, (n= 10). B. mRNA expression of STAT3 and SOCS3. n=6. In all mRNA expression experiments bars represent average mRNA levels expressed as arbitrary units normalized to the mean of wild type mice  $\pm$  S.E.M. C. Western blot analysis of protein expression of STAT3 and SOCS3. Ezrin is a non-variable protein showing equal protein loading. Each blot shows three representative samples from a blot containing six individual samples.

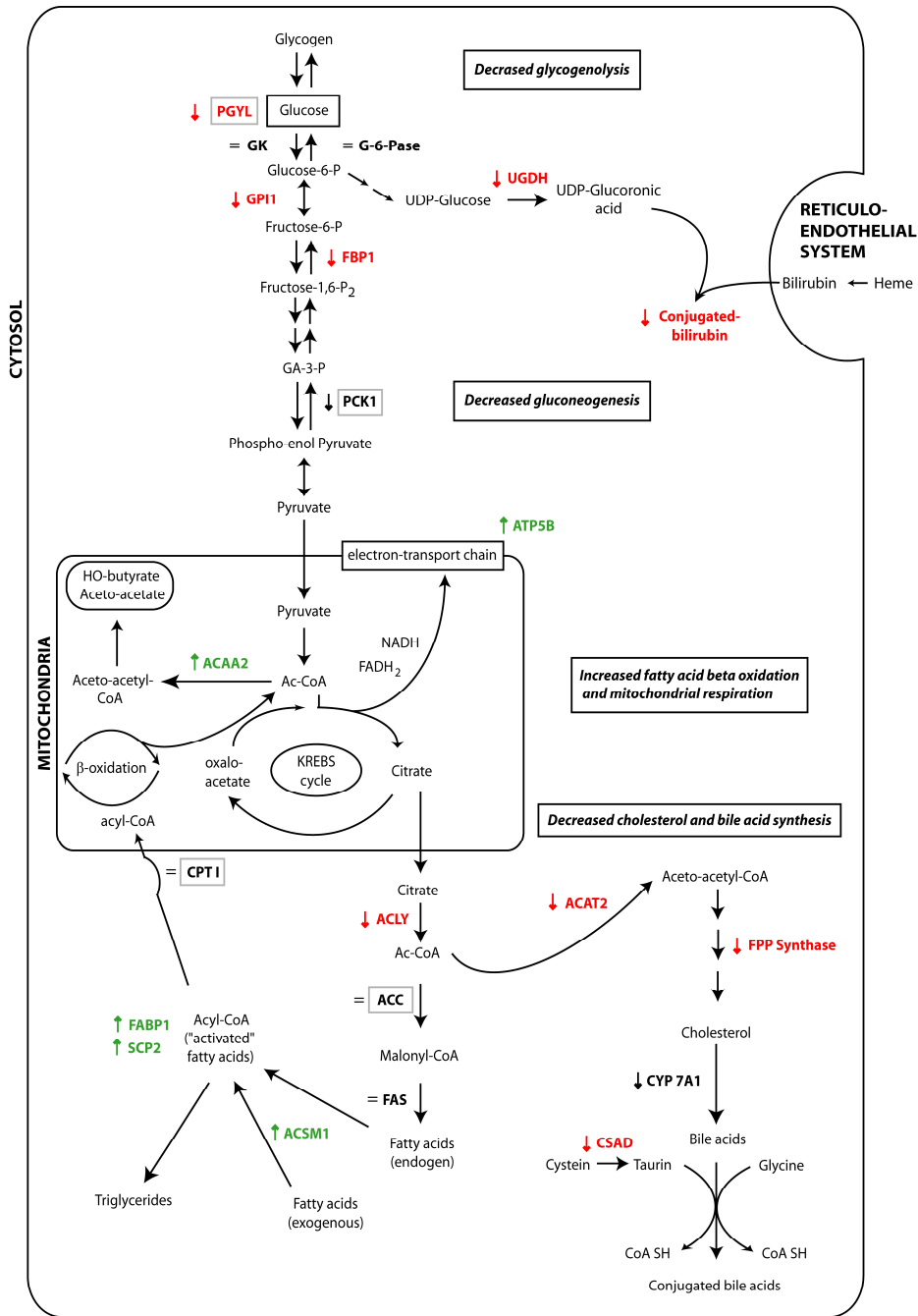


**FIG. 8. An overview of the functions of glucose- and lipid metabolic proteins identified by the two proteomic methods.** Up- or down-regulated proteins in the STAT6 knock-out mice are marked in green and red, respectively. Proteins marked in black are enzymes which were not identified in the proteomic study but whose expression was established by real-time PCR. Box around proteins refers to rate-regulating proteins. Arrows represent the direction of change, = represents no change. Up-regulated protein:

ACAA2: 3-ketoacyl-CoA thiolase, ACSM1: acyl-CoA synthetase, ATP5B: ATP synthase, FABP1: Fatty acid-binding protein, SCP2: Nonspecific lipid-transfer protein. Down-regulated protein: ACAT2: Acetyl CoA

acetyltransferase, ACLY: ATP Cytrate synthase, CSAD: Cysteine sulfinic acid decarboxylase, FPP Synthase: Farnesyl diphosphate synthase, GPII: Glucose phosphate isomerase, PCK1: Phosphoenolpyruvate carboxykinase, PYGL: Liver glycogen phosphorylase. Other abbreviations: ACC: Acetyl-Coenzyme A carboxylase, Ac-CoA: Acetyl-Coenzyme A, CoA: Coenzyme A, CPT1: Carnitin Palmoyltransferase, CYP7A1: Cytochrome P450 7A1, FADH<sub>2</sub>: Flavin adenine dinucleotide, FAS: Fatty acid synthase, FBP1: Fructose bisphosphatase 1, Fructose-1,6-P<sub>2</sub>: Fructose-1,6-bisphosphate, Fructose-6-P: Fructose-6-phosphate, GA-3-P: Glyceraldehyde-3-Phosphate, GK: Glucokinase, Glucose-6-P: Glucose-6-phosphatase, G-6-Pase: Glucose-6-phosphatase, NADH: Nicotinamide adenine dinucleotide.

### 2.5.6 *In silico* Promoter Analysis

STAT6 is a transcription factor, therefore changes in protein amount observed in the STAT6-deficient livers could be attributed to alterations in mRNA transcription of STAT6-dependent genes. Indeed, several proteins, *e.g.* GLO1, MUPs showed tight correlations between their mRNA and protein levels. In order to gain a better insight to the mechanism underlying the changes observed in the STAT6-deficient mice we performed *in silico* promoter analysis using different binding motifs, among them the consensus STAT6 binding element. The binding elements used for the analysis are listed in Table III.

**TABLE III** Oligo binding motives used for *in silico* promoter analysis.

For each motive the sequence and the total number of binding sites found in the down- or up-regulated proteins are indicated.

Motive	Sequence	Down-regulated proteins	Up-regulated proteins
STAT6	TTCNNNGAA	43	54
C/EBP	(A/G)TTGCG(C/T)AA(C/T)	0	0
AHRE-I (core)	GCGTG	118	116
AHRE-I (extended)	TNGCGTG	19	29
AHRE-I (full)	(T/G)NGCGTG(A/C)(G/C)A	1	5
AHRE-II	CATG(N6)C(T/A)TG	13	25
ARE	TGACNNNGC	38	78

First we analyzed the presence of STAT6 binding sequence in the promoter regions. 16 of the 21 down-regulated and 23 of the 28 up-regulated proteins contained one or more consensus STAT6 binding elements in their promoter regions, indicating that the presence of

the binding element is not directly linked to the observed changes in expression levels in the knock-out mice (Tables IV and V). Indeed, HSPA5 (Table V, #20) expression was up-regulated but the promoter region contained no STAT6 binding element. Moreover, the homologue selenium-binding proteins 1 and 2 were down-and up-regulated, respectively, in spite of the presence of several STAT6 consensus elements in the promoters of both proteins. Another family of transcription factors, the CCAAT/Enhancer Binding Proteins (C/EBPs), is a well known modifier of STAT6 regulated transcriptional activation (1). In addition, liver specific C/EBP $\beta$  knock-out mice display age-dependent hepatosteatosis (48). In our analysis none of the promoter regions of the identified proteins contained the classical binding element for C/EBP.

**TABLE IV** Transcription factor binding motives identified in the +5000/-1000 basepair regions of down-regulated proteins.

Number	Gene Symbol	Protein name	RefSeq	Chr.	Str	STAT6	AHRE			ARE
							I		II	
							CORE	EXT.	FULL	
1	Gstm2	Glutathione S-transferase Mu 2	NM_010359	chr3	-	2	2		1	1
2	Got1	Glutamate oxaloacetate transaminase 1	NM_010324	chr19	-	2	6	1	2	
3	Selenbp1	Selenium-binding protein 1	NM_009150	chr3	+	2	3			1
4	Gstm1	Glutathione S-transferase, Mu 1	NM_010359	chr3	-	2	2		2	1
5	Dbi	Acyl-CoA-binding protein	NM_007830	chr1	-	3	12		1	3
6	Mat1a	Methionine adenosyltransferase 1	NM_133653	chr14	+	2	1			2
7	Krt18	Keratin complex 1, acidic	NM_010664	chr15	+		7	3		2
8	Ass1	Argininosuccinate synthase	NM_007494	chr2	+	5	4	1		2
9	Adh1	Alcohol dehydrogenase 1	NM_007409	chr3	+		5			
10	Fbp1	Fructose biphosphatase 1	NM_019395	chr13						
11	EtfA	Electron transferring flavoprotein	NM_145615	chr9	-	2	5			1
12	Pygl	Liver glycogen phosphorylase	NM_133198	chr12	-	1	4		1	3
13	Ugdh	UDP-glucose 6-dehydrogenase	NM_009466	chr5	-		8	2	1	3
14	Fdps	Farnesyl pyrophosphate synthetase	NM_134469	chr3	-	1	6		1	1
15	Tuba6	Tubulin alpha-6 chain	NM_009448	chr15	+	1	7	1		2
16	Gpi1	Glucose phosphate isomerase 1	NM_008155	chr7	-	3	13	1	1	3
17	Acat3	Acetyl CoA transferase-like protein	NM_153151	chr17	-	4	5	2		1
18	Acat2	Acetyl CoA acetyltransferase, cytosolic	NM_009338	chr17	-	4	6	1	1	
19	Acly	ATP-citrate synthase	NM_134037	chr11	-	3	7	2		1
20	Cyca	Cytochrome C protein, somatic	NM_007808	chr6						
21	Csad	Cysteine sulfinic acid decarboxylase	NM_144942	chr15	-	4				

**TABLE V** Transcription factor binding motives identified in the up-regulated proteins.

Number	Gene Symbol	Protein Name	RefSeq	Chr.	Str	STAT6	AHRE I			AHRE II	ARE
							CORE	EXT.	FULL		
1	Ca3	Carbonic anhydrase 3	NM_007606	chr3	+	1	2				3
2	Fabp1	Fatty acid-binding protein   FABPL	NM_017399	chr6	+	1	1	2		1	1
3	Hba-a1	Hemoglobin alpha chain	NM_008218	chr11	+	1	3	2			
4	Sod1	Superoxide dismutase [Cu-Zn]	NM_011434	chr16	+		13	2		1	4
5	Rgn	Regulocalcin   SMP 30	NM_009060	chrX	+	1	5				3
6	Glo1	Lactoylglutathione lyase LGUL	NM_025374	chr17	-	1	3			1	3
7	Selenbp2	Selenium binding protein 2	NM_019414	chr3	+	3	3				2
8	Mup1a	Major urinary protein 1 MUP	NM_031188	chr4	-	3	1			2	1
9	Mup1b	Major urinary protein 1 MUP	NM_031188	chr4	-	3	1			2	1
10	Mup2	Major urinary protein 2 MUP	NM_008647	chr4	-	2	1			2	1
11	Mup6	Major urinary protein 6 MUP	NM_008648	chr4	-	2	1	1		2	1
12	Mup8, Mup11	Major urinary protein 8 & 11 MUP	NM_008649	chr4	-	3				1	2
13	Gpx1	Glutathione peroxidase 1	NM_008160	chr9	+	1	9				1
14	Alb	Serum albumin	NM_009654	chr5	+	1	2			1	
15	Hspd1	60 kDa heat shock protein	NM_010477	chr1	-	4	7	1	1		2
16	Hbb-b1	Hemoglobin beta-1 chain	NM_016956	chr7	-	1		1		1	
17	Acsm1	Medium-chain acyl-CoA synthetase	NM_054094	chr7	+		2				5
18	Krt18	Keratin complex 1, acidic	NM_010664	chr15	+		7	3			2
19	Uox	Urate oxidase	NM_009474	chr3	+	1	2				3
20	Hspa5	Heat shock 70kDa protein 5   GRP 78	NM_022310	chr2	+		8	2		1	1
21	Cyb5	Cytochrome b-5	NM_025797	chr18	+	2	4				8
22	Atp5b	ATP synthase, H+ transp. mitoch. F1 comp	NM_016774	chr10	+	1	6			1	1
23	Gstp1	Glutathione S-transferase P1									
24	Acaa2	3-ketoacyl-CoA thiolase, mitochondrial	NM_177470	chr18	+	1	8	3		3	1
25	Sep2	Nonspecific lipid-transfer protein	NM_011327	chr4	-	1	3				1
26	Nme2	Nucleoside diphosphate kinase B	NM_008705	chr11	-	4	2	1		1	1
27	Akr1c6	Estradiol 17 beta-dehydrogenase 5	NM_030611	chr13	+	1	1	1			1
28	Tst	Thiosulfate sulfurtransferase	NM_009437	chr15	-	3	11	2			2

We also extended our investigation to other proteins whose mRNA expression we analyzed in this study. Several of the proteins displayed STAT6 consensus sequence(s) in their promoter regions, *e.g.* ARG1, CYP7A1, FAS or G-6-Pase. Here again the presence of the binding element was not directly linked to the observed changes in expression levels as ARG1 was up-regulated, CYP7A1 was down-regulated while FAS and G-6-Pase showed no alterations (Table VI).

**TABLE VI Motives identified in the genes whose mRNA expression has been determined in the study.**

Number	Gene Symbol	Protein Name	RefSeq	Chr.	Str	STAT6	AHRE			ARE
							CORE	EXT.	FULL	
1	Arg1	Arginase 1, liver	NM_007482	chr10	-	3	3			1
2	Cyp7a1	Cytochrome P450, fam 7, sub a, poly 1	NM_007824	chr4	-	1	1	1		
3	Fasn	Fatty acid synthase	NM_007988	chr11	-	1	8	1		1
4	Pck1	Phosphoenolpyruvate carboxykinase	NM_011044	chr2	+			2		1
5	G6pc	Glucose-6-phosphatase, catalytic	NM_008061	chr11	+	1	2			3
6	Gck	Glucokinase	NM_010292	chr11	-		3			1
7	Soes3	Suppressor of cytokine signaling 3	NM_007707	chr11	-		11			1
8	Ahr	Aryl-hydrocarbon receptor (AHR)	NM_013464	chr12	-	3	5	1		1
9	Arnt	Aryl hydrocarbon receptor nucl. transloc.	NM_001037737	chr3	+		4			4

STAT6 knock-out mice are more susceptible to hypoxia/reperfusion induced liver injury (46, 49). Hypoxia-induced gene expression is mediated to a great extent by the hypoxia-inducible factor 1a (HIF-1 $\alpha$ ) (50). HIF-1 $\alpha$  belongs to the family of Per-Arnt-Sim (PAS) family of basic helix-loop-helix (bHLH) transcription factors. The bHLH/PAS family of proteins is intimately involved in the adaptive responses to generalized and cellular stress. One of the members of this family is the aryl-hydrocarbon receptor (AHR) known primarily for mediating the toxic effects of aromatic xenobiotics (reviewed in (51)). However, more recent data indicated a role for the AHR also in physiological processes, well beyond the adaptive response to xenobiotics, most importantly in hypoxia-mediated signaling (52). These data urged us to examine the presence of the different AHR-related binding sequences in the promoter regions of the genes identified by our proteomic study. The different nucleotide sequences of the consensus motifs were previously listed in Table III. Aryl-hydrocarbon receptor responsive element I (AHRE I) motif is the classical binding sequence for the aryl-hydrocarbon receptor. AHRE II has been recently described as a new binding element for a functionally related group of genes regulated by the AHR in cooperation with an additional DNA-binding protein, possibly the oestrogen receptor (53). The antioxidant responsive element (ARE) is responsible for mediating the indirect effects of dioxin, the classical activator of the AHR. The core pentanucleotide sequence of the AHRE I motif was found in virtually all promoters. By contrast, there were only 9 down- and 12 up-regulated proteins containing the extended or full motif. We identified 8 down- and 14 up-regulated proteins

containing the consensus AHRE II motif and 15 down- and 24 up-regulated proteins containing the ARE motif.

A large number of proteins (15 down-regulated and 23 up-regulated proteins) contained both STAT6 elements and one or several of the AHRE I, AHRE II or the ARE motifs. Most notably, the promoter regions of MUPs – the proteins showing the greatest increase in the STAT6 knock-out mice - contained the sequence of STAT6, AHRE II and ARE motifs. ARH acts as a heterodimer in association with the Aryl Hydrocarbon Receptor Nuclear Translocator (ARNT) (54). Interestingly, while the promoter region of the AHR contained several STAT6 elements, the promoter of ARNT was devoid of this sequence (Table VI, # 8 and 9).

## 2.6 Discussion

The aim of our investigation was to assess the impact of loss of signaling by STAT6, a transcription factor mediating the effects of two protective cytokines, IL-4 and IL-13, in liver.

In the first part of our study we compared the liver proteomes of wild type and STAT6 knock-out mice using two different techniques commonly used in proteomics, namely 2D gel electrophoresis and 2D nanoscale LC tandem mass spectrometry, also known as multidimensional protein identification technology (MudPIT) (55). The results illustrate well the complementarity of these two techniques, since about a third of all the differentially expressed proteins identified in this study were found by both techniques. The main advantage of 2D-PAGE remains in the fact that separation occurs at the protein level and this technique is well adapted to resolve protein isoforms (56) as shown for the different SBP1 and SBP2 isoforms or for the MUP protein family (57). On the contrary, separation occurs at the peptide level in shotgun liquid-based techniques such as the MudPIT approach. Thus, peptides issued from the digestion of a single protein are not anymore analyzed in the same nLC-MS/MS run as in the 2D-PAGE approach, but are scrambled over all the two dimensional SCX and C18 fractions, which renders isoforms identification less obvious. However, quantification of differentially expressed proteins remains a difficult task when comparing 2D gel maps. Indeed, direct comparison of different 2D gel images is rarely

evident and often requires some image warping. Thus, quantification based on spot intensity differences becomes limited even with a good normalization of image backgrounds. Therefore, gel-based techniques with covalently bound fluorescent dyes have been developed such as the 2D fluorescence differential gel electrophoresis (DIGE) technology (58, 59) to circumvent problems due to 2D maps comparison and leverage technical variability. But it has been shown recently that migration shifts exist between the small amount of labeled proteins (*i.e.* 1-2%) and the remaining unlabeled proteins, which can lead to a loss of sensitivity and thus a loss in protein identification reliability (60). On the contrary, with the liquid-based approach combined with tandem mass spectrometry quantification occurs by comparing peak areas of isotopically labeled compounds. In iTRAQ analysis, the ratio of two different MS/MS reporter ions (*i.e.* reporter 114 and 115) is calculated for each identified peptide in order to find differentially expressed proteins. MS-based quantitation is more accurate than gel image comparison, and tandem mass spectrometry is commonly used for its quantitative performance of low molecular weight compounds when using selective scanning mode such as selected reaction monitoring (SRM) (61). Recently, SRM has also been adapted for the quantitative analysis in proteomics and new strategies, such as the stable isotope standards and capture by anti-peptide antibodies (SISCAPA) method, have been developed for targeted proteomics analyses (62-64). Using these two complementary proteomic techniques we identified 20 down-regulated and 28 up-regulated proteins in the STAT6 knock-out mice.

In the next phase of our study we validated the physiological relevance of the identified proteins. The highest increase in expression was detected in case of the major urinary proteins (MUPs). MUPs received their name by their predominance in mouse urine constituting a “physiological proteinuria” (reviewed in (65)). MUPs are filtrated by kidney glomeruli freely due to their low (approximately 18kDa) molecular weights and their globular form. Major urinary proteins belong to the family of lipocalin proteins, characterized by an overall structure of eight  $\beta$ -sheets defining a  $\beta$ -barrel configuration. The hydrophobic core of the molecule binds volatile polar pheromones in the male urine and releases them slowly once deposited as a territorial “scent mark” (66, 67). MUPs are primarily produced in the liver in a sex dependent manner with the males having significantly higher expression levels than females (68, 69). MUPs are the products of a multigene family of approximately 30 genes and pseudogenes localized on mouse chromosome 4 displaying high sequence homology both at the mRNA and the protein levels (70). Transcription of MUPs can be

induced by testosterone, growth hormone, thyroxin, insulin and dexamethasone administration. Surprisingly, we found a decrease rather than an increase in testosterone levels, a finding that rules out the most common factor as the cause of the spectacular up-regulation of MUP expression in the knock-out mice. STAT6 knock-out mice display no noticeable differences in body size or weight arguing against an increase in growth hormone levels, as well. In addition, thyroid hormone and random fed insulin levels were not different between wild type and STAT6 knock-out mice (data not shown). Taken together, these data suggest the involvement of currently unidentified factor(s) in the regulation of MUP expression.

Results from other studies showed that MUP expression is often altered in conditions linked to liver dysfunction *e.g.* lipid accumulation or sclerosis though no direct correlation between MUP expression and the development of fatty liver disease could be established (71, 72). MUPs belong to the family of extracellular lipid-binding proteins, also referred to as “lipocalins” (73). Recently, serum retinol binding protein 4 (SRBP4), another member of the lipocalin family, has been shown to be increased in the white adipose tissue of high-fat diet fed and genetically obese (*ob/ob*) mice (74). When examining if a similar regulation of MUP expression occurs in the livers we found a down-regulation in two different genetically obese rodent models characterized by hepatosteatosis: *ob/ob* mice and *fa/fa* rats (Supplementary Material - Fig. S1). Taken together, these data also support a so far unappreciated role for MUP in liver lipid homeostasis though a more complex and less direct one than that of SRBP4 in the white adipose tissue.

The two proteomic analyses identified several members of diverse stress-related cellular networks related to the regulation of cytoplasmic selenium and glutathione concentrations. Moreover, we found a large number of proteins involved in the defense mechanism against heat shock and endoplasmatic reticulum stress.

One of the most important stress-response proteins are the selenium binding proteins. Selenium binding proteins (SBPs) belong to the family of selenium-containing proteins (43). In contrast to the subgroup of selenoproteins containing selenium incorporated in selenocystein by the use of a specific selenocysteil- tRNA, SBP molecules do not internally contain selenium but rather bind it externally in a chemically yet undetermined fashion (43). There are three different selenium-binding proteins: a 14 kDa protein called the liver fatty acid-binding protein (FABP1) and two homologue proteins called selenium binding protein 1

and 2 (SBP1 and SBP2). Selenium binding protein 2 has been described as the major target for acetaminophen in mouse liver cytosol and therefore is also known as the 56 kDa acetaminophen-binding protein (APBP, AP56) (35, 75-77). The two SBPs share a high degree of identity both at the mRNA (98%) and at the protein (96%) levels with a difference of mere 18 amino acids between their sequences. SBP1 has a slightly lower calculated molecular weight (52351.82) and higher pI value (5.97) when compared to SBP2 (MW= 52628.04 and pI= 5.78). In contrast to SBP1, the expression of SBP2 was up-regulated in STAT6-deficient mice. This opposite regulation of the two SBP isoforms was confirmed by 2-DE and iTRAQ analyses validating its physiological relevance. Indeed, in spite of their structural and apparent functional similarity SBP1 and SBP2 expression were found to be divergent in several previous studies (78-82). SBP2 was down-regulated in CCl<sub>4</sub>-induced liver injury, while administration of the AHR-ligand TCDD led to the up-regulation of this protein (31, 72, 83, 84). Clofibrate, a hypolipidemic compound acting through the peroxisome proliferator  $\alpha$  (PPAR- $\alpha$ ) was shown to protect cells from oxidative stress and the resultant cytotoxicity induced by H<sub>2</sub>O<sub>2</sub> treatment, a diverse array of hepatotoxic compounds and hypoxia-reoxygenation (85). Interestingly, SBP2 expression decreases after clofibrate treatment co-inciding with a decrease in hepatic lipid content (83, 84). An even more specific link between liver lipid homeostasis and SBP2 expression was indicated by the study of Park *et al.* where feeding of a hypercholesterinemia-inducing diet led to the down-regulation of SBP2 expression in the steatosis susceptible C57BL6/J but not in the resistant C3H strain (71). In this regard the increased SBP2 expression in the STAT6 knock-out mice could be viewed as an adaptive mechanism against the gradually developing lipid deposition and the consequential ROS accumulation leading to metabolic oxidative stress. Indeed, in addition to their role in selenium homeostasis, a direct antioxidant activity has been postulated for SBPs in analogy to other selenocysteine-containing enzymes *e.g.* glutathione peroxidase 1 (GPX1) (81). This point is substantiated by the fact that GPX1 have been identified as up-regulated in STAT6 knock-out mice.

Another selenium-containing protein, the 14 kDa fatty acid binding protein (FABP1, P12710) was also observed to be up-regulated in the livers of STAT6-null mice. Apart from its fatty acid binding function FABP1 has been shown to play a crucial role in the anticarcinogenic and growth inhibition functions of selenite by acting as a growth regulatory protein (32, 34, 86). FABP1 is composed of 127 amino acids containing seven methionine and one cysteine groups (87, 88). Notably, of all the amino acids, the sulphur containing

cysteine and methionine groups are the most easily oxidizable by different reactive oxygen species (ROS) (89). Thus, FABP1 may act as an effective endogenous cytoprotectant against hepatocellular oxidative stress (90).

Confirming the presence of increased stress in the livers of STAT6 knock-out mice, we found an increase in the expression of a third selenium-containing protein: the seleno-enzyme GPX1 (91). GPX1 takes part in regulating the availability of reduced glutathione, a major factor implicated in the cellular anti-oxidant defense system. In line with the alterations in GPX1 expression we found coordinated changes in the levels of other enzymes of this system. The overall picture that emerged was a decrease in glutathione anti-oxidative capacity in the STAT6 knock-out mice. This finding is in accordance with the sensitivity of STAT6 knock-out mice towards liver and kidney ischemia-reperfusion injury and with the protective effect of IL-4 and IL-13, the two STAT6-dependent cytokines against these insults (92). The importance of intact glutathione metabolism is emphasized by the finding that mice deficient for MAT1A, the enzyme regulating glutathione synthesis, develop spontaneous non-alcoholic hepatosteatosis (NASH) and hepatocellular carcinoma (93, 94). The importance of the intact function of the glutathione system was recently confirmed in a human study where a decrease in GSTM expression was reported in steatotic livers (95).

The glutathione system also plays an important role in the defense against the accumulation of toxic metabolic by-products. Toxic byproducts can be formed through lipid peroxidation and the formation of advanced glycation endproducts (AGEs). One of the enzymes involved in the elimination of these toxic metabolites is lactoylglutathione lyase / glyoxalase 1 (GLO1). GLO1 mediates the glutathione-conjugated elimination of methylglyoxal, a reactive  $\alpha$ -oxoaldehyde formed during lipid peroxidation, glycolysis or the degradation of glycated proteins (96, 97). GLO1 uses the reduced form of glutathione (GSH) for its detoxification function; therefore elevated GLO1 activity will further deplete cellular GSH stocks. Nitric oxide is a potent inhibitor of lipid peroxidation (98). We found an up-regulation of ARG1 expression in STAT6 knock-out mice implying lower cellular nitric oxide levels through direct competition with the nitric oxide synthase for their shared substrate, arginine. Thus, lower nitric oxide levels would further aggravate ROS accumulation and would contribute to the development of cellular stress.

In summary, the proteome of the STAT6-deficient mice presented an overall picture with a depletion of cellular defensive reserve to withstand oxidative stress and an up-

---

regulation of enzymes involved in the elimination of different reactive oxygen species and damaging metabolites.

Cellular stress is also linked to disturbances in ER function through a complex response known as the unfolded protein response (UPR). (99, 100) Metabolic and calcium disturbances, hypoxia or an unbalance in cellular redox or glycosilation state can all lead to stress within the endoplasmatic reticulum (ER) resulting in the release of  $\text{Ca}^{2+}$  and triggering cell injury or apoptotic response (101, 102). STAT6 knock-out mice displayed a strong up-regulation of HSPA5 expression, a hallmark of ER stress (103). HSPA5 has been shown to be activated by reduced  $\text{Ca}^{2+}$  concentration, to protect cells from oxidative/metabolic stress thus prevent cell death (83, 104-107). The ER stress and the activation of defensive mechanisms suggested by the increase in HSPA5 expression is in line with the up-regulation of regucalcin and GLO1 implying disturbed calcium homeostasis and an increase in protein glycosylation, respectively. The physiological importance of HSPA5 in liver function is underlined by a recent study identifying HSPA5 as one of the “focus” genes in experimental NAFLD (108).

HSPA5 belongs to the family of heat shock proteins. Expression of heat shock proteins can be induced by exposing the cells to conditions of environmental stress, including heat shock, oxidative stress, heavy metals, or to pathologic conditions, such as ischemia-reperfusion, inflammation, tissue damage, infection or mutant proteins associated with genetic diseases (109). Heat shock proteins function as molecular chaperones or proteases. Molecular chaperones are a class of proteins that interact with diverse protein substrates to assist in their folding, with a critical role during cell stress to prevent the appearance of folding intermediates or otherwise damaged molecules (109). Consequently, heat shock proteins assist in the recovery from stress either by repairing damaged proteins (protein refolding) or by degrading them, thus restoring protein homeostasis and promoting cell survival (109). In our study we identified another up-regulated heat shock protein: HSPD1 (HSP60). HSPD1 is a mitochondrial matrix protein that participates in a chaperone complex responsible for the proper folding of mitochondrial DNA encoded proteins and polypeptides. As the mitochondria generates copious amounts of free radicals, the chaperones promoting refolding of redox-modified proteins to prevent aggregation are of extreme importance (110). The up-regulation of this mitochondrial chaperone suggests a specific role for mitochondria-derived ROS production in the development of hepatocellular stress in STAT6 knock-out

mice. This finding is in line with a previous human studies showing mitochondrial deficiency in NASH biopsies (111, 112).

Cellular stress related to disturbed ER and mitochondrial functions is linked to unbalanced intracellular calcium homeostasis (102). Many different cellular mechanisms are influenced by cytoplasmic calcium concentrations including enzyme activity and protein synthesis (101). Perturbation of calcium homeostasis in STAT6 knock-out mice was suggested by the up-regulation of regucalcin, a protein playing a major role in regulating cellular calcium fluxes. Regucalcin is a 299- amino-acid protein preferentially expressed in hepatocytes and in renal tubular epithelia (reviewed in (113)). Expression of regucalcin decreases with age in rat and mouse liver in an androgen-independent manner hence its second name, senescence marker protein (SMP30) (114). Regucalcin is thought to play an important regulatory role in cytosolic  $\text{Ca}^{2+}$  homeostasis through modulating the activity of the plasma membrane, mitochondrial and microsomal  $\text{Ca}^{2+}$  pumps thus protecting the cell against a rise in cytosolic calcium content and the subsequent cellular stress and cell death (115). This protective function was also demonstrated *in vivo* using regucalcin knock-out mice. Indeed, these mice display signs of accelerated ageing: oxidative stress in the brain, pigment deposition in kidney tubular cells and elevated triglyceride deposition and mitochondria enlargement in liver (116-119). Regucalcin expression is regulated at the transcriptional level (115). Enhanced regucalcin promoter activity and expression have been observed upon stimulation with phorbol 12-myristate 13-acetate (PMA), dexamethasone and insulin in H4-II-E murine and in HepG2 human hepatoma cells. By contrast, TNF- $\alpha$  treatment resulted in reduced regucalcin protein amount (120-122). Based upon the contrasting regulation by insulin and TNF- $\alpha$  Solomon *et al.* suggested a role for regucalcin in hepatocyte insulin resistance (122). The importance of regucalcin in liver metabolism *in vivo* was confirmed by several proteomic and genomic studies. Most notably, an upregulation of regucalcin expression was identified in the livers of Han/Wistar rats resistant to the hepatotoxic drug tetrachlorodibenzo-*p*-dioxin (TCDD) when compared to the livers of the TCDD sensitive Long-Evans rats (31). By contrast, regucalcin was found to be down-regulated in livers of C57Bl/6 mice, a strain susceptible to atherogenic diet, compared to the resistant C3H/HeJ mice; and in the livers of senescence accelerated mice (SAM) (71, 82). Taken these data together, they suggest that the increased regucalcin expression observed in the STAT6 knock-out mice can be viewed as part of the cellular defense mechanism against the metabolic/calcium stress induced by the hepatocellular lipid deposition in these mice. In line

with the close relationship between calcium- and STAT6-mediated signaling are the data reporting the intertwining activation of these two pathways in polycystic kidney disease (12).

Several liver enzymes controlling lipid and glucose homeostasis were differentially expressed in STAT6 knock-out mice. Altogether, these changes suggested an increase in fatty acid metabolism due to excess exogenous fatty acid loading. The most prominent change was observed in case of the liver fatty acid binding protein, FABP1. Interestingly, another member of the family of fatty acid binding proteins, the adipocyte/macrophage aP2 has been shown to be inducible by IL-4 in human bronchial cells (HBCs) in a STAT6 dependent manner. This study also showed a contrasting regulatory mechanism regulating aP2 expression in HBCs and in murine 3T3L1 adipocytes pointing towards a complex tissue-specific network implicated in the regulation of this gene's expression (13). Our data concerning the up-regulation of FABP1 expression in STAT6 knock-out mice add a new element to our understanding of the regulation of expression of different fatty acid binding proteins *in vivo*. It is of interest that both FABP1 and STAT6 have been down-regulated in human hepatitis C protein expressing but not in steatotic Huh7 hepatocytes implying the possible involvement of these proteins in the development of steatosis-related inflammation and fibrosis (123, 124).

Concerning the liver lipid accumulation in STAT6 knock-out mice it is worthwhile to mention, that the mice used in this study were created using the Balbc/J inbred mouse background, a strain less frequently employed in metabolic studies. One related strain, Balb/cByJ was recently shown to display highly increased serum and liver triglyceride levels due to a deletion in the short-chain acyl-CoA dehydrogenase gene impairing fatty acid  $\beta$ -oxidation (125). Previous studies indicated that this mutation was absent from the Balbc/J strain, a result that we also confirmed in the mice used in these experiments ((126) and data not shown).

Comparing our results with those obtained from different rodent models of hepatosteatorosis we confirmed the relevance of several proteins. Regucalcin, carbonic anhydrase 3 and selenium binding protein 2 were up-regulated in our study while they were down-regulated in the atherogenic diet-sensitive C57BL6/J mice and in CCl<sub>4</sub> treated BALB/c mice indicating that these proteins are not likely to be determining factors in the development of hepatosteatorosis but rather reflect a general defensive mechanism against oxidative/metabolic stress (71, 72). By contrast, a more direct role can be confirmed for

HSPA5, which has been differentially expressed in several murine models of hepatosteatosis (72, 127). Up-regulation of HSPA5 in the STAT6 knock-out mice is likely aimed at alleviating ER stress, thus providing an efficient protection of hepatocytes. The efficiency of protection is evidenced by the lack of overt hepatic pathology in the STAT6 knock-out mice. Indeed, improving ER folding capacity by the administration of chemical chaperones was successfully applied to improve hepatosteatosis in the ob/ob mice (128). Moreover, a protective role for HSPA5 against the development of fatty liver was proposed in a recent study where a significant decrease of HSPA5 was reported in early stage hepatic steatosis (129).

Our proteomic data suggested that STAT6 exerts a protective effect against the development of non-alcoholic fatty liver disease (NAFLD) through a complex regulatory network involving metabolic enzymes and proteins involved in redox and cell cycle regulation. When comparing our data we found that several proteins identified in our study have been positively identified in studies exploring the network of aryl-hydrocarbon receptor (AHR) signaling. Indeed, recent data indicated that beside its major function as a xenobiotic receptor for aromatic compounds, the aryl-hydrocarbon receptor-mediated pathways play an important role in regulating metabolic homeostasis in pancreatic islet  $\beta$ -cells and in transmitting the effect of hypoxia on vascular endothelial growth factor expression in mice *in vivo* (51, 52, 130). Using *in silico* analysis we identified different AHR binding motifs in the promoter regions of the proteins with differential expression in STAT6 knock-out mice. Our results concerning the number of identified sites are not in complete agreement with previous studies due to using updated gene annotation from the UCSC database (mm8 versus mm5) and owing to the fact that since the publication date of the papers mentioned above additional untranslated region (UTR) exons were identified resulting in the modification of the position of the transcription start sites (31, 131). However, we confirmed the binding motifs in several proteins identified in those studies *e.g.* regucalcin, CA3, SBP2 and PCK1. While the verification of the functionality of the motifs found in the promoter regions is well beyond the scope of this study it is of interest that a relatively large percent of proteins contained one or more full or extended AHRE I and/or AHRE II elements when compared to our expectations based upon a previous phylogenetic analysis published by Boutros *et al.* (53).

The development of non-alcoholic fatty liver in STAT6 knock-out mice is in accordance with previous results demonstrating that these mice are prone to develop more

serious atherosclerotic lesions with enhanced lipid deposition in the aortic wall when challenged by a high-fat diet (132). The relevance of these results to human pathology was recently highlighted by data identifying STAT6 as one of the three mRNAs showing the greatest up-regulation in aortic atherosclerotic plaques (133). In addition, a recent study suggested an association between atherosclerosis and NAFLD (134). Proteomic studies conducted in human NAFLD did not identify STAT6 as a differentially expressed protein. It is not surprising given the very low abundance of this protein as demonstrated by the lack of detection both by 2D gel electrophoresis and iTRAQ analysis in our study. Microarray studies of human NAFLD did not reveal significant differences in STAT6 expression but identified several common proteins with our study (95, 111, 112). Moreover, STAT6 was down-regulated in hepatitis C virus protein expressing human hepatocytes (124). Hepatitis C virus infection is often associated with the occurrence of liver steatosis. These results confirm that the phenotype of STAT6 knock-out mice bears resemblance to the human pathology and imply a yet unappreciated, most likely indirect contribution of STAT6 to the development of NAFLD.

In summary, our study explored the effect of the suppression of IL-4 and IL-13-mediated anti-inflammatory signals in liver function by comparing the proteomes of wild type and STAT6 knock-out mice. To achieve this goal we employed two complementary techniques frequently used for differential analyses: 2D gel electrophoresis and 2D nLC-MS/MS combined with iTRAQ labeling technique. Based upon the identified proteins we revealed a so far unknown metabolic phenotype in the STAT6-deficient mice and showed the presence of latent liver steatosis. These results demonstrate a protective role for STAT6 against hepatic lipid deposition; a finding reminiscent of the protective role it plays against the development of atherosclerotic lipid accumulation. According to our results, a role for STAT6 in the context of non-alcoholic fatty liver disease in humans is a topic worth to be further explored.

---

## 2.7 Acknowledgements

We are grateful to colleagues who generously provided advice and reagents. We thank N. Desmeules, C. Manzin and S. Mouche (Department of Cell Physiology and Metabolism, University of Geneva) for excellent technical help; Prof. P. Bischof (Department of Gynecology and Obstetrics, University Hospital of Geneva) for the testosterone measurements, Dr. J-C. Sanchez, P. Arboit and N. Walter (Proteomic Platform, University of Geneva) for help with the 2-DE gel analysis; Prof. D. Hochstrasser and Dr. O. Golaz (Central Clinical Chemistry Laboratory of the University Hospital of Geneva) for serum measurements, Dr P. Descombes and C. Delucinge (Genomics Platform, NCCR “Frontiers in Genetics”, University of Geneva) for the promoter analysis and P. Boutros (Department of Pharmacology, University of Toronto) for providing the Bioperl scripts and valuable scientific comments. This work was supported from a grant from COST Action B17, No.C02.0097.

## 2.8 References

1. Hebenstreit, D., Wirnsberger, G., Horejs-Hoeck, J., and Duschl, A. (2006) Signaling mechanisms, interaction partners, and target genes of STAT6. *Cytokine Growth Factor Rev* 17, 173-188.
2. Borner, C., Woltje, M., Hollt, V., and Kraus, J. (2004) STAT6 transcription factor binding sites with mismatches within the canonical 5'-TTC...GAA-3' motif involved in regulation of delta- and mu-opioid receptors. *J Neurochem* 91, 1493-1500.
3. Kraus, J., Borner, C., and Hollt, V. (2003) Distinct palindromic extensions of the 5'-TTC...GAA-3' motif allow STAT6 binding in vivo. *Faseb J* 17, 304-306.
4. Abu-Amer, Y. (2001) IL-4 abrogates osteoclastogenesis through STAT6-dependent inhibition of NF-kappaB. *J Clin Invest* 107, 1375-1385.
5. Biola, A., Andreau, K., David, M., Sturm, M., Haake, M., Bertoglio, J., and Pallardy, M. (2000) The glucocorticoid receptor and STAT6 physically and functionally interact in T-lymphocytes. *FEBS Lett* 487, 229-233.
6. Litterst, C. M., and Pfitzner, E. (2001) Transcriptional activation by STAT6 requires the direct interaction with NCoA-1. *J. Biol. Chem.* 276, 45713-45721.

7. Valineva, T., Yang, J., Palovuori, R., and Silvennoinen, O. (2005) The transcriptional co-activator protein p100 recruits histone acetyltransferase activity to STAT6 and mediates interaction between the CREB-binding protein and STAT6. *J Biol Chem* 280, 14989-14996.
8. Yang, J., Aittomaki, S., Pesu, M., Carter, K., Saarinen, J., Kalkkinen, N., Kieff, E., and Silvennoinen, O. (2002) Identification of p100 as a coactivator for STAT6 that bridges STAT6 with RNA polymerase II. *Embo J* 21, 4950-4958.
9. Zimmermann, N., Mishra, A., King, N. E., Fulkerson, P. C., Doepker, M. P., Nikolaidis, N. M., Kindinger, L. E., Moulton, E. A., Aronow, B. J., and Rothenberg, M. E. (2004) Transcript signatures in experimental asthma: identification of STAT6-dependent and -independent pathways. *J Immunol* 172, 1815-1824.
10. Kaplan, M. H., Schindler, U., Smiley, S. T., and Grusby, M. J. (1996) Stat6 is required for mediating responses to IL-4 and for development of Th2 cells. *Immunity* 4, 313-319.
11. Aoudjehane, L., Podevin, P., Scatton, O., Jaffray, P., Dusanter-Fourt, I., Feldmann, G., Massault, P. P., Grira, L., Bringuier, A., Dousset, B., Chouzenoux, S., Soubrane, O., Calmus, Y., and Conti, F. (2007) Interleukin-4 induces human hepatocyte apoptosis through a Fas-independent pathway. *Faseb J* 21, 1433-1444.
12. Low, S. H., Vasanth, S., Larson, C. H., Mukherjee, S., Sharma, N., Kinter, M. T., Kane, M. E., Obara, T., and Weimbs, T. (2006) Polycystin-1, STAT6, and P100 function in a pathway that transduces ciliary mechanosensation and is activated in polycystic kidney disease. *Dev Cell* 10, 57-69.
13. Shum, B. O., Mackay, C. R., Gorgun, C. Z., Frost, M. J., Kumar, R. K., Hotamisligil, G. S., and Rolph, M. S. (2006) The adipocyte fatty acid-binding protein aP2 is required in allergic airway inflammation. *J Clin Invest* 116, 2183-2192.
14. Gao, B. (2005) Cytokines, STATs and liver disease. *Cell Mol Immunol* 2, 92-100.
15. Husted, T. L., and Lentsch, A. B. (2006) The role of cytokines in pharmacological modulation of hepatic ischemia/reperfusion injury. *Curr Pharm Des* 12, 2867-2873.
16. Li, J., Thorne, L. N., Punjabi, N. M., Sun, C. K., Schwartz, A. R., Smith, P. L., Marino, R. L., Rodriguez, A., Hubbard, W. C., O'Donnell, C. P., and Polotsky, V. Y. (2005) Intermittent hypoxia induces hyperlipidemia in lean mice. *Circ Res* 97, 698-706.
17. Savransky, V., Nanayakkara, A., Vivero, A., Li, J., Bevans, S., Smith, P. L., Torbenson, M. S., and Polotsky, V. Y. (2007) Chronic intermittent hypoxia predisposes to liver injury. *Hepatology* 45, 1007-1013.

18. Li, J., Grigoryev, D. N., Ye, S. Q., Thorne, L., Schwartz, A. R., Smith, P. L., O'Donnell, C. P., and Polotsky, V. Y. (2005) Chronic intermittent hypoxia upregulates genes of lipid biosynthesis in obese mice. *J Appl Physiol* 99, 1643-1648.
19. Inoue, H., Ogawa, W., Ozaki, M., Haga, S., Matsumoto, M., Furukawa, K., Hashimoto, N., Kido, Y., Mori, T., Sakaue, H., Teshigawara, K., Jin, S., Iguchi, H., Hiramatsu, R., LeRoith, D., Takeda, K., Akira, S., and Kasuga, M. (2004) Role of STAT-3 in regulation of hepatic gluconeogenic genes and carbohydrate metabolism in vivo. *Nat Med* 10, 168-174.
20. Hochstrasser, D. F., Frutiger, S., Paquet, N., Bairoch, A., Ravier, F., Pasquali, C., Sanchez, J. C., Tissot, J. D., Bjellqvist, B., and Vargas, R. (1992) Human liver protein map: a reference database established by microsequencing and gel comparison. *Electrophoresis* 13, 992-1001.
21. Arnold, R. J., Hrnčirova, P., Annaiah, K., and Novotny, M. V. (2004) Fast Proteolytic Digestion Coupled with Organelle Enrichment for Proteomic Analysis of Rat Liver. *J. Proteome Res.* 3, 653-657.
22. Ross, P. L., Huang, Y. N., Marchese, J. N., Williamson, B., Parker, K., Hattan, S., Khainovski, N., Pillai, S., Dey, S., Daniels, S., Purkayastha, S., Juhasz, P., Martin, S., Bartlet-Jones, M., He, F., Jacobson, A., and Pappin, D. J. (2004) Multiplexed Protein Quantitation in *Saccharomyces cerevisiae* Using Amine-reactive Isobaric Tagging Reagents. *Mol. Cell. Proteomics* 3, 1154-1169.
23. Tschäppät, V., Varesio, E., Signor, L., and Hopfgartner, G. (2005) The application of 2-D dual nanoscale liquid chromatography and triple quadrupole-linear ion trap system for the identification of proteins. *J. Sep. Sci.* 28, 1704-1711.
24. Hirsch, J., Hansen, K. C., Choi, S., Noh, J., Hirose, R., Roberts, J. P., Matthay, M. A., Burlingame, A. L., Maher, J. J., and Niemann, C. U. (2006) Warm Ischemia-induced Alterations in Oxidative and Inflammatory Proteins in Hepatic Kupffer Cells in Rats. *Mol. Cell. Proteomics* 5, 979-986.
25. Shilov, I. V., Seymour, S. L., Patel, A. A., Loboda, A., Tang, W. H., Keating, S. P., Hunter, C. L., Nuwaysir, L. M., and Schaeffer, D. A. (2007) The Paragon Algorithm: a Next Generation Search Engine that Uses Sequence Temperature Values and Feature Probabilities to Identify Peptides from Tandem Mass Spectra. *Mol. Cell. Proteomics* published online.
26. Seymour, S. L. (2005) Pro Group. *MCP Workshop: Criteria for Publication of Proteomic Data*, Paris, France.

27. Guo, Y., Singleton, P. A., Rowshan, A., Gucek, M., Cole, R. N., Graham, D. R. M., Van Eyk, J. E., and Garcia, J. G. N. (2007) Quantitative proteomics analysis of human endothelial cell membrane rafts. *Mol. Cell. Proteomics* 6, 689-696.
28. Cottrell, J. (2007) [http://www.matrixscience.com/help/decoy\\_help.html#MANUAL](http://www.matrixscience.com/help/decoy_help.html#MANUAL).
29. Karp, N. A., Spencer, M., Lindsay, H., O'Dell, K., and Lilley, K. S. (2005) Impact of Replicate Types on Proteomic Expression Analysis. *J. Proteome Res.* 4, 1867-1871.
30. Bligh, E. G., and Dyer, W. J. (1959) A rapid method of total lipid extraction and purification. *Can J Biochem Physiol* 37, 911-917.
31. Pastorelli, R., Carpi, D., Campagna, R., Airoidi, L., Pohjanvirta, R., Viluksela, M., Hakansson, H., Boutros, P. C., Moffat, I. D., Okey, A. B., and Fanelli, R. (2006) Differential expression profiling of the hepatic proteome in a rat model of dioxin resistance: correlation with genomic and transcriptomic analyses. *Mol. Cell. Proteomics* 5, 882-894.
32. Bansal, M. P., Mukhopadhyay, T., Scott, J., Cook, R. G., Mukhopadhyay, R., and Medina, D. (1990) DNA sequencing of a mouse liver protein that binds selenium: implications for selenium's mechanism of action in cancer prevention. *Carcinogenesis* 11, 2071-2073.
33. Strausberg, R. L., Feingold, E. A., Grouse, L. H., Derge, J. G., Klausner, R. D., Collins, F. S., Wagner, L., Shenmen, C. M., Schuler, G. D., Altschul, S. F., Zeeberg, B., Buetow, K. H., Schaefer, C. F., Bhat, N. K., Hopkins, R. F., Jordan, H., Moore, T., Max, S. I., Wang, J., Hsieh, F., Diatchenko, L., Marusina, K., Farmer, A. A., Rubin, G. M., Hong, L., Stapleton, M., Soares, M. B., Bonaldo, M. F., Casavant, T. L., Scheetz, T. E., Brownstein, M. J., Usdin, T. B., Toshiyuki, S., Carninci, P., Prange, C., Raha, S. S., Loquellano, N. A., Peters, G. J., Abramson, R. D., Mullahy, S. J., Bosak, S. A., McEwan, P. J., McKernan, K. J., Malek, J. A., Gunaratne, P. H., Richards, S., Worley, K. C., Hale, S., Garcia, A. M., Gay, L. J., Hulyk, S. W., Villalon, D. K., Muzny, D. M., Sodergren, E. J., Lu, X., Gibbs, R. A., Fahey, J., Helton, E., Kettelman, M., Madan, A., Rodrigues, S., Sanchez, A., Whiting, M., Madan, A., Young, A. C., Shevchenko, Y., Bouffard, G. G., Blakesley, R. W., Touchman, J. W., Green, E. D., Dickson, M. C., Rodriguez, A. C., Grimwood, J., Schmutz, J., Myers, R. M., Butterfield, Y. S., Krzywinski, M. I., Skalska, U., Smailus, D. E., Schnerch, A., Schein, J. E., Jones, S. J., and Marra, M. A. (2002) Generation and initial analysis of more than 15,000 full-length human and mouse cDNA sequences. *Proc. Natl Acad. Sci. USA* 99, 16899-16903.

34. Lanfear, J., Fleming, J., Walker, M., and Harrison, P. (1993) Different patterns of regulation of the genes encoding the closely related 56 kDa selenium- and acetaminophen-binding proteins in normal tissues and during carcinogenesis. *Carcinogenesis* 14, 335-340.
35. Pumford, N. R., Martin, B. M., and Hinson, J. A. (1992) A metabolite of acetaminophen covalently binds to the 56 kDa selenium binding protein. *Biochem Biophys Res Commun* 182, 1348-1355.
36. Knopf, J. L., Gallagher, J. F., and Held, W. A. (1983) Differential, multihormonal regulation of the mouse major urinary protein gene family in the liver. *Mol. Cell. Biol.* 3, 2232-2240.
37. Lee, T. S., and Chau, L. Y. (2002) Heme oxygenase-1 mediates the anti-inflammatory effect of interleukin-10 in mice. *Nat Med* 8, 240-246.
38. Takeuchi, D., Yoshidome, H., Kato, A., Ito, H., Kimura, F., Shimizu, H., Ohtsuka, M., Morita, Y., and Miyazaki, M. (2004) Interleukin 18 causes hepatic ischemia/reperfusion injury by suppressing anti-inflammatory cytokine expression in mice. *Hepatology* 39, 699-710.
39. Schroder, A. J., Pavlidis, P., Arimura, A., Capece, D., and Rothman, P. B. (2002) Cutting edge: STAT6 serves as a positive and negative regulator of gene expression in IL-4-stimulated B lymphocytes. *J. Immunol.* 168, 996-1000.
40. Morris, S. M., Jr. (2002) Regulation of enzymes of the urea cycle and arginine metabolism. *Annu Rev Nutr* 22, 87-105.
41. Rubbo, H., Darley-Usmar, V., and Freeman, B. A. (1996) Nitric oxide regulation of tissue free radical injury. *Chem Res Toxicol* 9, 809-820.
42. Rhee, S. G., Chae, H. Z., and Kim, K. (2005) Peroxiredoxins: a historical overview and speculative preview of novel mechanisms and emerging concepts in cell signaling. *Free Radic Biol Med* 38, 1543-1552.
43. Behne, D., and Kyriakopoulos, A. (2001) Mammalian selenium-containing proteins. *Annu Rev Nutr* 21, 453-473.
44. Atshaves, B. P., McIntosh, A. M., Lyuksyutova, O. I., Zipfel, W., Webb, W. W., and Schroeder, F. (2004) Liver fatty acid-binding protein gene ablation inhibits branched-chain fatty acid metabolism in cultured primary hepatocytes. *J. Biol. Chem.* 279, 30954-30965.
45. Glatz, J. F., and van der Vusse, G. J. (1996) Cellular fatty acid-binding proteins: their function and physiological significance. *Prog Lipid Res* 35, 243-282.

46. Shen, X. D., Ke, B., Zhai, Y., Gao, F., Anselmo, D., Lassman, C. R., Busuttill, R. W., and Kupiec-Weglinski, J. W. (2003) Stat4 and Stat6 signaling in hepatic ischemia/reperfusion injury in mice: HO-1 dependence of Stat4 disruption-mediated cytoprotection. *Hepatology* 37, 296-303.
47. Choi, Y., Shimogawa, H., Murakami, K., Ramdas, L., Zhang, W., Qin, J., and Uesugi, M. (2006) Chemical genetic identification of the IGF-linked pathway that is mediated by STAT6 and MFP2. *Chem Biol* 13, 241-249.
48. Inoue, Y., Inoue, J., Lambert, G., Yim, S. H., and Gonzalez, F. J. (2004) Disruption of hepatic C/EBPalpha results in impaired glucose tolerance and age-dependent hepatosteatosis. *J. Biol. Chem.* 279, 44740-44748.
49. Kato, A., Yoshidome, H., Edwards, M. J., and Lentsch, A. B. (2000) Reduced hepatic ischemia/reperfusion injury by IL-4: potential anti-inflammatory role of STAT6. *Inflamm Res* 49, 275-279.
50. Zhou, J., and Brune, B. (2006) Cytokines and hormones in the regulation of hypoxia inducible factor-1alpha (HIF-1alpha). *Cardiovasc Hematol Agents Med Chem* 4, 189-197.
51. Barouki, R., Coumoul, X., and Fernandez-Salguero, P. M. (2007) The aryl hydrocarbon receptor, more than a xenobiotic-interacting protein. *FEBS Lett.*
52. Ichihara, S., Yamada, Y., Ichihara, G., Nakajima, T., Li, P., Kondo, T., Gonzalez, F. J., and Murohara, T. (2007) A role for the aryl hydrocarbon receptor in regulation of ischemia-induced angiogenesis. *Arterioscler Thromb Vasc Biol* 27, 1297-1304.
53. Boutros, P. C., Moffat, I. D., Franc, M. A., Tijet, N., Tuomisto, J., Pohjanvirta, R., and Okey, A. B. (2004) Dioxin-responsive AHRE-II gene battery: identification by phylogenetic footprinting. *Biochem Biophys Res Commun* 321, 707-715.
54. Bock, K. W., and Kohle, C. (2006) Ah receptor: dioxin-mediated toxic responses as hints to deregulated physiologic functions. *Biochem Pharmacol* 72, 393-404.
55. Washburn, M. P., Wolters, D., and Yates, J. R., III (2001) Large-scale analysis of the yeast proteome by multidimensional protein identification technology. *Nature Biotechnol.* 19, 242-247.
56. Görg, A., Weiss, W., and Dunn, M. J. (2004) Current two-dimensional electrophoresis technology for proteomics. *Proteomics* 4, 3665-3685.
57. Valkova, N., Yunis, R., Mak, S. K., Kang, K., and Kultz, D. (2005) Nek8 mutation causes overexpression of galectin-1, sorcin, and vimentin and accumulation of the major urinary protein in renal cysts of jck mice. *Mol. Cell. Proteomics* 4, 1009-1018.

58. Tonge, R., Shaw, J., Middleton, B., Rowlinson, R., Rayner, S., Young, J., Pognan, F., Hawkins, E., Currie, I., and Davison, M. (2001) Validation and development of fluorescence two-dimensional differential gel electrophoresis proteomics technology. *Proteomics* 1, 377-396.
59. Ünlü, M., Morgan, M. E., and Minden, J. S. (1997) Difference gel electrophoresis. A single gel method for detecting changes in protein extracts. *Electrophoresis* 18, 2071-2077.
60. Hrebicek, T., Dürschmid, K., Auer, N., Bayer, K., and Rizzi, A. (2007) Effect of CyDye minimum labeling in differential gel electrophoresis on the reliability of protein identification. *Electrophoresis* 28, 1161-1169.
61. Hopfgartner, G., and Bourgoigne, E. (2003) Quantitative high-throughput analysis of drugs in biological matrices by mass spectrometry. *Mass Spectrometry Reviews* 22, 195-214.
62. Whiteaker, J. R., Zhao, L., Zhang, H. Y., Feng, L.-C., Piening, B. D., Anderson, L., and Paulovich, A. G. (2007) Antibody-based enrichment of peptides on magnetic beads for mass-spectrometry-based quantification of serum biomarkers. *Analytical Biochemistry* 362, 44-54.
63. Anderson, N. L., Anderson, N. G., Haines, L. R., Hardie, D. B., Olafson, R. W., and Pearson, T. W. (2004) Mass Spectrometric Quantitation of Peptides and Proteins Using Stable Isotope Standards and Capture by Anti-Peptide Antibodies (SISCAPA). *J. Proteome Res.* 3, 235-244.
64. Anderson, L., and Hunter, C. L. (2006) Quantitative Mass Spectrometric Multiple Reaction Monitoring Assays for Major Plasma Proteins. *Mol Cell Proteomics* 5, 573-588.
65. Cavaggioni, A., and Mucignat-Caretta, C. (2000) Major urinary proteins, alpha(2U)-globulins and aphrodisin. *Biochim Biophys Acta* 1482, 218-228.
66. Bacchini, A., Gaetani, E., and Cavaggioni, A. (1992) Pheromone binding proteins of the mouse, *Mus musculus*. *Experientia* 48, 419-421.
67. Zidek, L., Stone, M. J., Lato, S. M., Pagel, M. D., Miao, Z., Ellington, A. D., and Novotny, M. V. (1999) NMR mapping of the recombinant mouse major urinary protein I binding site occupied by the pheromone 2-sec-butyl-4,5-dihydrothiazole. *Biochemistry* 38, 9850-9861.
68. Finlayson, J. S., and Baumann, C. A. (1958) Mouse proteinuria. *Am J Physiol* 192, 69-72.

69. Finlayson, J. S., Potter, M., and Runner, C. R. (1963) Electrophoretic Variation And Sex Dimorphism Of The Major Urinary Protein Complex In Inbred Mice: A New Genetic Marker. *J. Natl Cancer Inst.* 31, 91-107.
70. Clissold, P. M., and Bishop, J. O. (1982) Variation in mouse major urinary protein (MUP) genes and the MUP gene products within and between inbred lines. *Gene* 18, 211-220.
71. Park, J. Y., Seong, J. K., and Paik, Y. K. (2004) Proteomic analysis of diet-induced hypercholesterolemic mice. *Proteomics* 4, 514-523.
72. Henkel, C., Roderfeld, M., Weiskirchen, R., Berres, M. L., Hillebrandt, S., Lammert, F., Meyer, H. E., Stuhler, K., Graf, J., and Roeb, E. (2006) Changes of the hepatic proteome in murine models for toxically induced fibrogenesis and sclerosing cholangitis. *Proteomics* 6, 6538-6548.
73. de Wolf, F. A., and Brett, G. M. (2000) Ligand-binding proteins: their potential for application in systems for controlled delivery and uptake of ligands. *Pharmacol Rev* 52, 207-236.
74. Yang, Q., Graham, T. E., Mody, N., Preitner, F., Peroni, O. D., Zabolotny, J. M., Kotani, K., Quadro, L., and Kahn, B. B. (2005) Serum retinol binding protein 4 contributes to insulin resistance in obesity and type 2 diabetes. *Nature* 436, 356-362.
75. Bansal, M. P., Cook, R. G., Danielson, K. G., and Medina, D. (1989) A 14-kilodalton selenium-binding protein in mouse liver is fatty acid-binding protein. *J. Biol. Chem.* 264, 13780-13784.
76. Pumford, N. R., Hinson, J. A., Benson, R. W., and Roberts, D. W. (1990) Immunoblot analysis of protein containing 3-(cystein-S-yl)acetaminophen adducts in serum and subcellular liver fractions from acetaminophen-treated mice. *Toxicol. Appl. Pharmacol.* 104, 521-532.
77. Hoivik, D. J., Manautou, J. E., Tveit, A., Mankowski, D. C., Khairallah, E. A., and Cohen, S. D. (1996) Evidence suggesting the 58-kDa acetaminophen binding protein is a preferential target for acetaminophen electrophile. *Fundam Appl Toxicol* 32, 79-86.
78. Kim, H., Kang, H. J., You, K. T., Kim, S. H., Lee, K. Y., Kim, T. I., Kim, C., Song, S. Y., Kim, H. J., Lee, C., and Kim, H. (2006) Suppression of human selenium-binding protein 1 is a late event in colorectal carcinogenesis and is associated with poor survival. *Proteomics* 6, 3466-3476.

79. Huang, K. C., Park, D. C., Ng, S. K., Lee, J. Y., Ni, X., Ng, W. C., Bandera, C. A., Welch, W. R., Berkowitz, R. S., Mok, S. C., and Ng, S. W. (2006) Selenium binding protein 1 in ovarian cancer. *Int J Cancer* 118, 2433-2440.
80. Li, L. S., Kim, H., Rhee, H., Kim, S. H., Shin, D. H., Chung, K. Y., Park, K. S., Paik, Y. K., Chang, J., and Kim, H. (2004) Proteomic analysis distinguishes basaloid carcinoma as a distinct subtype of nonsmall cell lung carcinoma. *Proteomics* 4, 3394-3400.
81. Mayr, M., Chung, Y. L., Mayr, U., McGregor, E., Troy, H., Baier, G., Leitges, M., Dunn, M. J., Griffiths, J. R., and Xu, Q. (2004) Loss of PKC-delta alters cardiac metabolism. *Am J Physiol Heart Circ Physiol* 287, H937-945.
82. Cho, Y. M., Bae, S. H., Choi, B. K., Cho, S. Y., Song, C. W., Yoo, J. K., and Paik, Y. K. (2003) Differential expression of the liver proteome in senescence accelerated mice. *Proteomics* 3, 1883-1894.
83. Giometti, C. S., Liang, X., Tollaksen, S. L., Wall, D. B., Lubman, D. M., Subbarao, V., and Rao, M. S. (2000) Mouse liver selenium-binding protein decreased in abundance by peroxisome proliferators. *Electrophoresis* 21, 2162-2169.
84. Chu, R., Lim, H., Brumfield, L., Liu, H., Herring, C., Ulintz, P., Reddy, J. K., and Davison, M. (2004) Protein profiling of mouse livers with peroxisome proliferator-activated receptor alpha activation. *Mol. Cell. Biol.* 24, 6288-6297.
85. Mehendale, H. M. (2000) PPAR-alpha: a key to the mechanism of hepatoprotection by clofibrate. *Toxicol. Sci.* 57, 187-190.
86. Milner, J. A. (1986) Inhibition of chemical carcinogenesis and tumorigenesis by selenium. *Adv Exp Med Biol* 206, 449-463.
87. Chan, L., Wei, C. F., Li, W. H., Yang, C. Y., Ratner, P., Pownall, H., Gotto, A. M., Jr., and Smith, L. C. (1985) Human liver fatty acid binding protein cDNA and amino acid sequence. Functional and evolutionary implications. *J. Biol. Chem.* 260, 2629-2632.
88. Gordon, J. I., Alpers, D. H., Ockner, R. K., and Strauss, A. W. (1983) The nucleotide sequence of rat liver fatty acid binding protein mRNA. *J. Biol. Chem.* 258, 3356-3363.
89. Vouquier, S., Mary, J., and Friguet, B. (2003) Subcellular localization of methionine sulphoxide reductase A (MsrA): evidence for mitochondrial and cytosolic isoforms in rat liver cells. *Biochem J* 373, 531-537.
90. Rajaraman, G., Wang, G. Q., Yan, J., Jiang, P., Gong, Y., and Burczynski, F. J. (2007) Role of cytosolic liver fatty acid binding protein in hepatocellular oxidative stress: effect of dexamethasone and clofibrate treatment. *Mol. Cell. Biochem.* 295, 27-34.

91. Rotruck, J. T., Pope, A. L., Ganther, H. E., Swanson, A. B., Hafeman, D. G., and Hoekstra, W. G. (1973) Selenium: biochemical role as a component of glutathione peroxidase. *Science* 179, 588-590.
92. Kato, A., Yoshidome, H., Edwards, M. J., and Lentsch, A. B. (2000) Regulation of liver inflammatory injury by signal transducer and activator of transcription-6. *Am J Pathol* 157, 297-302.
93. Lu, S. C., Alvarez, L., Huang, Z. Z., Chen, L., An, W., Corrales, F. J., Avila, M. A., Kanel, G., and Mato, J. M. (2001) Methionine adenosyltransferase 1A knockout mice are predisposed to liver injury and exhibit increased expression of genes involved in proliferation. *Proc Natl Acad Sci U S A* 98, 5560-5565.
94. Martinez-Chantar, M. L., Corrales, F. J., Martinez-Cruz, L. A., Garcia-Trevijano, E. R., Huang, Z. Z., Chen, L., Kanel, G., Avila, M. A., Mato, J. M., and Lu, S. C. (2002) Spontaneous oxidative stress and liver tumors in mice lacking methionine adenosyltransferase 1A. *Faseb J* 16, 1292-1294.
95. Younossi, Z. M., Baranova, A., Ziegler, K., Del Giacco, L., Schlauch, K., Born, T. L., Elariny, H., Gorreta, F., VanMeter, A., Younoszai, A., Ong, J. P., Goodman, Z., and Chandhoke, V. (2005) A genomic and proteomic study of the spectrum of nonalcoholic fatty liver disease. *Hepatology* 42, 665-674.
96. Mlakar, A., Batna, A., Dudda, A., and Spitteller, G. (1996) Iron (II) ions induced oxidation of ascorbic acid and glucose. *Free Radic Res* 25, 525-539.
97. Wells-Knecht, K. J., Zyzak, D. V., Litchfield, J. E., Thorpe, S. R., and Baynes, J. W. (1995) Mechanism of autoxidative glycosylation: identification of glyoxal and arabinose as intermediates in the autoxidative modification of proteins by glucose. *Biochemistry* 34, 3702-3709.
98. de Oliveira, C. P., Stefano, J. T., de Lima, V. M., de Sa, S. V., Simplicio, F. I., de Mello, E. S., Correa-Giannella, M. L., Alves, V. A., Laurindo, F. R., de Oliveira, M. G., Giannella-Neto, D., and Carrilho, F. J. (2006) Hepatic gene expression profile associated with non-alcoholic steatohepatitis protection by S-nitroso-N-acetylcysteine in ob/ob mice. *J Hepatol* 45, 725-733.
99. Marciniak, S. J., and Ron, D. (2006) Endoplasmic reticulum stress signaling in disease. *Physiol Rev* 86, 1133-1149.
100. Schroder, M., and Kaufman, R. J. (2005) The mammalian unfolded protein response. *Annu Rev Biochem* 74, 739-789.

101. Paschen, W. (2001) Dependence of vital cell function on endoplasmic reticulum calcium levels: implications for the mechanisms underlying neuronal cell injury in different pathological states. *Cell Calcium* 29, 1-11.
102. Orrenius, S., Zhivotovsky, B., and Nicotera, P. (2003) Regulation of cell death: the calcium-apoptosis link. *Nat Rev Mol Cell Biol* 4, 552-565.
103. Lee, A. S. (2001) The glucose-regulated proteins: stress induction and clinical applications. *Trends Biochem Sci* 26, 504-510.
104. Voccoli, V., Mazzoni, F., Garcia-Gil, M., and Colombaioni, L. (2007) Serum-withdrawal-dependent apoptosis of hippocampal neuroblasts involves Ca(++) release by endoplasmic reticulum and caspase-12 activation. *Brain Res* 1147, 1-11.
105. Ellis, R. J., and van der Vies, S. M. (1991) Molecular chaperones. *Annu Rev Biochem* 60, 321-347.
106. Cao, S. X., Dhahbi, J. M., Mote, P. L., and Spindler, S. R. (2001) Genomic profiling of short- and long-term caloric restriction effects in the liver of aging mice. *Proc. Natl Acad. Sci. USA* 98, 10630-10635.
107. Haas, I. G. (1994) BiP (GRP78), an essential hsp70 resident protein in the endoplasmic reticulum. *Experientia* 50, 1012-1020.
108. Sharma, M. R., Polavarapu, R., Roseman, D., Patel, V., Eaton, E., Kishor, P. B., and Nanji, A. A. (2006) Transcriptional networks in a rat model for nonalcoholic fatty liver disease: a microarray analysis. *Exp Mol Pathol* 81, 202-210.
109. Jolly, C., and Morimoto, R. I. (2000) Role of the heat shock response and molecular chaperones in oncogenesis and cell death. *J Natl Cancer Inst* 92, 1564-1572.
110. Parcellier, A., Gurbuxani, S., Schmitt, E., Solary, E., and Garrido, C. (2003) Heat shock proteins, cellular chaperones that modulate mitochondrial cell death pathways. *Biochem Biophys Res Commun* 304, 505-512.
111. Chiappini, F., Barrier, A., Saffroy, R., Domart, M. C., Dagues, N., Azoulay, D., Sebah, M., Franc, B., Chevalier, S., Debuire, B., Dudoit, S., and Lemoine, A. (2006) Exploration of global gene expression in human liver steatosis by high-density oligonucleotide microarray. *Lab Invest* 86, 154-165.
112. Sreekumar, R., Rosado, B., Rasmussen, D., and Charlton, M. (2003) Hepatic gene expression in histologically progressive nonalcoholic steatohepatitis. *Hepatology* 38, 244-251.

113. Fujita, T., Shirasawa, T., and Maruyama, N. (1999) Expression and structure of senescence marker protein-30 (SMP30) and its biological significance. *Mech. Ageing Dev.* 107, 271-280.
114. Fujita, T., Uchida, K., and Maruyama, N. (1992) Purification of senescence marker protein-30 (SMP30) and its androgen-independent decrease with age in the rat liver. *Biochim Biophys Acta* 1116, 122-128.
115. Yamaguchi, M. (2005) Role of regucalcin in maintaining cell homeostasis and function (review). *Int J Mol Med* 15, 371-389.
116. Maruyama, N., Ishigami, A., Kuramoto, M., Handa, S., Kubo, S., Imasawa, T., Seyama, K., Shimosawa, T., and Kasahara, Y. (2004) Senescence marker protein-30 knockout mouse as an aging model. *Ann N Y Acad Sci* 1019, 383-387.
117. Sato, T., Seyama, K., Sato, Y., Mori, H., Souma, S., Akiyoshi, T., Kodama, Y., Mori, T., Goto, S., Takahashi, K., Fukuchi, Y., Maruyama, N., and Ishigami, A. (2006) Senescence marker protein-30 protects mice lungs from oxidative stress, aging, and smoking. *Am J Respir Crit Care Med* 174, 530-537.
118. Son, T. G., Zou, Y., Jung, K. J., Yu, B. P., Ishigami, A., Maruyama, N., and Lee, J. (2006) SMP30 deficiency causes increased oxidative stress in brain. *Mech. Ageing Dev.* 127, 451-457.
119. Yumura, W., Imasawa, T., Suganuma, S., Ishigami, A., Handa, S., Kubo, S., Joh, K., and Maruyama, N. (2006) Accelerated tubular cell senescence in SMP30 knockout mice. *Histol Histopathol* 21, 1151-1156.
120. Murata, T., Shinya, N., and Yamaguchi, M. (1997) Expression of calcium-binding protein regucalcin mRNA in the cloned human hepatoma cells (HepG2): stimulation by insulin. *Mol. Cell. Biochem.* 175, 163-168.
121. Murata, T., and Yamaguchi, M. (1999) Promoter characterization of the rat gene for Ca<sup>2+</sup>-binding protein regucalcin. Transcriptional regulation by signaling factors. *J. Biol. Chem.* 274, 1277-1285.
122. Solomon, S. S., Buss, N., Shull, J., Monnier, S., Majumdar, G., Wu, J., and Gerling, I. C. (2005) Proteome of H-411E (liver) cells exposed to insulin and tumor necrosis factor-alpha: analysis of proteins involved in insulin resistance. *J. Lab. Clin. Med.* 145, 275-283.
123. De Gottardi, A., Vinciguerra, M., Sgroi, A., Moukil, M., Ravier-Dall'antonia, F., Paziienza, V., Pugnale, P., Foti, M., and Hadengue, A. (2007) Microarray analyses and

- molecular profiling of steatosis induction in immortalized human hepatocytes. *Lab Invest.*
124. Girard, S., Vossman, E., Misek, D. E., Podevin, P., Hanash, S., Brechot, C., and Beretta, L. (2004) Hepatitis C virus NS5A-regulated gene expression and signaling revealed via microarray and comparative promoter analyses. *Hepatology* 40, 708-718.
  125. Reue, K., and Cohen, R. D. (1996) Acads gene deletion in BALB/cByJ mouse strain occurred after 1981 and is not present in BALB/cByJ-fld mutant mice. *Mamm. Genome* 7, 694-695.
  126. Lin, X., Yue, P., Chen, Z., and Schonfeld, G. (2005) Hepatic triglyceride contents are genetically determined in mice: results of a strain survey. *Am J Physiol Gastrointest Liver Physiol* 288, G1179-1189.
  127. Van Greevenbroek, M. M., Vermeulen, V. M., and De Bruin, T. W. (2004) Identification of novel molecular candidates for fatty liver in the hyperlipidemic mouse model, HcB19. *J Lipid Res* 45, 1148-1154.
  128. Ozcan, U., Yilmaz, E., Ozcan, L., Furuhashi, M., Vaillancourt, E., Smith, R. O., Gorgun, C. Z., and Hotamisligil, G. S. (2006) Chemical chaperones reduce ER stress and restore glucose homeostasis in a mouse model of type 2 diabetes. *Science* 313, 1137-1140.
  129. Meneses-Lorente, G., Watt, A., Salim, K., Gaskell, S. J., Muniappa, N., Lawrence, J., and Guest, P. C. (2006) Identification of early proteomic markers for hepatic steatosis. *Chem Res Toxicol* 19, 986-998.
  130. Gunton, J. E., Kulkarni, R. N., Yim, S., Okada, T., Hawthorne, W. J., Tseng, Y. H., Roberson, R. S., Ricordi, C., O'Connell, P. J., Gonzalez, F. J., and Kahn, C. R. (2005) Loss of ARNT/HIF1beta mediates altered gene expression and pancreatic-islet dysfunction in human type 2 diabetes. *Cell* 122, 337-349.
  131. Tijet, N., Boutros, P. C., Moffat, I. D., Okey, A. B., Tuomisto, J., and Pohjanvirta, R. (2006) Aryl hydrocarbon receptor regulates distinct dioxin-dependent and dioxin-independent gene batteries. *Mol Pharmacol* 69, 140-153.
  132. Huber, S. A., Sakkinen, P., David, C., Newell, M. K., and Tracy, R. P. (2001) T helper-cell phenotype regulates atherosclerosis in mice under conditions of mild hypercholesterolemia. *Circulation* 103, 2610-2616.
  133. Satterthwaite, G., Francis, S. E., Suvarna, K., Blakemore, S., Ward, C., Wallace, D., Braddock, M., and Crossman, D. (2005) Differential gene expression in coronary

- 
- arteries from patients presenting with ischemic heart disease: further evidence for the inflammatory basis of atherosclerosis. *Am Heart J* 150, 488-499.
134. Brea, A., Mosquera, D., Martin, E., Arizti, A., Cordero, J. L., and Ros, E. (2005) Nonalcoholic fatty liver disease is associated with carotid atherosclerosis: a case-control study. *Arterioscler Thromb Vasc Biol* 25, 1045-1050.
135. Applera Corporation and MDS Sciex (2006) ProteinPilot Software Online Help v.1.0.15.

## 2.9 Supplementary Material

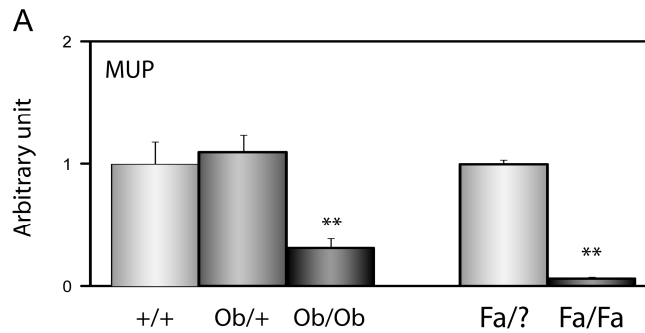


**FIGURE S1 Major Urinary Protein (MUP) mRNA levels in obese murine models.**

MUP mRNA level is significantly decreased in the livers of ob/ob mice and fa/fa rats, \*\* =  $p \leq 0.01$

**TABLE S1 Primers used for real-time PCR**

NAME	Entry	Forward	Reverse
Acetyl-Coenzyme A carboxylase (ACC)	NM_133360	taa acc agc act ccc gat tc	cca tcc tgt aag caa gag at
Albumin (ALB)	NM_009654	tgc ttt ttc cag ggg tgt gtt	tta ctt cct gca cta att tgg ca
Arginase 1 (ARG1)	NM_007482	tgg ctt gcg aga cgt aga c	gct cag gtg aat cgg cct ttt
Carnitine palmitoyltransferase (CPT1)	NM_013495	gca ctg cag ctc gca cat tac aa	ctc aga cag tac ctc ctt cag gaa a
Catalase (CAT)	NM_009804	atg gct ttt gac cca agc aa	cgg ccc tga agc ttt ttg t
Cyclophilin	XM_341363	caa atg ctg gac caa aca caa	gcc atc cag cca ttc agt ct
Cytochrome P450 7A1 (CYP7a1)	NM_007824	aca cca ttc ctg caa cct tc	gct gtc cgg ata ttc aag ga
Fatty acid binding protein (FABP1)	NM_017399	gag gag tgc gaa ctg gag ac	gtc gcc caa tgt cat ggt a
Fatty acid synthase (FAS)	NM_007988	gct gcg gaa act tca gga aat	aga gac gtg tca ctc ctg gac tt
Glucokinase (GK)	NM_010292	cag atc ctg gca gag ttc cag	cgg tcc atc tcc ttc tgc at
Glucose-6-phosphatase (G-6 Pase)	NM_008061	ctg tga gac cgg acc agg a	gac cat aac ata gta tac acc tgc tgc
Glutathione peroxidase 1 (GPX1)	NM_008160	gcg gcc ctg gca ttg	gga cca gcg ccc atc tg
Glyoxalase (GLO1)	NM_025374	gat ttg gtc aca ttg gga ttg c	tcc ttt cat ttt ccc gtc atc ag
Heat Shock 70 kDa protein 5 (HSPA5)	NM_022310	acc ccg aga aca cgg gtc tt	tgc cca cct cca ata tca act
Heme oxygenase (HO-1)	NM_010442	caa cag tgg cag tgg gaa ttt a	cca ggc aag att ctc cct tac
Major Urinary Protein (MUP)	NM_008647	gaa gct agt tct acg gga agg a	agg cca gga taa tag tat gcc a
Phosphoenolpyruvate carboxykinase (PCK1)	NM_011044	cca cag ctg ctg cag aac a	gaa ggg tcg cat ggc aaa
Regucalcin (RGN)	NM_009060	gaa cta cag gtg tgg gga gtc	tga ccg tat ccc atc gac aaa ta
Signal transducer and activator of transcription 3 (STAT3)	NM_213660	caa tac cat tga cct gcc gat	gag cga ctc aaa ctg ccc t
Superoxide dismutase (SOD1)	NM_011434	acc agt gca gga cct cat ttt a	tct cca aca tgc ctc tct tca tc
Suppressor of cytokine signaling 3 (SOCS3)	NM_007707	cct tca gct cca aaa gcc ag	gct ctc ctg cag ctt gcg

TABLE S2 Proteins identified in the livers of wild type and STAT6 knock-out mice by iTRAQ 2D nLC-MS/MS technique

N	Unused	%Cov	Nb unique peptides	Accession nb.	Protein Name	Species	KO / WT ratio	Error factor interval	EF	Std Dev.	n <sub>quant.</sub>
1	120.43	59.47	57	Q8C196	Carbamoyl-phosphate synthase	Mus musculus (Mouse)	0.95	[0.88 - 1.02]	1.07	0.13	109
2	50.20	59.38	24	Q8C7H3	Albumin	Mus musculus (Mouse)	0.94	[0.88 - 0.99]	1.06	0.12	127
		62.67		Q8C7C7		Mus musculus (Mouse)					
		59.38		Q3TV03		Mus musculus (Mouse)					
		59.38		P07724		Mus musculus (Mouse)					
3	43.88	78.00	21	Q8R1T8	Selenium binding protein 2	Mus musculus (Mouse)	1.70	[1.48 - 1.97]	1.15	0.08	9
		78.00		Q63936		Mus musculus (Mouse)					
		83.54		Q3UL72		Mus musculus (Mouse)					
4	39.83	83.54	18	Q35460	Betaine-homocysteine methyltransferase	Mus musculus (Mouse)	0.91	[0.76 - 1.09]	1.20	0.37	142
		89.20		Q3UEJ7		Mus musculus (Mouse)					
		89.20		F16400		Mus musculus (Mouse)					
5	32.48	89.20	15	P16400	Argininosuccinate synthetase	Mus musculus (Mouse)	0.87	[0.78 - 0.97]	1.11	0.19	98
		73.75		P16015		Mus musculus (Mouse)					
6	32.32	73.75	18	P16015	Carbonic anhydrase 3	Mus musculus (Mouse)	1.16	[1.02 - 1.31]	1.13	0.28	130
		37.92		Q8R0Y6		Mus musculus (Mouse)					
7	30.60	37.92	12	Q8R0Y6	1D-formyltetrahydrofolate dehydrogenase	Mus musculus (Mouse)	0.92	[0.83 - 1.02]	1.11	0.10	27
		37.92		Q8C1F2		Mus musculus (Mouse)					
8	30.57	44.80	13	P24549	Retinal dehydrogenase 1	Mus musculus (Mouse)	1.21	[0.77 - 1.91]	1.57	0.35	20
		66.90		Q3TF14		Mus musculus (Mouse)					
9	29.75	67.05	14	F10760	S-adenosylhomocysteine hydrolase	Rattus norvegicus (Rat)	0.96	[0.87 - 1.06]	1.11	0.12	35
		66.90		Q3U4D1		Mus musculus (Mouse)					
		63.43		Q5M9P0		Mus musculus (Mouse)					
		47.93		Q3UEH1		Mus musculus (Mouse)					
10	29.72	47.93	15	Q3UEH1	Fructose biphosphatase 1	Mus musculus (Mouse)	0.81	[0.87 - 0.97]	1.20	0.23	48
		88.07		Q58ET5		Mus musculus (Mouse)					
11	29.66	88.07	19	Q58ET5	Glutathione S-transferase, mu 1	Mus musculus (Mouse)	0.96	[0.75 - 1.24]	1.29	0.24	32
		39.79		Q8C2C7		Mus musculus (Mouse)					
		39.79		F03038		Mus musculus (Mouse)					
		40.54		Q3KQP2		Mus musculus (Mouse)					
12	28.74	40.54	15	Q3KQP2	Heat shock protein, 60 kDa	Mus musculus (Mouse)	1.03	[0.84 - 1.25]	1.22	0.35	81
		53.54		Q65G44		Rattus norvegicus (Rat)					
		53.54		F22791		Rattus norvegicus (Rat)					
		53.54		Q8N7N6		Mus musculus (Mouse)					
13	28.39	53.54	14	F22791	3-hydroxy-3-methylglutaryl-Coenzyme A synthase 2	Rattus norvegicus (Rat)	0.87	[0.80 - 1.26]	1.45	0.34	29
		53.54		Q8N7N6		Mus musculus (Mouse)					
		53.54		F54889		Mus musculus (Mouse)					
		68.42		Q61178		Mus musculus (Mouse)					
14	27.98	68.42	14	Q61178	Arginase 1	Mus musculus (Mouse)	0.92	[0.82 - 1.03]	1.12	0.20	80
		68.42		Q4FK78		Mus musculus (Mouse)					
		59.70		Q3UELO		Mus musculus (Mouse)					
		67.44		Q3TB74		Mus musculus (Mouse)					
15	27.68	66.89	13	P02088	Hemoglobin beta-1 subunit	Mus musculus (Mouse)	0.97	[0.88 - 1.07]	1.10	0.18	122
		70.05		Q3UER1		Mus musculus (Mouse)					
16	26.22	70.05	10	Q3UER1	Aldolase 2	Mus musculus (Mouse)	0.92	[0.70 - 1.22]	1.33	0.34	51
		62.64		Q3TJ66		Mus musculus (Mouse)					
17	24.85	50.47	12	Q61X12	Catalase	Mus musculus (Mouse)	1.10	[0.95 - 1.28]	1.16	0.18	40
		50.47		Q542K4		Mus musculus (Mouse)					
		50.47		Q3TVZ1		Mus musculus (Mouse)					
		50.47		Q8CBE3		Mus musculus (Mouse)					
		50.47		Q3UZ27		Mus musculus (Mouse)					
		50.47		Q3TVQ8		Mus musculus (Mouse)					
18	24.19	48.98	11	Q3UJF8	Acetyl-Coenzyme A acyltransferase 2	Mus musculus (Mouse)	1.13	[1.02 - 1.25]	1.11	0.12	42
		63.98		Q3TIT9		Mus musculus (Mouse)					
		58.44		Q8BWT1		Mus musculus (Mouse)					
		63.98		Q3UKH3		Mus musculus (Mouse)					
19	23.33	43.19	10	P26443	Glutamate dehydrogenase 1	Mus musculus (Mouse)	1.13	[0.97 - 1.30]	1.16	0.14	24
		40.50		F10880		Rattus norvegicus (Rat)					
		41.47		Q8C338		Mus musculus (Mouse)					
		42.27		Q5HZJ8		Mus musculus (Mouse)					
20	22.67	42.27	10	Q8C338	Isocitrate dehydrogenase 1 (NADP <sup>+</sup> )	Mus musculus (Mouse)	1.09	[0.97 - 1.22]	1.12	0.15	47
		42.27		Q3UAV7		Mus musculus (Mouse)					
		42.27		O88944		Mus musculus (Mouse)					
		42.27		Q3TJ51		Mus musculus (Mouse)					
21	22.22	89.95	10	P19157	Glutathione S-transferase P 1	Mus musculus (Mouse)	1.66	[1.38 - 2.01]	1.206	0.25	50
		31.63		Q71LX8		Mus musculus (Mouse)					
22	20.92	31.63	7	Q71LX8	Heat shock 90kDa protein 1, beta	Mus musculus (Mouse)	0.94	[0.77 - 1.15]	1.23	0.09	7
		31.63		Q86H55		Rattus norvegicus (Rat)					
		31.67		F11499		Mus musculus (Mouse)					
		27.94		F34058		Rattus norvegicus (Rat)					
23	20.40	31.63	10	Q3UJQ7	Epoxide hydrolase 2	Mus musculus (Mouse)	1.07	[0.96 - 1.22]	1.13	0.14	35
		35.20		Q3UQT1		Mus musculus (Mouse)					
24	19.49	35.20	8	F34058	Nonspecific lipid-transfer protein	Mus musculus (Mouse)	1.31	[1.13 - 1.52]	1.18	0.18	37
		29.43		P32020		Mus musculus (Mouse)					
25	19.12	52.17	9	Q3UD91	Glutamate oxaloacetate transaminase 2	Mus musculus (Mouse)	1.11	[0.87 - 1.43]	1.28	0.19	19
		44.65		F05202		Mus musculus (Mouse)					
		37.91		Q3TIP8		Mus musculus (Mouse)					
		52.03		Q8QW85		Mus musculus (Mouse)					
26	19.09	49.64	9	Q3TY87	Fumarylacetoacetate hydrolase	Mus musculus (Mouse)	1.00	[0.85 - 1.17]	1.17	0.16	33
		17.65		Q91WP9		Mus musculus (Mouse)					
27	18.88	17.65	10	Q91WP9	Liver glycogen phosphorylase	Mus musculus (Mouse)	0.80	[0.49 - 0.74]	1.23	0.15	15
		17.65		Q3UKJ0		Mus musculus (Mouse)					

N	Unused	%Cov	Nb unique peptides	Accession nb.	Protein Name	Species	KO / WT ratio	Error factor interval	EF	Std Dev.	n quart.
28	18.70	36.53	9	Q3UKA4	Alcohol dehydrogenase 1	Mus musculus (Mouse)	0.73	[0.67 - 0.80]	1.09	0.12	55
29	18.59	36.00	9	Q64442	Sorbitol dehydrogenase	Mus musculus (Mouse)	0.97	[0.80 - 1.19]	1.22	0.13	12
30	18.22	84.25	9	P12710	Fatty acid-binding protein, liver	Mus musculus (Mouse)	1.45	[1.26 - 1.68]	1.15	0.22	101
31	18.20	47.45	8	P49429	4-hydroxyphenylpyruvate dioxygenase	Mus musculus (Mouse)	0.98	[0.85 - 1.13]	1.15	0.14	29
32	18.15	52.17	8	Q64374	Regucalcin	Mus musculus (Mouse)	1.37	[1.13 - 1.65]	1.21	0.14	16
		48.15		Q3UJG3		Mus musculus (Mouse)					
33	17.88	56.10	7	Q669X5	Glyceraldehyde-3-phosphate dehydrogenase	Mus musculus (Mouse)	0.96	[0.76 - 1.21]	1.26	0.12	8
		56.10		Q669X2		Mus musculus (Mouse)					
		57.36		Q3THM2		Mus musculus (Mouse)					
		56.10		Q6U410		Mus musculus (Mouse)					
		52.85		Q4V783		Mus musculus (Mouse)					
		52.85		Q3UMT2		Mus musculus (Mouse)					
34	16.84	40.11	8	P11725	Ornithine carbamoyltransferase	Mus musculus (Mouse)	1.01	[0.89 - 1.15]	1.13	0.14	35
		40.11		P00481		Rattus norvegicus (Rat)					
		35.14		Q5M897		Rattus norvegicus (Rat)					
		33.90		Q8R1A8		Mus musculus (Mouse)					
35	15.95	25.77	7	Q77SZ0	Heat shock protein 9	Mus musculus (Mouse)	1.00	[0.79 - 1.26]	1.26	0.16	14
		25.77		P38847		Mus musculus (Mouse)					
		24.45		Q3VD16		Mus musculus (Mouse)					
		23.86		Q3TW83		Mus musculus (Mouse)					
		23.27		P48721		Rattus norvegicus (Rat)					
36	15.71	52.86	8	Q8ADD0	Peroxisome oxidase	Mus musculus (Mouse)	1.03	[0.71 - 1.50]	1.45	0.38	34
		53.57		Q63ZU7		Mus musculus (Mouse)					
37	15.51	40.53	8	Q3UBP6	Actin	Mus musculus (Mouse)	1.09	[0.82 - 1.30]	1.19	0.10	13
		40.53		Q3TVF6		Mus musculus (Mouse)					
		38.67		Q3TSB7		Mus musculus (Mouse)					
		37.97		Q3UBQ4		Mus musculus (Mouse)					
		36.27		Q3UAF7		Mus musculus (Mouse)					
		36.27		Q3UAF6		Mus musculus (Mouse)					
		36.27		Q3UA89		Mus musculus (Mouse)					
		36.27		Q3U5R4		Mus musculus (Mouse)					
38	15.37	89.38	6	P01942	Hemoglobin alpha subunit	Mus musculus (Mouse)	1.34	[1.21 - 1.48]	1.11	0.13	59
		89.73		Q61287		Mus musculus (Mouse)					
39	15.34	7.71	6	Q3UHT8	Fatty acid synthase	Mus musculus (Mouse)	0.98	[0.76 - 1.28]	1.30	0.12	6
		7.71		P19098		Mus musculus (Mouse)					
40	14.71	31.90	6	Q604P4	Heat shock protein 8	Mus musculus (Mouse)	1.01	[0.79 - 1.28]	1.27	0.16	13
		30.98		Q3UBA8		Mus musculus (Mouse)					
		30.98		Q3U9L2		Mus musculus (Mouse)					
		30.98		Q3U9G0		Mus musculus (Mouse)					
		30.98		Q3U9B4		Mus musculus (Mouse)					
		30.98		Q3U7E2		Mus musculus (Mouse)					
		30.98		Q3U7D7		Mus musculus (Mouse)					
		30.98		Q3TQ13		Mus musculus (Mouse)					
		30.98		Q3TH68		Mus musculus (Mouse)					
		30.98		Q3TEK2		Mus musculus (Mouse)					
		30.98		P83017		Mus musculus (Mouse)					
		30.29		Q3U764		Mus musculus (Mouse)					
		29.76		Q3ULM1		Mus musculus (Mouse)					
		27.55		Q3UGM0		Mus musculus (Mouse)					
		29.79		Q6NZD0		Mus musculus (Mouse)					
		29.10		Q3TF16		Mus musculus (Mouse)					
		29.39		Q3KQJ4		Mus musculus (Mouse)					
		29.33		Q3TRH3		Mus musculus (Mouse)					
41	14.48	34.24	7	Q9DD05	Delta-aminolevulinic acid dehydratase	Mus musculus (Mouse)	1.01	[0.82 - 1.25]	1.24	0.19	21
		34.24		P10518		Mus musculus (Mouse)					
42	14.37	63.35	5	Q544Y8	Glutathione S-transferase, alpha 3	Mus musculus (Mouse)	0.91	[0.82 - 1.01]	1.11	0.13	41
		63.35		Q9DCU1		Mus musculus (Mouse)					
43	13.87	35.56	7	Q91Y10	Argininosuccinate lyase	Mus musculus (Mouse)	1.06	[0.94 - 1.20]	1.13	0.11	21
		35.56		Q3UJH0		Mus musculus (Mouse)					
44	13.76	33.53	7	Q9CWN6	Leucine aminopeptidase 3	Mus musculus (Mouse)	1.20	[0.97 - 1.63]	1.37	0.24	16
		29.48		Q69P44		Mus musculus (Mouse)					
		31.35		Q3TFS5		Mus musculus (Mouse)					
45	13.45	29.29	6	Q61X93	S-adenosylmethionine synthetase	Mus musculus (Mouse)	0.78	[0.54 - 1.12]	1.44	0.23	14
46	13.03	20.80	6	Q62111	Serotransferrin	Mus musculus (Mouse)	0.96	[0.73 - 1.27]	1.32	0.16	9
		20.80		Q3UBW7		Mus musculus (Mouse)					
47	12.57	53.82	6	Q3UKG9	Triosephosphate isomerase	Mus musculus (Mouse)	1.10	[0.96 - 1.25]	1.14	0.12	21
		53.82		Q3UC04		Mus musculus (Mouse)					
48	12.47	63.36	6	Q9QXF8	Glycine N-methyltransferase	Mus musculus (Mouse)	0.94	[0.82 - 1.09]	1.16	0.14	25

N	Unused	%Cov	Nb unique peptides	Accession nb.	Protein Name	Species	KO / WT ratio	Error factor interval	EF	Std Dev.	n quant.
49	12.38	39.38	8	Q8KDB9	Alcohol sulfotransferase	Mus musculus (Mouse)	1.22	[ 0.99 - 1.50 ]	1.23	0.12	9
		39.38		Q8BGL3	Mus musculus (Mouse)						
		79.08		P08228	Superoxide dismutase [Cu-Zn]	Mus musculus (Mouse)	1.16	[ 1.04 - 1.29 ]	1.11	0.14	44
51	12.17	31.33	5	Q564E2	Lactate dehydrogenase 1, A chain	Mus musculus (Mouse)	1.07	[ 0.84 - 1.38 ]	1.27	0.17	21
		31.52		Q3UDU4	Mus musculus (Mouse)						
		31.33		Q3TI09	Mus musculus (Mouse)						
		31.33		Q3TCI7	Mus musculus (Mouse)						
		31.33		Q3THB4	Mus musculus (Mouse)						
		27.94		Q96K20	Mus musculus (Mouse)						
		31.33		P04642	Rattus norvegicus (Rat)						
		25.76		Q3TJE8	UDP-glucose dehydrogenase	Mus musculus (Mouse)	0.52	[ 0.41 - 0.66 ]	1.28	0.16	13
52	12.12	25.76	8	Q3TJ71		Mus musculus (Mouse)					
		25.76		O70475	Mus musculus (Mouse)						
		25.76		O70199	Rattus norvegicus (Rat)						
		50.75		P36700	Peroxisredoxin-1	Mus musculus (Mouse)	0.69	[ 0.29 - 1.64 ]	2.39	0.59	15
		56.10		Q3UJA1	Peptidylprolyl isomerase A	Mus musculus (Mouse)	1.16	[ 0.93 - 1.44 ]	1.24	0.11	9
53	11.98	50.75	5	Q3TE63		Mus musculus (Mouse)					
		56.10		Q3TE63	Mus musculus (Mouse)						
54	11.94	56.10	8	Q3UJA1		Mus musculus (Mouse)					
		56.10		Q3TE63	Mus musculus (Mouse)						
55	11.75	46.64	5	Q9DBJ1	Phosphoglycerate mutase 1	Mus musculus (Mouse)	1.05	[ 0.92 - 1.21 ]	1.15	0.09	13
		26.33		Q8R1P0	Malate dehydrogenase	Mus musculus (Mouse)	0.95	[ 0.75 - 1.20 ]	1.28	0.19	19
56	11.70	28.33	8	Q8GSM4		Rattus norvegicus (Rat)					
		28.33		P04638	Rattus norvegicus (Rat)						
		22.78		P06249	Mus musculus (Mouse)						
		33.03		Q8BMU7	Electron transferring flavoprotein, alpha-subunit.	Mus musculus (Mouse)	0.87	[ 0.78 - 0.97 ]	1.11	0.12	32
		33.03		Q5M7W0	Rattus norvegicus (Rat)						
		33.03		Q4V9X5	Mus musculus (Mouse)						
		33.03		Q3THD7	Mus musculus (Mouse)						
		24.92		Q8BMD3	Mus musculus (Mouse)						
57	11.40	33.03	8	Q96LC5		Mus musculus (Mouse)					
		33.03		P13803	Rattus norvegicus (Rat)						
		30.03		Q3V000	Mus musculus (Mouse)						
		27.12		P07871	3-ketoacyl-CoA thiolase	Rattus norvegicus (Rat)	0.99	[ 0.55 - 1.80 ]	1.81	0.22	5
		25.71		P21775	Rattus norvegicus (Rat)						
58	11.11	25.71	5	Q8VCH0		Mus musculus (Mouse)					
		22.18		P55264	Adenosine kinase	Mus musculus (Mouse)	0.79	[ 0.61 - 1.03 ]	1.30	0.12	7
		17.73		Q64840	Rattus norvegicus (Rat)						
		17.73		Q642G1	Rattus norvegicus (Rat)						
80	10.93	95.24	12	Q549D9	Hemoglobin beta minor	Mus musculus (Mouse)	1.08	[ 0.85 - 1.37 ]	1.27	0.24	32
		86.39		Q5D0E8	Mus musculus (Mouse)						
		78.95		Q01768	Nucleoside diphosphate kinase B	Mus musculus (Mouse)	1.16	[ 1.07 - 1.31 ]	1.11	0.08	9
81	10.22	69.08	5	P19804		Rattus norvegicus (Rat)					
		31.48		Q8CI38	Homogentisate 1, 2-dioxygenase	Mus musculus (Mouse)	0.89	[ 0.77 - 1.02 ]	1.15	0.10	15
		31.48		Q77PP2	Mus musculus (Mouse)						
		31.48		O09173	Mus musculus (Mouse)						
		23.37		Q6AYR0	Rattus norvegicus (Rat)						
82	10.07	24.59	4	Q61XD4	Formimidoyltetrahydrofolate cyclodeaminase	Mus musculus (Mouse)	0.96	[ 0.35 - 2.63 ]	2.73	0.44	7
		18.11		Q89818	Rattus norvegicus (Rat)						
		21.88		Q86JR7	Phosphoglucomutase	Mus musculus (Mouse)	1.04	[ 0.87 - 1.62 ]	1.58	0.19	7
83	9.95	22.95	4	Q6RJV4		Mus musculus (Mouse)					
		22.95		Q3UG53	Mus musculus (Mouse)						
		22.95		Q3U8X6	Mus musculus (Mouse)						
		21.39		P36852	Rattus norvegicus (Rat)						
		21.57		Q6D0F9	Mus musculus (Mouse)						
		20.79		Q499Q4	Rattus norvegicus (Rat)						
		10.80		Q3UF56	Pyruvate carboxylase	Mus musculus (Mouse)	1.00	[ 0.70 - 1.41 ]	1.42	0.15	7
		10.80		Q3TCQ3	Mus musculus (Mouse)						
84	9.83	10.80	5	Q3T9S7		Mus musculus (Mouse)					
		10.81		Q05920	Mus musculus (Mouse)						
		13.89		Q8BP64	Mus musculus (Mouse)						
		12.30		Q62043	Mus musculus (Mouse)						
		28.14		Q3UA81	Elongation factor 1-alpha 1	Mus musculus (Mouse)	0.94	[ 0.79 - 1.12 ]	1.19	0.13	15
		28.14		Q3TI13	Mus musculus (Mouse)						
		28.14		P10128	Mus musculus (Mouse)						
85	9.77	22.94	4	Q3UZQ3		Mus musculus (Mouse)					
		32.95		Q510F4	Glycerol-3-phosphate dehydrogenase	Rattus norvegicus (Rat)	0.94	[ 0.80 - 1.10 ]	1.17	0.08	8
		32.67		Q5DTS5	Mus musculus (Mouse)						
		33.05		P13707	Mus musculus (Mouse)						
		33.05		Q35077	Rattus norvegicus (Rat)						
86	9.64	26.05	4	Q91VV1	Phenylalanine hydroxylase	Mus musculus (Mouse)	0.99	[ 0.79 - 1.01 ]	1.13	0.06	8

N	Unused	%Cov	Nb unique peptides	Accession nb.	Protein Name	Species	KO / WT ratio	Error factor interval	EF	Std Dev.	n <sub>quant.</sub>									
66	9.49	26.11	3	Q3UEH8	Phosphoglycerate kinase 1	Mus musculus (Mouse)	0.94	[0.85 - 1.05]	1.11	0.04	6									
		26.05		Q6AYW2		Rattus norvegicus (Rat)														
		26.11		P16331		Mus musculus (Mouse)														
		26.38		Q5XJE7		Mus musculus (Mouse)														
		26.38		Q5M045		Rattus norvegicus (Rat)														
		26.38		Q3TPE6		Mus musculus (Mouse)														
		26.44		P16617		Rattus norvegicus (Rat)														
		26.44		P09411		Mus musculus (Mouse)														
23.26	Q3UKV8	Mus musculus (Mouse)																		
70	9.38	23.67	4	P03101	14-3-3 protein zeta/delta	Mus musculus (Mouse)	0.73	[0.38 - 1.40]	1.91	0.28	6									
71	9.35	65.96	5	Q9WVL0	Maleylacetoacetate isomerase	Mus musculus (Mouse)	1.22	[0.61 - 2.43]	2.00	0.49	17									
72	9.24	65.33	4	P70604	Estradiol 17 beta-dehydrogenase 5	Mus musculus (Mouse)	1.14	[1.01 - 1.29]	1.13	0.07	8									
73	9.13	18.73	4	Q8CEG4	Valosin containing protein	Mus musculus (Mouse)	0.91	[0.69 - 1.18]	1.30	0.10	6									
		18.73		Q8BSR6		Mus musculus (Mouse)														
		20.89		Q8BNF8		Mus musculus (Mouse)														
		18.73		Q3TXN9		Mus musculus (Mouse)														
		18.73		Q3TIM2		Mus musculus (Mouse)														
		18.73		Q3TFH9		Mus musculus (Mouse)														
		21.80		Q99JZ6		Mus musculus (Mouse)														
		21.80		Q9P9T8		Rattus norvegicus (Rat)														
21.80	Q3UJ73	Mus musculus (Mouse)																		
21.80	Q3TG26	Mus musculus (Mouse)																		
21.80	P04691	Rattus norvegicus (Rat)																		
19.02	Q3UF52	Mus musculus (Mouse)																		
19.02	Q3TIL1	Mus musculus (Mouse)																		
19.02	Q3TFB6	Mus musculus (Mouse)																		
25.08	Q9DCR1	Mus musculus (Mouse)																		
75	8.99	22.52	4	P14152	Malate dehydrogenase	Mus musculus (Mouse)	1.00	[0.89 - 1.12]	1.12	0.07	9									
		20.42		Q88989		Rattus norvegicus (Rat)														
76	8.74	47.54	3	Q9CPU0	Glyoxalase 1	Mus musculus (Mouse)	2.54	[2.14 - 3.02]	1.19	0.10	11									
77	8.59	19.52	4	Q9WUM5	Succinyl-CoA ligase [GDP-forming] alpha-chain	Mus musculus (Mouse)	0.60	[0.49 - 1.65]	1.84	0.22	5									
		19.52		Q6P7S4		Rattus norvegicus (Rat)														
		19.52		P13086		Rattus norvegicus (Rat)														
78	8.09	73.27	5	P15628	Glutathione S-transferase Mu 2	Mus musculus (Mouse)	0.64	[0.42 - 0.97]	1.52	0.18	7									
79	8.05	17.32	4	Q9DCW4	Electron transfer flavoprotein beta-subunit	Mus musculus (Mouse)	0.95	[0.80 - 1.12]	1.18	0.14	18									
		14.98		Q6FU3		Rattus norvegicus (Rat)														
80	8.02	10.29	4	Q3UEL5	Urocanate hydratase homolog	Mus musculus (Mouse)	0.97	[0.87 - 1.07]	1.11	0.07	13									
		8.88		Q8VC12		Mus musculus (Mouse)														
		26.64		Q91ZD7		Rattus norvegicus (Rat)														
81	7.96	24.18	5	Q8K3V8	Aldehyde dehydrogenase 2	Rattus norvegicus (Rat)	1.01	[0.85 - 1.20]	1.19	0.10	10									
		23.14		Q6Q289		Rattus norvegicus (Rat)														
		23.14		Q6Q288		Rattus norvegicus (Rat)														
		22.74		Q3UJW1		Mus musculus (Mouse)														
		22.74		Q3U9J7		Mus musculus (Mouse)														
		22.74		Q3U8I3		Mus musculus (Mouse)														
		22.74		Q3TVM2		Mus musculus (Mouse)														
		22.74		F47738		Mus musculus (Mouse)														
		22.74		P11884		Rattus norvegicus (Rat)														
		22.84		Q8VC30		Mus musculus (Mouse)														
		22.84		Q8VC30		Mus musculus (Mouse)														
		37.57		Q4FZE6		Major urinary protein 1						Mus musculus (Mouse)	25.54	-	-	-	1			
		84		7.41		25.78						6	Q80Y52	Heat shock protein 1, alpha	Mus musculus (Mouse)	0.87	[0.54 - 1.41]	1.62	0.15	4
						25.78							Q3TKA2		Mus musculus (Mouse)					
24.42	Q91XW0		Rattus norvegicus (Rat)																	
24.01	Q3UIF3		Mus musculus (Mouse)																	
27.83	Q9C5U3		Mus musculus (Mouse)																	
25.18	Q3TJU7		Mus musculus (Mouse)																	
23.08	Q3TDN8		Biphenyl hydrolase-like		Mus musculus (Mouse)	0.86	[0.19 - 3.83]	4.47	0.21	2										
86	7.25		13.42		3	Q9ESA0	Transketolase	Mus musculus (Mouse)	0.94	[0.78 - 1.12]	1.20		0.07		5					
		12.04	Q3UK62	Mus musculus (Mouse)																
		12.04	F40142	Mus musculus (Mouse)																
		10.11	P50137	Rattus norvegicus (Rat)																
		18.51	Q8CHT0	Mus musculus (Mouse)																
87	7.16	18.51	3	Q8CHT0	Aldehyde dehydrogenase 4A1	Mus musculus (Mouse)	1.04	[0.88 - 1.22]	1.18	0.11	12									
		13.08		Q5RJI3		Mus musculus (Mouse)														
		13.08		Q3UZJ1		Mus musculus (Mouse)														
		13.08		Q3UUX1		Mus musculus (Mouse)														
		13.08		Q3TW50		Mus musculus (Mouse)														
		13.08		Q3TEE7		Mus musculus (Mouse)														
88	7.15	13.08	3	Q5RJI3	Glucose phosphate isomerase 1	Mus musculus (Mouse)	0.83	[0.44 - 0.90]	1.42	0.17	7									
		13.08		Q3UZJ1		Mus musculus (Mouse)														
89	7.00	16.96	3	Q9DB19	Inorganic pyrophosphatase	Mus musculus (Mouse)	1.18	[0.92 - 1.63]	1.29	0.14	10									
		16.96		Q9DB19		Mus musculus (Mouse)														

N	Unused	%Cov	Nb unique peptides	Accession nb.	Protein Name	Species	KO / WT ratio	Error factor interval	EF	Std Dev.	n <sub>quant.</sub>									
90	6.67	17.01	3	Q8BTY3	Prolyl 4-hydroxylase, beta polypeptide	Mus musculus (Mouse)	1.02	[ 0.72 - 1.44 ]	1.41	0.13	5									
		16.96		Q3UA53		Mus musculus (Mouse)														
		11.78		Q499R7		Rattus norvegicus (Rat)														
		13.95		Q922C8		Mus musculus (Mouse)														
		13.95		Q3URP6		Mus musculus (Mouse)														
		13.95		Q3UJA8		Mus musculus (Mouse)														
		14.06		Q3UDR2		Mus musculus (Mouse)														
		13.95		Q3UBY9		Mus musculus (Mouse)														
		13.95		Q3UA23		Mus musculus (Mouse)														
		13.95		Q3U738		Mus musculus (Mouse)														
		13.95		Q3TWE3		Mus musculus (Mouse)														
		13.95		Q3TIM0		Mus musculus (Mouse)														
		13.95		Q3THC3		Mus musculus (Mouse)														
		13.95		Q3TGS0		Mus musculus (Mouse)														
		13.95		Q3TF72		Mus musculus (Mouse)														
91	6.66	20.71	3	Q3TI20	Tubulin alpha-6 chain	Rattus norvegicus (Rat)	0.67	[ 0.50 - 0.74 ]	1.11	0.05	8									
		20.71		P86373		Mus musculus (Mouse)														
		14.48		Q6UJ22		Mus musculus (Mouse)														
		92		6.73		12.47						3	Q8C153	Elongation factor 2	Mus musculus (Mouse)	1.15	[ 0.65 - 2.04 ]	1.77	0.08	2
						12.47							Q8BMA8		Mus musculus (Mouse)					
						12.69							Q8P9L9		Mus musculus (Mouse)					
						12.47							Q544E4		Mus musculus (Mouse)					
						12.47							Q3UZ14		Mus musculus (Mouse)					
						12.47							Q3UMI7		Mus musculus (Mouse)					
						12.47							Q3UDC8		Mus musculus (Mouse)					
						12.47							Q3UBL9		Mus musculus (Mouse)					
						12.47							Q3TX47		Mus musculus (Mouse)					
						12.47							Q3TW68		Mus musculus (Mouse)					
						12.47							Q3TLB1		Mus musculus (Mouse)					
						12.47							Q3TK17		Mus musculus (Mouse)					
12.47	Q3TJZ1		Mus musculus (Mouse)																	
12.49	P05197		Rattus norvegicus (Rat)																	
10.84	Q3TWX1		Mus musculus (Mouse)																	
93	6.49	11.39	3	Q9JX06	Annexin A6	Mus musculus (Mouse)	1.11	-	-	-	1									
		11.29		Q8BSS4		Mus musculus (Mouse)														
		11.29		Q3UI56		Mus musculus (Mouse)														
		11.29		Q3UDK4		Mus musculus (Mouse)														
		11.39		Q3TUI1		Mus musculus (Mouse)														
		11.31		P14824		Mus musculus (Mouse)														
		13.87		Q8CEX0		Mus musculus (Mouse)														
		11.67		Q3V224		Mus musculus (Mouse)														
		94		6.46		17.70						3	Q6VCH3	Serine (Or cysteine) proteinase inhibitor, clade A, member 3K	Mus musculus (Mouse)	1.10	[ 0.85 - 1.44 ]	1.30	0.12	7
						17.70							P07759		Mus musculus (Mouse)					
14.11	Q62267		Mus musculus (Mouse)																	
95	6.38		19.95		2	Q3UXC2	Eukaryotic translation initiation factor 4A1	Mus musculus (Mouse)	1.04	[ 0.82 - 1.32 ]	1.27		0.09		5					
			19.95			Q3TCK7		Mus musculus (Mouse)												
		19.95	Q3TFG3	Mus musculus (Mouse)																
		18.68	Q3TLL6	Mus musculus (Mouse)																
		25.78	Q3TSJ4	Mus musculus (Mouse)																
12.15	Q8BTU6	Mus musculus (Mouse)																		
96	6.29	19.29	3	Q8BH00	Aldh6a1 protein	Mus musculus (Mouse)	0.96	[ 0.83 - 1.11 ]	1.15	0.07	8									
		9.36		Q99LB7		Mus musculus (Mouse)														
97	6.22	16.96	3	Q8BU72	Sarcosine dehydrogenase	Mus musculus (Mouse)	1.38	[ 0.34 - 5.68 ]	4.11	0.20	2									
		16.96		Q8BU72		Mus musculus (Mouse)														
98	6.20	19.23	3	Q3U7H9	Peroxiredoxin 5	Mus musculus (Mouse)	0.95	[ 0.70 - 1.28 ]	1.35	0.13	6									
		19.05		P99029		Mus musculus (Mouse)														
99	6.18	18.15	3	Q80XJ7	Aldo-keto reductase family 1, member A4	Mus musculus (Mouse)	0.97	[ 0.62 - 1.62 ]	1.57	0.16	5									
		18.15		Q540D7		Mus musculus (Mouse)														
		18.15		Q3UJW9		Mus musculus (Mouse)														
100	6.17	18.72	3	Q5EBQ2	Phosphatidylethanolamine binding protein	Mus musculus (Mouse)	1.14	[ 0.90 - 1.44 ]	1.26	0.06	4									
		18.72		Q3TGC5		Mus musculus (Mouse)														
101	6.01	16.15	3	Q920E5	Farnesyl pyrophosphate synthetase	Mus musculus (Mouse)	0.76	[ 0.58 - 0.99 ]	1.31	0.18	12									
		16.15		Q3TMB3		Mus musculus (Mouse)														
		12.18		Q3US29		Mus musculus (Mouse)														
		16.15		Q5M8R9		Mus musculus (Mouse)														
102	6.01	14.01	3	Q9WVK7	Short chain 3-hydroxyacyl-CoA dehydrogenase	Rattus norvegicus (Rat)	1.16	[ 0.80 - 1.68 ]	1.44	0.18	8									
		14.01		Q61425		Mus musculus (Mouse)														

N	Unused	%Cov	Nb unique peptides	Accession nb.	Protein Name	Species	KO / WT ratio	Error factor interval	EF	Std Dev.	n quant.
103	8.00	18.80	3	Q91Z53	Glyoxylate reductase/hydroxypyruvate reductase	Mus musculus (Mouse)	0.80	[0.37 - 1.71]	2.14	0.28	5
104	8.00	7.17	3	Q910S9	Liver carboxylesterase 31 precursor	Mus musculus (Mouse)	0.94	[0.46 - 1.52]	1.81	0.28	8
		7.40		Q93980		Mus musculus (Mouse)					
		10.65		Q3UEJ0		Mus musculus (Mouse)					
		3.82		Q91XD5		Mus musculus (Mouse)					
		3.52		Q8VCU1		Mus musculus (Mouse)					
105	5.99	16.84	2	Q9DBE0	Cysteine sulfinic acid decarboxylase	Mus musculus (Mouse)	0.87	[0.83 - 0.70]	1.06	0.01	2
		16.84		Q8K586		Mus musculus (Mouse)					
106	5.89	15.79	3	Q9JLJ2	Aldehyde dehydrogenase 9, subfamily A1	Mus musculus (Mouse)	1.08	[0.87 - 1.72]	1.80	0.14	4
		15.08		Q3V1N7		Mus musculus (Mouse)					
		15.08		Q3U387		Mus musculus (Mouse)					
		15.79		Q3TMT4		Mus musculus (Mouse)					
		15.79		Q3THE7		Mus musculus (Mouse)					
		15.08		Q3TG52		Mus musculus (Mouse)					
		10.73		Q3UDG0		Mus musculus (Mouse)					
107	5.81	45.27	3	P11352	Glutathione peroxidase 1	Mus musculus (Mouse)	1.33	[1.07 - 1.65]	1.24	0.07	4
		37.31		Q5RJH8		Mus musculus (Mouse)					
		27.86		Q91WZ5		Rattus norvegicus (Rat)					
		38.62		Q8PDW8		Rattus norvegicus (Rat)					
		27.86		P04041		Rattus norvegicus (Rat)					
108	5.64	21.58	2	Q8BV14	Dihydropteridine reductase	Mus musculus (Mouse)	0.90	[0.86 - 1.19]	1.31	0.08	3
		15.35		P11348		Rattus norvegicus (Rat)					
109	5.45	16.07	2	Q9EQ20	Aldehyde dehydrogenase family 6, subfamily A1	Mus musculus (Mouse)	0.73	-	-	-	1
		16.07		Q8CIB4		Mus musculus (Mouse)					
		16.07		Q3TDA2		Mus musculus (Mouse)					
		12.91		Q8KDL1		Mus musculus (Mouse)					
110	5.40	19.35	3	Q8VCN5	Cystathionine gamma-lyase	Mus musculus (Mouse)	0.88	[0.37 - 2.12]	2.39	0.30	5
111	5.34	10.48	2	Q9DBM2	Peroxisomal bifunctional enzyme	Mus musculus (Mouse)	1.07	-	-	-	1
		10.45		Q91W49		Mus musculus (Mouse)					
112	5.31	31.08	2	Q3TJA2	Superoxide dismutase 2	Mus musculus (Mouse)	0.85	[0.33 - 2.19]	2.59	0.22	3
		31.08		P09871		Mus musculus (Mouse)					
		30.22		Q9NZM1		Mus musculus (Mouse)					
		24.32		Q3U8W4		Mus musculus (Mouse)					
113	5.30	4.67	3	Q91V92	ATP-citrate synthase	Mus musculus (Mouse)	0.51	[0.41 - 0.63]	1.24	0.09	8
		4.63		Q3V117		Mus musculus (Mouse)					
		4.67		Q3TED3		Mus musculus (Mouse)					
		5.41		Q8VIQ1		Rattus norvegicus (Rat)					
		7.77		Q9VDM8		Mus musculus (Mouse)					
		4.22		Q497C7		Rattus norvegicus (Rat)					
		4.18		P16838		Rattus norvegicus (Rat)					
		4.93		Q3UEA1		Mus musculus (Mouse)					
114	5.24	14.34	3	Q78JT3	3-hydroxyanthranilate 3,4-dioxygenase	Mus musculus (Mouse)	1.18	[0.76 - 1.77]	1.50	0.09	3
115	5.22	19.17	2	Q91W85	Acyl-Coenzyme A dehydrogenase, short chain	Mus musculus (Mouse)	-	-	-	-	0
		19.08		Q8IMX3		Rattus norvegicus (Rat)					
		19.17		Q07417		Mus musculus (Mouse)					
116	5.13	14.86	3	Q9QZT1	Acetyl-CoA acetyltransferase	Mus musculus (Mouse)	0.78	[0.51 - 1.19]	1.52	0.10	3
		14.86		Q3TQF7		Mus musculus (Mouse)					
		14.86		P17764		Rattus norvegicus (Rat)					
117	5.11	7.21	2	P16850	Acyl-CoA dehydrogenase, long-chain specific	Rattus norvegicus (Rat)	0.70	[0.12 - 4.04]	5.76	0.24	2
		9.07		P51174		Mus musculus (Mouse)					
118	5.09	8.98	2	Q9Z2V4	Phosphoenolpyruvate carboxykinase	Mus musculus (Mouse)	1.09	[0.96 - 1.24]	1.14	0.03	3
		8.98		Q8CI37		Mus musculus (Mouse)					
		8.98		Q8SSX3		Mus musculus (Mouse)					
		8.98		P07379		Rattus norvegicus (Rat)					
119	4.99	28.78	2	Q64471	Glutathione S-transferase theta-1	Mus musculus (Mouse)	0.70	[0.39 - 1.26]	1.80	0.08	2
		21.67		Q91X50		Mus musculus (Mouse)					
		16.74		Q01579		Rattus norvegicus (Rat)					
		21.67		Q8DCY6		Mus musculus (Mouse)					
120	4.98	10.85	2	Q91ZJ5	UTP-glucose-1-phosphate uridylyltransferase 2	Mus musculus (Mouse)	0.81	-	-	-	1
		7.67		Q4V819		Rattus norvegicus (Rat)					
121	4.88	14.77	2	Q00998	Alpha-1-antitrypsin	Mus musculus (Mouse)	-	-	-	-	0
		14.77		P07759		Mus musculus (Mouse)					
		13.11		P81105		Mus musculus (Mouse)					
122	4.86	40.20	2	Q4K176	Heat shock protein 1 (Chaperonin 10)	Mus musculus (Mouse)	1.08	[0.93 - 1.21]	1.14	0.08	10
		33.33		P97801		Rattus norvegicus (Rat)					
		33.66		P26772		Rattus norvegicus (Rat)					
		32.35		Q9J195		Mus musculus (Mouse)					
123	4.83	12.14	2	Q8P513	Alcohol dehydrogenase 2 / 5	Mus musculus (Mouse)	0.94	[0.51 - 1.72]	1.83	0.24	8

N	Unused	%Cov	Nb unique peptides	Accession nb.	Protein Name	Species	KO / WT ratio	Error factor interval	EF	Std Dev.	n quant.
		12.30		Q3TW83		Mus musculus (Mouse)					
		12.33		P28474		Mus musculus (Mouse)					
		12.33		P12711		Rattus norvegicus (Rat)					
124	4.75	14.14	2	Q545S0	Thiosulfate sulfurtransferase	Mus musculus (Mouse)	1.23	[ 1.00 - 1.39 ]	1.13	0.08	7
125	4.74	17.21	3	Q93092	Transaldolase	Mus musculus (Mouse)	0.82	[ 0.34 - 1.64 ]	2.38	0.31	5
		17.21		Q9EQS0		Rattus norvegicus (Rat)					
126	4.48	48.54	2	P81458	Pterin-4-alpha-carbinolamine dehydratase	Mus musculus (Mouse)	1.07	[ 0.91 - 1.28 ]	1.18	0.02	2
127	4.34	57.14	2	Q52KC4	Thioredoxin 1	Mus musculus (Mouse)	1.19	[ 0.37 - 3.88 ]	3.24	0.25	3
		47.12		P11232		Rattus norvegicus (Rat)					
128	4.30	12.83	2	Q91WS8	Acetyl-Coenzyme A dehydrogenase, medium chain	Mus musculus (Mouse)	0.94	[ 0.68 - 1.31 ]	1.39	0.05	2
		12.83		P45952		Mus musculus (Mouse)					
		10.69		P08503		Rattus norvegicus (Rat)					
129	4.29	21.28	2	Q91XE0	Glycine-N-acyltransferase	Mus musculus (Mouse)	1.04	[ 0.36 - 2.98 ]	2.87	0.14	2
130	4.28	7.33	2	Q3UEH4	Pyruvate kinase liver and red blood cell	Mus musculus (Mouse)	1.31	-	-	-	1
		7.37		Q3UEH4		Mus musculus (Mouse)					
		6.97		P12929		Rattus norvegicus (Rat)					
131	4.25	16.99	2	Q9QZV3	Dodecenoyl-Coenzyme A delta isomerase	Mus musculus (Mouse)	1.10	[ 0.50 - 2.43 ]	2.21	0.22	4
		16.98		P42125		Mus musculus (Mouse)					
		13.84		Q9DBN7		Mus musculus (Mouse)					
132	4.24	10.41	2	Q3UJH8	Glutamate oxaloacetate transaminase 1	Mus musculus (Mouse)	0.59	[ 0.34 - 0.999 ]	1.71	0.16	4
		9.47		P05201		Mus musculus (Mouse)					
133	4.11	14.88	2	Q8R4V3	Acetyl-CoA acetyltransferase	Mus musculus (Mouse)	0.67	[ 0.55 - 0.81 ]	1.22	0.09	7
		14.88		Q8CAY8		Mus musculus (Mouse)					
		14.88		Q80X81		Mus musculus (Mouse)					
		5.09		Q77P61		Rattus norvegicus (Rat)					
		12.34		Q5XI22		Rattus norvegicus (Rat)					
134	4.10	30.43	2	Q546F0	Macrophage migration inhibitory factor	Mus musculus (Mouse)	1.04	[ 0.95 - 1.15 ]	1.10	0.07	14
		30.70		P30904		Rattus norvegicus (Rat)					
135	4.04	17.42	2	P40938	Indolethylamine N-methyltransferase	Mus musculus (Mouse)	1.08	[ 0.85 - 1.37 ]	1.27	0.07	4
136	4.01	43.70	2	Q4VWZ5	Acyl-CoA-binding protein	Mus musculus (Mouse)	0.64	[ 0.58 - 1.63 ]	1.82	0.32	16
137	4.00	6.39	4	P21213	Histidine ammonia-lyase	Rattus norvegicus (Rat)	-	-	-	-	0
		5.78		Q8CE60		Mus musculus (Mouse)					
		5.78		P35492		Mus musculus (Mouse)					
138	4.00	14.18	2	Q9RDP3	Esterase D	Mus musculus (Mouse)	1.03	[ 0.81 - 1.75 ]	1.70	0.08	2
139	4.00	13.33	2	Q6DCM2	Glutathione S-transferase kappa 1	Mus musculus (Mouse)	0.95	[ 0.41 - 2.18 ]	2.30	0.19	3
		7.11		P24473		Rattus norvegicus (Rat)					
140	3.95	37.14	2	Q56A15	Cy5 protein	Mus musculus (Mouse)	0.60	[ 0.44 - 0.81 ]	1.36	0.07	3
141	3.95	19.08	2	Q8VCX1	3-oxo-5-beta-steroid 4-dehydrogenase	Mus musculus (Mouse)	0.70	-	-	-	1
142	3.80	18.08	2	Q4FZK2	Eukaryotic translation elongation factor 1 gamma	Mus musculus (Mouse)	0.64	[ 0.70 - 1.28 ]	1.35	0.11	5
		23.68		Q8R1N8		Mus musculus (Mouse)					
		14.87		Q4FZZ5		Rattus norvegicus (Rat)					
143	3.71	29.63	2	Q569N4	Heat-responsive protein 12	Mus musculus (Mouse)	0.71	[ 0.41 - 1.21 ]	1.72	0.11	3
144	3.68	21.29	2	Q91W19	Sulfotransferase family 1A, phenol-preferring, member 1	Mus musculus (Mouse)	0.99	-	-	-	1
		18.48		Q9R1S5		Mus musculus (Mouse)					
145	3.63	5.87	2	Q9DBT9	Dimethylglycine dehydrogenase	Mus musculus (Mouse)	1.22	[ 0.75 - 1.99 ]	1.63	0.12	3
		5.87		Q5EBH4		Mus musculus (Mouse)					
		4.32		Q83342		Rattus norvegicus (Rat)					
		4.32		Q6RKL4		Rattus norvegicus (Rat)					
146	3.40	5.66	2	Q9QYG0	NDRG2 protein	Mus musculus (Mouse)	1.17	[ 0.95 - 1.44 ]	1.23	0.05	3
		6.82		Q69ZM2		Mus musculus (Mouse)					
		5.88		Q3TY42		Mus musculus (Mouse)					
		5.88		Q3TI48		Mus musculus (Mouse)					
		3.50		Q8VI01		Rattus norvegicus (Rat)					
		3.64		Q8VI00		Rattus norvegicus (Rat)					
		3.64		Q9VBW2		Rattus norvegicus (Rat)					
		3.50		Q9VBU2		Rattus norvegicus (Rat)					
147	3.22	8.66	2	Q3UKT3	Ornithine aminotransferase	Mus musculus (Mouse)	1.19	-	-	-	1
		8.66		Q3UJK5		Mus musculus (Mouse)					
		8.66		P29758		Mus musculus (Mouse)					
		12.11		Q6LDF9		Rattus norvegicus (Rat)					
		6.15		P04182		Rattus norvegicus (Rat)					
148	3.15	13.33	3	Q6BPH1	Tyrosine 3-monooxygenase/tryptophan 5- monooxygenase activation protein	Mus musculus (Mouse)	1.36	-	-	-	1
		31.87		Q3V453		Mus musculus (Mouse)					
149	3.08	2.32	2	Q9ESH4	Aldehyde oxidase 3	Mus musculus (Mouse)	2.41	-	-	-	1
		2.32		Q8VI15		Mus musculus (Mouse)					
		1.72		Q8V657		Mus musculus (Mouse)					
		1.72		Q8V656		Mus musculus (Mouse)					
		2.83		Q8R387		Mus musculus (Mouse)					

N	Unused	%Cov	Nb unique peptides	Accession nb.	Protein Name	Species	KO / WT ratio	Error factor interval	EF	Std Dev.	n quant.
		2.83		Q54754		Mus musculus (Mouse)					
		0.90		Q9Z0U5		Rattus norvegicus (Rat)					
		0.90		Q5QE80		Rattus norvegicus (Rat)					
		0.82		Q9CW59		Mus musculus (Mouse)					
150	2.08	40.63	5	Q90ZX7	Aldehyde dehydrogenase 1a7	Mus musculus (Mouse)	1.01	[ 0.89 - 1.48 ]	1.47	0.05	2
		25.80		P13801		Rattus norvegicus (Rat)					
151	2.00	74.79	18	Q91X87	Selenium binding protein 1	Mus musculus (Mouse)	0.73	[ 0.65 - 0.82 ]	1.12	0.02	2
		70.13		P17563		Mus musculus (Mouse)					
152	2.00	37.57	3	Q9CXU8	Major urinary protein 1 / 11 & 8 / 6	Mus musculus (Mouse)	15.73	[ 5.29 - 46.77 ]	2.97	0.48	7
		31.11		Q68EV3		Mus musculus (Mouse)					
		31.11		P11588		Mus musculus (Mouse)					
		45.03		P04938		Mus musculus (Mouse)					
		37.78		P02762		Mus musculus (Mouse)					
153	2.00	12.83	2	Q91X22	Serpina protein 1a / 1b	Mus musculus (Mouse)	-	-	-	-	0
		12.83		Q3KQ04		Mus musculus (Mouse)					
		10.41		P22599		Mus musculus (Mouse)					
		10.41		Q8VC41		Mus musculus (Mouse)					
154	1.70	24.06	4	Q921H8	3-ketoacyl-CoA thiolase A	Mus musculus (Mouse)	-	-	-	-	0
		20.52		Q3UPU8		Mus musculus (Mouse)					
155	1.62	6.58	2	Q7TMN7	Annexin A4	Mus musculus (Mouse)	0.75	-	-	-	1
		6.58		Q5U362		Rattus norvegicus (Rat)					
		6.58		Q3UCL0		Mus musculus (Mouse)					
		6.60		P97429		Mus musculus (Mouse)					
		6.60		P55260		Rattus norvegicus (Rat)					
		6.13		Q8BSL2		Mus musculus (Mouse)					



# **3. Metabolic study**

**STAT6-deficient Mice Display  
Age-dependent Hepatosteatosis  
and Glucose Intolerance**



---

**STAT6-deficient mice display age-dependent hepatosteatosis and glucose intolerance**

**Joël Iff<sup>1</sup>, Wei Wang<sup>1</sup>, Sarah Mouche<sup>1</sup>, Celine Manzin<sup>1</sup>, Manlio Vinciguerra<sup>1</sup>, Emmanuel Varesio<sup>2</sup>, Gérard Hopfgartner<sup>2</sup>, Michelangelo Foti<sup>1</sup>, Françoise Rohner-Jeanrenaud<sup>1,3</sup> and Ildiko Szanto<sup>4,1,\*</sup>**

<sup>1</sup> Department of Cellular Physiology and Metabolism, Geneva Medical University Center, University of Geneva, 1211 Geneva 4, Switzerland

<sup>2</sup> Life Sciences Mass Spectrometry Laboratory, School of Pharmaceutical Sciences, University of Geneva, University of Lausanne, 1211 Geneva 4, Switzerland

<sup>3</sup> Laboratory of Metabolism, Division of Endocrinology, Diabetology, and Nutrition, Department of Internal Medicine, Faculty of Medicine, University of Geneva, Geneva, Switzerland.

<sup>4</sup> Department of Rehabilitation and Geriatrics, University of Geneva, 1211 Geneva 4, Switzerland

Corresponding author:

Ildiko Szanto, Department of Cellular Physiology and Metabolism, Geneva Medical University Center, University of Geneva, CH-1211 Geneva 4, Switzerland.

Phone: +41 (0)22 379 5238

Fax: +41 (0)22 379 5220

E-mail: [Ildiko.Szanto@medecine.unige.ch](mailto:Ildiko.Szanto@medecine.unige.ch)

---

### 3.1 Introduction

The incidence of obesity worldwide has increased drastically during recent decades. Consequently, obesity and the associated disorders now constitute a serious threat to the current and future health of all populations. Obesity is associated with an array of additional complications, including an increased risk of insulin resistance, type 2 diabetes, fatty liver disease, cardiovascular pathologies and degenerative disorders including dementia and airway diseases (1). The high occurrence of diabetes and the wide variety of pathologies associated with it makes this condition the focus of several different research fields.

Obesity and type 2 diabetes resides at the cross-road of metabolic and inflammatory signaling pathways with the adipose tissue as a major regulator of these processes (2). The chronic “inflammatory state” observed in obesity is characterized by abnormal cytokine production, an increase in acute phase reactants and a generalized cellular stress in different insulin target tissues (3). These findings are supported by the data showing that mice which lack the inflammatory mediator IKK are resistant to high fat diet induced obesity (4). Inflammatory responses can be transmitted through the innate or the adaptive immune system. The involvement of adaptive immune system in the development of insulin resistance was established a little over a decade ago by the finding that the inflammatory cytokine tumor necrosis factor- $\alpha$  (TNF- $\alpha$ ) is overexpressed in the adipose tissue of obese mice (5). These studies were followed by a landslide of discoveries demonstrating the involvement of a variety of inflammatory cytokines in the development of obesity-linked pathologies. More recently, the implication of the innate immune system was highlighted by the study of Shi et al. who reported that the innate immune receptor Toll like receptor 4 (TLR4) is crucial in mediating high fat diet induced inflammation, weight gain and insulin resistance (6). The inflammatory response that emerges in the presence of obesity seems to be predominantly linked to the adipose tissue, though other tissues, particularly the liver might be also involved (2). Metabolic, inflammatory and innate immune processes are also coordinately regulated by lipids (7). Several transcription factors, particularly those in the peroxisome-proliferator activated receptor (PPAR) and liver X receptor (LXR) families, appear to be crucial for modulating the intersection of these pathways. Activation of these transcription factors inhibits the expression of several genes involved in inflammatory response in macrophages and adipocytes (8). Thus, these transcription factors provide an interface for lipid metabolism, inflammatory response and adipose tissue differentiation.

As demonstrated above, significant research efforts have been devoted to unveil the role of increased inflammatory signals in the development of insulin resistance. By contrast, practically no study addressed the question if the lack of anti-inflammatory signals would have similar deleterious metabolic effects.

Two major anti-inflammatory cytokines are interleukin 4 and 13 (IL-4 and IL-13). These cytokines are produced by activated lymphocytes and mediate their signaling through a common transcription factor named Signal Transducer and Activator of Transcription 6 (STAT6). STAT6 is a ubiquitously expressed member of the STAT protein family involved in interleukin 4 and 13 (IL-4 and IL-13) signaling (reviewed in (9)). Upon stimulation, STAT6 is tyrosine phosphorylated and translocates to the nucleus as a homodimer. Once in the nucleus, STAT6 modulates gene transcription by binding to a specific palindromic DNA sequence (10, 11). Most STAT6-dependent genes display this sequence in their promoter regions (reviewed in (9)). In addition, STAT6 interacts with a wide variety of transcription factors and serves as a recruitment platform for the different members of the transcriptional machinery (12-16). Most importantly, STAT6 has been shown to attenuate the inflammatory signals mediated by the IKK/NF $\kappa$ B pathway (13, 17). Due to the multiple interaction partners of STAT6, mice deficient in STAT6 expression display complex STAT6-dependent and – independent transcriptional alterations (18).

In spite of the fact that STAT6 is expressed in a wide variety of tissues most of the research efforts to elucidate the molecular basis for the different effects of STAT6 have been attributed to its essential function in the immune system to pre-dispose T cells towards Th2 type differentiation (19). Recently, however, several studies indicated a function for STAT6 in different other cell types. Notably, STAT6 has been shown to be involved in adipocyte differentiation, kidney epithelial cell mechanosensation and regulation of apoptosis in human hepatoma cells (20, 21). Cytokines known to activate STAT6 play an important role in liver function. Notably, IL-4 and IL-13 injection activates STAT6 and protects against ischemia/reperfusion (I/R) injury (22, 23). Therefore, the lack of STAT6 activation leads to aggravated hypoxic injury both in liver and in the kidney (reviewed in (24)).

Liver I/R leads to abrupt changes in oxygen supply and alterations of substrate availability required for cellular metabolism. Cytokines play a crucial role in modulating hepatocyte metabolic adaptive responses to the hypoxic insult inflicted by the I/R (25). Intermittent hypoxia predisposes to liver injury and induces alterations in lipid homeostasis

---

(26-28). IL-6, an anti-inflammatory cytokine, protects against the development of fatty liver by activating STAT3 and regulating the expression of various glucose and lipid homeostasis genes (29). IL-4 and IL-13 display a similar protective effect against I/R injury, however the gene expression pattern regulated by their common effector molecule, STAT6, has not yet been investigated. A previous study indicated that STAT6 knock-out mice show increased aortic lipid plaque formation when challenged by an atherogenic diet (30). The relevance of these findings were confirmed when a human study reported increased STAT6 expression in the coronary artery intima of patients with advanced atherosclerosis (31). The above studies demonstrated that STAT6 is involved in the regulation of metabolic adaptation under different stress conditions such as hypoxia and suggested that it might be involved in the regulation of peripheral lipid deposition.

In summary, taking the currently available *in vitro* and *in vivo* data together, they establish a complex interaction between inflammatory, metabolic and hypoxia-regulated factors in the development of metabolic syndrome. The role of inflammatory signals in the control of these processes is well established, but data concerning the regulatory function of anti-inflammatory signals are still largely unavailable. STAT6, a mediator of anti-inflammatory signals, is at the crossroad of all the above mentioned pathways: the innate and lymphocyte mediated inflammatory reactions, lipid metabolism, hypoxia and the ROS production.

Therefore, based upon our current knowledge and the results derived from our previous study in the STAT6 knock-out mice it is quite relevant to ask if STAT6 might in fact be a major protector against the onset of metabolic disturbances. To answer this question we used STAT6- deficient mice and characterized their responses to high fat diet challenge.

## 3.2 Experimental Procedures

*Mice and high fat diet feeding* - All experiments were conducted in accordance with the regulatory guidelines of the Veterinary Office of the Canton of Geneva on the care and welfare of laboratory animals. The experimental protocol had been accepted by the Ethical Committee of the University of Geneva and the Veterinary Office of the Canton of Geneva. Mice had *ad libitum* access to water and standard chow (SDS Dietex) or high fat diet 60% of energy as fat (cat: D12108, Provimi Kliba). Balb/cJ wild-type and STAT6 knock-out male mice were obtained from Charles River Laboratories and were kept under regular animal housing conditions.

*Intraperitoneal glucose and insulin tolerance tests* - Mice were starved overnight for 16 hours and blood glucose was measured (Glucotrend Premium, Roche Diagnostics) from the tail vein before intra-peritoneal glucose (2 g/kg body weight) or insulin (1 U/kg body weight) injection and again at 15, 30, 60, 90 and 120 min afterwards.

*Serum measurements* - Blood was obtained from tail vein in a heparinized tube (BD Vacutainer) and immediately centrifuged. Plasma was stored at -80°C before use. Insulin plasma concentrations were measured by ELISA (Insulin ultrasensitive mouse ELISA, Mercodia AB). Starving values were obtained after 16 hours of food deprivation; random fed values were obtained four hours after the lights were off. Insulin resistance index (IRI) was calculated using the following formula: fasting glucose (mM) X fasting insulin (ng/ml) X \* 39.64 / 22.5. Total and HDL cholesterol and triglycerides were measured using DxC800 Beckman Coulter machine.

*Cold exposure* - Mice were starved overnight. Rectal temperature, body weight and glucose were measured at 5:00 pm before overnight starvation and the next morning at 9:00 am before cold (4°C) exposure. During the experiment blood glucose and rectal temperature were recorded at 0.5, 1, 2, 3 and 4 hours. At the end of the experiment, mice were placed at room temperature and were given access *ad lib.* to chow diet. Body weight, blood glucose and rectal temperature were again measured the following day at 9:00 am (24 hours after the beginning of cold exposure).

*Liver lipid content* - Liver lipids were extracted according to a modified Bligh and Dyer method (35). Briefly, liver pieces were pulverized in a mortar using liquid nitrogen then

left overnight in a chloroform:methanol (2:1, v:v) extraction solution. After filtration, lipids were washed once with water, then three times using 2 mM calcium chloride in water:methanol:chloroform (48:49:3, v:v:v) with the supernatant discarded each time. Finally, lipids were air dried and weighted in order to quantify total lipid amount. Triglycerides and cholesterol contents were determined with commercially-available enzymatic kits (Randox Labs.) (36, 37).

*RNA preparation and quantitative real-time RT-PCR* - Total RNA was prepared by homogenizing approximately 100-200 mg liver tissue in TRIZOL Reagent (Invitrogen) and was purified by using RNase free DNase in combination with the RNeasy Mini Kit (Qiagen). cDNA was synthesized from 2 µg of DNA-free RNA by Superscript II Reverse Transcriptase (Invitrogen). Primers and probes were designed by Primer Express software (Applied Biosystems) and are listed as a supplementary material in Table S1. The results were quantified by the  $\Delta\Delta C_t$  method using cyclophilin A as the standard internal non-variable gene to compensate for differences in RNA input and efficiency of cDNA synthesis. Results were expressed as arbitrary units compared to the average expression levels in wild-type mice and are represented as mean  $\pm$  S.E.M.

*Western blotting* - Liver tissues were snap frozen in liquid nitrogen immediately upon removal and were stored at  $-80^\circ\text{C}$  till processing. Tissues were homogenized in lysis buffer (25 mM HEPES, 0.5% Triton X100, 65 mM NaCl, 2.5 mM EDTA, 25 mM sodium pyrophosphate, 50 mM NaF, 2 mM PMSF, 9 mM sodium orthovanadate, one tablet of Complete Inhibitor Cocktail in 20 ml (Roche Diagnostics), pH 7.5. Protein concentration was measured by bicinchoninic acid (BCA) method (Pierce). Proteins were separated by SDS-PAGE, transferred onto nitrocellulose membranes and identified by immunoblotting. Primary antibodies were as follows: p-IR, IR, p-IRS2, p-SHC, SHC, SREBP1, p-IRS1 ser, P-IRS1-tyr, IRS1, Ezrin and STAT6 (Santa Cruz Biotechnology) and P-ACC, P-GSK3 $\beta$ , IRS2, JNK, p-JNK, p-MAPK, MAPK, p85 IRS (Cell Signaling). Secondary HRP-conjugated antibodies were from Biorad and Sigma-Aldrich. Signals were revealed by enhanced chemiluminescence and were recorded in Chemidoc XRS system (Biorad). Quantification of the detected bands was performed by using the Quantity One program (Biorad). Results were expressed as arbitrary units compared to the average expression levels in wild-type mice and are represented as mean  $\pm$  S.E.M.

---

*Statistical analysis* - Results were analyzed by Student's unpaired *t* test using the SigmaStat software (version 2.0 – SPSS, Chicago, IL, USA). Results with a *p* value less or equal than 0.05 were considered significant.

### **3.3 Results**

#### ***3.3.1 Starving hyperglycemia and hypoinsulinemia in STAT6 KO mice***

Serum glucose and insulin levels were determined in four-month-old wild-type and STAT6 KO mice. The mice were then divided into two groups: one group was given standard chow while the second group was fed a high fat containing diet for a period of ten weeks. Four-month-old STAT6 KO mice displayed elevated blood glucose and decreased plasma insulin levels upon overnight starving but no difference in the fed state (**Table 1**, 4 months). Ageing led to elevated starving but decreased fed glucose levels in both genotypes. These changes were accompanied by a tendency of lower insulin secretion in STAT6 KO mice in both fed and starved state (**Table 1**, 6.5 months chow diet). Ten weeks of high fat diet feeding led to the deterioration of metabolic balance in both genotypes; but again, STAT6 KO mice showed much more severe alterations than wild-type mice (**Table 1**, 6.5 months high fat diet).

**TABLE I Serum parameters in wild type and STAT6 knock-out mice.**

Results are expressed as mean  $\pm$  S.E.M., n.s. = non significant ( $p \geq 0.05$ ,  $p \geq 0.01$ ,  $p \geq 0.001$  determined by Student's *t* test). Number of mice is given in parentheses.

	WT	STAT6 KO	p value		
			WT vs KO	4 Mo vs 6 Mo	Chow vs High Fat
4 months					
Random fed					
Glucose (mM)	7.2 $\pm$ 0.1 (n=26)	7.3 $\pm$ 0.1 (n=26)	n.s.	-	-
Insulin (ng/ml)	0.88 $\pm$ 0.18 (n=11)	0.73 $\pm$ 0.13 (n=11)	n.s.	-	-
Starving					
Glucose (mM)	4.0 $\pm$ 0.1 (n=37)	4.5 $\pm$ 0.1 (n=47)	$p \leq 0.001$	-	-
Insulin (ng/ml)	0.25 $\pm$ 0.08 (n=11)	0.11 $\pm$ 0.01 (n=11)	$p \leq 0.05$	-	-
6 months chow diet					
Random fed					
Glucose (mM)	6.6 $\pm$ 0.1 (n=11)	6.9 $\pm$ 0.1 (n=9)	n.s.	WT $p \leq 0.01$ KO n.s.	-
Insulin (ng/ml)	0.34 $\pm$ 0.11 (n=9)	0.25 $\pm$ 0.04 (n=6)	n.s.	$p \leq 0.05$	-
Starving					
Glucose (mM)	4.9 $\pm$ 0.2 (n=23)	5.4 $\pm$ 0.2 (n=20)	n.s.	$p \leq 0.001$	-
Insulin (ng/ml)	0.13 $\pm$ 0.04 (n=7)	0.09 $\pm$ 0.01 (n=5)	n.s.	WT $p \leq 0.01$ KO n.s.	-
6 months high fat diet					
Random fed					
Glucose (mM)	7.6 $\pm$ 0.2 (n=16)	7.9 $\pm$ 0.2 (n=17)	n.s.	-	$p \leq 0.01$
Insulin (ng/ml)	2.56 $\pm$ 0.48 (n=9)	1.06 $\pm$ 0.21 (n=10)	$p \leq 0.01$	-	WT $p \leq 0.001$
Starving					
Glucose (mM)	5.8 $\pm$ 0.2 (n=16)	6.9 $\pm$ 0.3 (n=17)	$p \leq 0.01$	-	KO $p \leq 0.05$ $p \leq 0.01$
Insulin (ng/ml)	0.77 $\pm$ 0.19 (n=9)	0.30 $\pm$ 0.07 (n=9)	$p \leq 0.05$	-	$p \leq 0.05$

### 3.3.2 *STAT6 KO mice are glucose intolerant*

Our preceding study identified the presence of latent liver lipid accumulation in STAT6 KO mice. Liver steatosis is often associated with impaired glucose homeostasis; therefore we performed intraperitoneal glucose and insulin tolerance tests (GTT and ITT, respectively). At four months of age STAT6 knock-out mice displayed severely impaired glucose tolerance (**Fig. 1a**). By contrast, there was no difference in the response to insulin between wild-type and knock-out littermates, except a small but significant latency in glucose clearing observed at 15 minutes in the STAT6-deficient mice (**Fig. 1b**). Meanwhile aging led to higher fasting glucose levels (**Table 1**) it had no effect on the response to glucose administration in any genotype (**Fig. 1c** and compare to **Fig. 1a**). Interestingly, aging rendered mice of both genotypes more responsive to insulin (**Fig. 1d** and compare it to **Fig. 1b**). Ten weeks of high fat diet feeding lead to the development of pronounced glucose intolerance in wild-type mice resulting in blood glucose levels similar to the ones displayed by their STAT6 KO littermates on chow diet (**Fig. 1e**). By contrast, high fat diet did not further impair glucose intolerance in the knock-out mice (**Fig. 1e** and compare it to **Fig. 1c**). High fat diet resulted in the development of moderate insulin resistance in mice of both genotypes, evident only at the early time point of 15 minutes of insulin challenge ( $p \leq 0.01$  in both genotypes; chow diet vs. high fat diet) (**Fig. 1f** and compare it to **Fig. 1d**). In line with the lower insulin levels, STAT6 KO mice were more insulin sensitive judged by homeostasis model assessment-insulin resistance (HOMA-IR) (**Fig. 1g**). The lower serum insulin levels were reflected in a decrease in pancreas islet insulin content in chow fed STAT KO mice. By contrast, mice of both genotypes displayed the adaptive increase in insulin content upon high fat diet feeding (**Fig. 1h**).

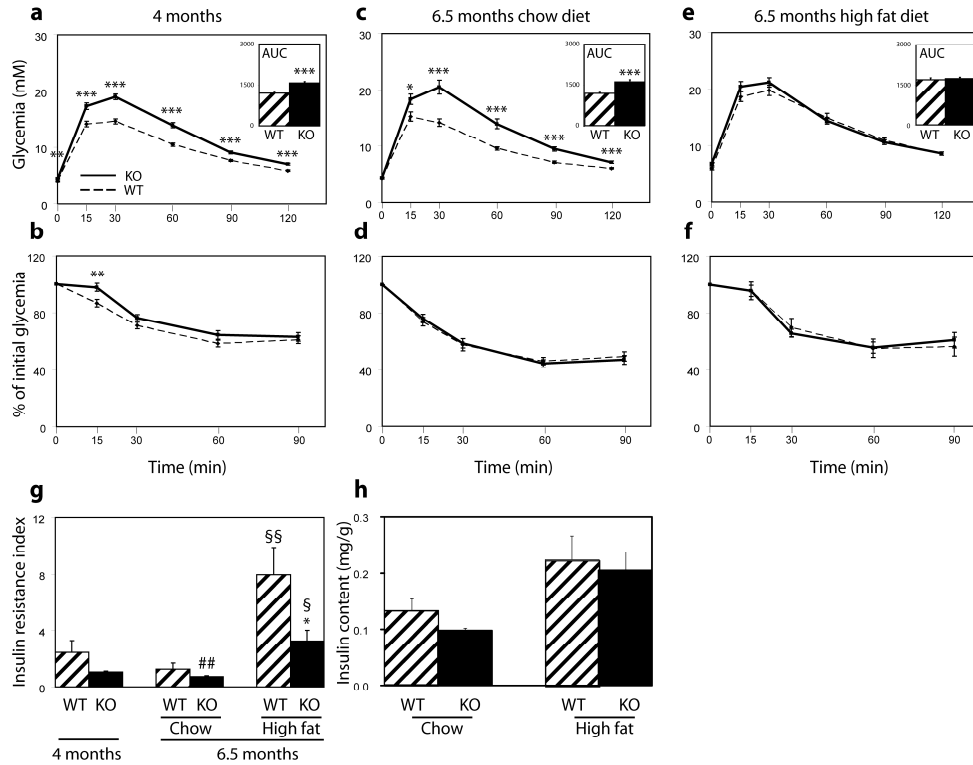


**FIG. 1. Characterization of glucose tolerance, insulin resistance and insulin production of WT and STAT6 KO mice at 4 months (n=40/genotype) and 6.5 months of age after ten weeks of chow or high fat diet (n=15/genotype/diet).**

(a, c, e) Blood glycemia was determined after intra-peritoneal (IP) glucose injection (2g/Kg) in 4 (a) and 6.5 months old (c) mice kept on chow diet and in 6.5 months mice after 10 weeks of high fat diet feeding (e). (Dashed line and bar: WT, full line and bar: STAT6 KO; AUC =Area Under the Curve; \*\*\* p < 0.001 WT vs. STAT6 KO). (b, d, f) Blood glycemia after IP insulin injection (1U/Kg). (\*\* p < 0.01, WT vs. KO). (g) HOMA-IR: homeostasis model assessment-insulin resistance (fasting glucose (mM) X fasting insulin (ng/ml) X 39.64 / 22.5. Data are presented as mean ± S.E.M.; n.s.: non-significant, #: p ≤ 6.5months vs. 4 months, (n= 8/genotype). (h) Insulin content of whole pancreas of 6.5 months old mice kept on chow or high fat diet.

### 3.3.3 Liver lipid storage and mobilization in STAT6 KO mice

Wild-type and STAT6 KO mice displayed similar calorie intake ( $58.9 \pm 3.6$  vs.  $56.6 \pm 2.6$  kJ/day and  $81.0 \pm 3.3$  vs.  $77.0 \pm 4.6$  kJ/day, wild-type vs. KO, chow and high fat diet, respectively) and body weight gain ( $4.4 \pm 2.2$  vs.  $13.8 \pm 5.9$  mg/day and  $76.7 \pm 13.6$  vs.  $74.6 \pm 13.7$  mg/day, wild-type vs. KO, chow and high fat diet, respectively). Serum cholesterol levels were elevated in STAT6 KO mice upon high fat diet challenge confirming the results of a previous study where feeding an atherogenic diet led to similar differences between STAT6 KO and wild-type mice (30) (**Fig. 2a-b**). By contrast, serum triglyceride levels were already significantly increased in chow fed knock-out mice and remained elevated after high fat diet feeding (**Fig. 2c**).

Our previous study demonstrated increased lipid deposition in the livers of STAT6 KO mice. To further characterize the consequences of the lack of STAT6 on whole body lipid metabolism we compared body composition and liver lipid content of wild-type and STAT6 KO mice. STAT6 KO mice displayed lower adiposity with a decrease in relative epididymal and intra-abdominal white adipose tissue mass (WAT<sub>e</sub> and WAT<sub>i</sub>, respectively) (**Fig. 2d,e,f**, Chow). High fat diet feeding resulted in a similar increase in WAT<sub>e</sub> and WAT<sub>i</sub> mass; however STAT6 KO mice displayed a selective increase in their liver weight compared to the wild-type mice (**Fig. 2d,e,f**, High fat Fed). Short-term fasting induces fuel and energy redistribution between adipose tissue and liver in order to maintain blood glucose levels by decreasing adipose tissue fat and liver glycogen depots. Overnight fasting revealed a dramatic difference in the metabolic adaptation in STAT6 KO mice. Wild-type Balb/cJ mice were resistant to starving-induced white adipose tissue lipolysis. By contrast, STAT6 knock-out mice responded with a significant loss in adipose tissue and liver mass suggesting exaggerated starving-induced reserve utilization in these mice (**Fig. 2d,e,f**, High fat Starved). Overnight starvation resulted in dramatic differences in liver metabolism as well. As we showed before, STAT6 KO mice displayed higher liver lipid levels than their wild-type littermates and this was further elevated upon high fat diet feeding (**Fig. 2g**). Acute starvation leads to hepatic lipid accumulation as a result of increased hepatic uptake of FFA released from the white adipose tissue. Indeed, upon overnight food deprivation wild-type mice increased their liver triglyceride and cholesterol contents. By contrast, STAT6 KO mice responded to starving by depleting the previously existing lipid reserves as well (**Fig. 2g,h,i**). Liver glycogen content was not significantly different between chow diet fed wild-type and

---

STAT6 KO mice. However, when fed a high fat diet, STAT6 KO mice failed to reduce glycogen accumulation but showed increased utilization during overnight starving (**Fig. 2j**).

To gain a better insight into the energy balance of STAT6 KO mice we measured the uncoupling protein 1 (UCP1) content in the brown adipose tissue. UCP1 is a brown adipocyte specific mitochondrial protein regulating energy dissipation. Basal UCP1 expression was significantly lower in STAT6 KO mice suggesting lower mitochondrial energy release. While high fat diet did not change this expression pattern, STAT6 KO mice failed to down-regulate UCP1 expression upon overnight starvation (**Fig. 2k**). To assess if an increase in the number of intercalating white adipocytes in the brown adipose mass is responsible for this dysregulation we compared the histological structure of the brown adipose tissue of wild-type and STAT6 KO mice but found no major morphological alteration (**Fig. 2l**). Cold induced stress increases UCP1-mediated thermogenesis in brown adipose tissue along with the induction of lipolysis in the white adipose tissue. In spite of the lower UCP1 expression, STAT6 KO mice were more efficient in keeping their body temperature when subjected to cold (4°C) challenge (**Fig. 2m**). Taken together, these data imply an intriguing scenario where the lack of STAT6 signaling leads to an imbalance in metabolic homeostasis, which becomes obvious during different metabolic stress conditions.

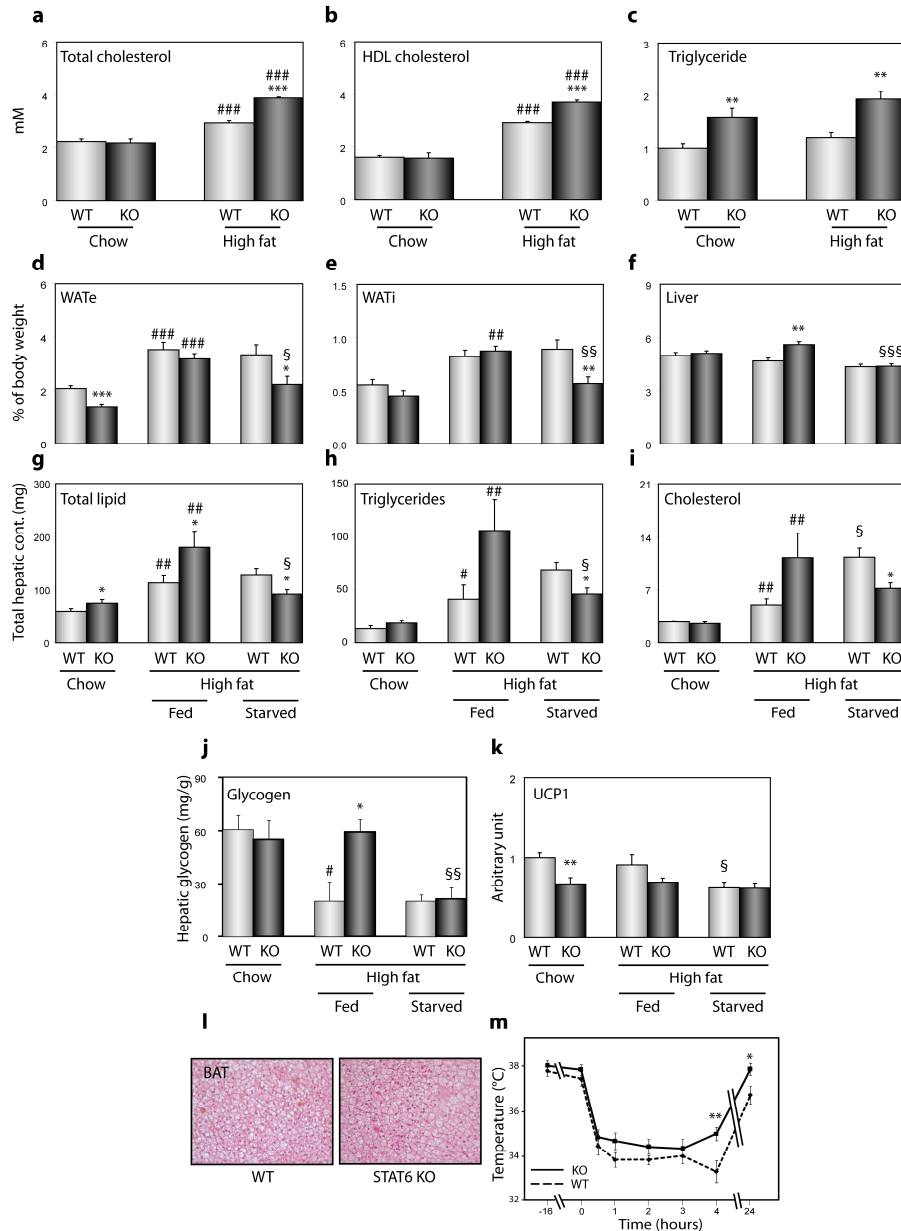


**FIG. 2. Characterization of plasma and liver content, lipid organ distribution and cold resistance between WT (grey bar) and STAT6 KO mice (full bar) on chow and high fat diet.**

(**a,b,c**) Serum levels of total cholesterol (**a**), high density lipoprotein (HDL) cholesterol (**b**) and triglycerides (**c**) were determined in mice kept on chow or high fat diet in fed mice or after overnight starvation. (\*\*  $p < 0.01$ , \*\*\*  $p < 0.001$  WT vs. KO; ###  $p < 0.001$  high fat vs. chow diet in the same genotype). (**d,e,f**) Epididymal white adipose tissue (WATe) (**e**), intra-abdominal white adipose tissue (WATi) (**e**) and liver (**f**) weights of WT and STAT6 KO mice. (\*  $p < 0.05$ , \*\* =  $p < 0.01$ , \*\*\*  $p < 0.001$  WT vs. KO; ###  $p < 0.001$  chow vs. high fat diet; §  $p < 0.05$ , §§§  $p < 0.001$  fed vs. starved). (**g, h, i**) Liver total lipid (**g**), triglyceride (**h**) and cholesterol levels (**i**). (\*  $p < 0.01$ , WT vs. KO; #  $p < 0.05$ , ##  $p < 0.01$ , ###  $p < 0.001$  chow vs. high fat diet; §  $p < 0.05$  fed vs. starved).

(j) Liver glycogen content of WT and STAT6 KO mice. (\*  $p < 0.01$  WT vs. KO; #  $p < 0.05$  chow vs. high fat diet; §§  $p < 0.01$  fed vs. starved). (k) Uncoupling protein 1 (UCP1) mRNA levels in brown adipose tissue (BAT). (\*\*  $p < 0.01$  WT vs. KO; §  $p < 0.01$  fed vs. starved). (e) Histology of the BAT of chow diet fed WT and STAT6 KO mice (Hematoxylin-eosin staining, magnification 5x.) (m) Resistance to cold stress in STAT6 KO mice. Mice were starved overnight at room temperature (-16 hours) and placed at 4°C (0 hours) for the times indicated. After 4 hours mice were transferred to room temperature and were given *ad lib.* access to food. Rectal temperature was measured at the times indicated. The graph represents mean  $\pm$  S.E.M.,  $n = 6-10$ /genotype. (\* =  $p < 0.05$ , \*\* =  $p < 0.01$ , \*\*\* =  $p < 0.001$  wild-type vs. STAT6 KO; ##  $p < 0.01$ , ### =  $p < 0.001$  high fat vs. chow diet; § =  $p < 0.05$ , §§§  $p < 0.001$  starved vs. fed).

### 3.3.4 *Histological changes in the liver and the white adipose tissue of STAT6 KO mice*

As shown previously by us and by others as well, there were no obvious changes in liver structure in control chow fed STAT6 KO mice by hematoxylin-eosin staining. By contrast, upon high fat diet feeding STAT6 KO mice developed centro-lobular micro- and macrovesicular hepatosteatosis while livers of control mice remained relatively intact with only mild microvesicular lipid deposition (**Fig. 3a** H.E.) This elevated lipid deposition was confirmed by the neutral lipid staining Oil-Red O (**Fig. 3a** Oil-Red O). Liver steatosis is often associated with collagen deposition in the intersinusoidal space resulting in liver fibrosis. Indeed, collagen staining showed the presence of increased deposition in STAT6 KO mice fed either chow or high fat diet (**Fig. 3a** Collagen). Increased serum levels of hepatic enzymes are often found in association with fatty liver disease as early indicators of impaired hepatic function. Interestingly, in spite of the dramatic high fat diet induced lipid accumulation in the livers of STAT6 KO mice, the respective serum alanine aminotransferase (ALT) ( $269.7 \pm 26.0$  vs.  $238.9 \pm 32.2$  U/l), aspartate transaminase (AST) ( $116.4 \pm 18.7$  vs.  $105.8 \pm 38.1$  U/l) and alkaline phosphatase (ALP) ( $14.4 \pm 0.5$  vs.  $15.8 \pm 0.9$  U/l) levels were identical in wild-type and STAT6 KO mice.

Chow diet fed STAT6 KO mice had lower WAT mass and higher insulin sensitivity. Adipocyte size is linked to insulin sensitivity as small adipocytes are insulin sensitive, while large adipocytes are insulin resistant. Adipocytes of STAT6 KO mice were smaller than those of wild-type mice. By contrast, high fat diet feeding resulted in the substantial hypertrophy of STAT6-null adipocytes, actually rendering the knock-out cells larger than the wild-type ones (**Fig. 3b, c**). No difference was observed in the mRNA expression of two markers of

adipocyte differentiation, the nuclear receptor peroxisome proliferator-activated receptor  $\gamma$  (PPAR $\gamma$ ) and the adipocyte fatty acid transporter AP2 (**Fig. 3d, e**).

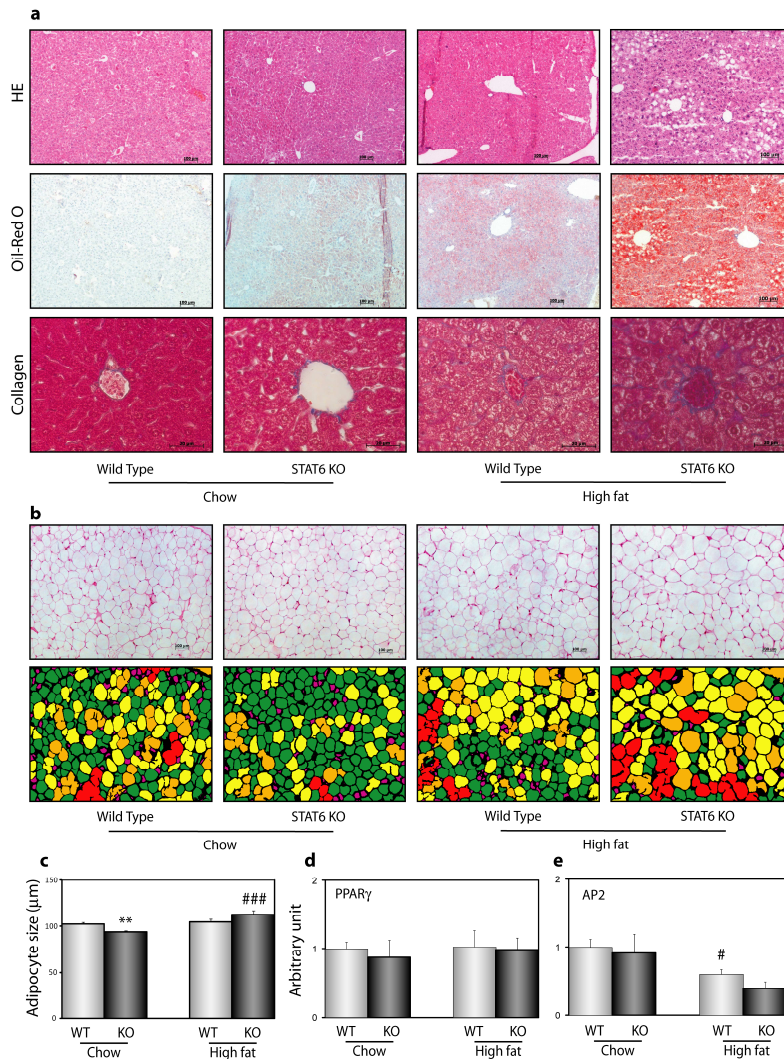


**FIG. 3. Comparison of liver and WATe histology of WT and STAT6 KO mice.**

(a) Histology of the liver stained by Hematoxylin-eosin (HE) (upper panels), the lipid staining Oil-Red-O (middle panels) and the collagen specific Masson staining (lower panels). (Magnification 10x). (b) Representative images of the WATe tissues from WT and STAT6 KO mice stained by hematoxylin-eosin (upper panels). The images were converted into computer assisted images where the adipocytes are colored according to their size with the increasing order of green, yellow, orange and red (lower panels). (c) Adipocyte size determined by quantification of random images taken from the epididymal adipose tissue of WT and STAT6 KO mice. (\*\*  $p < 0.01$  WT vs. KO; ###  $p < 0.001$  high fat vs. chow). (d,e) PPAR $\gamma$  mRNA measurement in WATe show no major differences between genotypes or food content. (e) AP2 mRNA measurement show a decrease in the WT animals (#  $p < 0.05$ ) after a high fat diet but no differences between genotypes.

### ***3.3.5 Differential protein and gene expression in the liver and white adipose tissue of STAT6 KO mice***

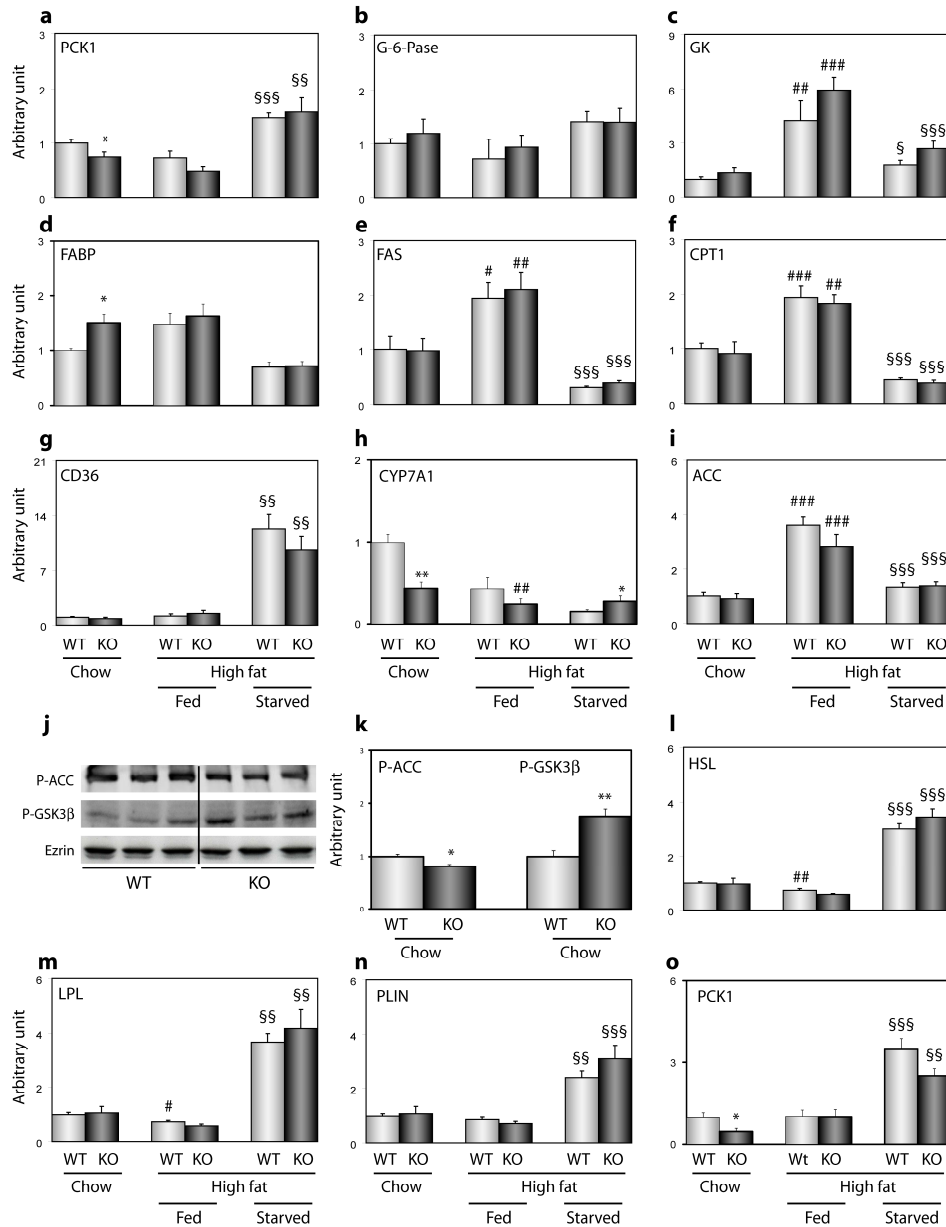
STAT6 is a transcription factor and our previous differential proteome analysis identified several differentially expressed enzymes involved in lipid, cholesterol and glucose metabolism in the livers of STAT6 KO mice. In order to understand the mechanism leading to glucose intolerance and liver lipid deposition in STAT6 KO mice, we measured key enzymes involved in these metabolic pathways. The key enzyme regulating glucose synthesis, PCK1, was down-regulated in STAT6 KO mice, but was induced to the same level as in the wild-type mice if subjected to overnight starvation. By contrast, the other key gluconeogenic enzyme, glucose 6 phosphatase (G-6-Pase) and the rate limiting enzyme of glycolysis, glucokinase (GK) showed no statistically significant alterations (**Fig. 4a-c**). Expression of liver fatty acid binding protein (FABP) was elevated in STAT6 KO mice to the same level as in high fat diet fed wild-type mice. Key genes of fatty acid (FA) synthesis (Fatty acid synthase (FAS)), FA oxidation (carnitine palmitoyltransferase 1 (CPT1)) and hepatocellular FA uptake (CD 36) also showed similar expression levels and regulation in wild-type and STAT6 KO mice (**Fig. 4d-g**). By contrast, CYP7A1, the rate limiting enzyme of cholesterol biosynthesis in rodents showed decreased expression in the STAT6 KO mice, most likely reflecting a compensatory mechanism against the liver accumulation of exogen cholesterol (**Fig. 4h**). Acetyl coenzyme A carboxylase (ACC) provides a pivotal step in fuel metabolism as it links fatty-acid and carbohydrate metabolism through the shared intermediate acetyl coenzyme A (CoA). The expression levels of this enzyme were similar in wild-type and STAT6 KO mice (**Fig. 4i**). By contrast, there was a significant difference in the phosphorylation state of both ACC and glycogen synthase kinase 3 $\beta$  (GSK3 $\beta$ ), one of the major regulatory enzymes of glycogen synthesis. Decreased phosphorylation of ACC signifies increased fatty acid synthesis and decreased fatty acid oxidation, while increased GSK3 $\beta$  phosphorylation represents increased glycogen synthesis, both predisposing to elevated nutrition storage becoming obvious under high fat diet conditions (**Fig. 4j, k, and see Fig. 2 h, j**).

Increased lipolysis in the WAT raises serum FFA concentrations and plays an important role in the development of liver steatosis. The activity of several white adipose tissue enzymes involved in this process is regulated at the transcriptional level. Therefore, we examined the expression of the adipocyte specific hormone-sensitive lipase (HSL), the

endothelial cell specific lipoprotein lipase (LPL) as well as that of perilipin, the enzyme regulating the release of tri-glyceride storage from adipocytes but found no differences between their expression levels and regulation in knock-out and wild-type mice (**Fig. 4l-n**). Phosphoenolpyruvate carboxykinase (PCK1) is an enzyme playing a major role in the synthesis of glycerol, used as the “back-bone” during the creation of triglycerides storage. Similar to the liver, we found a decrease in PCK1 expression in the white adipose tissue of STAT6-deficient mice (**Fig. 4o**). This finding is in line with the decreased WAT mass of STAT6 KO mice.

**FIG. 4. Expression of glucose and lipid homeostasis enzymes in the liver and the WAT of WT and STAT6 KO mice (see next page).**

(**a-i**) Liver mRNA expression of Phosphoenolpyruvate carboxykinase (PCK1) (**a**), glucose 6 phosphatase (G-6-Pase) (**b**), glucokinase (GK) (**c**), fatty acid binding protein (FABP) (**d**), fatty acid synthase (FAS) (**e**), carnitine palmitoyltransferase (CPT1) (**f**), CD36 (**g**), acetyl CoA Carboxylase (ACC) (**h**), and cytochrome P450 7A1 (CYP7A1) (**i**). (**j, k**) Western blot analysis (**j**) and its quantification (**k**) of liver glycogen synthase kinase 3 (P-GSK3 $\beta$ ) and acetyl CoA carboxylase (P-ACC) phosphorylation in WT and STAT6 KO mice. (**l,m,n,o**) White adipose tissue mRNA expression of hormone-sensitive lipase (HSL) (**l**), Lipoprotein lipase (LPL) (**m**), perilipin (PLIN) (**n**) and phosphoenolpyruvate carboxykinase (PCK1). (Bars represent mean  $\pm$  S.E.M.; \*  $p < 0.05$  WT vs. KO; #  $p < 0.05$ , ##  $p < 0.01$ , ###  $p < 0.001$  chow vs. high fat diet; §  $p < 0.05$ , §§  $p < 0.01$ , §§§  $p < 0.001$  fed vs. starved)



Excess accumulation of *de novo* synthesized fatty acids is a hallmark of both human and rodent liver steatosis (32, 33). Lipogenesis is regulated at the transcriptional level and altered expression of different transcriptional factors have been linked to the development of liver steatosis(34). Two major transcription factors are the peroxisome proliferator activated receptor- $\gamma$  (PPAR $\gamma$ ) and the sterol regulatory element-binding protein 1c (SREBP-1c). In the liver, STAT6 KO mice had elevated PPAR $\gamma$  levels compared to wild-type mice. By contrast, other members of the PPAR family, namely PPAR $\alpha$  and  $\beta$  and the PPAR $\gamma$  co-activator 1 $\alpha$

(PGC-1 $\alpha$ ) were not altered (**Fig. 5a**). The elevated PPAR $\gamma$  expression is in line with the decreased mRNA levels of PCK1, a known PPAR $\gamma$  target gene. SREBP proteins regulate endogen cholesterol synthesis in response to exogen cholesterol levels. The function of SREBP proteins is regulated through translocation from the endoplasmatic reticulum (ER) to the Golgi apparatus and activation by proteolytic cleavage. Accordingly, no difference was observed at the mRNA level. By contrast, STAT6 knock-out mice displayed elevated non-cleaved (non-activated) protein levels which indicates repression of cholesterol synthesis reflected in the decreased expression of CYP7A1 (**Fig. 5c,d, see Fig. 4h**).

Our previous study indicated that several genes differentially expressed in the knock-out mice lacked the consensus DNA binding sequence for STAT6, but contained various binding elements for the aryl-hydrocarbon receptor (AHR) in their promoter regions. Indeed, there was a tendency of higher expression levels of AHR and the related aryl-hydrocarbon receptor nuclear translocator (ARNT) in the chow diet fed knock-out mice. Moreover, high fat diet feeding resulted in an increase in both AHR and ARNT suggesting that these receptors might play a role in mediating the changes in gene expression related to metabolic stress (**Fig. 5e,f**). ARH activity is induced by dioxin, a hepatotoxic drug and one of the classical targets of this receptor is the induction of the cytochrome CYP1A1. When evaluating CYP1A1 expression we found no differences between STAT6 deficient and wild-type mice suggesting that ARH and ARNT have different signaling pathways and targets during toxic or metabolic assaults (**Fig. 5g**).

Another finding of our proteomic study was the revelation of signs of cellular stress in STAT6-deficient livers. Notably, we identified upregulation of the expression of the molecular chaperone 78 kD glucose regulated protein (GRP78) and that of glyoxalase (GLO) involved in the elimination of the advanced glycated endproducts (AGEs). GRP78 is a marker of endoplasmatic (ER) stress that has been casually linked to the development of insulin resistance, while up-regulation of GLO signifies a defense mechanism against increased cellular glucose and lipid load. Indeed, the expression of both genes remained elevated in the knock-out mice upon high fat diet feeding suggesting that they play an important role in the development of liver metabolic phenotype in these mice (**Fig. 5h**). CYP2E1 is a cytochrome enzyme, highly expressed in the livers and most commonly known to be linked to the development of cellular stress and alcoholic liver damage. However, the expression of this enzyme is also regulated by insulin and recent data indicated that it is

involved in the process leading to hepatic steatosis in obese and Type 2 diabetic patients. Interestingly, our previous proteomic analysis did not identify CYP2E1 as a differentially expressed protein in chow diet fed mice. Here we confirmed these data at the level of mRNA expression. Moreover, we also extended our observations to high fat diet fed mice where we found a significant up-regulation of this gene in the knock-out but not in wild type mice (**Fig. 5h**).

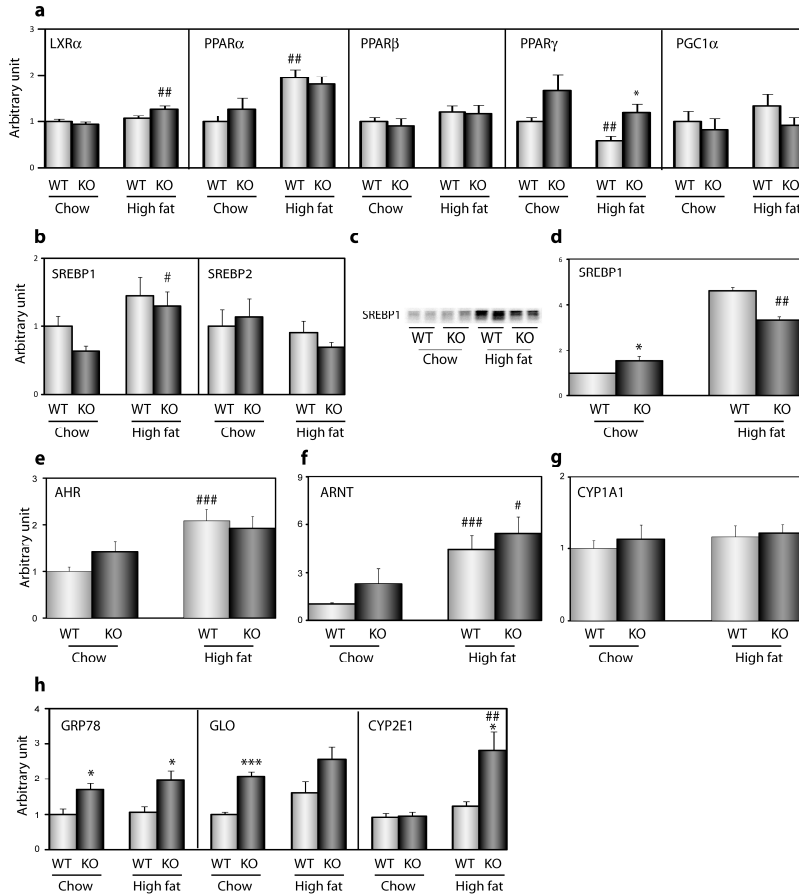


**FIG. 5. Elevated mRNA expression of lipid homeostasis transcription factors and stress-related proteins in the livers of STAT6 KO mice.**

(a, b) mRNA expression of Liver X receptor  $\alpha$  (LXR $\alpha$ ), peroxisome proliferator-activated receptor  $\alpha,\beta,\gamma$  (PPAR $\alpha$ , PPAR $\beta$ , PPAR $\gamma$ ), peroxisome proliferator-activated receptor  $\gamma$  coactivator 1  $\alpha$  (PGC1 $\alpha$ ) (a) and Sterol regulatory element-binding protein 1 and 2 (SREBP1, SREBP2) (b). (c, d) Western blot analysis (c) and quantification (d) of SREBP1c protein expression. (e, f, g) mRNA expression of the aryl hydrocarbon receptor (AHR) (e), aryl hydrocarbon receptor nuclear translocator (ARNT) (f) and cytochrome P450 1A1 (CYP1A1) (g). (h) mRNA expression of the 78kDa glucose regulated protein (GRP78), glyoxalase (GLO) and cytochrome P450 2E1 (CYP2E1). (Bars represent mean  $\pm$  S.E.M.; \*  $p < 0.05$  WT vs. KO; #  $p < 0.05$ , ##  $p < 0.01$ , ###  $p < 0.001$  chow vs. high fat diet).

### ***3.3.6 Insulin signaling in the livers of STAT6 KO mice***

Our data indicated that STAT6-deficient mice display higher sensitivity to insulin, particularly during high fat diet feeding (see **Fig. 1g**). Therefore, we compared the insulin-induced signaling pathways between high fat diet fed STAT6 KO and wild type mice injected by intraperitoneal insulin and sacrificed after 15 minutes (**Fig. 6a,b**). While we found no difference in insulin receptor expression or phosphorylation, there was a shift in the balance between IRS-1 and IRS-2 mediated signaling with an increase in IRS-1 and a decrease in IRS-2 phosphorylation. These data suggest an imbalance between insulin's mitogenic and metabolic effects which are linked to IRS-1 and IRS-2, respectively. In line with an increase in IRS-1-mediated mitogenic signaling the phosphorylation of p42/44 mitogen activated kinase (MAPK) was enhanced in the knock-out livers. Insulin also activates stress –related pathways, mediated largely by the members of the c-jun kinase (JNK) family. The 54 kDa JNK isoform has also been casually linked to the development of liver steatosis. In this context it is of interest that STAT6 KO mice showed a unique enhancement of insulin-induced phosphorylation/activation of this JNK isoform.

### ***3.3.7 Expression of STAT6 in liver steatosis***

The obese diabetic leptin deficient model (ob/ob) mice develop liver steatosis. To explore the possibility that decreased STAT6 mediated signaling is associated with the presence of liver steatosis we measured STAT6 mRNA and protein expression in the livers of this model of non-alcoholic fatty liver disease (NAFLD). Indeed, our data confirmed diminished levels of STAT6 expression in these mice (**Fig. 6c**). To further explore the significance of our findings in the context of human pathology we compared STAT6 expression between obese, non-diabetic subjects with and without the presence of liver steatosis. In keeping with the data obtained from the mouse model we found a significant down-regulation of STAT6 expression in humans with hepatosteatois (**Fig. 6d**).

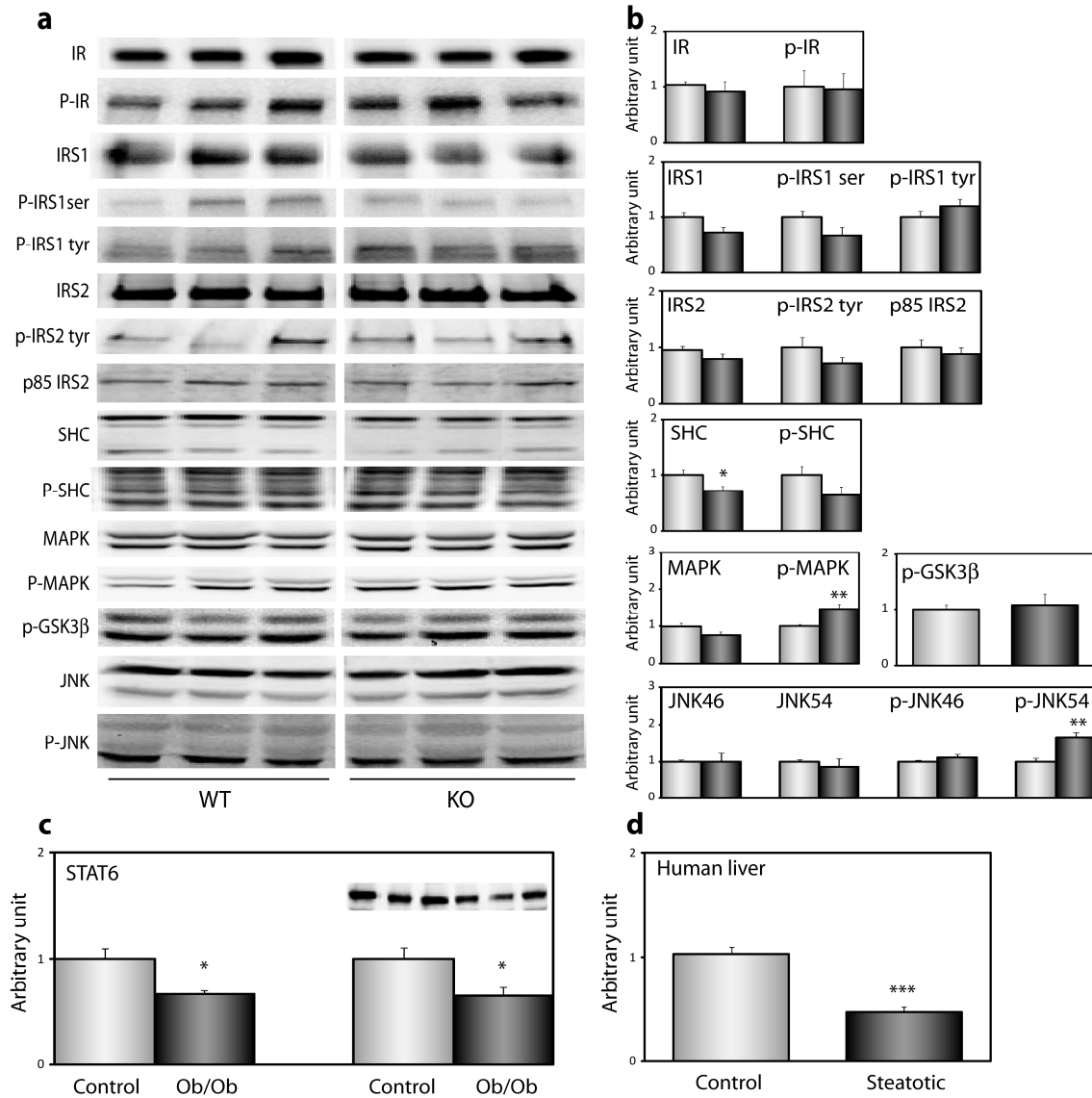


**FIG. 6. Decreased STAT6 expression is associated with hepatosteatosis.**

(a,b) Western blot analysis (a) and quantification (b) of the insulin-induced signaling/phosphorylation cascade. (insulin receptor (IR), phosphorylated insulin receptor (p-IR); (serine/ tyrosine- phosphorylated) insulin receptor substrate 1/2 (IRS1/2, p-IRS1 ser, p-IRS1/2 tyr); (phosphorylated) mitogen-activated protein kinase (p-MAPK); phosphorylated glycogen synthase kinase-3 β (p-GSK3β); (phosphorylated) 46 and 54 kDa c-Jun N-terminal kinase (JNK46/JNK54 and p-JNK46/p-JNK54). (Bars represent mean ±S.E.M, \* p < 0.05, \*\* p < 0.01 WT vs. KO). (c) STAT6 mRNA (left panel) and protein expression (right panel) in the livers of ob/ob mice. The gel above the right panel shows a representative Western blot. (\* p < 0.05 control vs. ob/ob) (d) Quantification of liver STAT6 mRNA levels in obese, non-diabetic patients with or without the presence of steatosis (steatotic and control, respectively). (\*\*\*) p < 0.001 control vs. steatotic liver).

---

### 3.4 Discussion

Our previous study uncovered the presence of hepatocellular stress and latent lipid accumulation in the livers of STAT6 KO mice. Liver steatosis is frequently associated with disturbed glucose and lipid homeostasis; therefore we explored these metabolic changes in mice deficient in STAT6 signaling. In the present study we have shown that the lack of STAT6 expression results in the development of age-dependent glucose intolerance and a decreased capacity to regulate metabolic balance under acute (overnight starving) or chronic (high fat diet feeding) challenges. We found that STAT6 knock-out mice display a pathologic distribution of fat deposition with a shift from the adipose tissue towards the liver. These data are in good correlation with previous murine and human studies where STAT6 expression was linked to peripheral fat deposition in the arterial wall. Furthermore, we demonstrate that STAT6-deficient mice store higher amount of liver glycogen and triglyceride under nutrition-rich conditions but use these stocks more extensively during starvation periods. Thus, the lack of STAT6-mediated signaling leads to the perturbation of the balance between energy storage and utilization in liver. This higher energy turn-over is also supported by the resistance of STAT6 KO mice to cold challenge which is accompanied by a compensatory decrease in the brown adipose tissue mediated heat generation indicated by the decreased expression of UCP-1, a molecule responsible for the majority of heat production through non-shivering thermogenesis.

The major significance of our study is that it identifies STAT6 as one of the molecules that is at the crossroad of inflammation and metabolic processes and whose expression is necessary for the fine tuning of the complex network regulating whole body nutritional partitioning, energy balance and the defense against metabolic assaults. The phenotype of STAT6 knock-out mice is even of greater importance taking into account the fact that most of these disturbances need an important timeframe to develop and remain subtle, but become evident and deleterious in the environment of metabolic stress closely resembling the process leading to the development of Type2 diabetes and liver steatosis. The predisposition towards the development of this complex phenotype is reflected at the level of gene expression as most of the genes that show differential expression in the knock-out mice basal (chow diet fed) state are regulated in the same direction in the wild type mice upon high fat diet feeding.

---

Our further experiments were focused on exploring one aspect of this complex phenotype: the link between impaired STAT6-mediated signaling and the development of liver steatosis. This correlation is supported by the decreased STAT6 expression detected in both murine and human steatotic livers.

Our previous proteomic study indicated that most of the differentially regulated proteins are probably not direct targets of STAT6. Indeed, in this study we identified up-regulation of the adipogenic receptor PPAR $\gamma$ , the compensatory down-regulation of SREBP1c activity leading to the suppression of endogen cholesterol biosynthesis, and the up-regulation of the xenobiotic receptors AHR and ARNT. The altered expression of PPAR $\gamma$  is reflected in the decreased expression of PCK1, while reduced SREBP1c activity is reflected in the diminished expression of CYP7A1. The potential role and the transcriptional targets of AHR and ARNT are more obscure. Importantly, however, AHR has been shown to participate in mediating the response to *in vivo* ischemia and reduced expression of ARNT has been linked to the development of insulin resistance in pancreatic islet  $\beta$  cells. These data suggest that these molecules are important mediators of physiological processes and have other, yet unappreciated functions than simple xenobiotic receptors. The fact that both receptors are up-regulated upon high-fat diet feeding without altering their conventional target gene involved in xenobiotic detoxification provides further indication of their potential involvement in the development of metabolic disturbances.

In summary, our study explored the effect of an imbalance in inflammatory mediators on the development of metabolic disturbances by using STAT6 knock-out mice, a model of decreased anti-inflammatory cytokine signaling. We demonstrated that these mice display latent metabolic disturbances that can aggravate and become obvious under stress conditions similar to those leading to the development of Type2 diabetes-related complications. These data indicate that mutations in STAT6, leading to decreased activity might be a so far unappreciated predisposing factor towards the development of diabetes-related complications. Moreover, these findings designate STAT6 as a potential therapeutic target in human hepatosteatosis.

---

### 3.5 Acknowledgements

We thank M. Klein. (Department of Cell Physiology and Metabolism, University of Geneva) and P. Quirighetti (Animal Core Facility, University of Geneva) for excellent technical help; R. James (Service of Endocrinology, University Hospital of Geneva) for liver lipids measurements, D. Hochstrasser, M. Fathi and O. Golaz (Central Clinical Chemistry Laboratory of the University Hospital of Geneva) for serum measurements and Sergei Startchik (Bioimaging Core Facility, University of Geneva) for help with the computational analysis of the white adipose tissue . This work was supported from a grant from COST Action B17, No.C02.0097.

### 3.6 References

1. Hotamisligil, G. S. (2006) Inflammation and metabolic disorders. *Nature* 444, 860-867.
2. Shoelson, S. E., Herrero, L., and Naaz, A. (2007) Obesity, inflammation, and insulin resistance. *Gastroenterology* 132, 2169-2180.
3. Wellen, K. E., and Hotamisligil, G. S. (2005) Inflammation, stress, and diabetes. *J Clin Invest* 115, 1111-1119.
4. Shoelson, S. E., Lee, J., and Yuan, M. (2003) Inflammation and the IKK beta/I kappa B/NF-kappa B axis in obesity- and diet-induced insulin resistance. *Int J Obes Relat Metab Disord* 27 Suppl 3, S49-52.
5. Hotamisligil, G. S., Shargill, N. S., and Spiegelman, B. M. (1993) Adipose expression of tumor necrosis factor-alpha: direct role in obesity-linked insulin resistance. *Science* 259, 87-91.
6. Shi, H., Kokoeva, M. V., Inouye, K., Tzameli, I., Yin, H., and Flier, J. S. (2006) TLR4 links innate immunity and fatty acid-induced insulin resistance. *J Clin Invest* 116, 3015-3025.
7. Yu, C., Chen, Y., Cline, G. W., Zhang, D., Zong, H., Wang, Y., Bergeron, R., Kim, J. K., Cushman, S. W., Cooney, G. J., Atcheson, B., White, M. F., Kraegen, E. W., and Shulman, G. I. (2002) Mechanism by which fatty acids inhibit insulin activation of insulin receptor substrate-1 (IRS-1)-associated phosphatidylinositol 3-kinase activity in muscle. *J Biol Chem* 277, 50230-50236.

8. Glass, C. K., and Ogawa, S. (2006) Combinatorial roles of nuclear receptors in inflammation and immunity. *Nat Rev Immunol* 6, 44-55.
9. Hebenstreit, D., Wirnsberger, G., Horejs-Hoeck, J., and Duschl, A. (2006) Signaling mechanisms, interaction partners, and target genes of STAT6. *Cytokine Growth Factor Rev* 17, 173-188.
10. Borner, C., Woltje, M., Holtt, V., and Kraus, J. (2004) STAT6 transcription factor binding sites with mismatches within the canonical 5'-TTC...GAA-3' motif involved in regulation of delta- and mu-opioid receptors. *J Neurochem* 91, 1493-1500.
11. Kraus, J., Borner, C., and Holtt, V. (2003) Distinct palindromic extensions of the 5'-TTC...GAA-3' motif allow STAT6 binding in vivo. *Faseb J* 17, 304-306.
12. Abu-Amer, Y. (2001) IL-4 abrogates osteoclastogenesis through STAT6-dependent inhibition of NF-kappaB. *J Clin Invest* 107, 1375-1385.
13. Biola, A., Andreau, K., David, M., Sturm, M., Haake, M., Bertoglio, J., and Pallardy, M. (2000) The glucocorticoid receptor and STAT6 physically and functionally interact in T-lymphocytes. *FEBS Lett* 487, 229-233.
14. Litterst, C. M., and Pfitzner, E. (2001) Transcriptional activation by STAT6 requires the direct interaction with NCoA-1. *J. Biol. Chem.* 276, 45713-45721.
15. Valineva, T., Yang, J., Palovuori, R., and Silvennoinen, O. (2005) The transcriptional co-activator protein p100 recruits histone acetyltransferase activity to STAT6 and mediates interaction between the CREB-binding protein and STAT6. *J Biol Chem* 280, 14989-14996.
16. Yang, J., Aittomaki, S., Pesu, M., Carter, K., Saarinen, J., Kalkkinen, N., Kieff, E., and Silvennoinen, O. (2002) Identification of p100 as a coactivator for STAT6 that bridges STAT6 with RNA polymerase II. *Embo J* 21, 4950-4958.
17. Nelson, G., Wilde, G. J., Spiller, D. G., Kennedy, S. M., Ray, D. W., Sullivan, E., Unitt, J. F., and White, M. R. (2003) NF-kappaB signalling is inhibited by glucocorticoid receptor and STAT6 via distinct mechanisms. *J Cell Sci* 116, 2495-2503.
18. Zimmermann, N., Mishra, A., King, N. E., Fulkerson, P. C., Doepker, M. P., Nikolaidis, N. M., Kindinger, L. E., Moulton, E. A., Aronow, B. J., and Rothenberg, M. E. (2004) Transcript signatures in experimental asthma: identification of STAT6-dependent and -independent pathways. *J Immunol* 172, 1815-1824.

19. Kaplan, M. H., Schindler, U., Smiley, S. T., and Grusby, M. J. (1996) Stat6 is required for mediating responses to IL-4 and for development of Th2 cells. *Immunity* 4, 313-319.
20. Aoudjehane, L., Podevin, P., Scatton, O., Jaffray, P., Dusanter-Fourt, I., Feldmann, G., Massault, P. P., Grira, L., Bringuier, A., Dousset, B., Chouzenoux, S., Soubrane, O., Calmus, Y., and Conti, F. (2007) Interleukin-4 induces human hepatocyte apoptosis through a Fas-independent pathway. *Faseb J* 21, 1433-1444.
21. Low, S. H., Vasanth, S., Larson, C. H., Mukherjee, S., Sharma, N., Kinter, M. T., Kane, M. E., Obara, T., and Weimbs, T. (2006) Polycystin-1, STAT6, and P100 function in a pathway that transduces ciliary mechanosensation and is activated in polycystic kidney disease. *Dev Cell* 10, 57-69.
22. Kato, A., Yoshidome, H., Edwards, M. J., and Lentsch, A. B. (2000) Reduced hepatic ischemia/reperfusion injury by IL-4: potential anti-inflammatory role of STAT6. *Inflamm Res* 49, 275-279.
23. Yoshidome, H., Kato, A., Miyazaki, M., Edwards, M. J., and Lentsch, A. B. (1999) IL-13 activates STAT6 and inhibits liver injury induced by ischemia/reperfusion. *Am J Pathol* 155, 1059-1064.
24. Gao, B. (2005) Cytokines, STATs and liver disease. *Cell Mol Immunol* 2, 92-100.
25. Husted, T. L., and Lentsch, A. B. (2006) The role of cytokines in pharmacological modulation of hepatic ischemia/reperfusion injury. *Curr Pharm Des* 12, 2867-2873.
26. Li, J., Thorne, L. N., Punjabi, N. M., Sun, C. K., Schwartz, A. R., Smith, P. L., Marino, R. L., Rodriguez, A., Hubbard, W. C., O'Donnell, C. P., and Polotsky, V. Y. (2005) Intermittent hypoxia induces hyperlipidemia in lean mice. *Circ Res* 97, 698-706.
27. Savransky, V., Nanayakkara, A., Vivero, A., Li, J., Bevans, S., Smith, P. L., Torbenson, M. S., and Polotsky, V. Y. (2007) Chronic intermittent hypoxia predisposes to liver injury. *Hepatology* 45, 1007-1013.
28. Li, J., Grigoryev, D. N., Ye, S. Q., Thorne, L., Schwartz, A. R., Smith, P. L., O'Donnell, C. P., and Polotsky, V. Y. (2005) Chronic intermittent hypoxia upregulates genes of lipid biosynthesis in obese mice. *J Appl Physiol* 99, 1643-1648.
29. Inoue, H., Ogawa, W., Ozaki, M., Haga, S., Matsumoto, M., Furukawa, K., Hashimoto, N., Kido, Y., Mori, T., Sakaue, H., Teshigawara, K., Jin, S., Iguchi, H., Hiramatsu, R., LeRoith, D., Takeda, K., Akira, S., and Kasuga, M. (2004) Role of STAT-3 in regulation of hepatic gluconeogenic genes and carbohydrate metabolism in vivo. *Nat Med* 10, 168-174.

- 
30. Huber, S. A., Sakkinen, P., David, C., Newell, M. K., and Tracy, R. P. (2001) T helper-cell phenotype regulates atherosclerosis in mice under conditions of mild hypercholesterolemia. *Circulation* 103, 2610-2616.
  31. Satterthwaite, G., Francis, S. E., Suvarna, K., Blakemore, S., Ward, C., Wallace, D., Braddock, M., and Crossman, D. (2005) Differential gene expression in coronary arteries from patients presenting with ischemic heart disease: further evidence for the inflammatory basis of atherosclerosis. *Am Heart J* 150, 488-499.
  32. Araya, J., Rodrigo, R., Videla, L. A., Thielemann, L., Orellana, M., Pettinelli, P., and Poniachik, J. (2004) Increase in long-chain polyunsaturated fatty acid n - 6/n - 3 ratio in relation to hepatic steatosis in patients with non-alcoholic fatty liver disease. *Clin Sci (Lond)* 106, 635-643.
  33. Shimomura, I., Shimano, H., Korn, B. S., Bashmakov, Y., and Horton, J. D. (1998) Nuclear sterol regulatory element-binding proteins activate genes responsible for the entire program of unsaturated fatty acid biosynthesis in transgenic mouse liver. *J Biol Chem* 273, 35299-35306.
  34. Browning, J. D., and Horton, J. D. (2004) Molecular mediators of hepatic steatosis and liver injury. *J Clin Invest* 114, 147-152.
  35. Bligh, E. G., and Dyer, W. J. (1959) A rapid method of total lipid extraction and purification. *Can J Biochem Physiol* 37, 911-917.
  36. Haarbo, J., Svendsen, O. L., and Christiansen, C. (1992) Progestogens do not affect aortic accumulation of cholesterol in ovariectomized cholesterol-fed rabbits. *Circ Res* 70, 1198-1202.
  37. James, R. W., and Pometta, D. (1990) Differences in lipoprotein subfraction composition and distribution between type I diabetic men and control subjects. *Diabetes* 39, 1158-1164.

# **4. Conclusion and perspectives**



---

The aim of this work was to evaluate the impact of the loss of STAT6, a transcription factor transducing the effect of the anti-inflammatory cytokines, IL-4 and IL-13. The link between increased pro-inflammatory signals and insulin resistance and type 2 diabetes is well established, but much less information is available about the potential role of decreased anti-inflammatory signals in these disorders. We hypothesized that a reduction of anti-inflammatory signaling in the organism would have similar deleterious effects as in the increase of pro-inflammatory mediators. To verify this hypothesis we decided to identify and quantify differences in protein liver expression in STAT6 knock-out mice. Liver has a particular implication in metabolic homeostasis, thus studying this organ was crucial to verify our hypothesis. The challenge of analyzing this complex organ convinced us to utilize two different proteomic techniques. The two techniques were two-dimensional gel electrophoresis (2-DE) with Coomassie blue staining and two-dimensional nanoscale liquid chromatography tandem mass spectrometry (2D nLC-MS/MS) with iTRAQ labeling. 2-DE performs the analysis on a protein base while (2D nLC-MS/MS) with iTRAQ labeling performs the analysis at the peptide level.

A recent publication from the group of M. Mann (1) described the identification of 3244 liver proteins with high confidence. In a first step they performed a large scale analysis of mouse liver tissues using several fractionation techniques followed by high accuracy mass spectrometry and identified 2210 proteins. To obtain this high amount of proteins, the authors had to use a number of different separative techniques, including centrifugal separation of membrane proteins from soluble ones, followed by 1D gel electrophoresis and nanoscale LC-MS/MS. Finally, the list of 3244 liver proteins was generated by merging their new data with that from the proteome obtained in a previous study (2). The aim of their work was the creation of a complete proteomic map of mouse liver and interestingly, they found only 220 proteins annotated as belonging to the cytoplasmic fraction.

Contrary to their effort to identify the whole mouse liver proteome, the focus of our investigation was to identify with certitude the most intense differences in protein expression resulting from the loss of STAT6. For this reason we used the two different separative techniques cited before: 2-DE and 2D nLC-MS/MS. Due to the specificity of each technique we decided to use full liver lyophilisate with 2-DE and cytosolic fraction solution with iTRAQ. Our investigations let us detect about 700 proteins with 2-DE, providing identification of 10 down- and 25 up-regulated proteins in the STAT6 KO mice. Moreover,

---

155 validated proteins were identified with iTRAQ, including 16 down- and 17 up-regulated in the STAT6 KO mice. Taken together, both 2-DE and iTRAQ gave complementary results with a total of 35 proteins for the 2-DE and 33 proteins for iTRAQ among which 21 were similar.

Regarding the relatively low number of differentially expressed proteins detected by 2-DE, it can be explained by the inherent limitation of densitometric spot comparison with 2-DE. The first limitation implies to exclude underlying spot and, the second one implies to correctly superimpose two different gels. Effectively, some differences exist during electrophoresis which can result in warping the gel while detecting the spots. To resolve this issue, we might have used a different technique such as two-dimensional difference gel electrophoresis (DIGE). In DIGE lysine labeling of the samples with the different dyes allows the reliable comparison of different samples because they are analyzed on the same gel. However, this approach requires an automatic spot picker linked to a laser detector, which is not of common use and drawbacks exist with this technique as well. Labeling induces a shift during migration and, due to poor labeling efficiency (1-2%), spot identification may be performed on wrong protein localization.

Although 2-DE and iTRAQ methods are different, they still provided similarities including 6 down- and 15 up-regulated proteins, representing about one third of all our identified proteins. There was only one protein that gave conflicting results, which finally revealed, after Taqman measurement, not to be regulated (albumin). One of the advantage of 2-DE is that post-translational modifications (PTM) or protein isoforms can be identified with more ease compared to 2D nLC-MS/MS. This identification is less obvious with liquid based approach because of the cleavage of proteins into peptides resulting in PTM loss. To conclude we can argue that 2D nLC-MS/MS based quantification is more selective than densitometric spot quantification because it uses at least a ratio between the two reporter ions (*i.e.*  $m/z$  114 and  $m/z$  115). This ratio is directly linked to the identification, while quantification and identification are separated into two different processes when using 2-DE. Proteomics revealed a higher amount of up-regulated protein in STAT6 KO mice. This was surprising due to the role of STAT6 which is a transcription factor, mostly involved in positive regulation of gene transcription.

This proteomic analysis was finally applied as a first screening of the difference of protein expression between a limited number of WT and STAT6 KO mice. For that reason,

most of the proteins of interest have then been confirmed by another specific quantitative technique. We used gene amplification (Taqman) and protein antibody detection (Western Blot) to confirm the proteomic identifications.

Among the up-regulated proteins, we identified fatty acid binding protein (FABP1). This protein is known to transport lipid across membranes, from the outer part of the cell to the intra-cellular compartments (3). Interestingly, ten of these proteins were stress or detoxification related proteins. These protein include regucalcin (RGN), heat shock 70 kDa protein 5 (HSPA5), heat shock protein 60 (HSPD1), lactoylglutathione lyase (GLO), glutathione peroxidase 1 (GPX1), glutathione S-transferase Mu 1 and 2 (GSTM1, GSTM2), glutathione S-transferase P1 (GSTP1), superoxide dismutase 1 (SOD1) and methionine adenosyltransferase 1 (MAT1A). This observation, together with the high increase of stress proteins in the liver, induced us to have a closer look at the hepatic structural content. This up-regulation of these stress protein, due to the removal of STAT6, was the result of an accumulation of harmful substances, leading to liver structural damages. We discovered that STAT6 KO mice were subjected to an increased liver lipid accumulation resembling the human non alcoholic fatty liver disease (NAFLD). To evaluate the harmful consequences on metabolism, we decided to challenge these mice with a high dose of glucose. According to our expectations, STAT6 KO mice had developed, together with NAFLD glucose intolerance, thereby unable to uptake glucose correctly.

Interestingly, one of the most intense up-regulating proteins found in STAT6 KO mice, Major Urinary Protein (MUP) has been shown to be regulated in metabolic disorders models. For example MUP is decreased in obese mice and rats suggesting a link between this protein and metabolic disorders. However, no human homologue is known so far.

To better characterize the latent metabolic disease identified with the proteomic approach, we started a feeding regime of high fat containing diet to WT and STAT6 KO mice. This nutritional challenge is comparable to dietary excesses characteristic to obese patients. This harmful diet induced an increase in circulating amount of total- and HDL-cholesterol as well as triglycerides in STAT6 KO animals. These increased levels of circulating lipids were accompanied, as expected, with elevated deposition of triglyceride and cholesterol in STAT6 KO livers. This lipid accumulation became evident by a specific lipid staining (Oil-Red O) on histological liver slices. This liver lipid accumulation resulted in an increased liver weight which was accompanied with lipid redistribution with a decrease in the

---

peripheral adipose tissue in the STAT6 KO animal. Therefore, STAT6 plays an important role in peripheral fat distribution. Interestingly these animals were not subjected to liver inflammation. However, a small trigger, like infection, could lead to a release of pro-inflammatory cytokines and initiate a fibrosis, which is related to the human non alcoholic steatohepatitis (NASH).

Finally this work could open a new field in identification of biomarkers in the detection of non alcoholic fatty liver disease (NAFLD). Moreover, STAT6 could constitute a genetic predisposition, explaining toward the development of fatty liver. We cannot say, for the moment if this transcription factor is the cause or the consequence of the development of the disease. However, activators of STAT6 could be one of the targets in developing new therapeutic compounds to treat patients with NAFLD.

- 
1. Shi R, Kumar C, Zougman A, et al. (2007) Analysis of the mouse liver proteome using advanced mass spectrometry. *J Proteome Res* **6**: 2963-2972.
  2. Foster LJ, de Hoog CL, Zhang Y, et al. (2006) A mammalian organelle map by protein correlation profiling. *Cell* **125**: 187-199.
  3. Weisiger RA. (2002) Cytosolic fatty acid binding proteins catalyze two distinct steps in intracellular transport of their ligands. *Mol Cell Biochem* **239**: 35-43.